



RADBOUD UNIVERSITY PRESS

Radboud Dissertation Series

Biomarker-driven immunotherapy for sarcoma

Stefanus Gerardus van Ravensteijn

Biomarker-driven immunotherapy for sarcoma

Stefanus Gerardus van Ravensteijn

Radboud Dissertation Series

ISSN: 2950-2772 (Online); 2950-2780 (Print) Published by RADBOUD UNIVERSITY PRESS Postbus 9100, 6500 HA Nijmegen, The Netherlands www.radbouduniversitypress.nl

Design: Proefschrift AIO | Guus Gijben Cover: Proefschrift AIO | Guntra Laivacuma

Printing: DPN Rikken/Pumbo

ISBN: 9789465150710

DOI: 10.54195/9789465150710

Free download at: https://doi.org/10.54195/9789465150710

© 2025 Stefanus Gerardus van Ravensteijn

RADBOUD UNIVERSITY PRESS

This is an Open Access book published under the terms of Creative Commons Attribution-Noncommercial-NoDerivatives International license (CC BY-NC-ND 4.0). This license allows reusers to copy and distribute the material in any medium or format in unadapted form only, for noncommercial purposes only, and only so long as attribution is given to the creator, see http://creativecommons.org/licenses/by-nc-nd/4.0/.

Biomarker-driven immunotherapy for sarcoma

Proefschrift ter verkrijging van de graad van doctor aan de Radboud Universiteit Nijmegen op gezag van de rector magnificus prof. dr. J.M. Sanders, volgens besluit van het college voor promoties in het openbaar te verdedigen op

> vrijdag 31 oktober 2025 om 12.30 uur precies

> > door

Stefanus Gerardus van Ravensteijn geboren op 16 juni 1991 te Oss

Promotoren:

Prof. dr. C.M.L. van Herpen

Prof. dr. H.M.W. Verheul (Erasmus MC)

Copromotoren:

Prof. dr. I.M.E. Desar

Dr. K.F. Bol

Manuscriptcommissie:

Prof. dr. I.C.M. van der Geest

Prof. dr. J.A. Schalken

Dr. W.J. van Houdt (Antoni van Leeuwenhoek)

Table of contents

Chapter 1	
General Introduction	Ş
Chapter 2	
Immunological and genomic analysis reveals clinically relevant distinctions	
between angiosarcoma subgroups	19
Chapter 3	
MYC amplification in angiosarcoma depends on etiological/clinical	
subgroups – diagnostic and prognostic value	45
Chapter 4	
Cemiplimab in locally advanced or metastatic secondary angiosarcomas	
(CEMangio): A phase II clinical trial and biomarker analyses	63
Chapter 5	
Exploring the relation between TGF-β pathway activity and response to	
checkpoint inhibition in patients with metastatic Melanoma	99

Chapter 6

The prognostic relevance of MRI characteristics in myxofibrosarcoma patients treated with neoadjuvant radiotherapy	125
Chapter 7 Summary, discussion, and future perspectives	143
Epilogue	
The safety risk of information overload and bureaucracy in oncology	
clinical trial conduct	159
Nederlandse Samenvatting	168
List of Abbreviations	174
Research Data Management	176
List of Publications	178
PhD Portfolio	180
Curriculum Vitae	182
Dankwoord	184





Chapter 1

General Introduction

Angiosarcomas and immune checkpoint inhibition

Angiosarcomas (AS) are rare and aggressive mesenchymal sarcomas with endothelial characteristics. They can be classified into primary AS (pAS), which occur de novo at various anatomical locations with unknown etiology, and secondary AS (sAS) which develop as a result of DNA damaging factors including radiotherapy (RT), ultraviolet (UV) radiation, or chronic lymphedema (Stewart Treves AS). (1-3)

In case of localized, non-metastatic disease, treatment of AS comprises of curative surgery, alone or in combination with (neo)adjuvant radiotherapy or chemotherapy. (4) Unfortunately, the risk of local recurrence or metastatic disease is greater than 50% despite intensive treatment. In case of locally advanced or metastatic disease, median overall survival is limited to 5-10 months, with palliative chemotherapy, mainly consisting of paclitaxel or doxorubicin. (5-7) Median progression free survival (PFS) of treatment with paclitaxel was limited to 4 months, and median overall survival (OS) was only 7.6 months in patients with unresectable AS in the ANGIOTAX study. (8) Pazopanib is the only non-cytotoxic drug approved for treatment of AS, with a response rate of 20% and a median PFS of only 3 months. (9) Thus far, patients with AS have not benefitted from the recent advances that led to new treatment options, such as immunotherapy. Despite improvements in survival in many solid tumor types over the past decade, survival for AS has not improved, urging the need for new treatment modalities.

Immune checkpoint inhibition (ICI) has become a key element in the treatment of various malignancies, such as melanoma, renal cell carcinoma, lungcancer, and cutaneous squamous cell carcinoma, but not sarcomas. (10-13) Due to the immune desert tumor microenvironment (TME) of sarcomas, low tumor mutational burden (TMB), and low programmed death-ligand 1 (PD-L1) expression, sarcomas in general are considered non-immunogenic tumors which respond poorly to ICI. (14) However, sarcomas are a heterogeneous disease with more than 100 histological subtypes, so general assumptions on primary ICI resistance might not be true for all subtypes and may vary within a subtype. There are anecdotal reports and small retrospective case series that have reported radiological responses to ICI in AS patients, in particular UV-AS. (15, 16) Florou et al. reported a response rate of 71% in a case series of seven predominantly cutaneous AS patients. D'Angelo et al. showed a partial response in three out of eight AS patients treated with nivolumab and bempegaldesleukin, a PEGylated interleukin-2. (17) These data raises the question whether a subgroup of AS might benefit from treatment with ICI.

1

AS are a heterogeneous subtype of sarcomas, with limited knowledge about the genomic landscape. Furthermore, no data are available on the immune cell composition of the TME in AS. The composition of the immune microenvironment is increasingly being recognized as a potential key biomarker in predicting response to ICI. In sarcomas, a CD8+ cytotoxic T-cell signature has been associated with favorable treatment outcomes following ICI, particularly when B-cells were abundantly present. (18) The presence of tertiary lymphoid structures (TLS), that comprises of aggregates of CD4+ and CD8+ T-cells, dendritic cells, and B-cell follicles, has also been recognized for positively predicting ICI response in soft tissue sarcomas STS. (19, 20) Therefore, we started in **chapter 2** by analyzing the immune environment and genomic landscape in AS. In the largest cohort of AS, so far, we describe clinical subgroups of AS, in order to explore those that might benefit from ICI-based treatment and combine the immunological landscape of AS with additional genetic data.

Next we aim to investigate the prevalence, and possible prognostic value of MYC, a proto oncogene that is involved in metabolism, proliferation, and angiogenesis. (21) MYC proteins are also associated with remodulation of the TME and upregulation of PD-L1 expression, creating possible resistance to ICI. (22) MYC amplifications may therefore provide an interesting opportunity for a targeted approach in boosting ICI response in AS. Therefore, we analyzed a heterogeneous, retrospective cohort of 110 AS patients, investigating prevalence of MYC amplifications among AS subgroups and its potential role as a prognostic indicator, as described in **chapter 3**. Given that detecting MYC amplifications using fluorescent in situ hybridization is both expensive and time consuming, we explored the use immunohistochemistry to determine MYC protein expression as a surrogate method, and investigated concordance between both techniques.

Prospective clinical trials investigating the efficacy of ICI in AS are lacking. Based on the tumor characteristics of sAS, and anecdotal reports of responses to ICI, a clinical trial was designed investigating the effectivity of ICI in sAS. In **chapter 4** we describe the results of de CEMangio trial, a prospective, single arm, multicenter, phase II clinical trial investigating the efficacy and safety of the PD-1 inhibitor cemiplimab in 18 patients with locally advanced or metastatic sAS. Extensive translational research was performed to identify biomarkers for response to cemiplimab.

Predictive and prognostic biomarkers

The ideal *predictive* biomarker would identify exactly which patients will benefit from a specific therapy and which patients will not. This predictive biomarker could help create personalized treatment plans, avoid unnecessary toxicity and procedures for patients, and reduce healthcare costs for society. Predictive biomarkers would need to be highly sensitive and specific, and should be easy to measure in blood, tumor tissue, or by using radiological techniques. (23)

So far, unambiguous biomarkers predicting response to ICI are lacking. TMB, microsatellite instability (MSI), and PD-L1 are the most studied biomarkers. (24-27) The KEYNOTE-158 study reported a positive association between high TMB (TMB-H; ≥10 mutations/megabase (mut/Mb)) and treatment response to the PD-1 inhibitor pembrolizumab in a cohort of advanced solid tumors. (28) Marabelle et al. reported an objective response rate of 29% in case of TMB-H compared to 6% in non-TMB-H patients. (29, 30) Based on these results, the Food and Drug Administration (FDA) approved pembrolizumab for TMB-H solid tumors independent of tumor origin. (28) In several tumor types, the combined positive score (CPS) for scoring PD-L1 positivity is used to make decisions regarding treatment initiation with ICI. (31-33) The CPS score incorporates the number of PD-L1 stained cells, including tumor cells, lymphocytes, and macrophages, divided by the number of viable tumor cells to calculate a score. However, it is increasingly clear that TMB and PD-L1 or PD-L1 derived scores such as CPS do not inequivalently predict ICI response and may vary between cancer types. Therefore, in chapter 4, we investigated not only known biomarkers such as TMB, but also other promising new biomarkers including circulating tumor DNA and the gut-microbiome.

Malignant melanoma is an aggressive form of skin cancer arising from melanocytes and ICI is the cornerstone of treatment. Unfortunately, only half of the patients respond to ICI treatment. (10, 34, 35) Like in other tumor types, a predictive biomarker for ICI response in melanoma is lacking. The TME, especially the interplay between the tumor and the immune system, has emerged as a key factor in the development of melanoma metastasis. Preclinical data indicate that TGF- β pathway activity mediates immune evasion by T-cell exclusion from the tumor and may therefore be predictive for response to ICI. (36-38) With the development of agents blocking the TGF- β signaling pathway, the role of TGF- β in treatment resistance to ICI becomes of clinical relevance. (39) In **chapter 5** we describe the results of a retrospective cohort study investigating the association between TGF- β signal transduction pathway activity

and resistance to ICI treatment in advanced melanoma. Furthermore, other pathway activities were analyzed to better understand their potential role in ICI resistance.

In a perfect world, the ideal prognostic biomarker would indicate the natural behavior of the cancer and its likelihood for disease recurrence, metastatic potential, and survival. Identifying the perfect prognostic biomarker could help select patients for less or more intense treatment depending on their chance of disease recurrence. By using the perfect prognostic biomarker, over- and undertreatment could be minimized.

Prognostic biomarkers might support the development of (de)intensified primary treatment strategies in high- or low risk patients diagnosed with solid malignancies. Myxofibrosarcoma (MFS) is a histological subtype of STS existing of fibroblasts and myxoid stroma, and most often presenting in the extremities. Treatment for localized disease involves neoadjuvant radiotherapy (nRT) followed by surgical resection. (40) Due an infiltrative growth pattern, local recurrence rates are high, ranging from 20-60%. (41, 42) In MFS magnetic Resonance Imaging (MRI) is standard of care at presentation and after nRT. While presence on pre-nRT MRI of longitudinal spreading, referred to as the "tail sign", is recognized as prognostic for local recurrence and OS, the role of post-nRT MRI is ambiguous. (43-45) Being able to identify high-risk patients in an early stage might support the development of intensified primary treatment and follow-up strategies for these patients, limiting disease recurrence. In chapter 6 we evaluate the prognostic relevance of MRI characteristics in 40 MFS patients who received nRT.

In **chapter 7**, a summary with general discussion and perspectives for future research on AS and predictive and prognostic biomarkers will be presented.

Epilogue: Clinical trial conduct

Drawing from the insights gained through the design of the translational research studies and the investigator-initiated clinical trial described in previous chapters, it becomes clear that the successful execution of such studies depends not only on scientific advance but also on the efficiency of trial design and regulatory progresses. Performance of clinical trials has led to major developments in the field of oncology, significantly improving the prognosis for patients with many tumor (sub)types. (46) In order to ensure patients' safety, an increase in regulatory aspects for proper clinical trial conduct has been implemented over the past decades. However, due to information overload and ineffective bureaucracy, patient safety might possibly be negatively impacted. Trial initiation time has increased from months to several years, limiting participation of patients in clinical trials, while trial costs have risen dramatically. (47-50) In the epilogue of this thesis, described in **chapter 8**, we provide an overview of the current regulatory aspects of clinical research, evaluating practical consequences of these regulations and propose specific improvements for optimal clinical trial conduct.

References

- Fayette J, Martin E, Piperno-Neumann S, Le Cesne A, Robert C, Bonvalot S, et al. Angiosarcomas, a heterogeneous group of sarcomas with specific behavior depending on primary site: a retrospective study of 161 cases. Ann Oncol. 2007;18(12):2030-6.
- Berebichez-Fridman R, Deutsch YE, Joyal TM, Olvera PM, Benedetto PW, Rosenberg AE, Kett DH. Stewart-Treves Syndrome: A Case Report and Review of the Literature. Case Rep Oncol. 2016;9(1):205-11.
- 3. Young RJ, Brown NJ, Reed MW, Hughes D, Woll PJ. Angiosarcoma. Lancet Oncol. 2010;11(10):983-91.
- von Mehren M, Kane JM, Agulnik M, Bui MM, Carr-Ascher J, Choy E, et al. Soft Tissue Sarcoma, Version 2.2022, NCCN Clinical Practice Guidelines in Oncology. J Natl Compr Canc Netw. 2022;20(7):815-33.
- Florou V, Wilky BA. Current and Future Directions for Angiosarcoma Therapy. Curr Treat Options Oncol. 2018;19(3):14.
- Fury MG, Antonescu CR, Van Zee KJ, Brennan MF, Maki RG. A 14-year retrospective review of angiosarcoma: clinical characteristics, prognostic factors, and treatment outcomes with surgery and chemotherapy. Cancer J. 2005;11(3):241-7.
- 7. Penel N, Italiano A, Ray-Coquard I, Chaigneau L, Delcambre C, Robin YM, et al. Metastatic angiosarcomas: doxorubicin-based regimens, weekly paclitaxel and metastasectomy significantly improve the outcome. Ann Oncol. 2012;23(2):517-23.
- 8. Penel N, Bui BN, Bay JO, Cupissol D, Ray-Coquard I, Piperno-Neumann S, et al. Phase II trial of weekly paclitaxel for unresectable angiosarcoma: the ANGIOTAX Study. J Clin Oncol. 2008;26(32):5269-74.
- van der Graaf WT, Blay JY, Chawla SP, Kim DW, Bui-Nguyen B, Casali PG, et al. Pazopanib for metastatic soft-tissue sarcoma (PALETTE): a randomised, double-blind, placebo-controlled phase 3 trial. Lancet. 2012;379(9829):1879-86.
- Larkin J, Chiarion-Sileni V, Gonzalez R, Grob JJ, Cowey CL, Lao CD, et al. Combined Nivolumab and Ipilimumab or Monotherapy in Untreated Melanoma. N Engl J Med. 2015;373(1):23-34.
- Migden MR, Rischin D, Schmults CD, Guminski A, Hauschild A, Lewis KD, et al. PD-1 Blockade with Cemiplimab in Advanced Cutaneous Squamous-Cell Carcinoma. N Engl J Med. 2018;379(4):341-51.
- Motzer RJ, Tannir NM, McDermott DF, Arén Frontera O, Melichar B, Choueiri TK, et al. Nivolumab plus Ipilimumab versus Sunitinib in Advanced Renal-Cell Carcinoma. N Engl J Med. 2018;378(14):1277-90.
- 13. de Castro G, Jr., Kudaba I, Wu YL, Lopes G, Kowalski DM, Turna HZ, et al. Five-Year Outcomes With Pembrolizumab Versus Chemotherapy as First-Line Therapy in Patients With Non-Small-Cell Lung Cancer and Programmed Death Ligand-1 Tumor Proportion Score ≥ 1% in the KEYNOTE-042 Study. J Clin Oncol. 2023;41(11):1986-91.
- 14. Tawbi HA, Burgess M, Bolejack V, Van Tine BA, Schuetze SM, Hu J, et al. Pembrolizumab in advanced soft-tissue sarcoma and bone sarcoma (SARCo28): a multicentre, two-cohort, singlearm, open-label, phase 2 trial. Lancet Oncol. 2017;18(11):1493-501.
- Florou V, Rosenberg AE, Wieder E, Komanduri KV, Kolonias D, Uduman M, et al. Angiosarcoma patients treated with immune checkpoint inhibitors: a case series of seven patients from a single institution. J Immunother Cancer. 2019;7(1):213.
- Sindhu S, Gimber LH, Cranmer L, McBride A, Kraft AS. Angiosarcoma treated successfully with anti-PD-1 therapy - a case report. J Immunother Cancer. 2017;5(1):58.

- D'Angelo SP, Richards AL, Conley AP, Woo HJ, Dickson MA, Gounder M, et al. Pilot study of bempegaldesleukin in combination with nivolumab in patients with metastatic sarcoma. Nat Commun. 2022;13(1):3477.
- 18. Petitprez F, de Reynies A, Keung EZ, Chen TW, Sun CM, Calderaro J, et al. B cells are associated with survival and immunotherapy response in sarcoma. Nature. 2020;577(7791):556-60.
- 19. Italiano A, Bessede A, Pulido M, Bompas E, Piperno-Neumann S, Chevreau C, et al. Pembrolizumab in soft-tissue sarcomas with tertiary lymphoid structures: a phase 2 PEMBROSARC trial cohort. Nat Med. 2022;28(6):1199-206.
- 20. Wang XX, Liu YP, Lu Y, Wu LH, Ren JY, Ji H, et al. Identifying specific TLS-associated genes as potential biomarkers for predicting prognosis and evaluating the efficacy of immunotherapy in soft tissue sarcoma. Front Immunol. 2024;15:1372692.
- 21. Baudino TA, McKay C, Pendeville-Samain H, Nilsson JA, Maclean KH, White EL, et al. c-Myc is essential for vasculogenesis and angiogenesis during development and tumor progression. Genes Dev. 2002;16(19):2530-43.
- 22. Han H, Jain AD, Truica MI, Izquierdo-Ferrer J, Anker JF, Lysy B, et al. Small-Molecule MYC Inhibitors Suppress Tumor Growth and Enhance Immunotherapy. Cancer Cell. 2019;36(5): 483-97 e15.
- FDA. FDA-NIH Biomarker Working Group. Silver Spring (MD): Food and Drug Administration (US); Bethesda (MD): National Institutes of Health (US); BEST (Biomarkers, EndpointS, and other Tools) Resource. 2016.
- 24. Davis AA, Patel VG. The role of PD-L1 expression as a predictive biomarker: an analysis of all US Food and Drug Administration (FDA) approvals of immune checkpoint inhibitors. J Immunother Cancer. 2019;7(1):278.
- Lu S, Stein JE, Rimm DL, Wang DW, Bell JM, Johnson DB, et al. Comparison of Biomarker Modalities for Predicting Response to PD-1/PD-L1 Checkpoint Blockade: A Systematic Review and Meta-analysis. JAMA Oncol. 2019;5(8):1195-204.
- Samstein RM, Lee CH, Shoushtari AN, Hellmann MD, Shen R, Janjigian YY, et al. Tumor mutational load predicts survival after immunotherapy across multiple cancer types. Nat Genet. 2019;51(2):202-6.
- 27. Zeverijn LJ, Geurts BS, Battaglia TW, van Berge Henegouwen JM, de Wit GF, Hoes LR, et al. The Innate Immune Landscape of dMMR/MSI Cancers Predicts the Outcome of Nivolumab Treatment: Results from the Drug Rediscovery Protocol. Clin Cancer Res. 2024;30(19):4339-51.
- 28. Marabelle A, Fakih M, Lopez J, Shah M, Shapira-Frommer R, Nakagawa K, et al. Association of tumour mutational burden with outcomes in patients with advanced solid tumours treated with pembrolizumab: prospective biomarker analysis of the multicohort, open-label, phase 2 KEYNOTE-158 study. Lancet Oncol. 2020;21(10):1353-65.
- 29. FDA. Highlights of prescribing information: KEYTRUDA https://www.accessdata.fda.gov/drugsatfda_docs/label/2024/125514s155lbl.pdf#page=161 [
- 30. Zheng M. Tumor mutation burden for predicting immune checkpoint blockade response: the more, the better. J Immunother Cancer. 2022;10(1).
- 31. Wainberg ZA, Fuchs CS, Tabernero J, Shitara K, Muro K, Van Cutsem E, et al. Efficacy of Pembrolizumab Monotherapy for Advanced Gastric/Gastroesophageal Junction Cancer with Programmed Death Ligand 1 Combined Positive Score ≥10. Clin Cancer Res. 2021;27(7):1923-31.
- 32. Cortes J, Rugo HS, Cescon DW, Im SA, Yusof MM, Gallardo C, et al. Pembrolizumab plus Chemotherapy in Advanced Triple-Negative Breast Cancer. N Engl J Med. 2022;387(3):217-26.

- 33. Bellmunt J, de Wit R, Fradet Y, Climent MA, Petrylak DP, Lee JL, et al. Putative Biomarkers of Clinical Benefit With Pembrolizumab in Advanced Urothelial Cancer: Results from the KEYNOTE-045 and KEYNOTE-052 Landmark Trials. Clin Cancer Res. 2022;28(10):2050-60.
- 34. Wolchok JD, Chiarion-Sileni V, Gonzalez R, Grob JJ, Rutkowski P, Lao CD, et al. Long-Term Outcomes With Nivolumab Plus Ipilimumab or Nivolumab Alone Versus Ipilimumab in Patients With Advanced Melanoma. J Clin Oncol. 2022;40(2):127-37.
- Postow MA, Chesney J, Pavlick AC, Robert C, Grossmann K, McDermott D, et al. Nivolumab and ipilimumab versus ipilimumab in untreated melanoma. N Engl J Med. 2015;372(21):2006-17.
- Tauriello DVF, Palomo-Ponce S, Stork D, Berenguer-Llergo A, Badia-Ramentol J, Iglesias M, et al. TGFbeta drives immune evasion in genetically reconstituted colon cancer metastasis. Nature. 2018;554(7693):538-43.
- 37. Loffek S. Transforming of the Tumor Microenvironment: Implications for TGF-beta Inhibition in the Context of Immune-Checkpoint Therapy. J Oncol. 2018;2018:9732939.
- Mariathasan S, Turley SJ, Nickles D, Castiglioni A, Yuen K, Wang Y, et al. TGFbeta attenuates tumour response to PD-L1 blockade by contributing to exclusion of T cells. Nature. 2018;554(7693):544-8.
- 39. Tauriello DVF, Sancho E, Batlle E. Overcoming TGFbeta-mediated immune evasion in cancer. Nat Rev Cancer. 2022;22(1):25-44.
- 40. Vanni S, De Vita A, Gurrieri L, Fausti V, Miserocchi G, Spadazzi C, et al. Myxofibrosarcoma landscape: diagnostic pitfalls, clinical management and future perspectives. Ther Adv Med Oncol. 2022;14:17588359221093973.
- 41. van der Horst CAJ, Bongers SLM, Versleijen-Jonkers YMH, Ho VKY, Braam PM, Flucke UE, et al. Overall Survival of Patients with Myxofibrosarcomas: An Epidemiological Study. Cancers (Basel). 2022;14(5).
- 42. Teurneau H, Engellau J, Ghanei I, Vult von Steyern F, Styring E. High Recurrence Rate of Myxofibrosarcoma: The Effect of Radiotherapy Is Not Clear. Sarcoma. 2019;2019:8517371.
- 43. Sambri A, Spinnato P, Bazzocchi A, Tuzzato GM, Donati D, Bianchi G. Does pre-operative MRI predict the risk of local recurrence in primary myxofibrosarcoma of the extremities? Asia Pac J Clin Oncol. 2019;15(5):e181-e6.
- 44. Spinnato P, Clinca R, Vara G, Cesari M, Ponti F, Facchini G, et al. MRI Features as Prognostic Factors in Myxofibrosarcoma: Proposal of MRI Grading System. Acad Radiol. 2021;28(11):1524-9.
- 45. Yoo HJ, Hong SH, Kang Y, Choi J-Y, Moon KC, Kim H-S, et al. MR imaging of myxofibrosarcoma and undifferentiated sarcoma with emphasis on tail sign; diagnostic and prognostic value. European Radiology. 2014;24(8):1749-57.
- 46. Arnold M, Rutherford MJ, Bardot A, Ferlay J, Andersson TM, Myklebust TA, et al. Progress in cancer survival, mortality, and incidence in seven high-income countries 1995-2014 (ICBP SURVMARK-2): a population-based study. Lancet Oncol. 2019;20(11):1493-505.
- 47. Dilts DM, Sandler AB, Cheng SK, Crites JS, Ferranti LB, Wu AY, et al. Steps and time to process clinical trials at the Cancer Therapy Evaluation Program. J Clin Oncol. 2009;27(11):1761-6.
- 48. Steensma DP, Kantarjian HM. Impact of cancer research bureaucracy on innovation, costs, and patient care. J Clin Oncol. 2014;32(5):376-8.
- Stewart DJ, Whitney SN, Kurzrock R. Equipoise lost: ethics, costs, and the regulation of cancer clinical research. J Clin Oncol. 2010;28(17):2925-35.
- 50. Pascarella G, Capasso A, Nardone A, Triassi M, Pignata S, Arenare L, et al. Costs of clinical trials with anticancer biological agents in an Oncologic Italian Cancer Center using the activity-based costing methodology. PLoS One. 2019;14(1):e021033





Chapter 2

Immunological and genomic analysis reveals clinically relevant distinctions between angiosarcoma subgroups

Stefan G. van Ravensteijn*, Yvonne M.H. Versleijen-Jonkers*, Melissa H.S. Hillebrandt-Roeffen, Marije E. Weidema, Maikel J.L. Nederkoorn, Kalijn F. Bol, Mark A.J. Gorris, Kiek Verrijp, Leonie I. Kroeze, Tessa de Bitter, Richarda M. de Voer, Uta E. Flucke, Ingrid M.E. Desar

*These authors contributed equally to this work

Abstract

Angiosarcomas (AS) are extremely rare and aggressive vascular malignancies subdivided in de novo primary AS (pAS) and secondary AS (sAS). We hypothesize that the combination of immunological and genomic profiles significantly differs between primary and secondary AS, with potential impact on treatment strategies and a role for immunotherapy. Tumor-infiltrating lymphocytes were analyzed using multiplex immunohistochemistry from 79 pAS and 178 sAS. Median cell density was significantly higher in sAS for CD3+ T-cells (p < 0.001), CD8+ cytotoxic T-cells (p = 0.033), CD4+ T-helper cells (p < 0.001) and FoxP3+ T-regulatory cells (p < 0.001). CD20+ B-cell density was comparable (p = 0.417). Comprehensive genomic profiling was performed in 25 pAS and 25 sAS. A (likely) pathogenic mutation was detected in 80% of pAS vs. 88% of sAS (p = 0.702). Amplifications were found in 15% of pAS vs. 84% of sAS (p < 0.001). DNA damage response (DDR) pathway mutations (p = 0.021) and MYC amplifications (p < 0.001) were predominantly seen in sAS. In conclusion we observed a clear and clinical relevant distinction in immune infiltration and genomic profiles between pAS and sAS. The T-cell infiltrated tumor microenvironment and frequent DDR gene mutations, especially in sAS, warrant clinical trials with immunotherapy

Introduction

Angiosarcomas (AS) are rare malignant mesenchymal tumors with endothelial characteristics. (1, 2) They comprise of primary (de novo) AS (pAS) which can develop at different anatomic sites with unknown etiology and secondary AS (sAS) which arise due to DNA damaging factors like ultra-violet (UV) light exposure, prior radiotherapy or chronic lymphedema (Stewart-Treves syndrome). (1-3)

Unfortunately, the risk of developing local recurrent or metastatic disease in AS exceeds 50%. Treatment for localized disease consists of surgery, either in combination with (neo)adjuvant chemo- or radiotherapy. In locally advanced or metastatic disease median survival is limited to 5-10 months and patients are primarily treated with palliative chemotherapy. The only approved non-cytotoxic drug used is the tyrosine kinase inhibitor pazopanib. (4, 5) Overall survival has not improved the last 10 years, emphasizing the need for better treatments. (6-8)

Immune checkpoint inhibition (ICI) has become the cornerstone in treatment of various malignant tumors except sarcomas. (9, 10) Most sarcomas have a poorly immune-infiltrated tumor microenvironment (TME) and are therefore considered less responsive to ICI. (11, 12) However, some case reports and small case series demonstrated promising responses in AS patients treated with ICI, especially in UV-associated AS (UV-AS). (13-17) D'Angelo et al reported a durable clinical response in 3/8 AS patients treated with a combination of nivolumab and bempegaldesleukin, a CD122-preferential interleukin-2 pathway agonist. (18) It remains however unclear which AS clinical subgroups may benefit from ICI treatment.

So far, unambiguous biomarkers to predict response to ICI are lacking. Tumor mutational burden (TMB) and programmed cell death ligand 1 (PD-L1) are the most studied biomarkers. It is increasingly clear that they do not inequivalently predict ICI response. (16, 18-22) In sarcomas the composition of immune cell subsets, especially B- and T-cells within the TME, might be more indicative. (23) Petitprez et al reported that in sarcomas, a CD8+ T-cell signature and PD-1 expression resulted in favorable outcomes when B-cells were highly present. (23) D'Angelo et al have shown that CD8+ T-cell infiltrates were correlated with an improved objective response rate after treatment with ICI in in a very limited population of AS among others. (18)

Due to the heterogeneity of AS, and the limited efficacy of the current generic therapeutic options, there is an urgent need for further characterization of their combined immunological and genomic landscape to detect subgroups that are likely to benefit from ICI based treatment strategies. These strategies could comprise ICI monotherapy and combinations boosting ICI response. (24) Until now, no data are available on the composition of immune cells in AS while comprehensive genetic analyses of AS are performed in limited patient numbers. (25, 26) We aim to investigate the immune environment in a large group of AS clinical subgroups, in order to explore those that might benefit from ICI based treatment and combine this with additional genetic data.

Methods

Objectives

The primary objective is to detect differences in the combined immunological and genomic profiles of primary versus secondary angiosarcomas. The secondary objectives are to explore both the immunological and genomic profile of clinical AS subgroups.

Patients

We retrospectively collected data and samples from the primary tumor of patients diagnosed with AS in the Netherlands between 1989 and 2015 by a nationwide search through PALGA (Dutch nationwide network and registry of histo- and cytopathology) and an additional search through the Pathology database of the Radboudumc (2015-2019). Clinical data were received from the nationwide Netherlands Cancer Registry. Ethical approval for the study was obtained from the local certified Medical Ethics Committee (2016-2686). Patients were categorized in 2 main clusters; pAS and sAS and 8 clinical subgroups based on location of the tumor and origin of the AS. pAS subgroups were divided into: Heart, primary breast, skin that is not UV associated, soft tissue and visceral. (8) sAS subgroups are: Radiotherapy associated AS (RT-AS), Stewart Treves AS and UV-AS. AS of the sun exposed skin of the head and neck area were classified as UV-AS. All samples were histopathologically reviewed and representative tumor cores were selected.

Tumor microenvironment

Tissue microarrays (TMAs) of formalin-fixed paraffin embedded (FFPE) AS tumor material from 257 patients was used for immune profiling. To correct for heterogeneity two 2 mm tumor cores per tumor were analyzed. Multiplex immunohistochemistry (mIHC) was performed on 4 µm thick tissue sections of TMAs by use of the Opal 7-color IHC kit and automated Bond RX stainer using primary antibodies against CD3, CD8, FoxP3, CD20 and CD56 to detect cytotoxic, regulatory

and T-helper cells, B-cells and Natural Killer (NK) cells. An antibody against ERG, a transcription factor expressed in endothelial cells, served as tumor marker (clone EPR3864, Abcam). Methods for panel optimization and validation were previously described. (27, 28) Multispectral images were generated by scanning the slides with the Vectra® Automated Quantitative Imaging System with software version 3.0.4 (PerkinElmer). Data were analyzed using inform software (Akoya Biosciences), extended with in-house developed software for cell identification, phenotyping and localization of immune cell subsets. (29)

Genomic Analysis

Sample selection for next generation sequencing (NGS) was based on an estimated percentage of tumor cells of at least 30% to ensure accurate analysis of microsatellite instability (MSI) and tumor mutational burden (TMB). Tumor material could not be older than 2005, and only primary located untreated samples were included for the genomic analysis. DNA was extracted from FFPE tissue, precipitated and quantified. Library preparation and sequencing was performed as described previously. (30, 31) Coverage tables and a variant call file for single- and multiple-nucleotide variants, including number and percentage of variant alleles, were provided. Genomic variants were filtered by excluding the following: 1) variants not overlapping with exons and splice site regions except those in the TERT promoter region, 2) synonymous variants, unless located in a splice site region, 3) variants present with a frequency >0.1% in the control population represented in The Exome Aggregation Consortium (ExAC) version 0.2, and 4) variants with a variant allele frequency of <5%. Identified candidate variants were confirmed using the software Alamut visual version 2.13. Variants were manually analyzed and classified based on the predicted pathogenicity into 5 classes: class 1, not pathogenic; class 2, unlikely pathogenic; class 3, variant of unknown significance; class 4, likely pathogenic; and class 5, pathogenic. Class 4 and 5 variants were considered potentially clinically relevant and are referred to in this article as (likely) pathogenic. Interpretation of pathogenicity for variants in tumor suppressor genes (TSGs) was based on three prediction tools (sorting intolerant from tolerant (SIFT), Polyphen-2 and Align-Grantham Variation Grantham Deviation (Align-GVGD) and for both TSG and oncogenes on various knowledge-based tools (ClinVar, OncoKB, InterVar)). Therapeutic targeting of tumor suppressor genes generally requires inactivation of both gene copies. Therefore, for class 4/5 variants in tumor suppressor genes we evaluated whether these affect one or two alleles based on relative coverage and/or variant allele frequencies (VAF) of the variant and nearby single nucleotide polymorphisms (SNPs). Presence of gene amplification was analyzed as previously described on the basis of median coverage normalization. (30) A relative coverage ≥3 was considered gene amplification. The number of gene copies was estimated by using the relative coverage corrected for the percentage of tumor cells in the sample. TMB analysis was based on both synonymous and non-synonymous variants (total TMB). A cutoff value of 10 mutations/Mb (mut/Mb) was considered high TMB. Mutational signatures were investigated in all tumors with a TMB ≥10 mutations/Mb by use of the COSMIC mutational signature v3. (30, 32).

Statistical analysis

Median values and interquartile ranges (IQR) were used to describe continuous variables. Count and percent were used for categorical variables. To compare variables across groups, the Fisher exact test was used for categorical variables and Mann-Whitney U test for continuous variables. Values were considered significant with a p value <0.05. Statistical analysis was performed using IBM SPSS statistics 25 and R (version 3.6.2).

Results

Patient characteristics are depicted in Table 1. The median cell densities of lymphocyte subsets for pAS (n = 79) and sAS (n = 178) are shown in Table 2 and Figure 1. Median density was significantly higher in sAS for CD3⁺ T-cells, CD4⁺ T-helper cells, CD8⁺ cytotoxic T-cells and FoxP3⁺ T-regulatory cells. The median count of CD20⁺ B-cells was not significantly different between pAS and sAS. NK cells were rarely observed in both subgroups and never more than 30 cells/mm² (median o cells/mm²).

Next, cell densities of specific AS subgroups were analyzed. A complete overview of the cell densities for individual subgroups is shown in Table 3. Within the sAS group, median cell density was significantly higher for all lymphocyte subsets in the UV-AS subgroup compared to the RT-AS group: CD3+ (p = 0.003), CD4+ (p = 0.004), CD8+ (p = 0.022) and FoxP3+ T-cells (p < 0.001) and CD20+ B-cells (p = 0.021). UV-AS also showed significantly higher densities across all lymphocyte subsets compared to de novo (not UV-associated) skin AS. Visceral AS showed the highest cell density of all pAS subgroups for CD3+ T-cells, CD4+ T-cells, CD8+ T-cells and CD20+ B-cells.

Table 1. Tumor location for the specific AS subgroups for both primary and secondary AS.

Primary AS	Location Total Group $(n = 79)$	Location TSO Selection $(n = 25)$		
Soft tissue	Leg $(n = 3)$ Neck $(n = 1)$ Face $(n = 1)$ Bottom $(n = 1)$ Retroperitoneal $(n = 1)$ Ureter $(n = 1)$ Abdomen $(n = 1)$ Mediastinum $(n = 1)$ Lumbar region $(n = 1)$	Leg $(n = 1)$ Face $(n = 1)$ Retroperitoneal $(n = 1)$ Mediastinum $(n = 1)$		
Primary breast	Mamma (<i>n</i> = 20)	Mamma $(n = 5)$		
Not UV associated skin	Leg $(n = 10)$ Abdomen $(n = 2)$ Foot $(n = 1)$ Thorax $(n = 1)$ Unknown $(n = 1)$	Leg (n = 4)		
Visceral	Liver $(n = 7)$ Intestine $(n = 6)$ Spleen $(n = 5)$ Kidney $(n = 3)$ Adrenal gland $(n = 1)$ Thyroid $(n = 4)$ Stomach $(n = 1)$ Pleura $(n = 1)$	Thyroid $(n = 2)$ Kidney $(n = 1)$ Adrenal gland $(n = 1)$ Liver $(n = 1)$ Stomach $(n = 1)$ Spleen $(n = 1)$		
Heart	Heart (<i>n</i> = 4) Aorta (<i>n</i> = 1)	Heart $(n = 4)$ Aorta $(n = 1)$		
Secondary AS	Location total group $(n = 178)$	Location TSO selection $(n = 25)$		
RT-associated	Mamma (n = 111) Thorax (n = 5) Abdomen (n = 3) Scalp (n = 2) Arm (n = 2) Peri-anal (n = 1) Bladder (n = 1) Shoulder (n = 1)	Mamma (n = 13)		
UV associated	Scalp $(n = 27)$ Face $(n = 10)$ Neck $(n = 1)$	Scalp $(n = 5)$ Face $(n = 1)$ Neck $(n = 1)$		
Stewart Treves	Arm $(n = 11)$ Leg $(n = 2)$ Mamma $(n = 1)$	Arm $(n=4)$ Mamma $(n=1)$		

Median cells/mm² (Interquartile Range)	Primary AS (n = 79)	Secondary AS (n = 178)	p-Value
CD3+ T-cells	245 (342)	456 (758)	p < 0.001
CD8+ T-cells	84 (129)	111 (217)	p=0.033
FoxP3+T-cells	22 (32)	43(95)	p < 0.001
CD4+ T-cells	127 (145)	247 (470)	p < 0.001
CD20+ B-cells	22 (73)	32 (121)	p=0.417

Table 3. Immune densities for all AS subgroups. Cell densities are reflected in cells/mm² with the IQR for all individual immune cell subclasses.

	Primary AS (<i>n</i> = 79)				Secondary AS (n = 178)			
Angiosarcoma Subgroup	Soft Tissue n = 11	Breast n=20	Skin Not UV n=15	Visceral n = 28	Heart n=5	RT- Associated n=126	UV Associated n=38	Stewart Treves n=14
Median Cells/mm² (IQR)								
CD3+ T-cells	245 (549)	234 (246)	232 (280)	362 (440)	110 (204)	355 (605)	817 (862)	588 (734)
CD8+ T-cells	99 (406)	78 (94)	74 (60)	140 (194)	15 (71)	101 (186)	184 (230)	87 (209)
FoxP3+T-cells	28 (63)	14 (35)	32 (50)	14 (25)	7 (27)	32 (60)	92 (161)	23 (35)
CD4+ T-cells	94 (137)	127 (118)	145 (143)	150 (246)	88 (107)	190 (355)	461 (460)	457 (608)
CD20+ B-cells	26 (82)	22 (38)	15 (11)	67 (139)	12 (34)	21 (98)	44 (145)	88 (130)

Genomic landscape

Genomic analysis was performed on tumor DNA from a subgroup of 50 patients (25 pAS and 25 sAS). Median TMB was 3.2 mut/Mb (range 0.8–11.9) in pAS vs. 3.9 mut/Mb (range 0.0–99.6) in sAS (p = 0.572). Figure 2 shows the median TMB per subgroup. TMB High (TMB-H; \geq 10 mut/Mb) was found in 6 tumors (12%) divided over three subgroups, i.e., UV-AS (n = 3/7; median TMB 9.4 mut/Mb), visceral AS (n = 2/7; median TMB 3.2 mut/Mb) and primary skin AS (n = 1/4; median TMB 5.6 mut/Mb). Visceral AS with TMB-H were located in the adrenal gland and liver. None of the 50 tumors showed MSI.

Mutational signature analysis was performed for tumors with TMB-H (Figure S1). Single-base substitution signatures 7a (SBS7a) and SBS7b, associated with UV damage

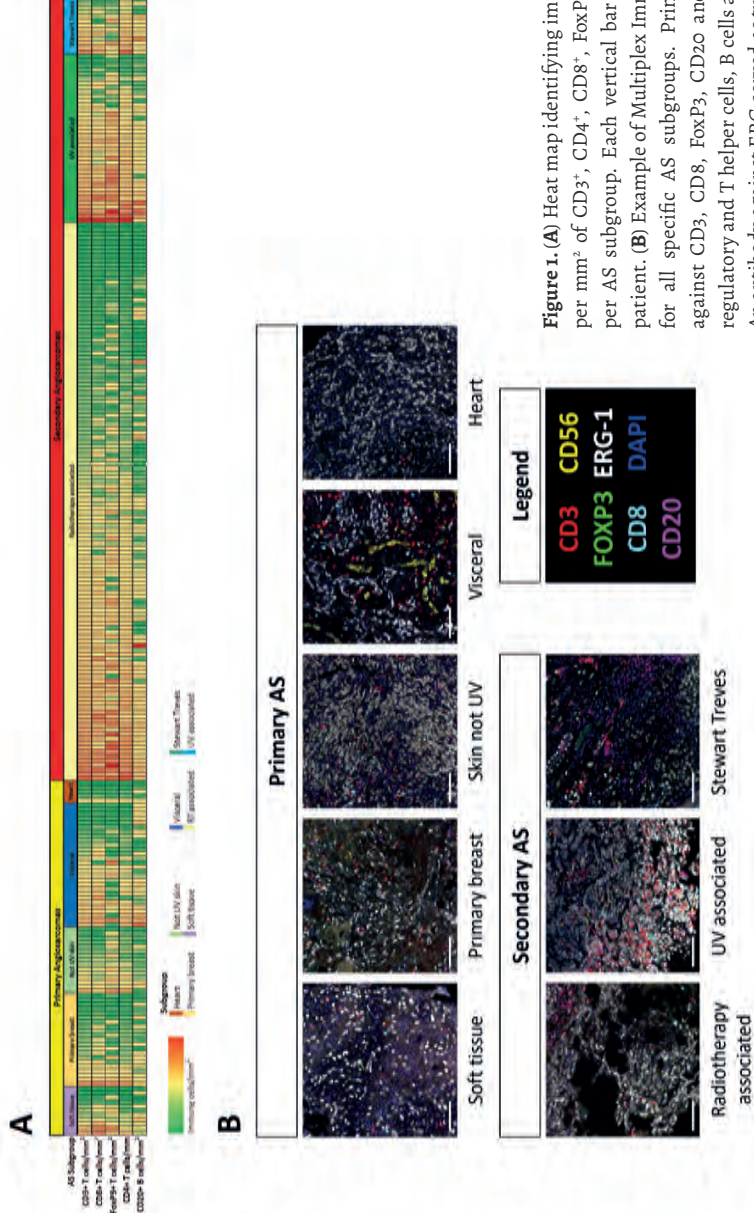


Figure 1. (A) Heat map identifying immune cell infiltrate densities per mm² of CD3⁺, CD4⁺, CD8⁺, FoxP3⁺ T cells and CD2o⁺ B-cells per AS subgroup. Each vertical bar representing an individual patient. (B) Example of Multiplex Immunohistochemistry images for all specific AS subgroups. Primary antibodies were used against CD3, CD8, FoxP3, CD2o and CD56 to detect cytotoxic, regulatory and T helper cells, B cells and Natural Killer (NK) cells. An antibody against ERG served as tumor marker.

were detected in three tumors, all UV-AS. In one visceral AS an SBS1 signature was detected, associated with endogenous mutational processes initiated by deamination of 5-methylcytosine to thymine and generated over time. No clear mutational signature was found in the patient classified as a not UV associated skin AS.

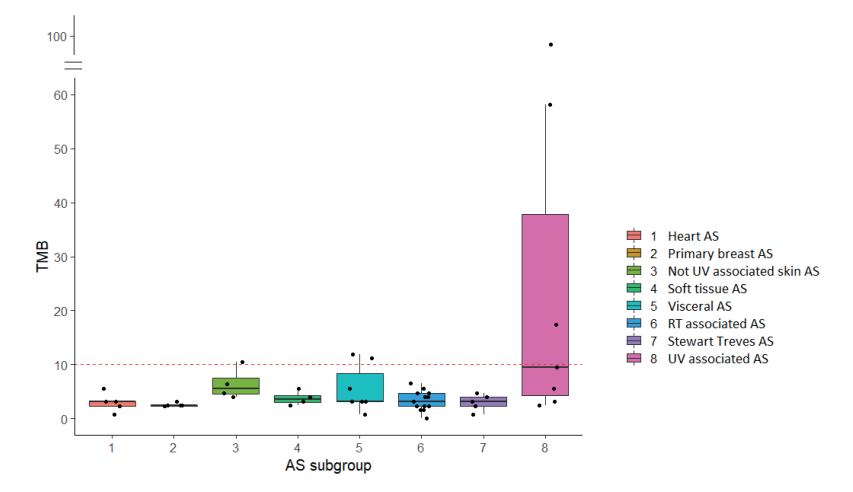


Figure 2. Median TMB per AS subgroup. High TMB (≥10 mut/Mb) was detected in 6 tumors (12%) in three subgroups: 3 UV associated AS, 2 Visceral AS and 1 not UV associated skin AS.

A (likely) pathogenic mutation or gene amplification was identified in 80% of pAS vs. 100% of sAS (p = 0.110). Figure 3 depicts the genetic alterations that occurred within more than one tumor sample.

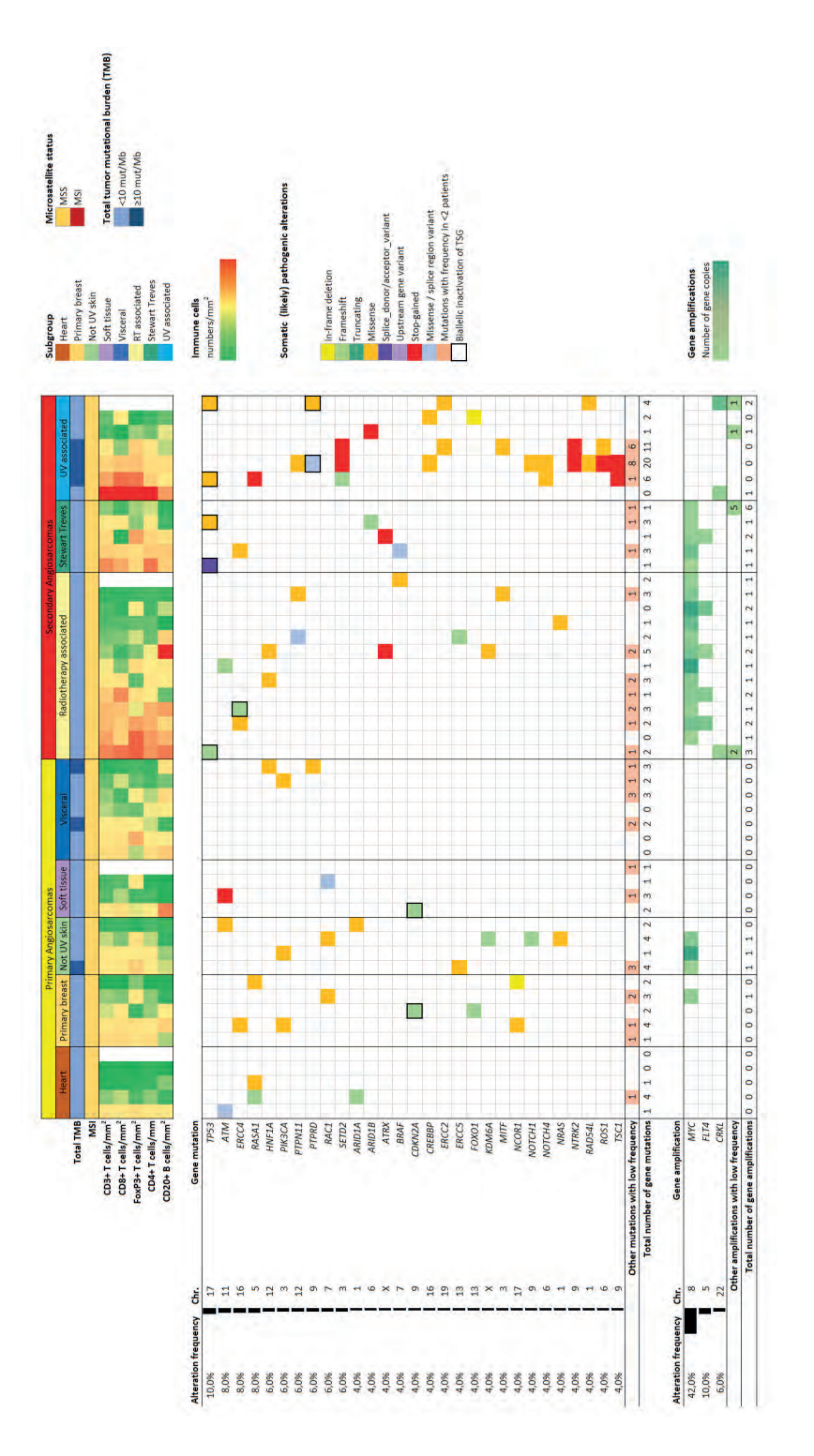


Figure 3. Genomic and immunological landscape of 50 angiosarcoma tumor samples. (Likely) Pathogenic mutations and gene amplifications detected in \geq 2 tumors are reflected in this figure. Cell densities for CD3+, CD8+, FoxP3+, CD4+T cells and CD20+B cells are reflected based on the number of cells/mm2-

Figure S2 provides a full overview of all (likely) pathogenic alterations (class 4/5). At least one (likely) pathogenic mutation was detected in 80% of the pAS vs. 88% of the sAS, (p = 0.702). The most frequently mutated gene was TP53, exclusively identified in sAS (20%, (p = 0.025)). Biallelic inactivation of the Tumor Suppressor Gene (TSG) was seen in all TP53 mutated cases. Other frequently found mutated genes were ERCC4 (8%), ATM (8%), RASA1 (8%), HNF1A (6%), PIK3CA (6%), PTPN11 (6%), RAC1 (6%) and SETD2 (6%). SETD2 mutations were discovered in 43% of UV-AS, but in no other AS subtype. Mutations in the DNA damage response (DDR) pathway were encountered in 24% of pAS vs. 60% of sAS (p = 0.021), with affection of the following genes: ATM, ATRX, BRIP1, CHEK2, ERCC2, ERCC3, ERCC4, ERCC5, FANCF, FANCI, MSH2, MSH3, TP53 and XRCC2. DDR mutations were found in 54% of RT-AS, 57% of UV-AS and 80% of Stewart Treves AS.

Amplifications were detected in 16% of pAS vs. 84% of sAS ($p \le 0.01$). MYC amplifications being the most frequent, were found in 16% of pAS vs. 68% of sAS ($p \le 0.01$) with 100% of the Stewart Treves AS, 92% of the RT-AS, 75% of the not UV associated skin AS and 20% of the primary breast AS. MYC amplifications were not discovered in any of the pAS located in the heart, soft tissue or visceral organs nor in UV-AS. FLT4 was amplified only in sAS (20%, p = 0.025)) and were seen in 31% of RT-AS, always in combination with a MYC amplification. CRKL amplifications were present in 12% of sAS (8% of RT-AS and 14% UV-AS) and none of the pAS.

Figure S3 shows all identified mutations that are classified as variant of unknown significance (class 3). In all tumor samples at least one class 3 mutation was found. Mutations in MAGI2 (20%), ZFHX3 (20%), TET1 (18%), FAT1(16%), FLT4 (16%), ICOSLG (16%) and LRP1B (16%) were most often present.

Combined Immunological and Genomic Profiles

Combined immunological and genomic data were available for 47 tumor samples (Figure 3). These samples showed similar lymphocyte cell densities compared to the entire cohort. Tumors with a DDR mutation (n = 21, 42%) had significantly higher cell densities for all lymphocyte subsets compared to AS without a DDR mutation including CD3+ (p = 0.004), CD8+ (p = 0.025), FoxP3+ (p = 0.010) and CD4+ (p = 0.004) T-cells and CD20+ B-cells (p = 0.031). Cell densities for all TILs were comparable in AS with and without MYC amplification.

Immunological and genomic data were analyzed for AS subgroups. UV-AS show the highest density for all T-cell subsets and the highest median TMB of all AS. TMB-H sAS were exclusively UV-AS. A (likely) pathogenic mutation or amplification was

seen in 86% of the UV-AS. Stewart Treves AS represent the group with the second highest CD₃⁺ and CD₄⁺ T-cell density and the highest CD₂0⁺ B-cell density. A (likely) pathogenic alteration was present in 100% of this subgroup and 80% of the cases had a DDR pathway mutation. Of all pAS, visceral AS showed the highest cell density for all TILs and the highest TMB. A (likely) pathogenic mutation was found in 4 out of 7 (57%) visceral AS. A DDR pathway mutation was identified in one visceral AS (14%). The subgroup with the lowest lymphocyte density were AS of the heart. In 60% (n = 3) of these tumors a (likely) pathogenic mutation was found. A DDR pathway mutation was identified in one of them (20%).

Discussion

In this study we showed the heterogeneity of immunological and genomic profiles in pAS and sAS subgroups. Especially in sAS, the high immune cell density, high TMB and presence of DDR gene mutations suggest possible responsiveness to ICI. Both in pAS and sAS a high frequency of (likely) pathogenic mutations and gene amplifications were identified, with patterns that could potentially be used in boosting strategies to stimulate ICI response.

One of the main findings was a significantly higher T-cell density in sAS compared to pAS. A high T-cell density was in particular found in UV-AS, and Stewart Treves AS and to a lesser extent in RT-AS. T-cell rich TME, especially by means of CD8+ T-cells, has been reported as a favorable prognostic factor with regards to survival outcomes in other high grade sarcomas. (33) High CD8+ T-cell density has also been correlated with improved ORR to ICI in several sarcoma subtypes including AS. (18) Interestingly, cell densities of FoxP3+ T-cells, known for their possible immunosuppressive role within the TME, were also significantly higher in sAS compared to pAS in our study. No difference was found in B-cell infiltration between pAS and sAS. This could be explained by the relatively high B-cell density in visceral AS. With its high density of T- and B-cells, visceral AS seem to represent a specific subgroup with an immunological profile that could render them more susceptible to immunotherapy compared to other pAS.

TMB-H was present in six tumors (12%), including three UV-AS (50%), two visceral AS (33%) and one not UV associated skin AS (17%). This is in line with earlier studies showing TMB-H in especially UV-AS. (16, 25, 26, 34) Espejo-Freire reported TMB-H in 26% of AS (total n=143), predominantly of the Head and Neck (H/N) (63%). (26) One could argue that at least a subset of their cases are UV associated as expected for

this anatomic area. Visceral AS showed the second highest TMB of our AS subgroups. This finding is also underpinned by the results of Espejo-Freire et al showing TMB-H in 14% of visceral AS. Their and our data support the hypothesis that UV-associated and visceral AS may in particular benefit from ICI treatment.

The distinction between UV-AS and non-UV associated AS of the skin is based on tumor location. Interestingly, our TMB-H UV-AS showed mutational signatures with a clear pattern associated with UV damage. (30, 35) In contrast, no UV associated signature was found in the skin not-UV associated tumor with TMB-H. In half of the tumors classified as UV-AS, no TMB-H was detected. Although only a small number of AS had sufficient mutations to perform mutational signature analysis, these signatures support the clinical relevance of defining pAS and sAS in the skin. Interestingly, Chan et al. also identified more mutated and UV driven profiles in approximately half the H/N AS (n=35). The others showed more mutationally quiet tumors with low TMB. (34) Weidema et al demonstrated two distinct clusters within 11 UV-AS, using DNA methylation profiling. (36) The use of mutational signatures has also been described in the literature as a potential biomarker for response to ICI. (37) Subsequent research needs to assess the possible prognostic or predictive role of mutational signatures in AS.

In our study (likely) pathogenic mutations were identified in up to 84% of the tested tumors. Many of these mutations are druggable targets, e.g. BRAF, CHEK2, PIK3CA, NRAS, EGFR, ATM, CDKN2A and RAD54L mutations.

PIK3CA mutations were present in three pAS (breast, skin, visceral) (6% of tumors). The same frequency has been reported by Espejo-Freire et al and Rosenbaum et al, while Painter et al. demonstrated with 21% a more frequent occurrence. (16, 25, 26) Interestingly, all tumors harboring a PIK3CA mutation in these studies were also pAS and almost exclusively located in the breast.

The DDR pathway is known to induce genomic instability and tumor evolution. DDR inhibition has shown to increase TMB and upregulate PD-L1 expression. (38, 39) It also affects interaction between cancer cells and the host immune system and is associated with an activated immune microenvironment. (40) We found DDR gene mutations in 24% of pAS and 60% of sAS. Tumors with a DDR mutation had significantly higher cell densities for all lymphocyte subsets compared to AS without a DDR mutation. Teo et al showed the association between DDR alterations and ICI treatment response in urothelial cell carcinoma patients. (41) Several clinical trials are currently investigating combination treatment with ICI and DDR targeted therapy drugs such as PARP, CDK4/6, ATR and WEE1-inhibitors. (42)

MYC amplifications provide another interesting opportunity for boosting ICI response. (43) MYC proteins are associated with tumorigenesis and therapeutic resistance through gene amplification, translocation and mRNA upregulation. They are known to remodulate the tumor microenvironment, creating resistance to ICI. (43) Han et al showed that MYC inhibition upregulated PD-L1 expression on tumor cells and increased the number of CD3+, CD4+, and CD8+ T-cells, thereby sensitizing otherwise refractory tumors for ICI treatment. (43) Several studies have shown that combination therapy with an anti PD-1 agent and a drug inhibiting the MYC pathway could be an interesting strategy to boost ICI response. The CDK7 inhibitor THZ1 in combination with ICI showed promising results in treatment for non-small cell lung cancer. (44) THZ1 inhibits MYC transcriptional activity through downregulating the p38α pathway. In our study, MYC was amplified in 68% of sAS. MYC amplifications were not exclusively present in RT-AS, but also in other AS subgroups. Interestingly, none of the UV-AS showed a MYC amplification, which is in concordance with previously reported studies (25, 26). For all MYC amplified pAS and sAS, therapeutic strategies based on MYC inhibition warrant further investigation.

PD-L1 status has been investigated before in AS subtypes. High PD-L1 and PD-1 expression were predominantly shown in UV-associated, visceral, and soft tissue AS. RT-AS showed predominantly high PD-L1 expression. (45) The value of PD-L1 and PD-1 expression as predictive biomarker of response to immunotherapy is limited as has been discussed extensively before. (46)

Although ICI treatment is currently not registered for AS, several clinical trials are being conducted to evaluate their efficacy in AS patients. Table 4 depicts the main ongoing clinical trials that include AS patients. Where NCTo5026736 includes both pAS and sAS for treatment with sintilimab, NCT04873375 inclusion is limited to sAS for treatment with cemiplimab. Other trials are evaluating combination treatments with ICI and targeted therapy or chemotherapy.

Our study has some limitations. Angiosarcomas are considered a heterogeneous disease, for which multiple classifications exist. The WHO classification does not define pAS and sAS, nor clinical subgroups. (47) Clinical subgroups have been defined in various ways previously, with pAS and sAS used most based on tumor etiology. (8, 25, 26, 45) We used the same classification as we did before. (8) For a rare and heterogenous disease, subgroups do matter. For example, T-cell densities were high in the visceral group but not in the heart subgroup. Taken together (supplementary 4) this difference is not recognized. In clinics, heart AS represent an AS subtype with an aggressive behavior and less treatment opportunities.

Specific clinical subgroups harbor only small numbers of patients, limiting our ability to draw definite conclusions. Second, for analyzing the TME of this large set of tumor samples, we used TMAs generated from tumor cores. Tumor cores may only represent a specific area within a heterogeneous tumor but were expected to better predict responsiveness to ICI than superficial infiltration within the edges of a tumor, especially since the detection of a tumor border in typically infiltrative growing AS is difficult. Furthermore, our data provide an insight in the TME of AS, but a clear cutoff value for using specific TILS as a (predictive) biomarker has not been established, complicating its use in clinical practice. Finally, one could remark that the TSO500 panel is a targeted NGS assay that does not comprise all genes. It does however include the vast majority of druggable cancer related genes, providing a clear overview for potential treatment options.

Conclusions

We showed a clear distinction in immunological and genomic profiles between pAS and sAS, with a T-cell infiltrated TME and frequent DDR gene mutations especially in sAS. Given the heterogeneity of angiosarcomas and the observed differences even between sAS subsets, clinical trials are needed to investigate the potential of immunotherapy.

Table 4. Main ongoing clinical trials evaluating ICI in Angiosarcoma patients.

Study NCT Registry Number	Agent	Study Population	Phase	Recruitment Status
NCT03277924	Nivolumab + Sunitinib	Soft tissue and bone sarcomas	I/II	Active, recruiting
NCT03138161	Nivolumab + Ipilimumab + Trabectidin	Soft tissue sarcomas (including angiosarcomas)	I/II	Active, recruiting
NCT04873375	Cemiplimab	Secondary Angiosarcomas	II	Active, recruiting
NCT05026736	Sintilimab	Angiosarcomas	II	Active, recruiting
NCT04784247	Pembrolizumab + Lenvatinib	Soft tissue and bone sarcomas (including angiosarcomas)	II	Active, recruiting
NCT03512834	Avelumab + Paclitaxel	Angiosarcomas	II	Active, recruiting
NCT04339738	Nivolumab + paclitaxel; Nivolumab + cabozantinib	Skin and visceral angiosarcoma	II	Active, recruiting
NCT04551430	Nivolumab + Ipilimumab + Cabozantinib	Soft tissue sarcomas (including angiosarcomas)	II	Active, recruiting
NCT03069378	Pembrolizumab + Talimogene Laherparepvec (T-VEC)	Soft tissue sarcomas (including cutaneous angiosarcomas)	II	Active, recruiting
NCT04668300	Durvalumab + Oleclumab	Soft tissue sarcomas (including angiosarcomas)	II	Active, recruiting
NCT04095208	Nivolumab + Relatlimab	Soft tissue sarcomas (including angiosarcomas)	II	Active, recruiting
NCT04741438	Nivolumab + Ipilimumab	Soft tissue sarcomas (including angiosarcomas)	III	Active, recruiting
NCT02834013	Nivolumab + Ipilimumab	Rare tumors (including angiosarcomas)	III	Active, recruiting
NCT02815995	Durvalumab + Temelimumab	Soft tissue and bone sarcomas (including angiosarcomas)	II	Active, not recruiting

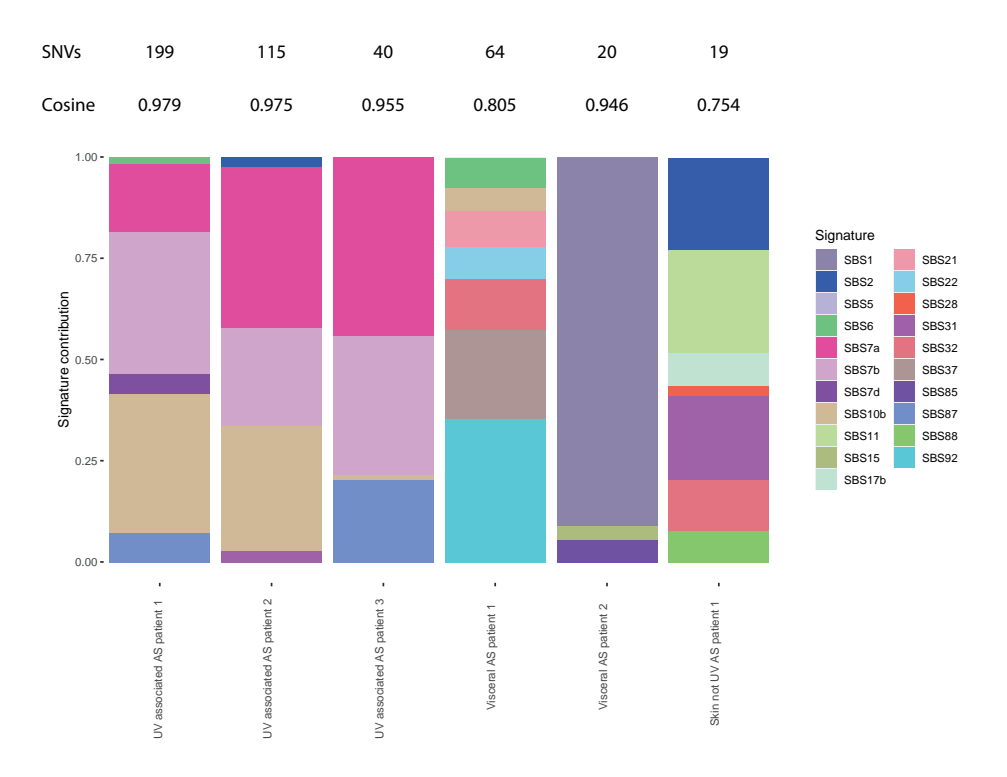
References

- 1. Young RJ, Brown NJ, Reed MW, Hughes D, Woll PJ. Angiosarcoma. Lancet Oncol. 2010;11(10):983-91.
- 2. Fayette J, Martin E, Piperno-Neumann S, Le Cesne A, Robert C, Bonvalot S, et al. Angiosarcomas, a heterogeneous group of sarcomas with specific behavior depending on primary site: a retrospective study of 161 cases. Ann Oncol. 2007;18(12):2030-6.
- Berebichez-Fridman R, Deutsch YE, Joyal TM, Olvera PM, Benedetto PW, Rosenberg AE, Kett DH. Stewart-Treves Syndrome: A Case Report and Review of the Literature. Case Rep Oncol. 2016;9(1):205-11.
- van der Graaf WT, Blay JY, Chawla SP, Kim DW, Bui-Nguyen B, Casali PG, et al. Pazopanib for metastatic soft-tissue sarcoma (PALETTE): a randomised, double-blind, placebo-controlled phase 3 trial. Lancet. 2012;379(9829):1879-86.
- Kollar A, Jones RL, Stacchiotti S, Gelderblom H, Guida M, Grignani G, et al. Pazopanib in advanced vascular sarcomas: an EORTC Soft Tissue and Bone Sarcoma Group (STBSG) retrospective analysis. Acta Oncol. 2017;56(1):88-92.
- Florou V, Wilky BA. Current and Future Directions for Angiosarcoma Therapy. Curr Treat Options Oncol. 2018;19(3):14.
- Lahat G, Dhuka AR, Hallevi H, Xiao L, Zou C, Smith KD, et al. Angiosarcoma: clinical and molecular insights. Ann Surg. 2010;251(6):1098-106.
- 8. Weidema ME, Flucke UE, van der Graaf WTA, Ho VKY, Hillebrandt-Roeffen MHS, Dutch Nationwide N, et al. Prognostic Factors in a Large Nationwide Cohort of Histologically Confirmed Primary and Secondary Angiosarcomas. Cancers (Basel). 2019;11(11).
- Andre T, Shiu KK, Kim TW, Jensen BV, Jensen LH, Punt C, et al. Pembrolizumab in Microsatellite-Instability-High Advanced Colorectal Cancer. N Engl J Med. 2020;383(23):2207-18.
- Postow MA, Chesney J, Pavlick AC, Robert C, Grossmann K, McDermott D, et al. Nivolumab and ipilimumab versus ipilimumab in untreated melanoma. N Engl J Med. 2015;372(21):2006-17.
- 11. Tawbi HA, Burgess M, Bolejack V, Van Tine BA, Schuetze SM, Hu J, et al. Pembrolizumab in advanced soft-tissue sarcoma and bone sarcoma (SARC028): a multicentre, two-cohort, single-arm, open-label, phase 2 trial. Lancet Oncol. 2017;18(11):1493-501.
- 12. Zhu MMT, Shenasa E, Nielsen TO. Sarcomas: Immune biomarker expression and checkpoint inhibitor trials. Cancer Treat Rev. 2020;91:102115.
- Florou V, Rosenberg AE, Wieder E, Komanduri KV, Kolonias D, Uduman M, et al. Angiosarcoma patients treated with immune checkpoint inhibitors: a case series of seven patients from a single institution. J Immunother Cancer. 2019;7(1):213.
- 14. Momen S, Fassihi H, Davies HR, Nikolaou C, Degasperi A, Stefanato CM, et al. Dramatic response of metastatic cutaneous angiosarcoma to an immune checkpoint inhibitor in a patient with xeroderma pigmentosum: whole-genome sequencing aids treatment decision in end-stage disease. Cold Spring Harb Mol Case Stud. 2019;5(5).
- 15. Sindhu S, Gimber LH, Cranmer L, McBride A, Kraft AS. Angiosarcoma treated successfully with anti-PD-1 therapy a case report. J Immunother Cancer. 2017;5(1):58.
- 16. Rosenbaum E, Antonescu CR, Smith S, Bradic M, Kashani D, Richards AL, et al. Clinical, genomic, and transcriptomic correlates of response to immune checkpoint blockade-based therapy in a cohort of patients with angiosarcoma treated at a single center. J Immunother Cancer. 2022;10(4).

- 17. Hamacher R, Kampfe D, Reuter-Jessen K, Pottgen C, Podleska LE, Farzaliyev F, et al. Dramatic Response of a PD-L1-Positive Advanced Angiosarcoma of the Scalp to Pembrolizumab. JCO Precis Oncol. 2018;2:1-7.
- D'Angelo SP, Richards AL, Conley AP, Woo HJ, Dickson MA, Gounder M, et al. Pilot study of bempegaldesleukin in combination with nivolumab in patients with metastatic sarcoma. Nat Commun. 2022;13(1):3477.
- Davis AA, Patel VG. The role of PD-L1 expression as a predictive biomarker: an analysis of all US Food and Drug Administration (FDA) approvals of immune checkpoint inhibitors. J Immunother Cancer. 2019;7(1):278.
- Lu S, Stein JE, Rimm DL, Wang DW, Bell JM, Johnson DB, et al. Comparison of Biomarker Modalities for Predicting Response to PD-1/PD-L1 Checkpoint Blockade: A Systematic Review and Meta-analysis. JAMA Oncol. 2019;5(8):1195-204.
- Samstein RM, Lee CH, Shoushtari AN, Hellmann MD, Shen R, Janjigian YY, et al. Tumor mutational load predicts survival after immunotherapy across multiple cancer types. Nat Genet. 2019:51(2):202-6.
- 22. Taube JM. Unleashing the immune system: PD-1 and PD-Ls in the pre-treatment tumor microenvironment and correlation with response to PD-1/PD-L1 blockade. Oncoimmunology. 2014;3(11):e963413.
- 23. Petitprez F, de Reynies A, Keung EZ, Chen TW, Sun CM, Calderaro J, et al. B cells are associated with survival and immunotherapy response in sarcoma. Nature. 2020;577(7791):556-60.
- 24. Vikas P, Borcherding N, Chennamadhavuni A, Garje R. Therapeutic Potential of Combining PARP Inhibitor and Immunotherapy in Solid Tumors. Front Oncol. 2020;10:570.
- 25. Painter CA, Jain E, Tomson BN, Dunphy M, Stoddard RE, Thomas BS, et al. The Angiosarcoma Project: enabling genomic and clinical discoveries in a rare cancer through patient-partnered research. Nat Med. 2020;26(2):181-7.
- Espejo-Freire AP, Elliott A, Rosenberg A, Costa PA, Barreto-Coelho P, Jonczak E, et al. Genomic Landscape of Angiosarcoma: A Targeted and Immunotherapy Biomarker Analysis. Cancers (Basel). 2021;13(19).
- Gorris MAJ, Halilovic A, Rabold K, van Duffelen A, Wickramasinghe IN, Verweij D, et al. Eight-Color Multiplex Immunohistochemistry for Simultaneous Detection of Multiple Immune Checkpoint Molecules within the Tumor Microenvironment. J Immunol. 2018;200(1):347-54.
- 28. Gorris MAJ, van der Woude LL, Kroeze LI, Bol K, Verrijp K, Amir AL, et al. Paired primary and metastatic lesions of patients with ipilimumab-treated melanoma: high variation in lymphocyte infiltration and HLA-ABC expression whereas tumor mutational load is similar and correlates with clinical outcome. Journal for ImmunoTherapy of Cancer. 2022;10(5):e004329.
- 29. Sultan S, Gorris MAJ, van der Woude LL, Buytenhuijs F, Martynova E, van Wilpe S, et al. A Segmentation-Free Machine Learning Architecture for Immune Land-scape Phenotyping in Solid Tumors by Multichannel Imaging. bioRxiv. 2021;2021.10.22.464548.
- 30. Kroeze LI, de Voer RM, Kamping EJ, von Rhein D, Jansen EAM, Hermsen MJW, et al. Evaluation of a Hybrid Capture-Based Pan-Cancer Panel for Analysis of Treatment Stratifying Oncogenic Aberrations and Processes. J Mol Diagn. 2020;22(6):757-69.
- de Bitter TJJ, Kroeze LI, de Reuver PR, van Vliet S, Vink-Borger E, von Rhein D, et al. Unraveling Neuroendocrine Gallbladder Cancer: Comprehensive Clinicopathologic and Molecular Characterization. JCO Precis Oncol. 2021;5.

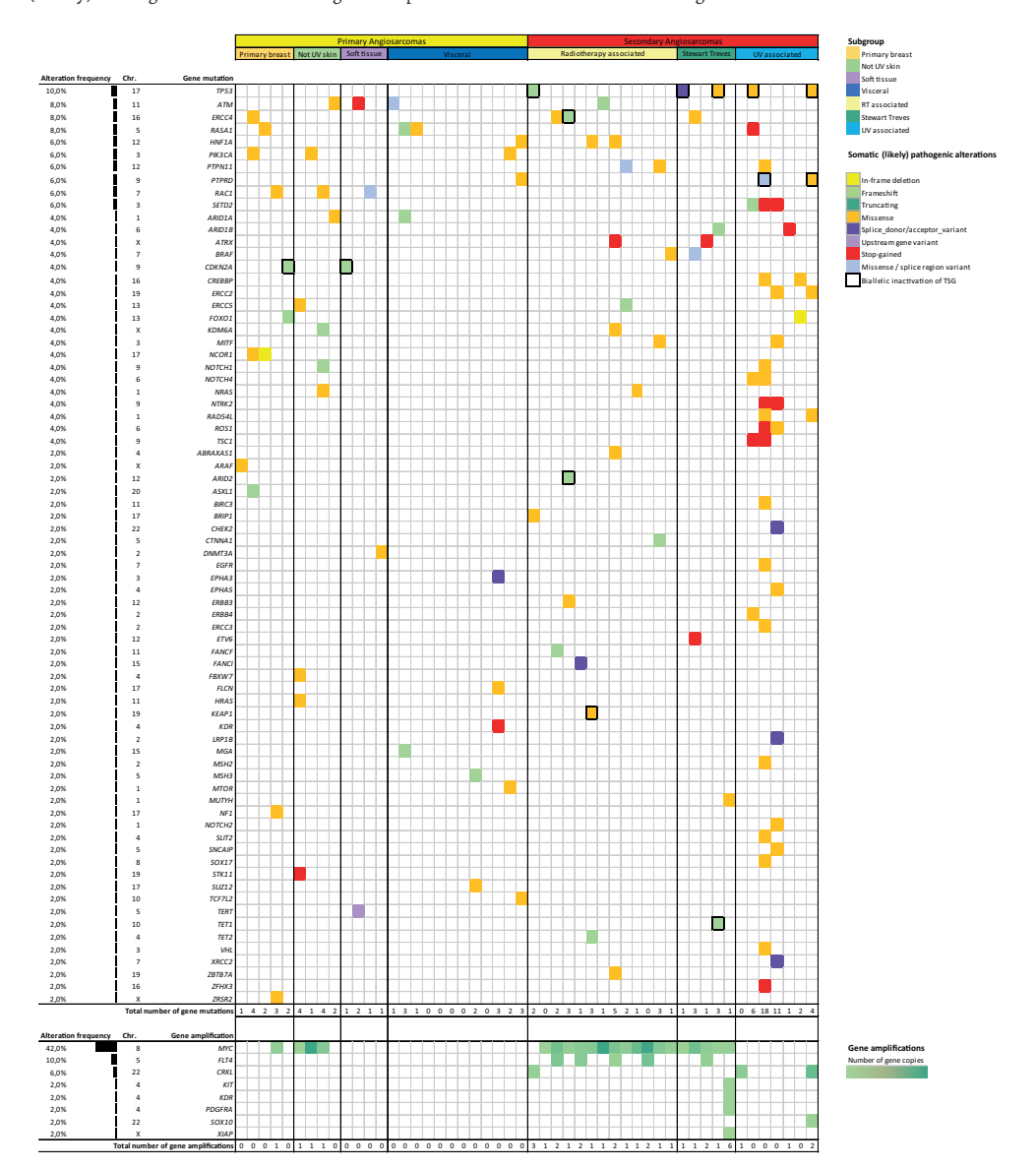
- 32. Tate JG, Bamford S, Jubb HC, Sondka Z, Beare DM, Bindal N, et al. COSMIC: the Catalogue Of Somatic Mutations In Cancer. Nucleic Acids Res. 2019;47(D1):D941-D7.
- 33. Boxberg M, Steiger K, Lenze U, Rechl H, von Eisenhart-Rothe R, Wortler K, et al. PD-L1 and PD-1 and characterization of tumor-infiltrating lymphocytes in high grade sarcomas of soft tissue prognostic implications and rationale for immunotherapy. Oncoimmunology. 2018;7(3):e1389366.
- 34. Chan JY, Lim JQ, Yeong J, Ravi V, Guan P, Boot A, et al. Multiomic analysis and immunoprofiling reveal distinct subtypes of human angiosarcoma. J Clin Invest. 2020;130(11):5833-46.
- Alexandrov LB, Kim J, Haradhvala NJ, Huang MN, Tian Ng AW, Wu Y, et al. The repertoire of mutational signatures in human cancer. Nature. 2020;578(7793):94-101.
- 36. Weidema ME, van de Geer E, Koelsche C, Desar IME, Kemmeren P, Hillebrandt-Roeffen MHS, et al. DNA Methylation Profiling Identifies Distinct Clusters in Angiosarcomas. Clin Cancer Res. 2020;26(1):93-100.
- Wang S, Jia M, He Z, Liu XS. APOBEC3B and APOBEC mutational signature as potential predictive markers for immunotherapy response in non-small cell lung cancer. Oncogene. 2018;37(29):3924-36.
- 38. Brown JS, Sundar R, Lopez J. Combining DNA damaging therapeutics with immunotherapy: more haste, less speed. Br J Cancer. 2018;118(3):312-24.
- Conway JR, Kofman E, Mo SS, Elmarakeby H, Van Allen E. Genomics of response to immune checkpoint therapies for cancer: implications for precision medicine. Genome Med. 2018;10(1):93.
- 40. Sun W, Zhang Q, Wang R, Li Y, Sun Y, Yang L. Targeting DNA Damage Repair for Immune Checkpoint Inhibition: Mechanisms and Potential Clinical Applications. Front Oncol. 2021;11:648687.
- 41. Teo MY, Seier K, Ostrovnaya I, Regazzi AM, Kania BE, Moran MM, et al. Alterations in DNA Damage Response and Repair Genes as Potential Marker of Clinical Benefit From PD-1/PD-L1 Blockade in Advanced Urothelial Cancers. J Clin Oncol. 2018;36(17):1685-94.
- 42. Peyraud F, Italiano A. Combined PARP Inhibition and Immune Checkpoint Therapy in Solid Tumors. Cancers (Basel). 2020;12(6).
- 43. Han H, Jain AD, Truica MI, Izquierdo-Ferrer J, Anker JF, Lysy B, et al. Small-Molecule MYC Inhibitors Suppress Tumor Growth and Enhance Immunotherapy. Cancer Cell. 2019;36(5):483-97 e15.
- 44. Wang J, Zhang R, Lin Z, Zhang S, Chen Y, Tang J, et al. CDK7 inhibitor THZ1 enhances antiPD-1 therapy efficacy via the p38alpha/MYC/PD-L1 signaling in non-small cell lung cancer. J Hematol Oncol. 2020;13(1):99.
- 45. Tomassen T, Weidema ME, Hillebrandt-Roeffen MHS, van der Horst C, group* P, Desar IME, et al. Analysis of PD-1, PD-L1, and T-cell infiltration in angiosarcoma pathogenetic subgroups. Immunol Res. 2022;70(2):256-68.
- 46. Gibney GT, Weiner LM, Atkins MB. Predictive biomarkers for checkpoint inhibitor-based immunotherapy. Lancet Oncol. 2016;17(12):e542-e51.
- 47. eds WCoTEB. World Health Organization classification of soft tissue and bone tumours. Lyon: IARC Press; 2020.

Supplementary 1: Overview mutational signatures High-TMB

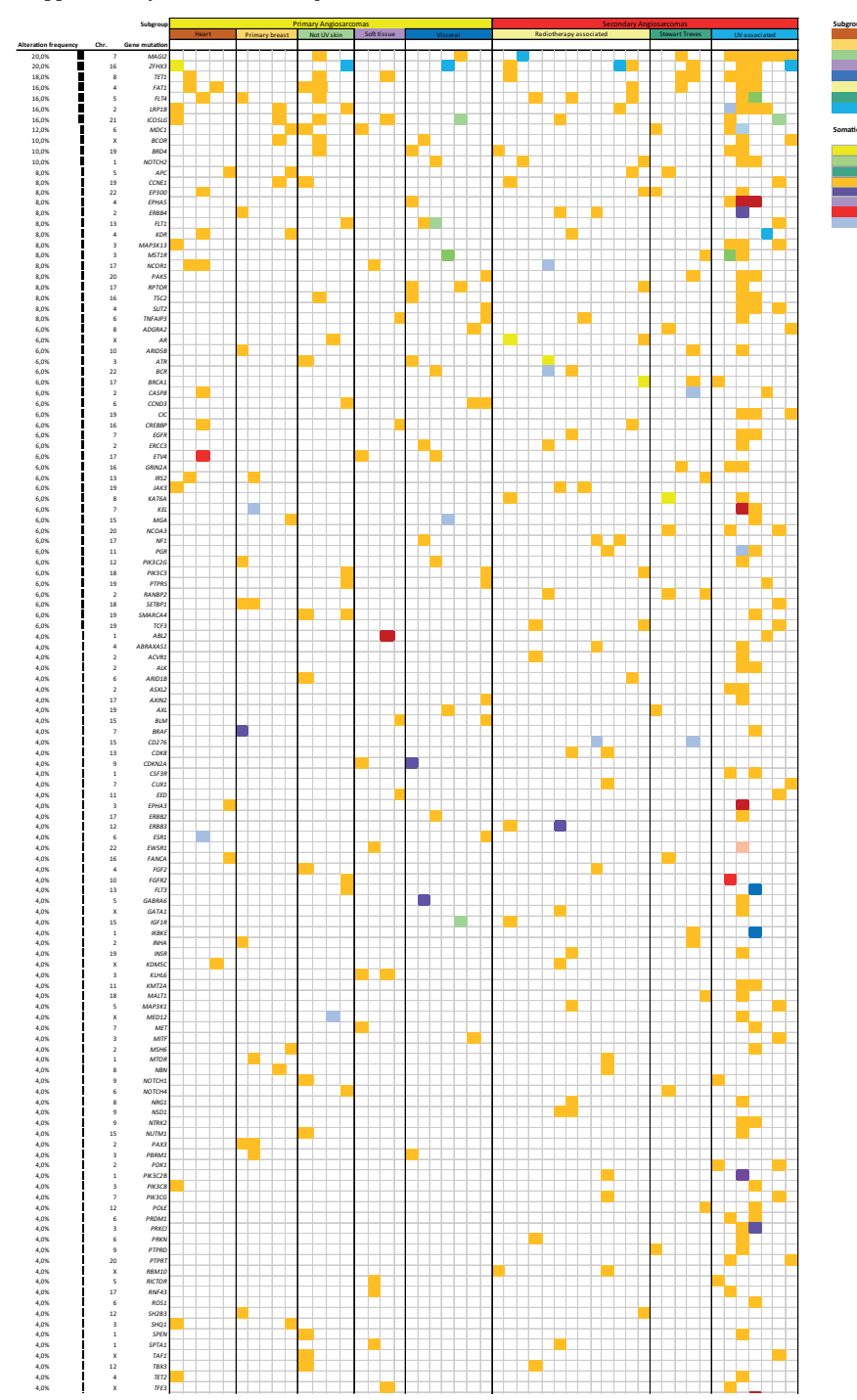


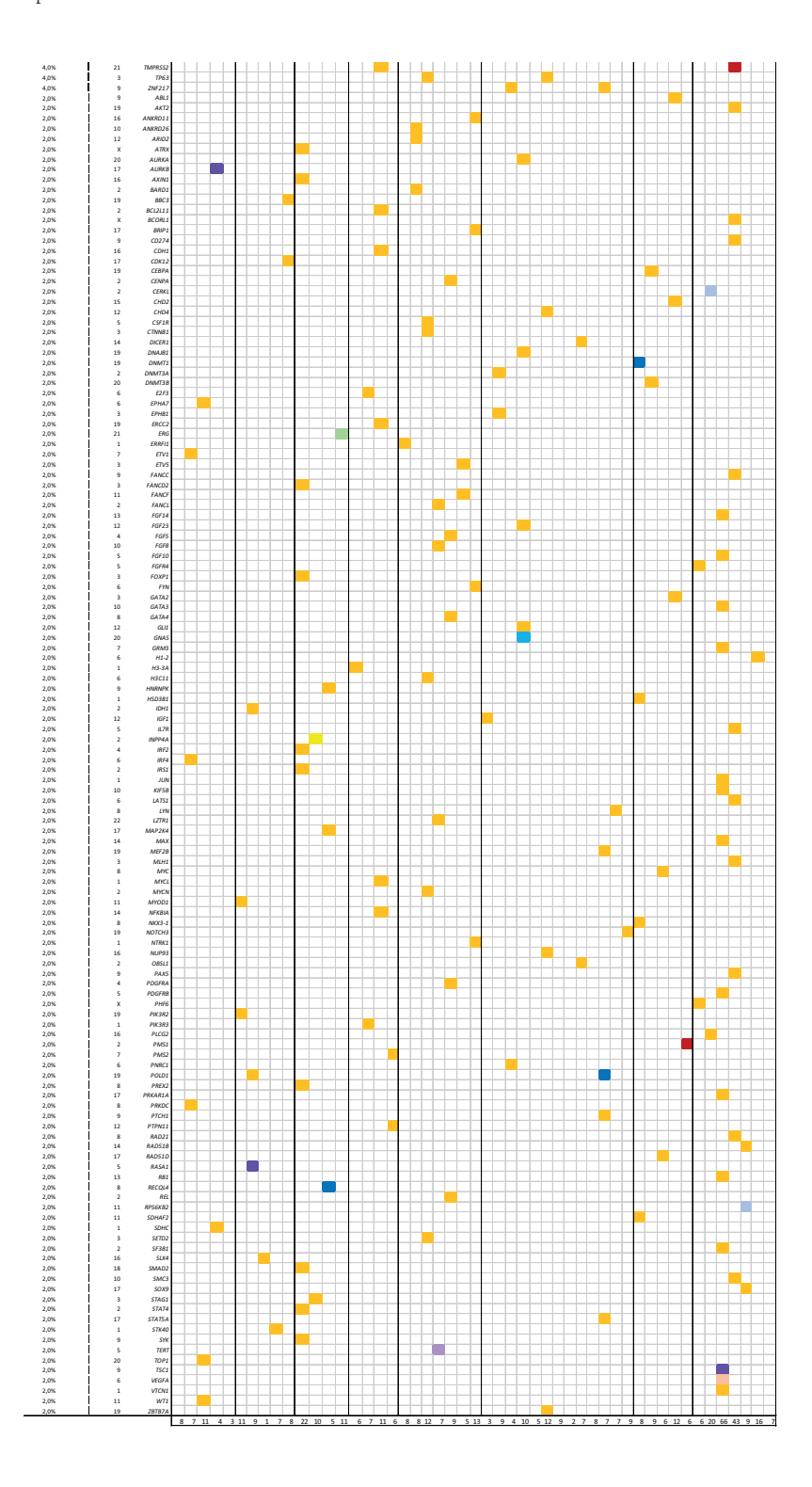
Supplementary figure 1: Mutational signatures in patients classified as high TMB (>10 mut/Mb). Signature recognition was measured using cosine similarity. SNV; Single Nucleotide Variation.

Supplementary 2: Genomic and immunological landscape of 50 angiosarcoma tumor samples. All (Likely) Pathogenic mutations and gene amplifications are reflected in this figure



Supplementary 3: Overview of all possible mutations





Supplementary 4:

Immune cell densities for AS subgroups. Cell densities are reflected in cells/mm² with the IQR for all individual immune cell subclasses. This table reflects the combined data of the visceral and hearts AS subgroup taken together in one subgroup (visceral).

Primary AS (n=	79)				Secondary AS	(n=178)	
Angiosarcoma Subgroup	Soft tissue n=11	Breast n=20	Skin not UV n=15	Visceral n=33	RT associated n=126	UV associated n=38	Stewart Treves n=14
Median cells/m	m² (IQR)						
CD3+ T-cells	245 (549)	234 (246)	232 (280)	336 (450)	355 (605)	817 (862)	588 (734)
CD8+ T-cells	99 (406)	78 (94)	74 (60)	109 (203)	101 (186)	184 (230)	87 (209)
FoxP3+ T-cells	28 (63)	14 (35)	32 (50)	12 (25)	32 (60)	92 (161)	23 (35)
CD4+ T-cells	94 (137)	127 (118)	145 (143)	129(237)	190 (355)	461 (460)	457 (608)
CD20+ B-cells	26 (82)	22 (38)	15 (11)	38 (122)	21 (98)	44 (145)	88 (130)





Chapter 3

MYC amplification in angiosarcoma depends on etiological/clinical subgroups – diagnostic and prognostic value

Stefan G. van Ravensteijn*, Ariane G. Hogeboom-Gimeno*, Ingrid M.E. Desar, Melissa H.S. Hillebrandt-Roeffen, Patricia H.J. van Cleef, Johannes J. Bonenkamp, Uta E. Flucke, Yvonne M.H. Versleijen-Jonkers

^{*} These authors contributed equally to this work

Abstract

Angiosarcomas (AS) are rare and heterogeneous malignant vascular tumors with a dismal prognosis. We undertook a retrospective study of AS cases with the intent of elucidating the prevalence of MYC amplification amongst different etiological/clinical subgroups and identifying MYC's potential as a prognostic biomarker.

Retrospective collection of data and tumor samples from 110 patients diagnosed with AS in the Netherlands was conducted. Histopathological review and investigation of MYC gene amplification and MYC protein overexpression (using fluorescent *in situ* hybridization and immunohistochemistry, respectively) was performed.

MYC amplification was identified in 50.9% of cases and predominantly present in secondary AS (sAS) (especially radiotherapy-associated and Stewart-Treves AS, both 92.9%). Within the primary AS (pAS) subgroup, skin non-UV-associated AS (69.2%) and primary breast AS (29.4%) demonstrated MYC amplification. MYC protein overexpression was observed in 47.7% of all tumors with an overall sensitivity and specificity of 75% and 81% respectively. There was no significant difference in median overall survival (OS) between patients with MYC and non-MYC amplified AS. Patients with AS displaying MYC protein overexpression had significantly shorter OS than those without (p=0.028).

Although MYC amplification is characteristic for secondary radiotherapy-associated and Stewart-Treves AS, it is not exclusive to these groups and can also be found in a subset of pAS. Overall concordance of FISH and IHC is rather poor. Only primary breast AS showed 100% concordance. Therefore MYC expression as surrogate marker should be used with caution. The role of MYC/MYC as a prognostic indicator is undefined, however resulting tailored treatment options could be considered.

Introduction

Angiosarcomas (AS) are a group of rare and highly aggressive mesenchymal malignancies with endothelial differentiation. They represent <1% of sarcomas and may arise in virtually any anatomic location, with the majority being cutaneous (1-3). Peak incidence is in the 7th decade (4). Clinicopathological and molecular diversity is substantial. AS are divided into primary, without known etiology, or secondary subgroups. The latter occur due to DNA damaging factors like ultraviolet (UV) light exposure, radiotherapy or in the setting of chronic lymphedema (Stewart-Treves AS) (5). The overall prognosis is poor with a high rate of tumor-related death. Therapeutic options are limited and are often chemotherapy-based when surgery alone experiences its limitation.

MYC is a proto-oncogene located on chromosome 8q24 that regulates proliferation, metabolism, stem cell renewal and plays a key role in angiogenesis (8,9). It is therefore not surprising that overexpression of the corresponding protein contributes to AS biology (10).

Studies have shown that a high percentage of predominantly post-irradiation AS are characterized by amplified MYC (11, 12). MYC amplification has also been detected in Stewart-Treves AS, although few cases (n=1-4 per study) have been reported so far (12-19). Only a small proportion of primary AS have demonstrated amplification of this gene, including small numbers per clinical/etiological subgroup without distinction between UV-associated and non-UV associated tumors (20, 21).

To this end, we sought to analyze a heterogeneous retrospective cohort (n=110) of AS in order to discern prevalence of MYC gene amplification (using fluorescent *in situ* hybridization) with special interest for clinical/etiological subgroups and concordance with the corresponding protein expression (using immunohistochemistry). We also investigated possible differences in overall survival between MYC amplified versus non-amplified groups to elucidate the potential role of MYC as a prognostic indicator.

Material and methods

Patients

We retrospectively collected data and tumor samples (formalin-fixed paraffinembedded tissue) from patients diagnosed with AS in the Netherlands between 1989 and 2015 by a nationwide search through PALGA (Dutch nationwide network and registry of histo- and cytopathology) and an additional search through the pathology database of the Radboud university medical center (Radboudumc) from 2015 to 2019. Data on tumor location and previous radiotherapy treatment were received from the Netherlands Cancer Registry and were linked to data from PALGA. Ethical approval for the study was obtained from the local certified Medical Ethics Committee of Radboudumc, The Netherlands (file number 2016-2686).

Patients were categorized in seven AS subgroups based on tumor location and whether they were considered primary or secondary. Primary AS subgroups were: primary breast, skin non-UV associated, soft tissue and visceral. Secondary AS subgroups were: radiotherapy (RT) associated, Stewart-Treves and UV-associated. Establishment of UV association was based on whether the tumor occurred on sun-exposed skin (i.e., head and neck) or not. All samples were histopathologically reviewed, including evaluation of sun damage in UV-associated cases.

Fluorescence in situ hybridization (FISH)

For MYC amplification detection, FISH was performed on 4 µm-thick formalin-fixed paraffin-embedded (FFPE) sections of AS tissue microarrays (TMAs) with one or two 2 mm cores per tumor from representative areas to correct for heterogeneity. In short, TMA sections were pretreated with 10 mM sodium citrate buffer (pH6) at 96°C for 10 min, followed by a digestion step with pepsin (200 U/ml) for 15 min at 37°C. The ZytoLight ® SPEC MYC/CEN 8 Dual Color Probe (Z-2092, Zytovision) was applied to the sections, heat denatured for 10 minutes at 80°C and hybridized at 37°C overnight. Finally, sections were mounted with a solution containing both DAPI and Vectashield (Vector Laboratories). Signals were scored using a Leica DM4 B fluorescent microscope with Leica LAS X software (Leica microsystems). Digital images were captured at 100x magnification. Generally 2 cores per tumor were analyzed. Per core 20 nuclei were examined. An amplification was defined as clustering of MYC signals or at least 10 signals per nucleus.

Immunohistochemistry

Immunohistochemistry was performed on 4 µm-thick FFPE sections of AS TMAs. Staining was performed in the Dako Omnis automated stainer (Agilent) using the EnVision FLEX, High pH kit (Agilent) and rabbit monoclonal antibody against c-Myc (clone EP121, 1:50, Z2258RL, Zeta Corporation).

All IHC stainings were scored by two independent observers. In case of observer discrepancies a third observer was consulted. MYC intensity was scored as 0 (negative), 1 (weak), 2 (positive) and 3 (strong) as shown in **figure 1**. A score of 0-1 was considered

negative, whereas a score of 2-3 was considered positive. The percentage of cells with nuclear expression was used to calculate an H-score. The H-score is obtained by the formula: staining intensity (0-3) * % stained tumor nuclei, providing a range of o to 300. Digital images were generated with VisionTekTM (Sakura, version 2.6) and analyzed at 20x magnification.

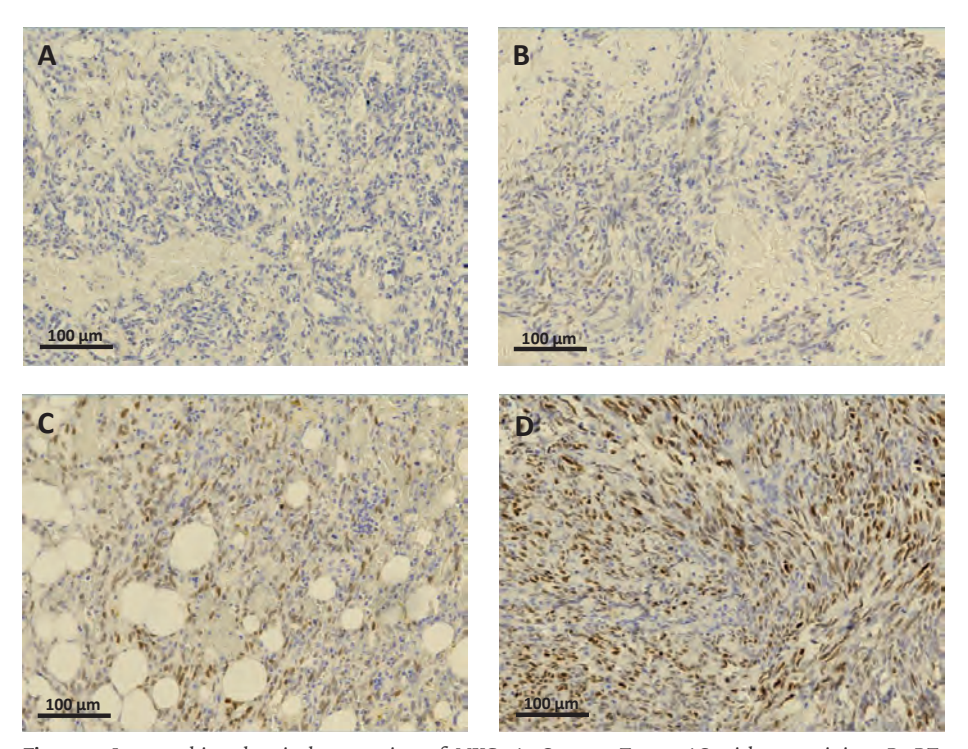


Figure 1: Immunohistochemical expression of MYC. A. Stewart Treves AS without staining; B. RTassociated AS with weak staining; C. RT-associated AS with positive staining; D. Stewart Treves AS with strong staining.

Copy number assessment

Copy number assessment was manually performed on 13 angiosarcomas based on array data by a proprietary algorithm based on the R package conumee after additional baseline correction as described previously (22). For 23 angiosarcomas the presence of MYC amplification was analyzed on the basis of median coverage normalization using next generation sequencing data (23). A relative coverage ≥3 was considered gene amplification.

Statistical analysis

Descriptive statistics were used describing baseline patient characteristics. Means or medians were used as applicable. The Fisher exact test, T-test and Mann-Whitney U tests were used. Crude survival was estimated using the Kaplan-Meier method, with survival differences between patient subgroups being assessed through log-rank testing. Values were found significant with a p value <0.05. Statistical analysis was performed using IBM SPSS statistics 25 and R (version 3.6.2).

Results

Patient characteristics

A total of 110 cases were included in our study. The patients characteristics are summarized in **table 1**. The median patients age was 74 years (range 14-96). The majority of patients was female (n=81, 73.6%). In total, 43 (39.1%) of the cases were classified as primary AS (pAS) and 67 (60.9%) as secondary AS (sAS).

Fluorescence in situ hybridization

A summary of the MYC status is shown in table 1. MYC amplification was identified in 50.9% (56/110) of the tumors. The majority of MYC amplifications were found in sAS (59.7%, 40/67), versus 37.2% in pAS (16/43, p=0.031). MYC was predominantly amplified in radiotherapy-associated (92.9%, 26/28, p<0.001) and Stewart-Treves AS (92.9%, 13/14, p<0.001), whereas only one skin UV-associated AS (4%, 1/25, p<0.001) was positive. Within the pAS subgroup, 69.2% of all skin non-UV-associated AS (9/13, p=0.237) showed MYC amplification, while only 22.2% of soft tissue AS (2/9, p=0.093) and 29.4% of primary breast AS (5/17, p=0.069) were positive and none of the visceral AS (0/4, p=0.057). Histological assessment of UV damage could be confirmed in 11 UV-associated cases by histological detection of the degradation of fibrillar collagen and elastic fibers. Evaluation in the other cases was not possible due to the limited presence of normal tissue. Four cases with high tumor mutational burden were assessable for UV signature analysis by targeted next generation sequencing using COSMIC mutational signature v3. A UV signature could be identified in 3/3 UV-associated AS, whereas no clear mutational signature was detected in 1/1 non UV-associated AS (23).

Immunohistochemistry

Immunohistochemical staining was evaluable on 109 tumor samples as shown in **table 1**. MYC protein expression was observed in 47.7% of all tumors (52/109). Positive staining was present in 39.5% (17/43) of pAS vs 53.0% (35/66) of sAS (p=0.177).

The majority of radiotherapy-associated AS (67.9%, 19/28, p=0.016) and 25% (6/24, p=0.019) of UV-associated AS were positive. Expression was also seen in 71.4% (10/14, p=0.084) of Stewart-Treves AS. Immunoreactivity was present in 53.8% (7/13, p=0.770) of skin non-UV-associated AS and in 50% (2/4, p=1.00) of visceral AS. Positive reaction was displayed in only 33.3% (3/9, p=0.493) of soft tissue AS and in 29.4% (5/17, p=0.119) of primary breast AS. Furthermore, an H-score was calculated as shown in **table 1**. The mean H-score (staining intensity (0-3) * % stained tumor nuclei) was statistically comparable for pAS (H-score=55.0) and sAS (H-score=70.5), p=0.254. Radiotherapy-associated AS (H-score=95.4) and Stewart-Treves AS (H-score=80.3) showed the highest H-score. The lowest H-score was seen in UV-associated AS (H-score=35.8).

Concordance FISH and IHC

To evaluate the concordance between FISH and IHC, sensitivity and specificity were calculated using MYC amplification status as the gold standard for all 109 tumor samples (table 2). The overall sensitivity and specificity were 75% and 81%, respectively. Sensitivity and specificity for identifying MYC amplification by means of IHC staining were 81% and 85% for pAS and 73% and 77% for sAS, respectively. Sensitivity ranged from 100% in both primary breast and UV-associated AS to 50% in soft tissue AS. Specificity was 100% for primary breast, skin non-UV associated, and Stewart-Treves AS. Visceral and radiotherapy-associated AS showed the lowest specificity at 50%.

	All patients	MYC amplification	No MYC amplification	p-value	IHC MYC Positive	IHC MYC Negative	p-value	IHC H-score Mean (IQR)	p-value
Number of patients (%)	110	56 (50.5)	54 (49.5)		52 (47.7)	57 (52.3)			
Age (median (range))	74 (14-96)	74 (14-95)	74 (27-96)	0.439	75 (14-95)	71 (27-96)	0.149		
Sex – Male – Female	29 (26.4) 81 (73.6)	5 (17.2) 51 (63.0)	24 (82.8) 30 (37.0)	<0.001	10 (34.5) 42 (52.5)	19 (65.5) 38 (47.5)	0.129		
AS subgroup N (%) - Primary AS - Secondary AS	43 (39.1) 67 (60.9)	16 (37.3) 40 (59.7)	27 (62.7) 27 (40.3)	0.031	17 (39.5) 35 (53.0)	26 (60.5) 31 (47.0)	0.177	55.0 (70.0) 70.5 (116.5)	0.254
AS subgroup N (%) Soft Tissue	9 (8.2)	2 (22.2)	7 (77.8)	0.093	3 (33.3)	(9.99) 9	0.493	57.3 (91.5)	
Primary Breast AS Skin non-UV associated	17 (15.56) 13 (11.8)	5 (29.4) 9 (69.2)	12 (70.6) 4 (30.8)	0.069	5 (29.4) 7 (53.8)	12 (70.6) 6 (46.2)	0.119	52.2 (78.0) 56.2 (63.0)	
- Upper leg (4) - Lower leg (5) - Abdomen (1) - Thorax (1) - Foot (1)									
- Unknown (1) Visceral - Kidney (1) - Liver (1)	4 (3.6)	(0) 0	4 (100)	0.057	2 (50.0)	2 (50.0)	1.00	58.3 (130.8)	
- Thyroid gland (1) - Rectum (1) Radiotherapy-associated* - Breast (23) - Scalp (1) - Upper leg (1) - Abdomen (1) - Thorax (1) - Peri-anal (1)	28 (25.5)	26 (92.9)	2 (7.1)	0.001	19 (67.9)	9 (32.1)	0.016	95.4 (176.3)	

eq
nu
nti
ပိ
e 1:
abl
H

	All patients	MYC amplification	No MYC amplification	p-value	IHC MYC Positive	IHC MYC IHC MYC p-value Positive Negative	p-value	IHC H-score p-value Mean (IQR)	p-value
UV-associated** - Scalp (19) - Neck (1)	25 (22.7) 1 (4)	1(4)	24 (96)	<0.001	6 (25.0)	<0.001 6 (25.0) 18 (75.0)	0.019	35.8 (47.8)	
– Face (5) Stewart Treves***	14 (12.7)	13 (92.9)	1 (7.1)	<0.001	10 (71.4) 4 (28.6)	4 (28.6)	0.084	80.3 (102.0)	
– Upper arm (8) – Lower arm (3)									
– Upper leg (1) – Lower leg (1)									

^{*}Radiotherapyassociated AS without MYC amplification were located at the scalp and peri-anal

^{**}UVassociated AS with MYC amplification was located the face

^{***} StewartTreves AS without MYC amplification was located the Upper Arm

Table 2: Sensitivity and specificity for MYC protein expression after immunohistochemical staining using MYC amplification status identified using FISH as standard.

	Sens	Spec
MYC IHC		
All patients	75	81
Primary AS	81	85
Soft Tissue	50	71
Primary Breast	100	100
Skin not UV	78	100
Visceral	-	50
Secondary AS	73	77
Radiotherapy-associated	69	50
UV-associated	100	78
Stewart Treves	77	100

Correlation between FISH and copy number assessment

We previously performed Copy Number Variation (CNV) analysis on thirteen (22) and genomic profiling on twenty-three (23) AS samples included in this study. Copy number assessment and MYC amplification status was correlated as shown in **figure 2**. Two out of thirteen cases showed MYC amplification by CNV analysis and eight out of twenty-three cases by genomic profiling, all of which were confirmed by FISH. One case without amplification by genomic profiling was positive using FISH. The reason for this discrepancy was a relative DNA coverage of 2.7 whereas our threshold for amplification was 3.0.

Overall Survival

There was no significant difference in median overall survival (OS) between patients with a MYC amplified tumor (15.2 months) and non-amplified tumor (12.2 months), p=0.615 (table 3, figure 3). Patients with AS containing positive MYC IHC staining showed a significantly shorter OS compared to patients with AS containing negative staining (12.7 vs 17.7 months, p=0.028) (table 3, figure 4).

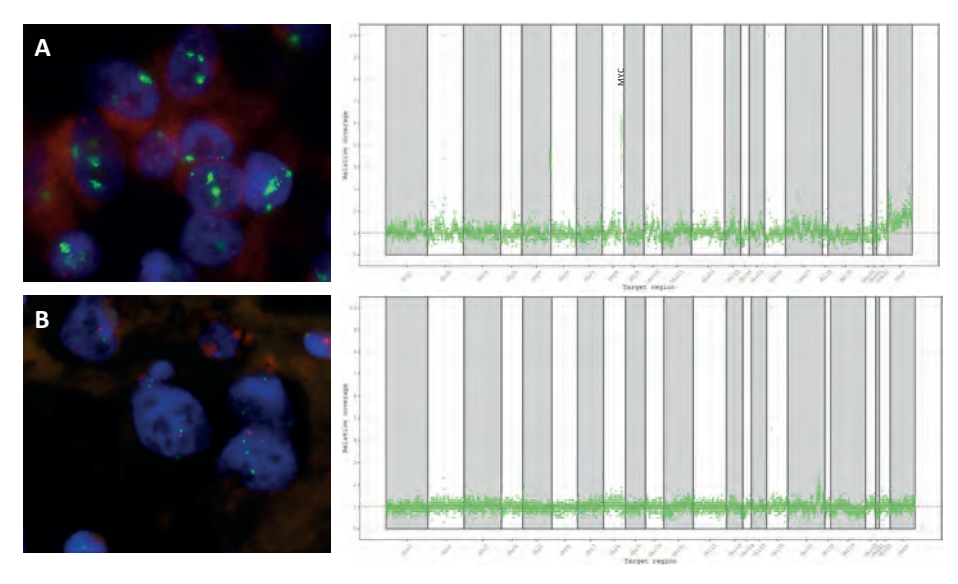


Figure 2: MYC amplification by FISH and genomic profiling. Left figures showing MYC signals (green) versus centromere 8 signals (red) by FISH analysis. Right figures showing copy number variations in the same tumor by genomic profiling. Vertical bars represent chromosomes 1-22, X and Y. On the Y axis a relative coverage of one corresponds to an equal number of copies as in the set of normal controls (2 copies of a gene region). A relative coverage of >1 or <1 indicates additional copies or loss of a copy, respectively. A. MYC amplification in Stewart Treves AS; B. No MYC amplification in soft tissue AS.

Table 3: Overall survival in months. p-values are calculated using the log-rank test.

	Median OS in months (95% CI)	p-value
Amplification status		0.615
MYC amplification	15.2 (9.5-20.9)	
No MYC amplification	12.2 (2.6-21.8)	
MYC IHC status		0.028
IHC Positive	12.7 (6.9-18.5)	
IHC negative	17.7 (7.2-28.3)	

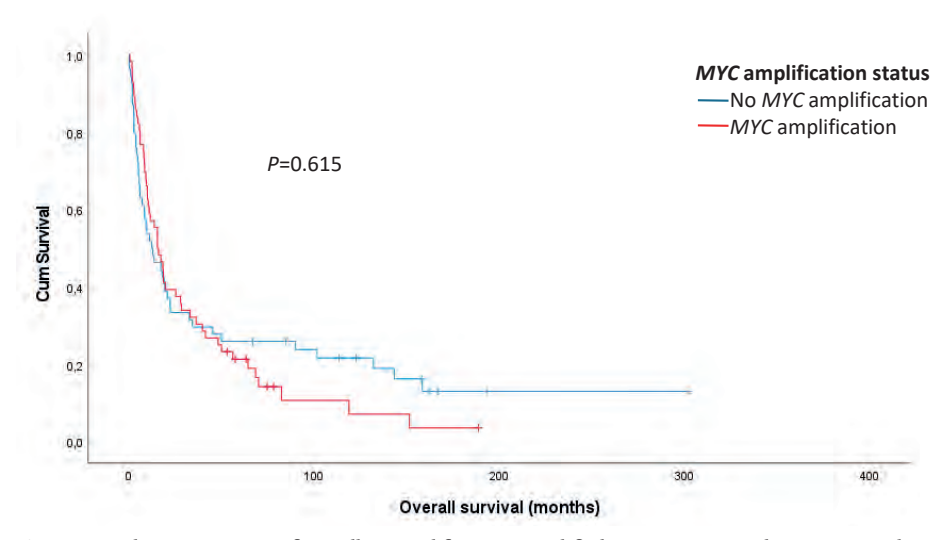


Figure 3: Kaplan-Meier curve of overall survival for MYC amplified tumors compared to tumors without the presence of a MYC amplification.

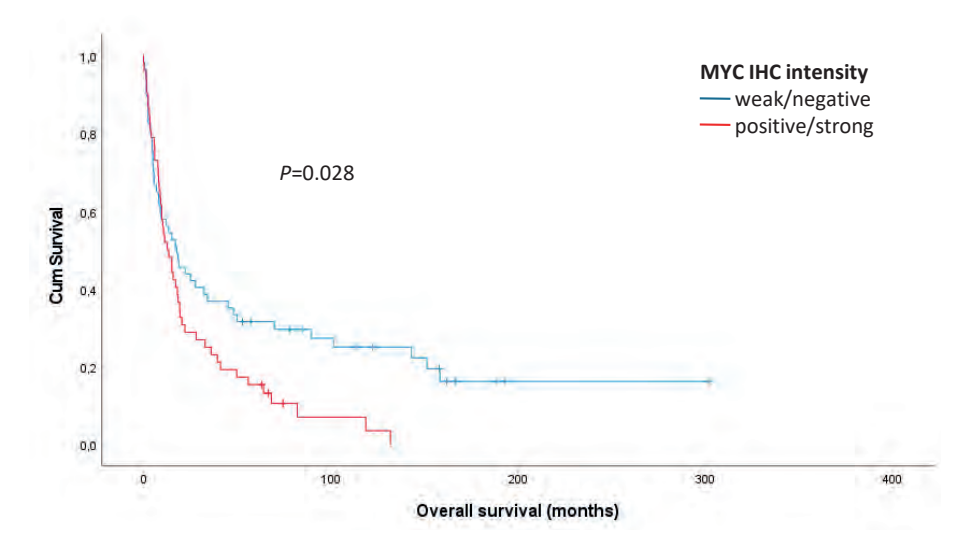


Figure 4: Kaplan-Meier curve of overall survival for patients with and without positive IHC staining.

Discussion

It has been shown that MYC amplification in AS upregulates the miR-17-92 cluster leading to downregulation of thrombospondin-1, a potent endogenous inhibitor of angiogenesis, and consequently to uncontrolled proliferation of malignant endothelial cells. Also, the potential MAML1 oncogene seems to play a role in MYC amplified AS (19).

In concordance with the reported studies, we showed MYC amplification to be predominantly present in radiotherapy-associated and Stewart-Treves AS (both 93%). The latter strengthens the evidence from very small studies (12-20). However, for unknown reasons, only 71% of our Stewart-Treves AS demonstrated MYC immunoreactivity. For hypothetic explanations see below.

Compared with the literature, MYC amplification is also present in some clinical/etiological subgroups of pAS with mainly skin non-UV-associated AS (69%) but also primary breast (29%) and soft tissue AS (22%) being positive. Furthermore, we do see a remarkable difference between UV-associated sAS versus non-UV-associated pAS of the skin based on MYC amplification (4% versus 69%, respectively). This mirrors the initial description of amplified MYC in a minority (13%) of AS of sun-exposed skin by Shon *et al* (21). Also, we previously observed a clear difference in the occurrence of high tumor mutational burden as well as the presence of T-cell subsets, both significantly higher in UV-associated AS compared to non-UV-associated (23).

Our classification, mainly based on anatomic location, is not entirely appropriate because not all cutaneous head and neck AS are necessarily exclusively UV-driven (24). Vice versa, evidence was found of UV mutational signatures in cutaneous AS of the trunk and extremities (25). We recently detected UV mutational signatures in three out of three AS occurring on sun-exposed area (head and neck) in contrast to the one non-UV-associated skin AS (23). Although these results support our classification method, we realize this is a small number of cases analyzed. Ideally, more evidence derived from clinicopathological features and genomic profiling would have provided a more solid rationale.

MYC amplification was detected in 29% of our primary breast AS. This is in stark contrast to prior series which have reported amplified MYC mainly in secondary mammary AS with few exceptions (12, 17, 26). Our results support that pathogenesis of primary versus secondary breast AS may converge more than previously thought. The absence of MYC amplification within visceral AS in our study may reflect the

small number of tumors included (n=4), since a recent study described the presence of it in 3/12 (25%) visceral AS confirming the biological role in primary AS of different sites (27).

Concordance of FISH and IHC was overall rather poor, although only primary breast AS showed 100% match. This coincides with results previously reported and reaffirms the role of MYC IHC as a diagnostic tool in mammary tumors (17). In contrast, the lower sensitivity and specificity of MYC IHC in AS of other sites, as also reported by Shon *et al.* (21), speaks against its utility as a surrogate marker in general. Lack of correlation between *MYC* gene amplification and protein overexpression as described in other tumors point to alternative mechanisms for protein overexpression, e.g decreased mRNA degradation, increased transcription/translation or epigenetic mechanisms (8, 28). Alternative possible explanations for discordance include: non-specific immunostaining interpreted as positive or low threshold IHC positivity. Furthermore, low expression levels of MYC could be the result of underestimation due to tumor heterogeneity or fixation artifacts across the tissue and the risk of sampling error by using two tumor cores per sample.

Although our study did not show any significant difference in overall survival in patients with MYC-amplified AS versus non-amplified, as also reported by Shon *et al.* (21), patients with AS displaying MYC protein overexpression had significantly shorter OS than those without. This finding should be interpreted with caution since established prognostic indicators (such as size, age or stage at diagnosis) or differences in treatment could act as confounding factors. Furthermore, as mentioned above, we cannot exclude the role of potential lack of specificity of MYC antibodies or low positivity interpretation threshold. Studies with adjustment for known prognostic factors are necessary to determine the significance of this finding. Concordance of FISH and copy number assessment by CNV analysis (22) or genomic profiling (23) was almost 100%, confirming the usability of these techniques for determination of the MYC status except when DNA coverage is too low.

The high frequency of MYC amplifications in AS and the potential correlation with the respecting protein showing poor survival makes MYC targeting a theoretically attractive strategy for future treatment of MYC amplified angiosarcomas, which warrants further investigation (29).

In summary, we have demonstrated that MYC amplification may be found in a variety of AS occurring in different anatomic locations and settings. Although characteristic of radiotherapy-associated and Stewart-Treves secondary AS, MYC amplification

is certainly not exclusive to these groups with a subset of primary AS also being amplified, especially amongst those of the skin and breast. We were unable to demonstrate the role of MYC as a prognostic indicator. Relative discordance between status of MYC and the corresponding protein suggests that alternative mechanisms for protein overexpression may be involved. Identification of MYC-positive AS may become significant as targeted therapy evolves.

References

- 1. Young RJ, Brown NJ, Reed MW, Hughes D, Woll PJ. Angiosarcoma. Lancet Oncol. 2010;11(10):983-91.
- 2. Rouhani P, Fletcher CD, Devesa SS, Toro JR. Cutaneous soft tissue sarcoma incidence patterns in the U.S.: an analysis of 12,114 cases. Cancer. 2008;113(3):616-27.
- 3. Fayette J, Martin E, Piperno-Neumann S, Le Cesne A, Robert C, Bonvalot S, et al. Angiosarcomas, a heterogeneous group of sarcomas with specific behavior depending on primary site: a retrospective study of 161 cases. Ann Oncol. 2007;18(12):2030-6.
- 4. Antonescu C. Malignant vascular tumors--an update. Mod Pathol. 2014;27 Suppl 1:S30-8.
- Weidema ME, Flucke UE, van der Graaf WTA, Ho VKY, Hillebrandt-Roeffen MHS, Dutch Nationwide N, et al. Prognostic Factors in a Large Nationwide Cohort of Histologically Confirmed Primary and Secondary Angiosarcomas. Cancers (Basel). 2019;11(11).
- 6. Buehler D, Rice SR, Moody JS, Rush P, Hafez GR, Attia S, et al. Angiosarcoma outcomes and prognostic factors: a 25-year single institution experience. Am J Clin Oncol. 2014;37(5):473-9.
- Lahat G, Dhuka AR, Hallevi H, Xiao L, Zou C, Smith KD, et al. Angiosarcoma: clinical and molecular insights. Ann Surg. 2010;251(6):1098-106.
- 8. Gurel B, Iwata T, Koh CM, Jenkins RB, Lan F, Van Dang C, et al. Nuclear MYC protein overexpression is an early alteration in human prostate carcinogenesis. Mod Pathol. 2008;21(9):1156-67.
- 9. Baudino TA, McKay C, Pendeville-Samain H, Nilsson JA, Maclean KH, White EL, et al. c-Myc is essential for vasculogenesis and angiogenesis during development and tumor progression. Genes Dev. 2002;16(19):2530-43.
- 10. Feller JK, Mahalingam M.c-myc and cutaneous vascular neoplasms. Am J Dermatopathol. 2013;35(3):364-9.
- 11. Kuba MG, Xu B, D'Angelo SP, Rosenbaum E, Plitas G, Ross DS, et al. The impact of MYC gene amplification on the clinicopathological features and prognosis of radiation-associated angiosarcomas of the breast. Histopathology. 2021;79(5):836-46.
- 12. Guo T, Zhang L, Chang NE, Singer S, Maki RG, Antonescu CR. Consistent MYC and FLT4 gene amplification in radiation-induced angiosarcoma but not in other radiation-associated atypical vascular lesions. Genes Chromosomes Cancer. 2011;50(1):25-33.
- Manner J, Radlwimmer B, Hohenberger P, Mossinger K, Kuffer S, Sauer C, et al. MYC high level gene amplification is a distinctive feature of angiosarcomas after irradiation or chronic lymphedema. Am J Pathol. 2010;176(1):34-9.
- 14. Harker D, Jennings M, McDonough P, Mauskar M, Savory S, Hosler GA, Vandergriff T. MYC amplification in angiosarcomas arising in the setting of chronic lymphedema of morbid obesity. J Cutan Pathol. 2017;44(1):15-9.
- 15. Requena C, Rubio L, Lavernia J, Machado I, Llombart B, Sanmartin O, et al. Immunohistochemical and Fluorescence In Situ Hybridization Analysis of MYC in a Series of 17 Cutaneous Angiosarcomas: A Single-Center Study. Am J Dermatopathol. 2018;40(5):349-54.
- 16. Huang SC, Zhang L, Sung YS, Chen CL, Kao YC, Agaram NP, et al. Recurrent CIC Gene Abnormalities in Angiosarcomas: A Molecular Study of 120 Cases With Concurrent Investigation of PLCG1, KDR, MYC, and FLT4 Gene Alterations. Am J Surg Pathol. 2016;40(5):645-55.
- Ginter PS, Mosquera JM, MacDonald TY, D'Alfonso TM, Rubin MA, Shin SJ. Diagnostic utility of MYC amplification and anti-MYC immunohistochemistry in atypical vascular lesions, primary or radiation-induced mammary angiosarcomas, and primary angiosarcomas of other sites. Hum Pathol. 2014;45(4):709-16.

- 18. Mentzel T, Schildhaus HU, Palmedo G, Buttner R, Kutzner H. Postradiation cutaneous angiosarcoma after treatment of breast carcinoma is characterized by MYC amplification in contrast to atypical vascular lesions after radiotherapy and control cases: clinicopathological, immunohistochemical and molecular analysis of 66 cases. Mod Pathol. 2012;25(1):75-85.
- Italiano A, Thomas R, Breen M, Zhang L, Crago AM, Singer S, et al. The miR-17-92 cluster and its target THBS1 are differentially expressed in angiosarcomas dependent on MYC amplification. Genes Chromosomes Cancer. 2012;51(6):569-78.
- 20. Motaparthi K, Lauer SR, Patel RM, Vidal CI, Linos K. MYC gene amplification by fluorescence in situ hybridization and MYC protein expression by immunohistochemistry in the diagnosis of cutaneous angiosarcoma: Systematic review and appropriate use criteria. J Cutan Pathol. 2021;48(4):578-86.
- 21. Shon W, Sukov WR, Jenkins SM, Folpe AL. MYC amplification and overexpression in primary cutaneous angiosarcoma: a fluorescence in-situ hybridization and immunohistochemical study. Mod Pathol. 2014;27(4):509-15.
- 22. Weidema ME, van de Geer E, Koelsche C, Desar IME, Kemmeren P, Hillebrandt-Roeffen MHS, et al. DNA Methylation Profiling Identifies Distinct Clusters in Angiosarcomas. Clin Cancer Res. 2020:26(1):93-100.
- 23. van Ravensteijn SG, Versleijen-Jonkers YMH, Hillebrandt-Roeffen MHS, Weidema ME, Nederkoorn MJL, Bol KF, et al. Immunological and Genomic Analysis Reveals Clinically Relevant Distinctions between Angiosarcoma Subgroups. Cancers (Basel). 2022;14(23).
- 24. Painter CA, Jain E, Tomson BN, Dunphy M, Stoddard RE, Thomas BS, et al. The Angiosarcoma Project: enabling genomic and clinical discoveries in a rare cancer through patient-partnered research. Nat Med. 2020;26(2):181-7.
- 25. Chan JY, Lim JQ, Yeong J, Ravi V, Guan P, Boot A, et al. Multiomic analysis and immunoprofiling reveal distinct subtypes of human angiosarcoma. J Clin Invest. 2020;130(11):5833-46.
- Fraga-Guedes C, Andre S, Mastropasqua MG, Botteri E, Toesca A, Rocha RM, et al. Angiosarcoma and atypical vascular lesions of the breast: diagnostic and prognostic role of MYC gene amplification and protein expression. Breast Cancer Res Treat. 2015;151(1):131-40.
- Zhang J, Gong H, Wang Y, Zhang G, Hou P. Angiosarcoma of the visceral organs: A morphological, immunohistochemical, and C-MYC status analysis. Pathol Res Pract. 2022;238:154118.
- 28. Morrison C, Radmacher M, Mohammed N, Suster D, Auer H, Jones S, et al. MYC amplification and polysomy 8 in chondrosarcoma: array comparative genomic hybridization, fluorescent in situ hybridization, and association with outcome. J Clin Oncol. 2005;23(36):9369-76.
- 29. Duffy MJ, O'Grady S, Tang M, Crown J. MYC as a target for cancer treatment. Cancer Treat Rev. 2021;94:102154.





Chapter 4

Cemiplimab in locally advanced or metastatic secondary angiosarcomas (CEMangio): A phase II clinical trial and biomarker analyses

S.G. van Ravensteijn, J.J. de Haan, H. Gelderblom, M.J.L. Nederkoorn, M.H.S. Hillebrandt-Roeffen, M.A.J. Gorris, T.J.J. de Bitter, A. Boleij, A. Gusinac, Thomas H.A. Ederveen, U.E. Flucke, J.J. Bonenkamp, F.M. Speetjens, S.E.J. Kaal, M. Smits, K.F. Bol, C.M.L. van Herpen, Y.M.H. Versleijen-Jonkers, and J.M.E. Desar

Abstract

Background

Angiosarcomas (AS) are rare vascular sarcomas. Secondary AS (sAS) arise from DNA damaging factors like radiotherapy (RT-AS), UV radiation (UV-AS) or chronic lymphedema (Stewart-Treves AS). Prognosis for advanced AS is poor with limited treatment options. Immune checkpoint inhibition (ICI) is not approved for AS, but high intratumoral T-cell density and frequent mutations in sAS may support efficacy.

Methods

This prospective, single-arm, multicenter phase II trial, assessed the efficacy and safety of cemiplimab (350 mg intravenous 3-weekly) in patients with locally advanced or metastatic sAS using a Simon's two stage design. The primary outcome was best overall response rate (BORR) within 24 weeks of treatment. Secondary outcomes included time to response (TTR), duration of response (DOR), progression-free survival (PFS), overall survival (OS) and predictive biomarkers for treatment response.

Results

Eighteen patients were treated with cemiplimab (12 RT-AS, 3 UV-AS, 3 Stewart-Treves AS). The BORR was 27.8% (4 partial responses, 1 complete response), with a TTR of 2.6 months and a DOR of 6.9 months. The median PFS was 3.7 months and OS 13.1 months. Grade \geq 3 immune related adverse events occurred in 33.3% of patients. High tumor mutational burden was observed in 3 UV-AS, two of which showed a response. High intratumoral CD3+ (p=0.019), CD4 (p=0.046) CD8+ (p=0.026) and FoxP3+ (p=0.026) T-cell densities, low platelet-to-lymphocyte ratio (p=0.026) and Colidextribacter abundance were associated with response.

Conclusion

Cemiplimab shows promising effectivity in sAS and warrants further investigation. Promising predictive blood and tissue biomarkers were identified indicating potential for improved patient selection.

Translational relevance

While sarcomas are generally considered immune cold tumors and unlikely to respond to immune checkpoint inhibitors (ICI), our prospective study highlights that specific secondary angiosarcoma (sAS) subgroups may benefit from ICI treatment. Extensive biomarker analysis revealed the predictive value of high intratumoral T-cell density,

low platelet-lymphocyte ratio, and gut microbiome abundance of Colidextribacter for treatment response to ICI. For the first time in AS, circulating tumor DNA showed to be a predictor of treatment response, as early as 3 weeks after treatment initiation. This study paves the way for the treatment of sAS patients with immunotherapy and biomarker-driven clinical trials in rare cancers by identifying patient subgroups with possible susceptibility to immunotherapy.

Introduction

Angiosarcomas (AS) are rare and aggressive soft tissue sarcomas with endothelial characteristics that can be subdivided in primary (de novo; pAS) and secondary AS (sAS).(1-3) Secondary AS arise due to DNA damaging factors like previous radiotherapy (RT) and ultraviolet (UV) radiation or due to chronic lymphedema (Stewart-Treves AS).(1, 3) The prognosis of locally advanced and metastatic AS is very poor, with a median overall survival (OS) of 5-10 months.(4, 5) Treatment primarily consists of palliative chemotherapy, predominantly with paclitaxel or doxorubicin.(6) The ANGIOTAX study reported a median progression free survival (PFS) of 4.0 months and OS of 7.6 months in patients with unresectable AS treated with paclitaxel.(7) Pazopanib, an oral multi-tyrosine kinase inhibitor, is the only non-cytotoxic drug approved for treating AS, with a response rate of 20% and a median PFS of 4.6 months.(8) In the past decade, survival for AS has not improved, highlighting the urgent need for new treatment strategies.(4, 9)

The development of Immune checkpoint inhibitors (ICI) was a major breakthrough in the treatment of many solid cancers, but not sarcomas. Sarcomas are in general considered immune cold tumors with a poorly immune-infiltrated tumor microenvironment (TME), low tumor mutational burden (TMB) and low Programmed Death-Ligand 1 (PD-L1) expression, all of which are potential biomarkers of response to ICI treatment.(10, 11) Despite an overall immune-cold phenotype, small case series have shown that a subgroup of AS might benefit from treatment with ICI.(12, 13) Florou et al. retrospectively reported a response rate of 71% in seven patients with predominantly cutaneous AS. These patients were treated with various ICIs both off label and in clinical trials.(12) D'Angelo et al. showed a clinical response in three out of eight AS patients treated with nivolumab and the CD122-preferential interleukin-2 agent bempegaldesleukin.(13)

We and others have shown that AS is a heterogeneous group of malignancies with significant differences between pAS and sAS in clinical behavior, genetic background and immunological landscape.(1, 14-16) sAS are characterized by a more T-cell infiltrated TME, including higher densities of CD4⁺ T-helper cells and CD8⁺ cytotoxic T-cells, compared to pAS.(1, 17) In sarcomas, several studies have indicated a possible correlation between T-cell and B-cell infiltration of the TME and response to ICI.(10, 13) Furthermore, a high TMB (TMB-H; TMB≥10 mutations/megabase (mut/Mb)) is reported in over 50% of UV-AS.(1, 16, 18) sAS are also characterized by the frequent presence of mutations in genes involved in the DNA Damage Response (DDR) pathway.(1) Alterations of the DDR pathway are known to induce genomic instability, increased TMB and are associated with an activated TME, indicating possible susceptibility to ICI.(19)

However, unambiguous biomarkers predicting response to ICI are lacking. Promising biomarkers associated with response to ICI or survival, such as circulating tumor DNA (ctDNA) levels, the gut-microbiome, interferon-gamma (IFN-gamma) level, the neutrophil-to-lymphocyte ratio (NLR) and platelet-to-lymphocyte ratio (PLR) have not yet been investigated in AS. Patient selection is essential to avoid unnecessary treatment and subsequent risk of toxicity for non-responders to ICI. Therefore in this study we aimed to identify possible predictive biomarkers for ICI response in sAS.

Given the complex genetic background of sAS, characterized by UV-mediated DNA damage and frequent MYC expression, sAS show some similarities to CSCC.(20) The PD-1 inhibitor cemiplimab has demonstrated favorable results in the treatment of Cutaneous Squamous Cell Carcinoma (CSCC), with an objective response rate of 40-50% in patients with locally advanced or metastatic disease.(21) We aimed to investigate the efficacy of cemiplimab in sAS with a translational focus on predictive biomarkers for treatment response to ICI.

Methods

Design and participants

The CEMangio trial is an investigator initiated, open label, multicenter, single arm, phase II clinical trial of cemiplimab monotherapy across three academic sarcoma expertise centers in the Netherlands. Adult patients with an Eastern Cooperative Oncology Group (ECOG) performance status of 0-2 and histologically confirmed locally advanced or metastatic sAS were included. Patients unfit for chemotherapy in the first line of systemic treatment and patients in advanced lines of treatment were included. Adequate hepatic, renal, and bone marrow function was required. At least

one measurable baseline lesion per Response Evaluation Criteria in Solid Tumors (RECIST) version 1.1 was mandatory.

Key exclusion criteria were active autoimmune disease requiring systemic immunosuppressive treatments; prior treatment with ICI; continuous corticosteroid treatment; history of pneumonitis in the last five years; anticancer treatment other than radiotherapy within 30 days of cemiplimab. Detailed eligibility criteria can be found in the study protocol (appendix).

This study protocol and all amendments were approved by the appropriate Medical Ethical Board (CMO Arnhem-Nijmegen, 2021-12959), and conducted in accordance with the principles of the Declaration of Helsinki and the guidelines of the international conference on harmonization for good clinical practice. All patients provided written informed consent before enrollment.

Procedures

Patients were treated with cemiplimab 350 mg intravenously every 3 weeks for up to 96 weeks or until disease progression, unacceptable toxicity, or withdrawal of consent. Tumor response evaluations were scheduled baseline, after 6 and 12 weeks, and every 12 weeks thereafter. Adverse events were graded according to the National Cancer Institute Common Terminology Criteria for Adverse Events (CTCAE) version 5.0. Treatment interruptions were applied based on the guidance of the summary of product characteristics, as registered with the European Medicine Agency.

Outcomes

The primary endpoint was the best overall response rate (BORR) within 24 weeks of cemiplimab treatment, according to RECIST 1.1 or daylight photography. BORR was defined as the proportion of patients who had a partial response (PR) or complete response (CR) to therapy. Secondary endpoints included median time to response (TTR), defined as the time between treatment initiation and the first date of an objective response; median duration of response (DOR), defined as the time between first measurement of CR or PR and the first date of recurrent or progressive disease (PD) or death; PFS, defined as the time between start of treatment and the first date of recurrence or PD or death from any cause; OS, defined as the time between the start of treatment and death from any cause. Other secondary outcomes included safety, sAS subtype responses, and translational endpoints.

Translational research

Secondary outcomes included associations between tumor characteristics and treatment response. A detailed description of the material and methods for the translational research component of this study is provided in the supplementary materials and methods. In summary, tumor biopsies, stool samples and blood samples were collected at prespecified timepoints. Next generation sequencing (NGS) and multiplex immunohistochemistry (IHC) were performed on tumor biopsies. The gut microbiome was analyzed using 16s rRNA sequencing. Peripheral blood was used for determination of interferon-gamma (IFN-gamma) levels, neutrophilto-lymphocyte ratio (NLR), platelet-to-lymphocyte ratio (PLR), ctDNA analysis and flow cytometry of peripheral blood mononuclear cells (PBMCs). Responders were classified as patients with either a CR or PR as best overall response (BOR). Non-responders were classified as patients with either stable disease (SD) or PD as BOR.

Statistical analysis

Primary and secondary clinical efficacy outcomes were assessed according to the intention-to-treat principle among enrolled patients. All patients who received at least one dose of cemiplimab were assessed for safety. The data cutoff date was October 18th, 2024. A Simon's two-stage design was used.(22) The null hypothesis that the true response rate is 10% was tested against a one-sided alternative. In the first stage, 13 patients were accrued. In case of one or fewer responses in the first 13 patients, the study would be stopped. Otherwise, 5 additional patients would be accrued for a total of 18 patients. The null hypothesis would be rejected if 4 or more responses were observed in 18 patients. This design yielded a type I error rate of 10% and power of 90% when the true response rate is 34%. This 34% was in concordance with the trial conducted by Migden et al., treating patients with locally advanced or metastatic CSCC with cemiplimab.(23) Patient characteristics were summarized using means or medians as applicable. Crude survival was estimated using the Kaplan-Meier method, with survival differences between patient subgroups assessed through log-rank testing. Values were found statistically significant with a p value <0.05. For patients with response, without disease progression or who did not die, censoring was applied at the time of their last contact with the study team for DOR and PFS analysis. For OS, patients without a survival event were censored at the time of last known survival. Statistical analyses were performed using IBM SPSS Statistics, version 22.0.0.1 and R studio, version 3.6.2.

Results

Study enrollment started in January 2022. After inclusion of 13 patients, in concordance with the Simon's Two Stage Design, an interim analysis was conducted. The prespecified criteria were met, and 5 additional patients were accrued until December 2023 for a total number of 18 patients. All patients were included for analysis of the primary endpoint. The baseline characteristics are presented in **Table 1**. All enrolled patients received at least one dose of cemiplimab. The median follow-up was 11.0 months. The median age of the patients was 72 years (range 51 to 94). Patients enrolled included 12 RT-AS (66.7%), 3 UV-AS (16.7%), and 3 Stewart-Treves AS (16.7%). The proportion of patients with locally advanced disease and distant metastases were 27.8% and 72.2%, respectively. Cemiplimab was first line systemic treatment in 10 patients (55.6%), second line in 6 patients (33.3%), and third line in 2 patients (11.1%).

Table 1: Baseline demographics and disease characteristics

Gender n (%)	
Male	5 (27.8)
Female	13 (72.2)
Median age in years (range)	72 (51-94)
WHO Performance Status n (%)	
0	6 (33.3)
1	8 (44.4)
2	4 (22.2)
Angiosarcoma subgroup n (%)	
Radiotherapy associated	12 (66.7)
UV associated	3 (16.7)
Stewart-Treves	3 (16.7)
Metastatic status n (%)	
Locally advanced	5 (27.8)
Distant metastases	13 (72.2)
Prior lines systemic treatment n (%)	
0	10 (55.6)
1	6 (33.3)
2	2 (11.1)
Prior radiotherapy for angiosarcoma n (%)	
Yes	8 (44.4)
No	10 (55.6)
Prior surgery for angiosarcoma n (%)	
Yes	9 (50.0)
No	9 (50.0)

Treatment outcomes

The BORR within 24 weeks was 27.8%, with 4 patients (22.2%) achieving a PR (2 RT-AS, 2 UV-AS) and 1 patient (5.6%) a CR (RT-AS; Figure 1A). One patient with a PR (UV-AS) at 24 weeks developed a CR at week 60. The null hypothesis would be rejected if 4 or more responses were observed in 18 patients, Therefore, with 5 objective responses, the primary endpoint of this study was met. Two patients report an ongoing CR at the data cutoff date, while both are no longer on treatment. One patient reached the maximum treatment duration at 96 weeks, and the other patient stopped due to an immune-related dermatitis. One patient with a PR developed early disease progression, within weeks after radiological response. The median TTR was 2.6 months (range 1.2-5.4), and the median DOR was 6.9 months (range 0.43-not reached). The median PFS was 3.7 months (range 1.1-not reached, Figure 1B) and the median OS was 13.1 months (range 2.1-not reached, Figure 1C). An adverse event (AE) of any kind was reported by all patients, with 10 patients (55.6%) experiencing a grade ≥3 AE (Supplementary Table 1). Grade 3 or higher immunerelated adverse events occurred in 6 patients (33.3%). Serious adverse events (SAEs) were reported in 6 patients (33.3%) (**Supplementary Table 2**). Treatment was stopped in 3 patients due to immune-related AEs: one patient with grade 3 hepatitis, another with grade 4 hepatitis and one patient due to grade 2 dermatitis. One patient died after a rapid clinical deterioration followed by multi-organ failure, including liverand kidney, of unknown origin and without a typical immune-related pattern. Because causality could not be fully excluded, a possible relationship with the study drug was reported.

Genomic landscape

Genomic analysis was performed on DNA extracted from tumor tissue from 17 patients. In one patient, DNA was insufficient for analysis. The median total TMB was 3.1 mut/Mb (range 0.0-124.7). **Supplementary Figure 1** shows the median TMB for all individual patients, compared to the BOR. TMB-H (≥10 mut/Mb) was found in all 3 UV-AS, all showing single-base substitution signature 7a, associated with UV damage. The 2 patients with the highest TMB (60.2 and 124.7 mut/Mb) showed a PR as BOR at 24 weeks. The patient with 124.7 mut/Mb eventually developed a CR. None of the tumors showed microsatellite instability. A (likely) pathogenic mutation or gene amplification was identified in 88.2% of tumors. **Figure 2** depicts all genetic alterations identified. Mutated genes found in more than one patient were *TP53* (23.5%), *TET2* (11.8%), *APC* (11.8%), *CHEK2* (11.8%), *RASA1* (11.8%), and *LRP1B* (11.8%). Mutations in genes of the DDR pathway were encountered in 9 tumor samples (52.9%). No association between treatment response and presence of a DDR mutation was found (*p*=1.00). Amplifications were detected in 64.7%, *MYC* amplifications being

the most frequent (35.3%). MYC amplifications were only detected in RT-AS (6/12) and were not related to treatment response (p=0.39). Amplification of CRKL (11.8%) and HIST2H3D (11.8%) were only detected in patients with PD as BORR.

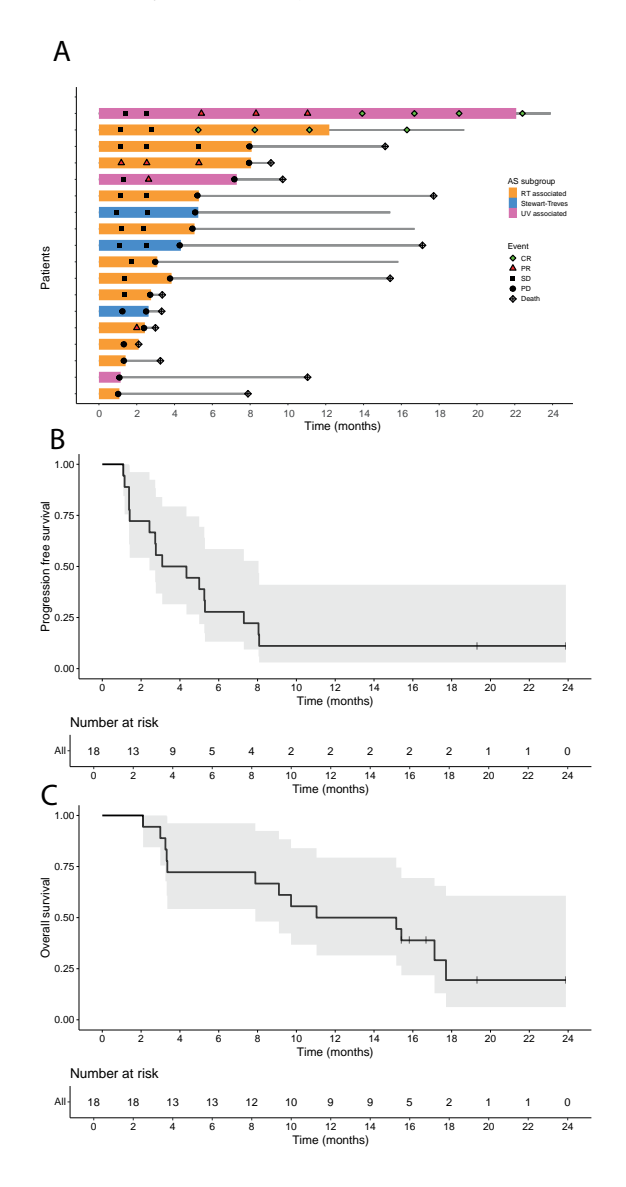


Figure 1: Treatment efficacy. A: Swimmer plot reflecting the radiological response to cemiplimab in secondary angiosarcomas over time in months per patient. Colored bar reflects treatment duration cemiplimab. B: Kaplan-Meier estimate reflecting the median progression-free survival including 95% confidence interval (grey) C: Kaplan-Meier estimate reflecting the median overall survival including 95% confidence interval (grey). Abbreviations: Complete response (CR), partial response (PR), progressive disease (PD), radiotherapy AS (RT-AS), stable disease (SD).

Circulating tumor DNA

Of the 18 patients included, 11 were eligible for ctDNA analysis based on the presence of a mutation or amplification in tumor tissue that is detectable with the targeted ctDNA-NGS panel.

A specific mutation was detected in the tumor tissue of 5 patients. One patient was excluded from the ctDNA analysis because of low coverage. In the four remaining patients 15 mutations in total were detected in the tumor tissue of which 13 were also detected with ctDNA-NGS at baseline, resulting in a true positive rate of 87% for small variant detection (**Supplementary Table 3**).

In one of the 4 patients, the *TP53* mutation identified in the tumor tissue (p.Gln317*, **Supplementary Table 3**), was only detected at baseline in ctDNA after manual inspection of the bam file. The other tumor-derived variant that was present in tissue, was not detected in ctDNA at any timepoint. The locus-specific coverage of both tumor-derived variants was sufficient to reliably detect them in ctDNA at each timepoint, suggesting that missing those variants was likely the result of low ctDNA shedding. Hence, in this patient ctDNA dynamics could not be used to correlate with treatment response.

In total, ctDNA was used to monitor treatment response in 9 patients (2 responders and 7 non-responders). In three patients (1 responder and 2 non-responders) this was based on a mutation in FGFR2, ARIDIA or TP53 and in the remaining six patients (1 responder and 5 non-responders), this was based on the presence of a MYC amplification. In both responders, ctDNA converted from detectable to undetectable values at 3 weeks, preceding a radiological response (Figure 3). The responding patient that developed progressive disease at a later timepoint, showed a sharp increase in ctDNA abundance prior to radiological disease progression. In all non-responders ctDNA remained detectable, with one patient showing a decrease in ctDNA abundance. Despite an initial decrease in ctDNA abundance, one non-responder with a mutation in ARIDIA experienced early disease progression at 6 weeks, unfortunately no ctDNA was collected at this timepoint. In all patients with a MYC amplification, ctDNA increase preceded radiological disease progression.

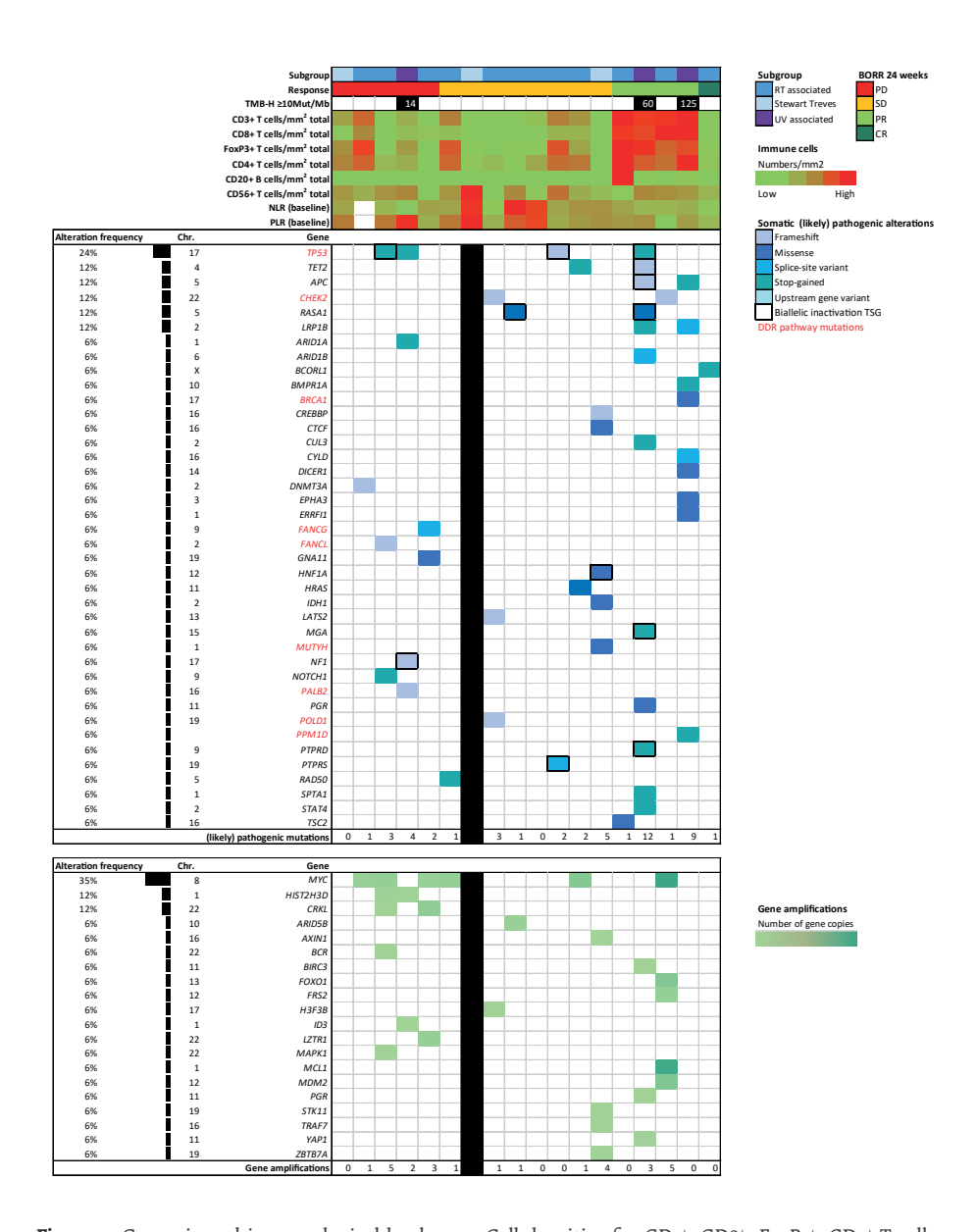


Figure 2: Genomic and immunological landscape. Cell densities for CD3+, CD8+, FoxP3+, CD4+ T-cells, CD20+ B cells and CD56+ natural killer cells are reflected based on the total number of intratumoral cells/mm². (Likely) Pathogenic mutations and gene amplifications are reflected in this figure. Abbreviations: Complete response (CR), neutrophil-lymphocyte Ratio (NLR), partial response (PR), platelet-Lymphocyte Ratio (PLR), progressive disease (PD), stable disease (SD), tumor mutational burden (TMB).

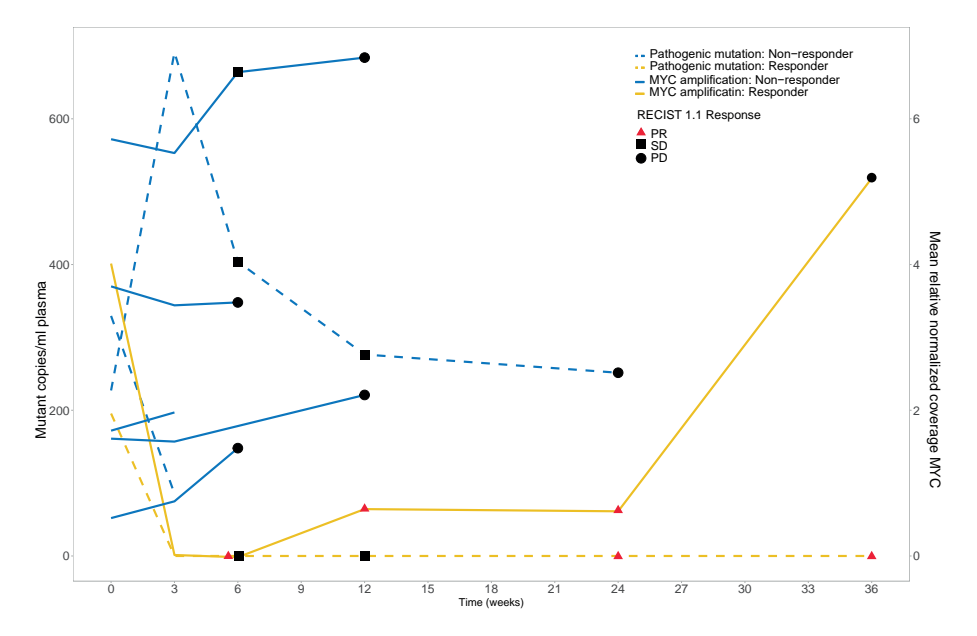


Figure 3: Circulating tumor DNA (ctDNA) in Angiosarcomas. ctDNA levels over time in three patients with a pathogenic mutation (TP53, ARADIA and FGFR2; dashed line, in mutant copies per ml plasma) and ctDNA depicted as mean relative coverage of MYC amplification over time in six patients. Symbols indicate radiological response at time of ctDNA collection. Responder is defined as CR or PR as best overall response rate (BOR). Non-responder is defined as SD or PD as BOR. Abbreviations: Partial response (PR), progressive disease (PD), stable disease (SD).

Immunological landscape

Multiplex IHC was performed on baseline tumor biopsies from all 18 patients. **Figure 4** shows examples of multiplex IHC performed on a baseline and 12-week tumor sample. Only six tumor samples at 12 weeks of treatment were available, limiting the ability to draw any conclusion regarding changes in cell density. The median cell densities of lymphocyte subsets are shown in **Supplementary Table 4** and **Figure 2**. In responders, median density was significantly higher for total CD3+ (p=0.019), CD8+ cytotoxic (*p*=0.026), FoxP3+ regulatory T-cells (*p*=0.026) and CD4+ helper (p=0.046) (**Supplementary Table5**). The median density for CD20+ B-cells and CD56+ natural killer (NK) cells was not significantly different between responders and non-responders. While the 4 patients with a PR as BOR showed the highest intratumoral lymphocyte density compared to all other samples, the patient with a CR as BOR had a relatively low density for CD3+, CD4+, and CD8+ T-cells.

Peripheral blood mononuclear cells (PBMCs) were available from 18 patients at baseline and of 11 patients after 12 weeks on treatment. Immune cell composition was comparable between baseline and 12 weeks for CD4⁺ and CD8⁺ T-cells, CD20⁺

B-cells, and CD56+ NK-cells and no difference was seen between responders and non-responders (data not shown). In all 11 patients with paired samples, a complete drop of PD-1+ CD4+ T-cells (median 41.9% vs 1.2%, p<0.01) and PD-1+ CD8+ T-cells (median 41.6% vs 1.3%, p<0.01) after 12 weeks of treatment was detected, regardless of response (supplementary Figure S2). Interference of cemiplimab binding was expected and confirmed by a second experiment revealing a comparable drop in detection of the PD-1+ CD4+ T-cells and PD-1+ CD8+ T-cells, after in vitro incubation of the PBMCs with cemiplimab.

Inflammatory biomarkers

Baseline neutrophil-lymphocyte ratio (NLR), platelet-lymphocyte ratio (PLR), and white blood cell count (WBC) were calculated (Figure 2). Median NLR (3.3 in responders vs 4.2 in non-responders, p=0.082) and WBC (7.6 in responders versus 6.4 in non-responders, p=0.924) were not significantly different. Median PLR was significantly higher in non-responders compared to responders (321 versus 182, p=0.026). IFN-gamma levels were analyzed at baseline and several timepoints during treatment. No significant difference in median IFN-gamma levels between responders and non-responders was found.

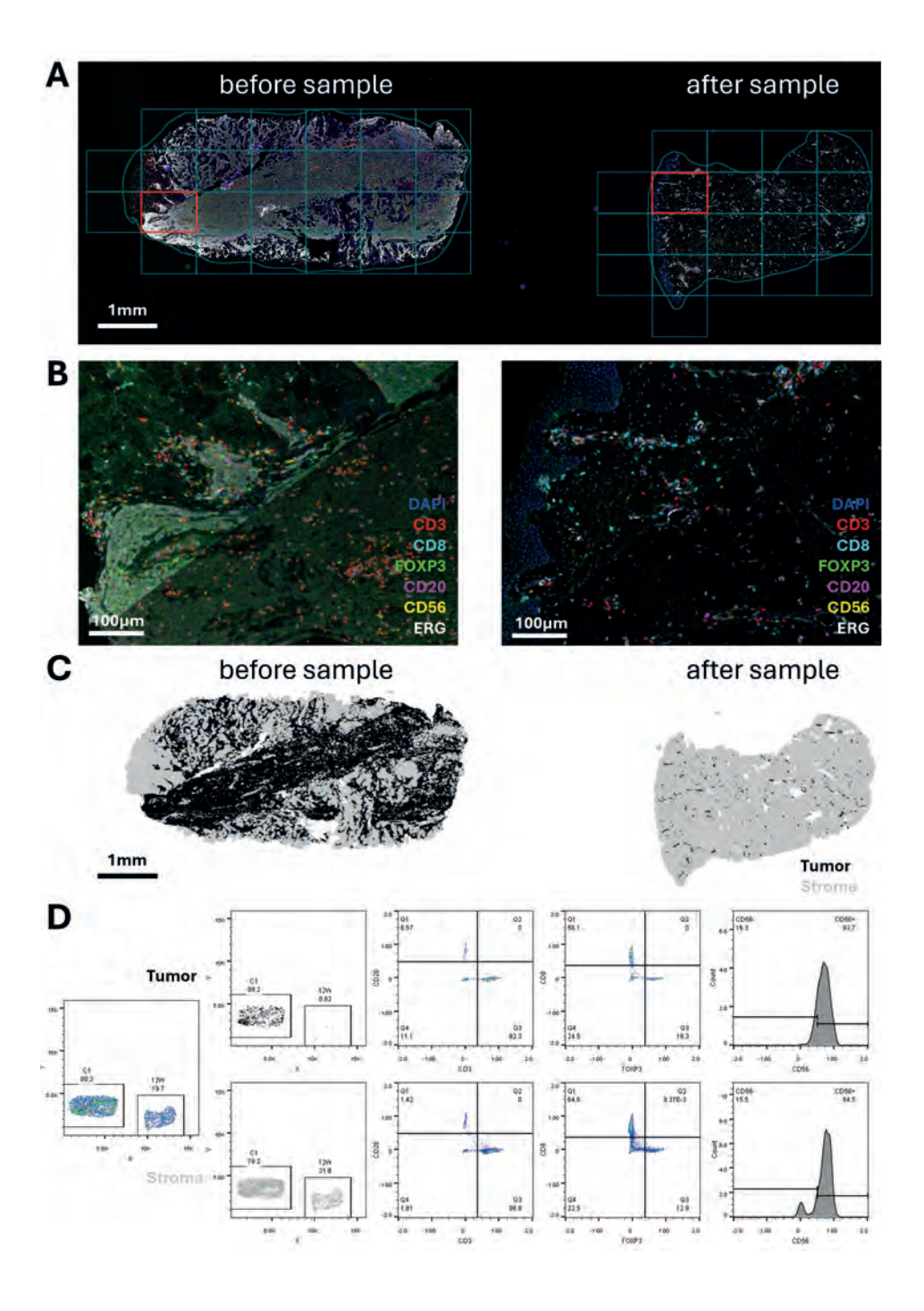


Figure 4: Multiplex imaging and data processing of angiosarcoma samples. A: Multiplex IHC stained slides were multispectral imaged at 20x and regions of analysis were selected using Phenochart. Redhighlighted regions are displayed in B. B: Images were unmixed using inForm to visualize the markers: CD3 (red), FOXP3 (green), CD8 (cyan), CD20 (magenta), CD56 (yellow), ERG (white), DAPI (blue) and autofluorescence (not shown) and lymphocytes were subsequently detected based on immune marker expression using ImmuNet in before (left) and after (right) samples. Colors show inferred intensity of surface marker expression for lymphocytes detected by the algorithm. C: A tissue segmentation algorithm was trained using inForm to recognize tumor (black) versus stroma areas (grey) based on DAPI, ERG and autofluorescence. D: Lymphocytes that are recognized ImmuNet were exported as FCS file and were phenotyped based on inferred marker expression. The gating strategy first separated T-cells (CD3⁺CD20⁻) from B-cells (CD3⁻CD20⁺). Next, T cells were further separated into cytotoxic T cells (CD3+CD8+FOXP3-), regulatory T cells (CD3+CD8-FOXP3+) and helper T cells (CD3+CD8-FOXP3-). NK cells (CD56*) were gated from cells negative for CD3 and CD20. This gating strategy was applied on lymphocytes detected in the tumor and stroma region separately. Abbreviations: Flow cytometry standard (FCS), immunohistochemistry (IHC), region of interest (ROI).

Gut microbiome

Baseline stool samples were available from 15 patients (5 responders and 10 nonresponders). Data regarding antibiotic use were available for 14 patients. In the year preceding cemiplimab treatment, 57.1% of the patients reported antibiotic use (75% of responders versus 50% of non-responders), while 28.6% reported use in the 3 months before ICI treatment (0% of responders versus 40% of non-responders). During the study, antibiotics were prescribed for 21.4% of the study participants (25% of responders versus 20% of non-responders).

The alpha diversity, or within-sample diversity, was comparable between responders and non-responders and between AS subgroups (Figure 5A, Supplementary Figure 3. Principal Coordinate Analysis (PCoA) is depicted for the first two principal components with UniFrac distances (Figure 5B), showing no significant difference between responders and non-responders. The relative abundance of microbial taxa on the phylum and genus level is shown in Figure 5C and 5D. The genus Colidextribacter was significantly higher abundant in responders (Figure 5E and 5F). In non-responders, Ruminococcus gnavus group and Pseudoflavonifractor genera were significantly overrepresented. Although not significant, a relative overrepresentation was observed for taxa Agathobacter, Christensenellaceae, Ruminococcus and Streptococcus in responders, and for Escherichia/Shigella in non-responders. Although not in the top 10 of most discriminative genera, Akkermansia was present in 40% of responders and 20% of non-responders (p>0.05). Paired samples from 9 patients showed no significant change in microbiota composition between baseline and 12 weeks of treatment (Supplementary Figure 3).

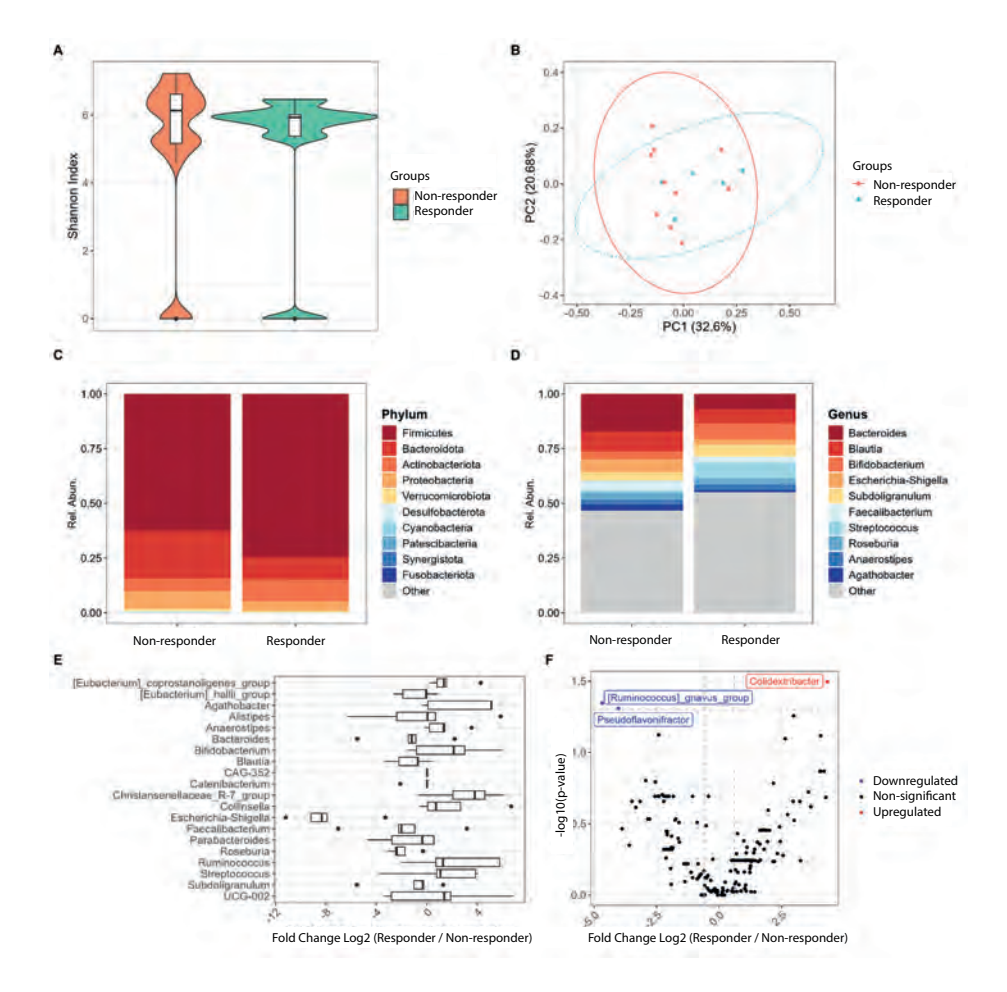


Figure 5: Fecal microbiome analysis A: Violin boxplots showing the Shannon diversity index for responders and non-responders. B: Principal Coordinate Analysis (PCoA) is shown for the first two principal components based on Weighted UniFrac distances. The first two principal components (PC1/PC2) explain at least 50% of the distances. The eclipse for each group is drawn based on the multivariate normal distribution. C/D: The relative abundance for the top 10 most abundant bacteria on phylum and genus taxonomic level. E: The top 20 most relative abundant genera are selected to calculate the fold change \log_2 (responder / non-responder) abundance. The boxplots contain fold change \log_2 values based on multiple comparisons between responders and non-responders. F: The fold change \log_2 values between responders and non-responders for all genera are shown. The x-axis contains the mean fold change \log_2 values, and the y-axis contains the Mann Whitney two-sample test p-values with \log_{10} transformation. The significant up- or downregulated genera are labeled if p<0.05 and with an abundance level ratio above 0.6 (increase) or below -0.6 (decrease). Note that taxa that are classified as "uncultured" are excluded from the analysis, or labelled as "Other". Responder is defined as stable disease or progressive disease BOR.

Discussion

In this phase II study, cemiplimab showed promising efficacy in the treatment of locally advanced or metastatic sAS. The CEMangio trial prospectively studied the use of anti-PDI ICI monotherapy, reporting a BORR of 27.8%, a median PFS of 3.7 months, and a median OS of 13.1 months. Two patients (11%) have an ongoing CR. Our findings align with the reported ORR of 25% in a prospective cohort of 16 pAS and sAS patients treated with a combination of ipilimumab and nivolumab by Wagner et al.(24) Furthermore, two other recent retrospective cohort studies reported similar response rates, ranging from 20-25%, in cohorts treating both pAS and sAS with ICI-based regimens.(25, 26) These findings collectively suggest a comparable efficacy across different studies and treatment protocols, highlighting the potential of ICI as a viable therapeutic option for sAS.

Particularly notable is the high response rate observed in UV-AS. We documented an ORR in 2/3 (67%) UV-AS patients, with all UV-AS tumors exhibiting the single-base substitution signature 7a, indicative of UV-induced damage. Wagner et al. reported an objective response in 60% of the scalp/face AS in their study, and in one out of 2 RT-AS, while no response was found in any of the pAS.(24) Similarly, a 60% response rate in 14 scalp/face AS in a retrospective study involving pembrolizumab has been reported.(25) In a retrospective study including several subgroups of AS, a response rate of 43% was reported in the 14 cutaneous AS of the head and neck treated with an ICI based regimen.(26) This might be indicative that especially UV-AS are susceptible to ICI therapy, possibly due to the high TMB associated with UV-AS.(1, 16, 18) In our study, all patients with TMB-H were UV-AS, with the 2 patients reporting the highest TMB showing a PR and CR, respectively. In a cohort of 143 sarcomas, 26% exhibited TMB-H, with 63% of these cases occurring in AS of the head and neck.(16) Previously, we also reported a high TMB in 43% of UV-AS (3/7).(1) None of the Stewart-Treves AS responded to treatment in our study. Interestingly, in contrast to our results, Rosenbaum et al. suggested potential sensitivity to ICI in Stewart-Treves AS, reporting clinical benefits with a PR in both patients in their retrospective cohort.(26) It must be remarked that both studies only included small numbers of Stewart-Treves AS, limiting the ability to draw rigid conclusions.

In our study, (likely) pathogenic mutations were identified in 88.2% of the tumors. Many of these mutations are druggable targets, e.g. BRCA1, CHECK2, IDH1, NOTCH1, PALB2, TSC2. Deficiencies in the DDR pathway are known to induce genomic instability and tumor evolution. DDR pathway mutations impair DNA repair, and thereby increase TMB and upregulate PD-L1 expression. This leads to an

enhanced immunogenicity in tumors due to the increased presence of neoantigens, consequently, tumors with DDR pathway mutations are associated with an immune-infiltrated microenvironment and may be more susceptible to ICI.(19, 27) Several clinical trials are currently investigating combination therapies using DDR pathway inhibitors, such as poly-ADP ribose polymerase inhibitors (PARPi), along with ICI.(27, 28) We did not find a significant association between the presence of DDR pathway mutations and response to ICI. This might be the result of the small numbers included. However, the high incidence of DDR pathway mutations in sAS, and reports suggesting potential synergy with combination strategies involving ICI and DDR inhibitors, indicate an interesting opportunity for future research in AS.

MYC amplifications, which are typically considered a hallmark of RT-AS, were observed in only 50% of RT-AS, and did not correlate with treatment response.(1, 15) CRKL amplifications have often been identified in AS, with frequencies ranging from 6-27%.(1, 12, 26) We only detected a CRKL amplification in two patients without response to cemiplimab. Overexpression of CRKL proteins is associated with poor prognosis in various solid tumors.(29) CRKL plays an essential role in T-cell migration, NK-cell expansion, and cell growth. Xie et al. reported that CRKL overexpression impedes CD8+ T-cell infiltration by mobilizing tumor-associated neutrophils, thereby limiting ICI effectivity in patients with hepatocellular carcinoma.(30) The frequent occurrence of MYC and CRKL amplifications warrants further research in larger cohorts of AS patients treated with ICI, since our findings might be influenced by the small numbers while MYC and CRKL amplifications are emerging as potential druggable targets.(31, 32)

Circulating tumor DNA (ctDNA) is increasingly recognized as a potential early response predictor to ICI in several tumor types including sarcomas, but was never investigated in AS before.(33, 34) We showed that a decline in ctDNA, as early as three weeks after treatment initiation, accurately predicted therapy response in responding patients, preceding a radiological response. We also demonstrated a clear increase of ctDNA in patients with evolving radiological disease progression. Real time monitoring by means of ctDNA could enable clinicians to assess effectiveness of ICI sooner than radiological imaging, which often is conducted after 12 weeks of treatment, allowing for timely adjustment of the treatment plan. This highlights the potential of ctDNA as a valuable tool in optimizing patient management.(35)

We found significantly higher intratumoral CD3+, CD4+, CD8+, and FoxP3+ T-cell density in baseline tumor samples of responders to ICI. The tumor immune microenvironment, and in particular the presence of CD8+ T-cells, have been reported as potential predictive biomarkers for treatment response to ICI.(13, 36, 37) CD8+

T-cell infiltrates correlated with improved response in AS treated with nivolumab and bempegaldesleukin.(13) Moreover, a high T-cell density was an independent prognostic factor for survival in soft tissue sarcoma.(37) Interestingly, in our study the patient who exhibited a CR had a relatively low T-cell density. This highlights a limitation in using intratumoral lymphocyte density as a sole predictive biomarker, possibly explained by the heterogeneous nature of the TME with sampling bias.

An early increase in PD-1+CD8+ peripheral T-cells has been reported as a possible predictive biomarker for ICI response in solid tumors.(38) We found no association between baseline and 12 week peripheral immune cell composition and treatment response. In our study, after 12 weeks of treatment, the immune cell composition in peripheral blood showed almost no PD-1+ T-cells. A second experiment confirmed that this drop in detection of PD-1 positive T-cells was due to therapeutic binding of cemiplimab, as was also previously reported for nivolumab and pembrolizumab in other studies with solid tumors.(38) In peripheral blood of HIV patients, cemiplimab PD-1 receptor occupancy of more than 70 percent correlated with undetectable PD-1 expression, which was achieved at levels of 1µg/ml cemiplimab concentration.(39) To gain a more comprehensive insight, in future studies, peripheral T-cell analysis during the first couple weeks of treatment could be a valuable next step.

Inflammatory biomarkers detected in peripheral blood could offer an easily accessible and minimally invasive method for predicting treatment response to ICI. Key inflammatory cells, such as neutrophils, lymphocytes, and platelets, interact with the TME and may help cancer cells evade immune surveillance.(40) Indicative for an inflammatory and pro-oncogenic state, we report a significantly higher PLR in nonresponders. PLR has been correlated with PFS and OS in gastric cancer patients treated with ICI.(41) In contrast to previous studies, NLR and IFN-gamma were comparable between responders and non-responders in our trial.(42, 43) We did observe a significant increase in IFN-gamma levels in a patient that at that timepoint developed ICI-induced hepatitis. An increase in IFN-gamma levels has been suggested as an indicator for immune-related AEs.(44) Mixed signals on NLR and IFN-gamma, and the association between low PLR and response to ICI warrant further exploration to determine their role as predictive biomarker.

The gut microbiome may influence response to ICI. Our results are consistent with previous reports, showing a significant association with response to ICI and enrichment of Colidextribacter.(45) Furthermore, we identified non-significant changes of relative abundance in responders of Agathobacter, Ruminococcus and Streptococcus, genera that have been frequently associated with ICI response.(46, 47) Presence of Ruminococcus gnavus and Pseudoflavonifractor was significantly associated with non-response to ICI, in concordance with earlier studies.(48) Escherichia Shigella was non-significantly enriched in non-responders in our study, as also shown by He et al, who investigated the influence of the gut microbiome on ICI response in NSCLC patients.(49) Of all bacterial genera, Akkermansia is most often associated with response to ICI.(46) Akkermansia was present in 40% of the responders in our study, compared to 20% of the non-responders (non-significant difference). There is increasing evidence that antibiotic use limits the benefit of ICIs.(46) Interestingly, all four patients in our study that received antibiotic treatment in the three months prior to treatment were non-responders, emphasizing the importance of appropriate antibiotic use in close proximity to ICI treatment.

Our study has some limitations. We included only 18 patients, in a single-arm design, which may affect the generalizability of our findings. Furthermore, despite limiting inclusion to sAS, the cohort remains heterogeneous, comprising of UV-AS, RT-AS, and Stewart-Treves AS. However, despite the small sample size, this cohort provides valuable insights for sAS treatment. Importantly, the study's extensive translational research component has allowed us to deepen our understanding of this rare disease in context of ICI and provided important leads for future research in AS. Future research could focus on combining ICI with chemotherapy as a first line of systemic therapy for metastatic or locally advanced sAS, as ICI combined with paclitaxel showed promising results in AS of the head and neck in the Alliance A091902 trial. Furthermore, the NADINA trial recently showed the value of neoadjuvant ipilimumabnivolumab in melanoma.(50) Neoadjuvant ICI as monotherapy or combined with chemotherapy, could be a valuable next step to investigate in resectable sAS, in order to reduce recurrence rates and improve long term survival.

Conclusion

Cemiplimab shows promising effectivity in sAS, particular in UV-AS and RT-AS. We showed that a T-cell infiltrated TME, TMB-H, low PLR, and *Colidextribacter* abundance are potential biomarkers for treatment response to ICI in sAS. Furthermore, this study highlights the potential added value of ctDNA in early response prediction. Future prospective clinical trials are needed to validate our findings in a larger cohort to determine the place and optimal regimen of ICI in sAS.

Acknowledgements

The authors thank the Radboudumc Technology Center Microscopy for use of their PhenoImager HT system. The authors thank K. Verrijp and P. Aroca Lara for their support in the multiplex IHC analysis.

References

- van Ravensteijn SG, Versleijen-Jonkers YMH, Hillebrandt-Roeffen MHS, Weidema ME, Nederkoorn 1. MJL, Bol KF, et al. Immunological and Genomic Analysis Reveals Clinically Relevant Distinctions between Angiosarcoma Subgroups. Cancers (Basel). 2022;14(23).
- Young RJ, Brown NJ, Reed MW, Hughes D, Woll PJ. Angiosarcoma. Lancet Oncol. 2010;11(10):983-91. 2.
- Fayette J., Martin E., Piperno-Neumann S., Le Cesne A., Robert C., Bonvalot S., et al. Angiosarcomas, a 3. heterogeneous group of sarcomas with specific behavior depending on primary site: a retrospective study of 161 cases. Ann Oncol. 2007;18(12):2030-6.
- Florou V, Wilky BA. Current and Future Directions for Angiosarcoma Therapy. Curr Treat Options 4. Oncol. 2018:19(3):14.
- Fury MG, Antonescu CR, Van Zee KJ, Brennan MF, Maki RG. A 14-year retrospective review of 5. angiosarcoma: clinical characteristics, prognostic factors, and treatment outcomes with surgery and chemotherapy. Cancer J. 2005;11(3):241-7.
- Penel N, Italiano A, Ray-Coquard I, Chaigneau L, Delcambre C, Robin YM, et al. Metastatic angiosarcomas: doxorubicin-based regimens, weekly paclitaxel and metastasectomy significantly improve the outcome. Ann Oncol. 2012;23(2):517-23.
- Penel N, Bui BN, Bay JO, Cupissol D, Ray-Coquard I, Piperno-Neumann S, et al. Phase II trial of weekly paclitaxel for unresectable angiosarcoma: the ANGIOTAX Study. J Clin Oncol. 2008;26(32):5269-74.
- Kollar A, Jones RL, Stacchiotti S, Gelderblom H, Guida M, Grignani G, et al. Pazopanib in advanced vascular sarcomas: an EORTC Soft Tissue and Bone Sarcoma Group (STBSG) retrospective analysis. Acta Oncol. 2017;56(1):88-92.
- Weidema ME, Flucke UE, van der Graaf WTA, Ho VKY, Hillebrandt-Roeffen MHS, Dutch Nationwide N, et al. Prognostic Factors in a Large Nationwide Cohort of Histologically Confirmed Primary and Secondary Angiosarcomas. Cancers (Basel). 2019;11(11).
- Petitprez F, de Reynies A, Keung EZ, Chen TW, Sun CM, Calderaro J, et al. B cells are associated with survival and immunotherapy response in sarcoma. Nature. 2020;577(7791):556-60.
- D'Angelo SP, Shoushtari AN, Agaram NP, Kuk D, Qin LX, Carvajal RD, et al. Prevalence of tumorinfiltrating lymphocytes and PD-L1 expression in the soft tissue sarcoma microenvironment. Hum Pathol. 2015;46(3):357-65.
- Florou V, Rosenberg AE, Wieder E, Komanduri KV, Kolonias D, Uduman M, et al. Angiosarcoma patients treated with immune checkpoint inhibitors: a case series of seven patients from a single institution. J Immunother Cancer. 2019;7(1):213.
- D'Angelo SP, Richards AL, Conley AP, Woo HJ, Dickson MA, Gounder M, et al. Pilot study of bempegaldesleukin in combination with nivolumab in patients with metastatic sarcoma. Nat Commun. 2022;13(1):3477.
- Weidema ME, van de Geer E, Koelsche C, Desar IME, Kemmeren P, Hillebrandt-Roeffen MHS, et al. DNA Methylation Profiling Identifies Distinct Clusters in Angiosarcomas. Clin Cancer Res. 2020;26(1):93-100.
- 15. Hogeboom-Gimeno AG, van Ravensteijn SG, Desar IME, Hillebrandt-Roeffen MHS, van Cleef PHJ, Bonenkamp JJ, et al. MYC amplification in angiosarcoma depends on etiological/clinical subgroups - Diagnostic and prognostic value. Ann Diagn Pathol. 2023;63:152096.
- 16. Espejo-Freire AP, Elliott A, Rosenberg A, Costa PA, Barreto-Coelho P, Jonczak E, et al. Genomic Landscape of Angiosarcoma: A Targeted and Immunotherapy Biomarker Analysis. Cancers (Basel). 2021;13(19).

- Tomassen T, Weidema ME, Hillebrandt-Roeffen MHS, van der Horst C, group* P, Desar IME, et al. Analysis of PD-1, PD-L1, and T-cell infiltration in angiosarcoma pathogenetic subgroups. Immunol Res. 2022;70(2):256-68.
- 18. Painter CA, Jain E, Tomson BN, Dunphy M, Stoddard RE, Thomas BS, et al. The Angiosarcoma Project: enabling genomic and clinical discoveries in a rare cancer through patient-partnered research. Nat Med. 2020;26(2):181-7.
- 19. Sun W, Zhang Q, Wang R, Li Y, Sun Y, Yang L. Targeting DNA Damage Repair for Immune Checkpoint Inhibition: Mechanisms and Potential Clinical Applications. Front Oncol. 2021;11:648687.
- 20. Hepburn LA, McHugh A, Fernandes K, Boag G, Proby CM, Leigh IM, Saville MK. Targeting the spliceosome for cutaneous squamous cell carcinoma therapy: a role for c-MYC and wild-type p53 in determining the degree of tumour selectivity. Oncotarget. 2018;9(33):23029-46.
- Migden MR, Rischin D, Schmults CD, Guminski A, Hauschild A, Lewis KD, et al. PD-1 Blockade with Cemiplimab in Advanced Cutaneous Squamous-Cell Carcinoma. N Engl J Med. 2018;379(4):341-51.
- 22. Simon R. Optimal two-stage designs for phase II clinical trials. Control Clin Trials. 1989;10(1):1-10.
- 23. Migden MR, Khushalani NI, Chang ALS, Lewis KD, Schmults CD, Hernandez-Aya L, et al. Cemiplimab in locally advanced cutaneous squamous cell carcinoma: results from an open-label, phase 2, single-arm trial. Lancet Oncol. 2020;21(2):294-305.
- 24. Wagner MJ, Othus M, Patel SP, Ryan C, Sangal A, Powers B, et al. Multicenter phase II trial (SWOG S1609, cohort 51) of ipilimumab and nivolumab in metastatic or unresectable angiosarcoma: a substudy of dual anti-CTLA-4 and anti-PD-1 blockade in rare tumors (DART). J Immunother Cancer. 2021;9(8).
- 25. Ravi V, Subramaniam A, Zheng J, Amini B, Trinh VA, Joseph J, et al. Clinical activity of checkpoint inhibitors in angiosarcoma: A retrospective cohort study. Cancer. 2022;128(18):3383-91.
- 26. Rosenbaum E, Antonescu CR, Smith S, Bradic M, Kashani D, Richards AL, et al. Clinical, genomic, and transcriptomic correlates of response to immune checkpoint blockade-based therapy in a cohort of patients with angiosarcoma treated at a single center. J Immunother Cancer. 2022;10(4).
- 27. Teo MY, Seier K, Ostrovnaya I, Regazzi AM, Kania BE, Moran MM, et al. Alterations in DNA Damage Response and Repair Genes as Potential Marker of Clinical Benefit From PD-1/PD-L1 Blockade in Advanced Urothelial Cancers. J Clin Oncol. 2018;36(17):1685-94.
- 28. Ramalingam SS, Thara E, Awad MM, Dowlati A, Haque B, Stinchcombe TE, et al. JASPER: Phase 2 trial of first-line niraparib plus pembrolizumab in patients with advanced non-small cell lung cancer. Cancer. 2022;128(1):65-74.
- 29. Li Z, Wu X, Chen S, Zhong J, Qiu X, Kpegah J, et al. Identification of CRKL as an oncogenic biomarker for prognosis and immunotherapy in melanoma, and its potential molecular mechanism. Genomics. 2023;115(3):110634.
- Xie P, Yu M, Zhang B, Yu Q, Zhao Y, Wu M, et al. CRKL dictates anti-PD-1 resistance by mediating tumor-associated neutrophil infiltration in hepatocellular carcinoma. J Hepatol. 2024;81(1):93-107.
- 31. Park T. Crk and CrkL as Therapeutic Targets for Cancer Treatment. Cells. 2021;10(4).
- 32. Han H, Jain AD, Truica MI, Izquierdo-Ferrer J, Anker JF, Lysy B, et al. Small-Molecule MYC Inhibitors Suppress Tumor Growth and Enhance Immunotherapy. Cancer Cell. 2019;36(5):483-97 e15.
- 33. Tolmeijer SH, van Wilpe S, Geerlings MJ, von Rhein D, Smilde TJ, Kloots ISH, et al. Early Ontreatment Circulating Tumor DNA Measurements and Response to Immune Checkpoint Inhibitors in Advanced Urothelial Cancer. Eur Urol Oncol. 2024;7(2):282-91.
- 34. Bui NQ, Nemat-Gorgani N, Subramanian A, Torres IA, Lohman M, Sears TJ, et al. Monitoring Sarcoma Response to Immune Checkpoint Inhibition and Local Cryotherapy with Circulating Tumor DNA Analysis. Clin Cancer Res. 2023;29(14):2612-20.

- 35. Wyatt AW, Litière S, Bidard FC, Cabel L, Dyrskjøt L, Karlovich CA, et al. Plasma ctDNA as a treatment response biomarker in metastatic cancers: evaluation by the RECIST working group. Clin Cancer Res. 2024.
- 36. van der Woude LL, Gorris MAJ, Wortel IMN, Creemers JHA, Verrijp K, Monkhorst K, et al. Tumor microenvironment shows an immunological abscopal effect in patients with NSCLC treated with pembrolizumab-radiotherapy combination. J Immunother Cancer. 2022;10(10).
- 37. Boxberg M, Steiger K, Lenze U, Rechl H, von Eisenhart-Rothe R, Wortler K, et al. PD-L1 and PD-1 and characterization of tumor-infiltrating lymphocytes in high grade sarcomas of soft tissue prognostic implications and rationale for immunotherapy. Oncoimmunology. 2018;7(3):e1389366.
- 38. Kim KH, Cho J, Ku BM, Koh J, Sun JM, Lee SH, et al. The First-week Proliferative Response of Peripheral Blood PD-1(+)CD8(+) T Cells Predicts the Response to Anti-PD-1 Therapy in Solid Tumors. Clin Cancer Res. 2019;25(7):2144-54.
- 39. Gay CL, Bosch RJ, McKhann A, Cha R, Morse GD, Wimbish CL, et al. Safety and Immune Responses Following Anti-PD-1 Monoclonal Antibody Infusions in Healthy Persons With Human Immunodeficiency Virus on Antiretroviral Therapy. Open Forum Infect Dis. 2024;11(3):ofad694.
- 40. Diakos CI, Charles KA, McMillan DC, Clarke SJ. Cancer-related inflammation and treatment effectiveness. Lancet Oncol. 2014;15(11):e493-503.
- Gou M, Zhang Y. Pretreatment platelet-to-lymphocyte ratio (PLR) as a prognosticating indicator for gastric cancer patients receiving immunotherapy, Discov Oncol. 2022;13(1):118.
- 42. Capone M, Giannarelli D, Mallardo D, Madonna G, Festino L, Grimaldi AM, et al. Baseline neutrophil-to-lymphocyte ratio (NLR) and derived NLR could predict overall survival in patients with advanced melanoma treated with nivolumab. J Immunother Cancer. 2018;6(1):74.
- 43. Kanai T, Suzuki H, Yoshida H, Matsushita A, Kawasumi H, Samejima Y, et al. Significance of Quantitative Interferon-gamma Levels in Non-small-cell Lung Cancer Patients' Response to Immune Checkpoint Inhibitors. Anticancer Res. 2020;40(5):2787-93.
- 44. Nuñez NG, Berner F, Friebel E, Unger S, Wyss N, Gomez JM, et al. Immune signatures predict development of autoimmune toxicity in patients with cancer treated with immune checkpoint inhibitors. Med. 2023;4(2):113-29.e7.
- 45. Newsome RC, Gharaibeh RZ, Pierce CM, da Silva WV, Paul S, Hogue SR, et al. Interaction of bacterial genera associated with therapeutic response to immune checkpoint PD-1 blockade in a United States cohort. Genome Med. 2022;14(1):35.
- 46. Routy B, Le Chatelier E, Derosa L, Duong CPM, Alou MT, Daillere R, et al. Gut microbiome influences efficacy of PD-1-based immunotherapy against epithelial tumors. Science. 2018;359(6371):91-7.
- 47. Gopalakrishnan V, Spencer CN, Nezi L, Reuben A, Andrews MC, Karpinets TV, et al. Gut microbiome modulates response to anti-PD-1 immunotherapy in melanoma patients. Science. 2018;359(6371):97-103.
- 48. Lee KA, Thomas AM, Bolte LA, Björk JR, de Ruijter LK, Armanini F, et al. Cross-cohort gut microbiome associations with immune checkpoint inhibitor response in advanced melanoma. Nat Med. 2022;28(3):535-44.
- He D, Li X, An R, Wang L, Wang Y, Zheng S, et al. Response to PD-1-Based Immunotherapy for Non-Small Cell Lung Cancer Altered by Gut Microbiota. Oncol Ther. 2021;9(2):647-57.
- 50. Blank CU, Lucas MW, Scolyer RA, van de Wiel BA, Menzies AM, Lopez-Yurda M, et al. Neoadjuvant Nivolumab and Ipilimumab in Resectable Stage III Melanoma. N Engl J Med. 2024.

Supplementary materials and methods

Genomic analysis

Sample selection for next generation sequencing (NGS) was conducted with the criterion of having at least 30% tumor cell content to ensure precise analysis of tumor mutational burden (TMB) and microsatellite instability (MSI). DNA was extracted from formalin-fixed paraffin embedded (FFPE) tissue, subsequently precipitated and quantified. Library preparation and sequencing were performed as described previously. (1, 2) Coverage tables and a variant call file were generated for both singleand multiple-nucleotide variants, including the number and percentages of variant alleles. Genomic variants were filtered by excluding: (1) variants outside exon and splice site regions except those in the TERT promoter region, (2) synonymous variants, unless they were located in a splice site region, (3) variants with a frequency > 0.1% in the control population represented in The Exome Aggregation Consortium (ExAC) version 0.2, and (4) variants with a variant allele frequency of less than 5%. Candidate variants were validated using Alamut Visual Plus version 1.7.1. Variants were manually analyzed and classified into 5 categories based on predicted pathogenicity: class 1 (not pathogenic), class 2 (unlikely pathogenic), class 3 (variant of unknown significance), class 4 (likely pathogenic), and class 5 (pathogenic). Classes 4 and 5 were considered potentially clinically relevant and are referred to as (likely) pathogenic in this article. Pathogenicity interpretations for variants in tumor suppressor genes (TSGs) utilized three prediction tools (sorting intolerant from tolerant (SIFT), Polyphen-2 and Align-Grantham Variation Grantham Deviation (Align-GVGD) and for both TSG and oncogenes various knowledge-based resources (ClinVar, OncoKB, InterVar) were used). Therapeutic targeting of tumor suppressor genes typically necessitates the inactivation of both alleles. Thus, for class 4/5 variants in TSGs, we assessed whether these affected one or both alleles by examining relative coverage and/or variant allele frequencies (VAF) of the variant and adjacent single nucleotide polymorphisms (SNPs). Gene amplification was evaluated as previously described based on median coverage normalization, with a relative coverage of ≥ 3 indicating amplification. (1) The number of gene copies was estimated by adjusting the relative coverage for the percentage of tumor cells in the sample. TMB analysis was based on non-synonymous variants (total TMB), with a threshold of 10 mutations/Mb (mut/ Mb) considered high TMB (TMB-H). Mutational signatures were analyzed in tumors with a TMB ≥10 mutations/Mb using the COSMIC mutational signature v3. (1, 3) Responders were classified with either a complete response (CR) or partial response as best overall response rate (BORR). Non responders were classified as patients with either stable disease (SD) or progressive disease (PD) as BORR.

Circulating tumor DNA

Blood samples were collected at prespecified timepoints. Blood samples (30 ml per sample) were collected in EDTA tubes and processed within two hours using two centrifugation steps. The first at $2,000 \times g$ for 10 minutes to isolate plasma and the second at $16,000 \times g$ for 10 minutes to remove cellular debris. Plasma was stored at -80° C until further processing.

Isolation of cfDNA from 4 to 10 ml plasma was performed manually using the QIAamp Circulating Nucleic Acid kit or automated using the QIAsymphony instrument (Qiagen, Hilden, Germany). DNA concentrations were measured using the Qubit High Sensitivity kit (Thermo Fisher) and 50 ng cfDNA input was used. Targeted NGS was performed by using an in-house developed NGS test. (4) The NovaSeq6000 system (Illumina) was used for sequencing, producing 2x150 base pair paired-end reads. Analysis was conducted as described previously by Tolmeijer et al and Hofste et al. (4, 5) Variants were filtered by excluding; (1) variants outside exons and splice site regions, (2) synonymous variants, (3) variants present with a frequency > 0.1% in the control population represented in the ExAC (0.2) database, (4) variants with less than 5 variant reads, (5) variants with only alternative reads on the forward or the reverse read, and (6) mutations with low confidence according to the Mutect2 quality filter. Only variants that were detected in the tissue were retrieved. The number of mutant molecules per ml plasma was calculated by using the mean mutant VAF, the volume of plasma used for isolation, and the total number of cfDNA molecules. (5)

In the cases in which a MYC amplification was detected in tissue, copy number analysis was performed as described by Tolmeijer et al. (5) Per sample the coverage per probe was divided by the overall median coverage of the sample to obtain a normalized coverage per probe. The normalized coverage was divided by the median normalized coverage of healthy cfDNA samples (n=22), processed similarly, to obtain a relative normalized coverage per probe. Per gene, the median relative normalized coverage was calculated. Amplification was defined as a median relative normalized coverage > 0.3.

Multiplex immunohistochemistry, multispectral imaging, and analysis

Sections of 4 μ m thickness were cut from FFPE biopsies before treatment and, if available, at 12 weeks of treatment. Samples belonging to one patient were mounted to one glass slide. Multiplex immunohistochemistry (mIHC) was performed on the Bond RX system using a panel to detect cytotoxic-, regulatory- and helper T-cells, B-cells and Natural Killer (NK) cells, as described before. (6, 7) An antibody against erythroblast transformation-specific-related gene (ERG), a transcription factor

expressed in endothelial cells, served as tumor marker (clone EPR3864, Abcam, Cambridge, United Kingdom). Whole tissue multispectral imaging was performed with the PhenoImager HT (Akoya Biosciences) at 20x magnification using the Vectra Polaris software (V1.0.13, Akoya Biosciences). All areas with containing tissue were selected for inForm batch processing with Phenochart (V1.2.0, Akoya Biosciences). Different Phenochart annotations were made to separate before treatment samples from after treatment tissue. Representative images were selected with Phenochart to train an algorithm with inForm image-analysis software (V.2.6.0, Akoya Biosciences) for spectral unmixing of Opal fluorophores, removal of autofluorescence signal, and tissue segmentation. For tissue segmentation, the algorithm was trained to recognize tumor, stroma and background based on the presence of ERG, DAPI, and autofluorescence. This algorithm was used to batch process whole tissue images. Cell identification was performed with ImmuNet. (8) Immune cell data was saved into Flow Cytometry Standard (FCS) files and subsequent phenotyping and localization of lymphocyte cell subsets was performed with Flow Jo (V10, Tree Star Inc., Ashland, OR). Immune cells were classified as CD3+ general- (CD3+), CD8+ cytotoxic- (CD3+, CD8+), FOXP3+ regulatory- (CD3+, FOXP3+) or CD4+ helper- (CD3+, CD8-, FOXP3-) T-cells, CD20+ B-cells (CD20+) or CD56 natural killer cells (CD56+). Infiltration of lymphocyte subsets was expressed in cell density by dividing the absolute cell counts by the surface area (cells/mm²) of the tissue region in consideration (total tissue, tumor, or stroma).

Flow cytometry staining on PBMCs

For flow cytometry peripheral blood mononuclear cells (PBMCs) were isolated and cryopreserved at baseline and if available at 12 weeks of treatment. PBMCs were thawed and stained first with a fixable viability dye eFluor 780 (65-0865-12, eBioscience). After washing with automacs staining buffer (130-091-221, Miltenyi Biotech) cells were stained with the following antibodies: CD8 FITC (555366 BD Biosciences), TIM-3 PE (119704, Biolegend), CD20 PERCP (130-113-376, Miltenyi Biotech), CD3 PE-Cy7 (25-0038-42, Invitrogen), CD56 APC (130-113-305, Miltenyi Biotech), CD4 APC-R700 (564975, BD Biosciences), PD-1 BV421 (329920, Biolegend) LAG-3 superbright 600 (63-2239-42, Invitrogen) and PD-L1 BV711 (329722, Biolegend). The stained cells were washed twice with staining buffer and fluorescence was analyzed with the BD FACS Lyric. A positive control was consistently used. A second experiment was conducted due to the steep decrease in PD-1 positive CD4+ and CD8+ T-cells at 12 weeks. The second experiment included PBMCs from baseline and 12 weeks of three patients. Two conditions were tested per timepoint. The first condition comprised of a culture with RPMI and Human Serum (HS), and served as the control. The second condition included RPMI, HS and 10ug/ml cemiplimab. After an incubation period of 66 hours at 37°C and 5% CO2, flow cytometry was conducted as described above. Data analysis was performed in BD FACSuite software version 1.5.0.925 (BD Biosciences).

Gut microbiome

OM-200.100 kits (OMNIgene®•GUT, DNA Genotek, Ottawa, Canada) were used to collect and stabilize DNA for quantitative gut microbiome profile analysis. Illumina 16S rRNA marker-gene amplicon libraries were generated and sequenced at BaseClear BV (Leiden, The Netherlands) on an Illumina MiSeq paired-end 300 system. The paired-end sequencing data was split using the demultiplexing tool bclfastq (version 2.20) in order to generate FASTQ read sequence files. Pre-processing of reads was performed with the Illumina Chastity filter, and reads containing the PhiX control signal were removed. The remaining reads were adapter-trimmed with a minimum length of 50 bp. A custom QIIME2-based Nextflow pipeline (version 23.10.1) was used for processing of the 16S marker-gene sequences. (9, 10) First, reads were primer-trimmed with cutadapt (forward: CCTACGGNGGCWGCAG, reverse: GGACTACHVGGGTATCTAATCC) with a minimum length of 20 bp and untrimmed reads were discarded (11). Trimmed paired-end reads were then merged into single reads via Paired-End reAd mergeR (PEAR) (12). Reads are then imported in QIIME2 via "qiime2 tools import" as 'SingleEndFastqManifestPhred33V2' format. (10) Denoising is performed via "qiime2 dada2 denoise-paired" set at default settings except for the discard of forward reads with number of expected errors higher than 3 (default 2), chimera-method is set to 'consensus' and the fold-change versus the abundance of the sequence being tested is set to 2 (default 1). (10) The latter entails that sequences that are being tested as chimeric should be more abundant than the parent sequence. The construction of a phylogenetic tree was done using "qiime2 phylogeny align-to-treemafft-fasttree". (10) Classification of representative sequences was accomplished by "qiime2 feature-classifier classify-consensus-vsearch" via VSEARCH alignment against the SILVA-138 database (Ref NR 99; i.e. non-redundant 99% identity) as a 16S reference database for taxonomic classification. (10, 13)

Analysis of 16S rRNA marker-gene sequencing data

Rstudio IDE (version 2023.12.1) with a R-base (version 4.3.3) was used for data analysis. First, the obtained rooted phylogenetic tree from "qiime2 phylogeny alignto-tree-mafft-fasttree" and table with taxonomy and their counts as BIOM format were loaded into R. (10) The data was used to select the "Bacteria" domain, and data TSS normalization (Total Sum Scaling) was performed by dividing, for each sample, the counts for each taxon by the sum total counts for that respective sample. Alpha diversity metrics by the Shannon index were computed after rarefaction by "qiime2 diversity core-metrics-phylogenetic" with default settings. (10) Tabular formats were data wrangled and visualized with the use of "tidyverse" and "patchwork" in R. Principal Coordinate Analysis (PCoA) with weighted UniFrac distances was computed by R package "rbiom". All visualization was achieved via data wrangling with R packages "tidyverse" and "patchwork". Permutational Multivariate Analysis of Variance (PERMANOVA) was applied on the weighted UniFrac distances to compute differences in beta diversity between selected study groups. (14, 15) The fold change of \log_2 bacterial expression between two groups was tested with the Mann-Whitney test with continuity correction in the normal approximation for the p-value. (16) Enrichment of operational taxonomic units (OTUs) was compared between responders and non-responders. In the end, we yielded on average 17,165 \pm 3,312 (standard deviation) number of reads on which taxonomic classification was performed (lowest sample had 12,942 reads). On taxonomic level, 1,882 Amplicon Sequence Variants (ASVs) were identified on bacterial domain.

Interferon-gamma detection

Plasma samples were collected using EDTA tubes for IFN-gamma analysis. Samples were stored at -80°C. MILLIPLEX® Human Cytokine/Chemokine/Growth Factor Panel A kit (MERCK, Darmstadt, Germany) was used. IFN-gamma detection limit was \geq 5.01 pg/ml. Analysis was performed using a Flexmap3D® with xPONENT® software (Luminex, Austin, TX).

References

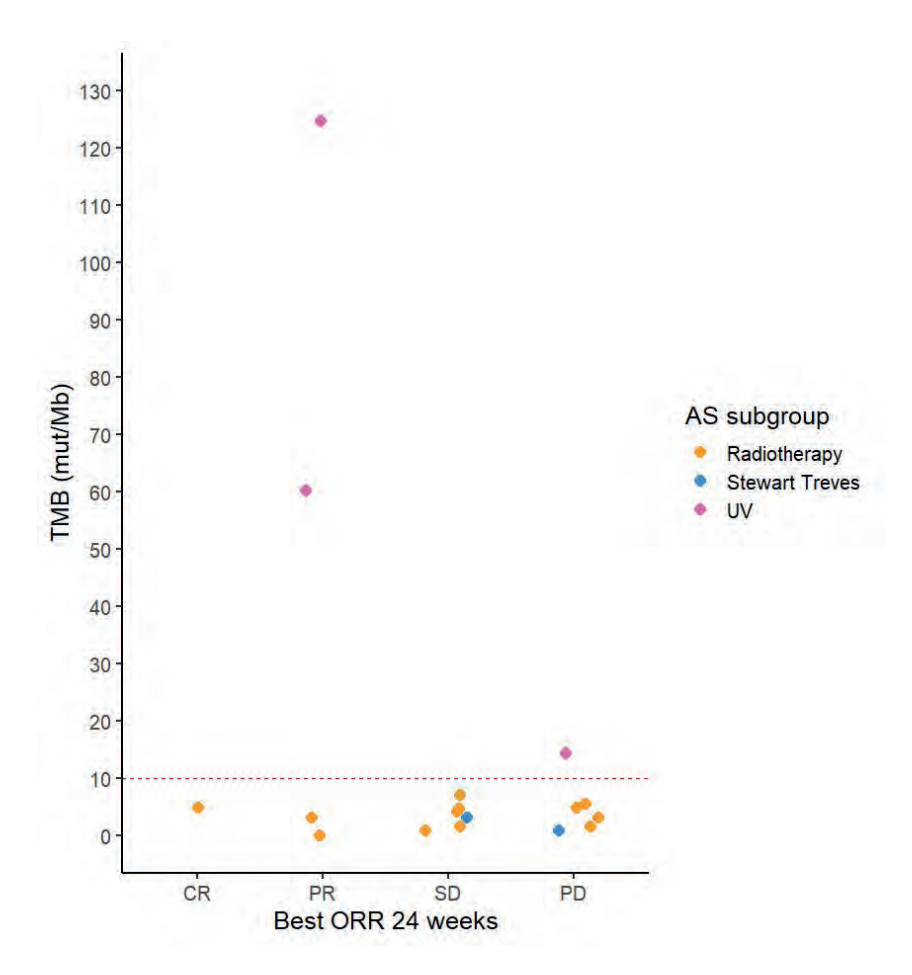
- Kroeze LI, de Voer RM, Kamping EJ, von Rhein D, Jansen EAM, Hermsen MJW, et al. Evaluation of a Hybrid Capture-Based Pan-Cancer Panel for Analysis of Treatment Stratifying Oncogenic Aberrations and Processes. J Mol Diagn. 2020;22(6):757-69.
- de Bitter TJJ, Kroeze LI, de Reuver PR, van Vliet S, Vink-Borger E, von Rhein D, et al. Unraveling Neuroendocrine Gallbladder Cancer: Comprehensive Clinicopathologic and Molecular Characterization. JCO Precis Oncol. 2021;5.
- Tate JG, Bamford S, Jubb HC, Sondka Z, Beare DM, Bindal N, et al. COSMIC: the Catalogue Of Somatic Mutations In Cancer. Nucleic Acids Res. 2019;47(D1):D941-D7.
- Hofste LSM, Geerlings MJ, von Rhein D, Tolmeijer SH, Weiss MM, Gilissen C, et al. Circulating 4. Tumor DNA-Based Disease Monitoring of Patients with Locally Advanced Esophageal Cancer. Cancers (Basel). 2022;14(18).
- Tolmeijer SH, Boerrigter E, Sumiyoshi T, Kwan EM, Ng SWS, Annala M, et al. Early On-treatment Changes in Circulating Tumor DNA Fraction and Response to Enzalutamide or Abiraterone in Metastatic Castration-Resistant Prostate Cancer. Clin Cancer Res. 2023;29(15):2835-44.
- Gorris MAJ, Martynova E, Sweep MWD, van der Hoorn IAE, Sultan S, Claassens M, et al. Multiplex Immunohistochemical Analysis of the Spatial Immune Cell Landscape of the Tumor Microenvironment. J Vis Exp. 2023(198).
- van Ravensteijn SG, Versleijen-Jonkers YMH, Hillebrandt-Roeffen MHS, Weidema ME, Nederkoorn MJL, Bol KF, et al. Immunological and Genomic Analysis Reveals Clinically Relevant Distinctions between Angiosarcoma Subgroups. Cancers (Basel). 2022;14(23).
- Sultan S, Gorris MAJ, Martynova E, van der Woude LL, Buytenhuijs F, van Wilpe S, et al. ImmuNet: A Segmentation-Free Machine Learning Pipeline for Immune Landscape Phenotyping in Tumors by Multiplex Imaging. Biology Methods and Protocols. 2024.
- Di Tommaso P, Chatzou, M., Floden, E. W., Barja, P. P., Palumbo, E., & Notredame, C. Nextflow enables reproducible computational workflows. Nature Biotechnology. 2017:316-9.
- 10. Bolyen E RJ, Dillon MR. Reproducible, interactive, scalable and extensible microbiome data science using QIIME 2. Nature Biotechnology. 2019:852-7.
- Martin M. Cutadapt removes adapter sequences from high-throughput sequencing reads. EMBnetjournal. 2011.
- J. Zhang KK, T. Flouri, A. Stamatakis. PEAR: A fast and accurate Illimuna Paired-End reAd mergeR. Bioinformatics. 2014.
- Quast C PE, Yilmaz P, Gerken J, Schweer T, Yarza P, Peplies J, Glöckner FO. The SILVA ribosomal RNA gene database project: improved data processing and web-based tools. Nucl Acids Res. 2013.
- 14. Anderson MJ. Permutational Multivariate Analysis of Variance (PERMANOVA). Wiley StatsRef: Statistics Reference Online. 2017 11 17.
- Martinez Arbizu P. pairwiseAdonis: Pairwise multilevel comparison using adonis. GitHub [Internet]. 2020.
- Wolfe MHaDA. Nonparametric Statistical Methods. New York: John Wiley & Sons. 1973:68-75.

Supplementary Table 1: Safety summary adverse events

Adverse Event	Grade 3	Grade 4	Grade 5
Alanine Aminotransferase increase		1 (5.6%)	
Anemia	1 (5.6%)		
Aspartate Aminotransferase increase	1 (5.6%)		
Diarrhea	1 (5.6%)		
Fatigue	1 (5.6%)		
Fever	1 (5.6%)		
Gamma-glutamyl transferase increase	1 (5.6%)		
Hematemesis	1 (5.6%)		
Hypertension	1 (5.6%)		
Lymphocyte count decrease	1 (5.6%)		
Multi organ failure			1 (5.6%)
Tumor hemorrhage	1 (5.6%)		

Supplementary Table 2: Serious Adverse Events

dapprenientary rable 2. serious naverse Events				
Serous Adverse Event	Relationship	Grade		
Hepatitis	Related	3		
Dermatitis	Related	2		
Multi-organ failure	Possibly related	5		
Hematemesis	Unlikely related	3		
Tumor hemorrhage	Unlikely related	3		
Pulmonary embolism	Unrelated	3		



Supplementary Figure 1: Tumor Mutational Burden. Total tumor mutational burden correlated to best overall response rate at 24 weeks of treatment with cemiplimab. Abbreviations Angiosarcoma (AS), Best overall response rate (BORR), complete response (CR), partial response (PR), progressive disease (PD), stable disease (SD), tumor mutational burden (TMB).

Supplementary Table 3: Results of the ctDNA-NGS analysis. Overview of ctDNA-NGS data of the patients in which mutations were detected in the tumor tissue which are detectable with the targeted ctDNA-NGS panel. Abbreviation Limit of Detection (LoD).

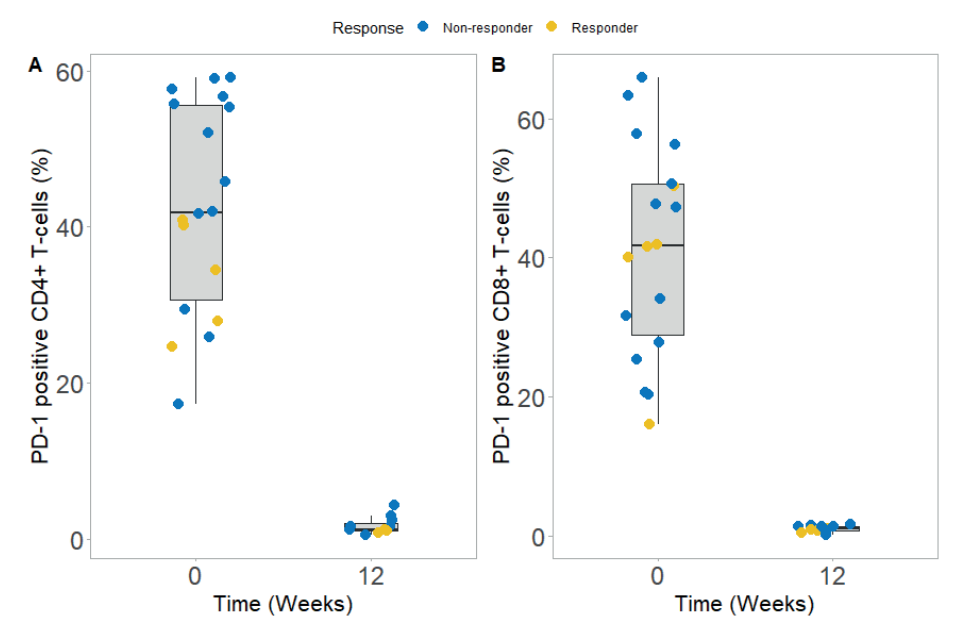
			Va	riant details (Hg19)		orboration at 11	tissue details	form of the state of		cfDNA de	tails	history at a			
Patient_ID	Gene	HVGS	HVGSc (transcript)	HVGSp	Pathogenicity	variant detected in tissue (yes/no)	Variant allele fraction (VAF)	cfDNA collection timepoint (treatment cycle)	variant detected in cfDNA (yes/no)	position	variation reads	Variant allele fraction (VAF)	locus specific LoD	median covera; sample	
CEM004	APC	chr5-g-112154942C>T	c.1213C>T (NM_000038.6)	p.(Arg405*)	PA5	yes	15	1 2	yes no	1988 3038 1500	11	0.50 2 0.07 0 0.00	0.53 0.35 0.70	17 26 13	571 0.39
								5	no	1500 1842 5259		0.00	0.57	15 15	571 0.67
								9 13 17	no no	5259 4774 3250		0.00	0.20 0.22 0.32	40 40 26	0.26
								21	no no	3250 4716 3814		0.00	0.32 0.22 0.28	35	0.27
	RO51	chr6-g.117641183T>C	c.5788A>G (NM_002944.3)	p.(Thr1930Ala)	PA3	yes	15	1	no no	3814 2146 3584		0.00 2 0.00 0 0.00	0.29 0.49 0.29	35 17 26	791 0.59
								3	no no	1625 2086	1	0.00	0.65		339 0.78
								9	no no	5670 5086		0.00	0.19 0.21	43	376 0.24
								17 21	no no	3254 5103		0.00	0.32	26	576 0.39
	NRG1	chr8:g:32453481G>A	c. 236G>A (NM_013956.5)	p.(Arg79GIn)	PAS	yes	43	25	no yes	4402 1763	- 1	0.00	0.24	33	324 0.32
	MANUA	Cital g. 324334020-7		p.pegraum	1~	,,	1	2	no no	2442 1303	-	0.00	0.43	26	571 0.39
								5	no no	1501 3878		1 0.07	0.70	15	
								13 17	no no	3633 2249		0.03	0.29	40	0.26
								21	no no	3283 2883		0.00	0.32	35	0.27
	FGFR2	chr10-g-123258012C>1	c.1669S>A (NM_000141.5)	p.(AspSS7Asn)	PA3	yes	26	1 2	yes no	1581 2244	15	S 0.95	0.66	17	
								3	no no	1185 1292		0.00	0.89	15	
								9	no no	3666 3179		0.00	0.29	43	376 0.24 341 0.26
								17 21	no no	2049 3111		0.00	0.51 0.34	26 35	576 0.39
	FGFR2	chr10:g.123298225C-1	c.629G>A (NM_000141.5)	p.(Arg210Gin)	PA3	yes	22	25 1	no yes	2733 1661	-	0.00	0.38	33	324 0.32
								2	no no	2649 1254		0.00	0.40	26 13	
								5	no no	1600 4479		0.00	0.66	15 43	571 0.67 376 0.24
								13 17	no no	4008 2686		0.02	0.26	40	0.26
								21 25	no no	3986 3339		0.00	0.26	35	0.27
	RNF43	chr17:g.56435503G>A	c.1634C>T (NM_017763.6)	p.(Ser545Phe)	PA3	yes	10	1 2	yes no	2324 3506	1	3 0.56 0 0.00	0.45	13 26	71 0.39
								3	no no	1939 2040		0.00	0.54 0.51	13 15	339 0.78 571 0.67
								9	no no	6037 5563		0.02	0.17 0.19	43	376 0.24
								17 21	no no	3873 5565		0.00	0.27	26 35	576 0.39
	RNF43	chr17:g.56435888C>1	c.1249S>A (NM_017763.6)	p.(Gly417Arg)	PAS	Wis	20	25	no Wes	4307 2280	1	0.00	0.24	33	91 0.59
				,				2 3	yes no no	3487 1897		0.00	0.90	13	339 0.78
								5	no no	1957 6180		0.00	0.54 0.17	15 43	571 0.67
								13 17 21	no no	5774 4103		0.00	0.18	40	0.26 0.39
								21 25	no no	5751 4620		0.00	0.18 0.23	35	0.27
	STK11	chr19:g.1226570G>A	c.1226G>A (NM_000455.5)	p. (Arg409GIn)	PAS	yes	23	1 2	yes no	1498 2230		6 0.40 0 0.00	0.70	17 26	71 0.39
								3	no no	1267 1386		0.00	0.83	15	71 0.67
								9	no no	4131 3700		0.00	0.25 0.28	43	0.26
								17 21	no no	2774 3945		0.00	0.27	26	058 0.27
CEM009	ARID1A	chr1:g.27088677C>G	c.2286C>G (NM_006015.6)	p.(Tyr762*)	PA4	yes	51	25 1	no yes	3014 4810	561		0.35	33	551 0.30
	RNF43	chr17:g.56435323GvA	c.1814C>T (NM_017763.6)	p. (Ala605Val)	PA3	yes	24	2	yes	8922 5562	8:	6 0.11	0.12	63	551 0.30
	TP53	chr17:g.7577058C>A	c.880G>T (NM_000546.6)	p.(Glu294*)	PA5	yes	43	2	yes yes	9490 4843	22	6 0.06 2 4.58	0.11	63	551 0.30
	TP53	577498_7577499delinsTT	_782+1delinsAA (NM_000546.6)	p.(7)	PA4	yes	41	2	yes yes	8418 4656	51	2 11.00	0.12	63	551 0.30
CEM012		12179255_112179256de		p.(Glu2655fs)	PA4	yes	10	2 1	yes no	8516 1987	71	9 0.93	0.12	63 18	701 0.16 904 0.58
								3 5	no no	2181 2748		0.00	0.48 0.38	15 25	0.42
	TP53	chr17-g,7576897G>A	c.949C>T (NM_000546.6)	p.(Gln317*)	PA5	yes	69	EOT 1	no yes	2294 2507	-	0.00	0.46	15	0.58
								3 5	no no	2665 3310		0.00	0.39 0.32		503 0.42
CEM014	TP53	chr17:g,7577549de	c.732del (NM_000546.6)	p. (Gly245fs)	PA4	yes	58	EOT 1	no yes	2405 2793	32	0.00	0.44	15 30	0.35
								2	yes yes	3420 4961	594 645	5 13.00	0.31 0.21	48	967 0.22
								5 EOT	yes yes	4535 3257	400 290	1 8.93	0.23 0.32	43 30	0.35
CEM015	IDH1	chr2:g, 209113113G>A	c.394C>T (NM_005896.4)	p. (Arg132Cys)	PAS	yes	17	1 2	no no	45 48	- 0	0.00	23.25 21.80		42 24.91 63 16.61
								3 5	no no	104 245		0.00	10.07 4.28		119 8.80 278 3.77
\Box	-	-	l				\Box	9	no	116	_	0.00	9.03		127 8.25

Supplementary Table 4: Immune cell infiltrate density in tumor vs stroma. Immune cell infiltrates are depicted for baseline tumor samples from secondary AS. Cell densities are reflected in cells/mm2 with the interquartile range (IQR) for all individual immune cell subclasses. The median total number of immune cell subclasses is shown. In addition the cell densities in both the tumor stroma, and tumor tissue are individually reported.

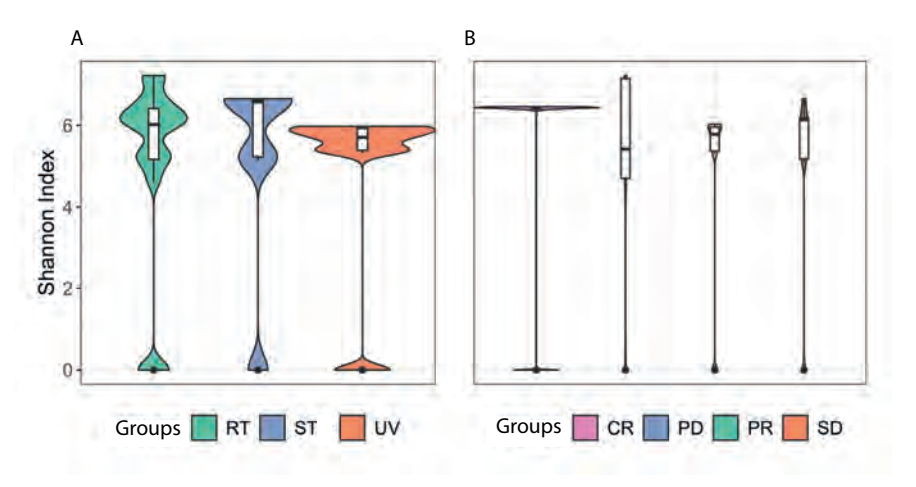
	Total	Stroma	Tumor
Median cells/mm² (IQR)			
CD3 ⁺ T-cells	207 (522)	304 (1027)	42 (57)
CD8 ⁺ T-cells	53 (194)	59 (216)	10 (22)
FoxP3+ T-cells	51 (132)	59 (178)	8 (18)
CD4 ⁺ T-cells	107 (165)	147 (268)	20 (27)
CD20+ B-cells	11 (93)	11 (100)	12 (73)
CD56 ⁺ NK-cells	15 (13)	13 (12)	8 (14)

Supplementary Table 5: Immune cell infiltrate density in responders vs non-responders. Immune cell infiltrates are depicted for responders (partial or complete response to cemiplimab) and non-responders (stable disease or progressive disease) as best overall response rate. The total number of cells/mm² (stromal and tumor) is depicted with the interquartile range (IQR).

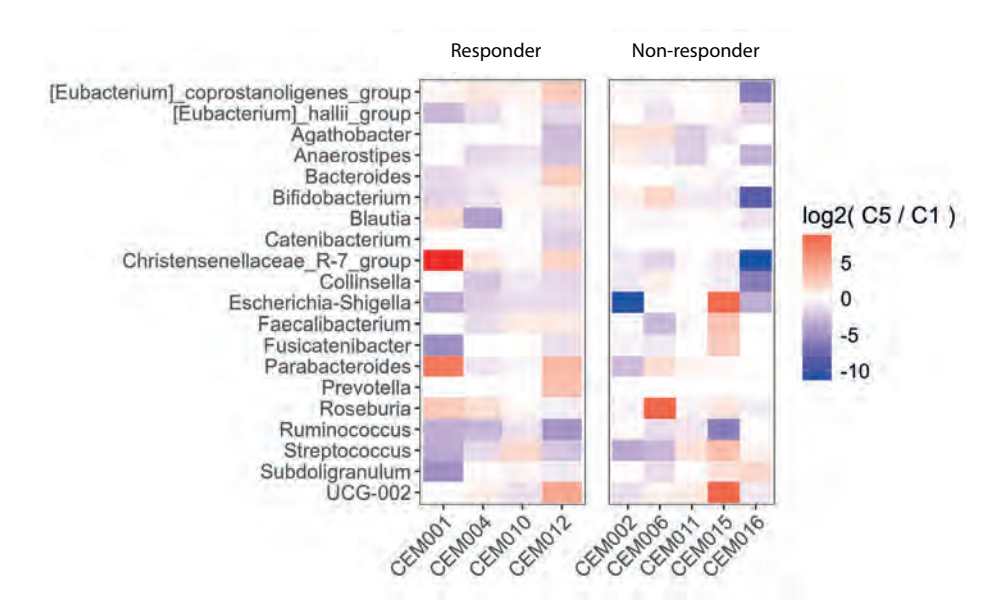
	Responders (n=5)	Non-responders (n=13)	p-value
Median cells/mm² (IQR)			
CD3 ⁺ T-cells	805 (567)	124 (270)	p=0.019
CD8 ⁺ T-cells	400 (309)	32 (53)	p=0.026
FoxP3 ⁺ T-cells	149 (129)	16 (95)	p=0.026
CD4 ⁺ T-cells	222 (250)	67 (141)	p=0.046
CD20+ B-cells	153 (284)	10 (27)	p=0.117
CD56 ⁺ NK-cells	15 (13)	16 (14)	p=0.924



Supplementary Figure 2: Decreased PD-1 expression after cemiplimab treatment in peripheral blood T-cells. PD-1 expression on CD4⁺ and CD8⁺ T-cells measured in peripheral blood at baseline and after 12 weeks of treatment with cemiplimab. Responder is defined as a partial or complete response to cemiplimab as best overall response. Non-responders is defined as stable disease or progressive disease as best overall response.



Supplementary Figure 3: Shannon diversity index at baseline for AS subgroups and according to best overall response rate. Boxplot showing the Shannon diversity index at baseline for each angiosarcoma subgroup (A) and based on best overall response (B). Abbreviations: Complete response (CR), partial response (PR), progressive disease (PD), radiotherapy (RT), stable disease (SD), Stewart-Treves (ST), ultraviolet (UV).



Supplementary Figure 4: Change in gut microbiome during treatment with cemiplimab. The top 20 most relative abundant genera are displayed, except for "uncultured" genera. The fold change log2 is computed based on paired samples for each cycle 5 (12 weeks) versus cycle 1 (baseline). Responder is defined as a partial or complete response to cemiplimab as best overall response. Non-responders is defined as stable disease or progressive disease as best overall response.





Chapter 5

Exploring the relation between TGF-β pathway activity and response to checkpoint inhibition in patients with metastatic Melanoma

Stefan G. van Ravensteijn, Avital L. Amir, Daniele V.F. Tauriello, Carla M.L. van Herpen, Marye. J. Boers-Sonderen, Yvonne J.W. Wesseling, Anne G.C. van Brussel, Diederick M. Keizer, Henk M.W. Verheul and Kalijn F. Bol

Abstract

Introduction

Immune checkpoint inhibition (ICI) is highly effective for the treatment of melanoma, but intrinsic resistance is present in a subgroup of patients. TGF- β pathway activity may play a role in this resistance by preventing T-cells from entering the tumor microenvironment, causing immune escape. We investigated the association of TGF- β signal transduction pathway activity with resistance to ICI treatment in advanced melanoma. Furthermore, other pathway activities were analyzed to better understand their potential role in ICI resistance.

Method

The activity of 8 signaling pathways (TGF- β , Hedgehog, MAPK, AR, NOTCH, PI3K, JAK/STAT1-2 and NFkB) was analyzed from tumor tissue from patients with advanced melanoma. Pathway activity scores (PAS) were explored for associations with survival and response to ICI in 34 patients (19 non-responders and 15 responders). A second, independent method to investigate the predictive value of TGF- β pathway activation was conducted by determining levels of phosphorylated SMAD2.

Results

The mean TGF- β PAS of responders versus non-responders was 53.9 vs 56.8 (p=0.265). No significant relation with progression-free survival was detected for TGF- β activity (p=0.078). No association between pSMAD2 staining and treatment response or survival was identified. In contrast, Hedgehog scores of responders versus non-responders were 35.7 vs 41.6 (p=0.038). High Hedgehog PAS was the sole significant predictor of resistance to ICI (OR 0.88, p=0.033) and worse progression-free survival (HR 1-1.1, p=0.012).

Conclusion

TGF- β pathway activation showed no significant relation with treatment response to ICI or survival in patients with advanced melanoma. Hedgehog PAS was identified as a possible biomarker associated with both treatment response and survival.

Introduction

Malignant melanoma is an aggressive form of skin cancer arising from melanocytes. In 2020 alone, melanoma was the cause of death for at least 57.000 patients globally. (1) For patients with distant metastatic disease, treatment with immune checkpoint inhibition (ICI) is the cornerstone together with BRAF/MEK inhibitors. Nivolumab and pembrolizumab, agents targeting programmed cell death 1 (PD-1), are first-line treatment. They are registered as monotherapy, or in combination with ipilimumab, an agent blocking cytotoxic T-lymphocyte-associated antigen 4 (CTLA-4) in both the metastatic and (neo)adjuvant setting. (2, 3)

The introduction of ICI has significantly prolonged survival of patients with metastatic melanoma, inducing durable responses in some patients. (4, 5) However, only up to half of patients respond to treatment with ICI, with response rates varying between 45–58%. (4-6) Treatment with checkpoint inhibition comes with a risk of adverse events, mainly immune-mediated phenomena, that can cause significant morbidity and sometimes leads to death. Grade 3-4 adverse events are reported in 10–17% of the patient treated with monotherapy anti-PD-1 agents and in up to 55% of the patients with combined treatment with anti-PD1 and anti-CTLA-4 agents. (4, 5) With a high risk of toxicity and a limited number of patients responding, there is need for both a predictive biomarker to select patients who can obtain a durable response to ICI and ways to overcome primary treatment resistance.

So far, unambiguous biomarkers to predict response to ICI are lacking. The tumor microenvironment (TME), especially the interplay between the tumor and the immune system, has emerged as a key factor in melanoma metastasis. Preclinical data indicate that TGF-\$\beta\$ pathway activity mediates immune evasion by T-cell exclusion from the tumor and may therefore be predictive for response. (7-10) TGF-\u03b3 is a pleiotropic cytokine that plays key roles during embryogenesis and in tissue homeostasis. It can also exhibit both tumor-suppressor and -promoting roles, affecting proliferation and growth, angiogenesis, extracellular matrix remodeling, and immune evasion. (11, 12) The TGF-β pathway is activated through ligand binding to the type II receptor (TGF-βR2) and recruitment of the type I receptor (TGF-βR1). A hetero-oligomeric complex is formed with TGF-βR2 and TGF-βR1. This initiates phosphorylation of the downstream target proteins SMAD2 and SMAD3, which allows them to form a complex with SMAD4 and regulate expression of target genes, such as ID1, SERPINE1, and inhibitory Smads (SMAD6 and SMAD7). (13, 14) SMAD7 interacts with TGF-BR1 and interferes with the activation of SMAD2 and SMAD3, functioning as a negative feedback loop to prevent continuous activation. (15, 16)

The hypothesis that TGF-β activation in the TME represents a primary mechanism of immune evasion is supported by preclinical data in diverse tumor types including melanoma. (17) It has been reported in melanoma cell lines that cross-talk between programmed death ligand 1 (PD-L1) and TGF-B exists, which could possibly affect ICI response. (18) Blocking TGF-β signaling in mice, either by deleting SMAD4 or using small molecule TGF-\$\beta\$ inhibitors like Galunisertib, inhibits tumor growth and formation of metastases and renders tumor more susceptible to ICI. (7, 19) Underlying mechanisms are thought to be the impaired migration of regulatory T-cells and restricted cytotoxic CD8+ T-cell function. (9, 20). In addition, deletion of the negative feedback loop by SMAD7 resulted in increased tumor growth and metastasis formation. (19) The data support the correlation between low SMAD7 transcript levels with poor survival in patients with melanoma or pancreatic cancer. (19, 21) Elevated TGF-\(\beta \) signaling was also suggested to counteract anti-tumor immunity by restricting the movement of T-cells into the TME, in patients with metastatic urothelial cell carcinoma treated with an anti-PD-L1 agent. (9) Moreover, high TGFBR1 and TGFBR2 expression were significantly associated with treatment resistance and reduced OS. (9)

With the development of agents blocking the TGF- β signaling pathway, the role of TGF- β in treatment resistance to ICI becomes of clinical relevance. (11) Therefore, this study investigated the hypothesis that an elevated level of activity of the TGF- β pathway is associated with ICI treatment resistance in melanoma and might be used as a predictive biomarker for response to ICI. We investigated TGF- β signal transduction pathway activity by means of quantitative target gene expression and also by assessment of SMAD2 phosphorylation. Furthermore, the role of other signal transduction pathways associated with tumor immunity was investigated, such as the Hedgehog (Hh) pathway. (22, 23) Understanding mechanisms of resistance to ICI could help develop strategies to overcome resistance and more personalized treatment.

Methods

Patients and treatment

In this retrospective cohort study, patients were included with cutaneous metastatic melanoma who received monotherapy with an anti-PD-1 agent as first line treatment. To increase the chance of finding clinically relevant differences, tumor samples were retrospectively collected, selecting responders and non-responders based on the presence and duration of a response. Response to ICI was based on the Response

Evaluation Criteria in Solid Tumors (RECIST) version 1.1. (24) Patients were treated with either Nivolumab or Pembrolizumab between January 2016 and November 2021 at the Radboudumc, a large academic hospital in the Netherlands. All data were retrieved from the electronic patient files. Formalin-Fixed Paraffin-Embedded (FFPE) material of primary tumor and metastatic lesion (both pre-treatment) and follow up data were obtained for all included patients. Patients treated with an anti-PD-1 agent that reached either a partial response (PR) or complete response (CR), with a duration of response (DOR) exceeding six months were classified as responders. Patients with progressive disease (PD) within six months after starting treatment were classified as non-responders. We selected 20 responders and 20 non-responders. Because of the exploratory nature of biomarker discovery in this study, no formal sample size calculation was performed.

Study design

The relation between TGF- β signaling activity and treatment resistance to ICI was the primary outcome measure. Secondary aims were the relation between progression free survival (PFS) and overall survival (OS) and TGF-\$\beta\$ activity. The difference in TGF-β pathway activity was explored in both primary tumors and matched metastatic lesions. Variables taken into account were age, sex, ICI agent, BRAF mutation status, presence of brain metastasis, lactate dehydrogenase (LDH) level, location of metastatic lesions, ECOG performance score, and melanoma subtype (i.e. superficial spreading, acral lentiginous or nodular). TGF-β was assessed in two separate ways. First, by calculating TGF-β PAS using OncoSIGNal (InnoSIGN, Eindhoven, the Netherlands), and secondly, by using a recombinant monoclonal anti-phospho-SMAD2 antibody staining. The OncoSIGNal signal transduction pathway activity test also provided a PAS for seven other oncogenic pathways: Mitogen-Activated Protein Kinase (MAPK), Androgen Receptor (AR), Notch, Hedgehog (Hh), Phosphoinositide 3-Kinase (PI3K), Nuclear Factor kappa B (NFxB), and Janus Kinase/Signal Transducer and Activator of Transcription (JAK-STAT1/2). The study complied with the relevant national regulations, institutional policies and the Helsinki Declaration. The medical ethical board of the Radboudumc approved the study (METC-2017-3164).

Signaling pathway activity score (PAS)

FFPE slides were annotated by a dedicated melanoma pathologist for areas with at least 50% tumor content from which mRNA was isolated. From these samples, PAS were measured using the OncoSIGNal pathway activity profiling PCR test (InnoSIGN). The OncoSIGNal test quantitatively measures functional activity using RT-qPCR to determine the mRNA expression of selected target genes of the pathway, as well as a number of housekeeping genes for normalization and quality control.

Computational algorithms translate the mRNA expression into an activity score for each pathway on a scale from 0-100 where 0 indicates the lowest probability of an active pathway, and inversely, 100 the highest probability of an activity pathway. (25) This Bayesian approach of expressing the odds of a pathway being active or inactive based on quantitative measurements of target gene sets has previously been validated and published in multiple tumor types for different pathways. (26-33)

Immunohistochemistry

Immunohistochemistry analysis was performed on 4 µm-thick FFPE tissue sections of melanoma primary tumor and metastatic lesions to investigate pSMAD2 expression. Colon carcinoma samples served as positive controls. Sections were deparaffinized in xylol and rehydrated through a graded ethanol into water series. Antigen retrieval was performed by heating the slides in 10 mM sodium citrate buffer pH6 for 20 min at 100°C. Endogenous peroxidase activity was blocked with 3% H₂O₂ in distilled water for 10 min at RT. Next, sections were incubated with monoclonal rabbit anti-phospho-SMAD2 (Ser465/467) (1:50, clone 138D4, #3108, Cell Signaling Technology, Danvers, MA, USA) in SignalStain® Antibody Diluent (#8112, Cell Signaling Technology) in a humidified chamber overnight at 4°C. Subsequently, a 15 min incubation step at RT with EnVision FLEX+ Rabbit LINKER (Agilent, Santa Clara, CA, USA) was performed, followed by 30 min incubation at RT with EnVision FLEX /HRP (Agilent, Santa Clara, USA). Antibody binding was visualized using the Envision Flex Dab+ Substrate Chromogen System (Agilent) for 10 min at RT. Finally, slides were counterstained with haematoxylin, dehydrated and mounted with a covereslip. pSMAD2 staining's were scored by two independent observers. In case of observer discrepancies a dedicated melanoma pathologist was consulted. Stainings were scored based on the percentage of cells stained and the intensity of the staining as described in table 1. Only tumor cells with a nuclear staining were counted. A mean score of o or 1 point was considered negative and a mean score of 2 or 3 was considered positive. (34)

Table 1: Scoring system for pSMAD2 staining

	Percentage of cells stained						
Intensity	<10%	10-30%	30-50%	>50%			
No staining	0	0	0	0			
Weak staining	0	0	1	1			
Moderate staining	0	1	2	3			
Strong staining	1	2	3	3			

Statistical analysis

Descriptive statistics were used describing baseline patient characteristics. Means or medians were used as applicable. χ^2 tests, t-tests, and Mann-Whitney U tests were used. Values were found statistically significant with a p value <0.05. Crude survival is estimated using the Kaplan-Meier method, with survival differences between patient subgroups being assessed through log-rank testing. Univariate Cox proportional hazard regression was performed to identify factors associated with PFS and OS. Individual pathway scores were included as continuous variables. Furthermore, age, WHO-ECOG performance status, neutrophil-lymphocyte ratio (NLR), LDH value (normal vs abnormal), BRAF mutation status (mutated vs wildtype), presence of brain metastasis, number of organs involved, the anatomic site of metastasis, presence of ulceration, dermal mitosis or satellite lesions, and Breslow thickness were included as covariates. Variables with a p value <0.1 in the univariate analysis were subjected to multivariate regression analysis. Statistical analyses were performed using IBM SPSS Statistics, version 22.0.0.1 and R studio, version 3.6.2.

Results

Patient characteristics

Forty patients were selected for PAS analysis from a metastatic lesion; in six patients PAS analysis was unsuccessful. A total of thirty-four patients with melanoma treated with immunotherapy had sufficient tumor tissue available from a metastatic lesion for PAS analysis. Of these 34 patients, a matched primary tumor sample was available in 31 patients. In total 19 patients classified as non-responder and 15 as responder. Of the 15 responders, four patients (26.7%) had a PR and 11 patients (73.3%) a CR. Patient and tumor characteristics were comparable between responders and non-responders except for the number of cycles of immunotherapy administered (p<0.001), treatment duration (p<0.001), and the best overall response (p<0.001) (**table 2**).

 Table 2: Patient characteristics, sorted for responders and non-responders.

	Number of patients (N=34)				
Characteristics, N (%)	Responder (N=15)	Non-Responder (N=19)	p-value		
Median age at initial diagnosis (range)	65 (28-75)	64 (46-80)	0.391		
Gender			0.724		
Male	9 (60)	13 (68)			
Female	6 (40)	6 (32)			
Primary Melanoma					
Median Breslow Thickness, mm (range)	2.8 (0.7-4.2)	4.5 (0.5-9.5)	0.157		
Ulceration present			0.087		
Yes	3 (21)	10 (53)			
No	11 (79)	9 (47)			
Metastatic melanoma					
Time between initial diagnosis and distant metastasis, months (range)	24 (5-133)	16 (2-206)	0.430		
LDH elevated			1.00		
Yes	3 (20)	4 (21)			
No	12 (80)	15 (79)			
BRAF mutation			1.00		
Yes	8 (53)	10 (53)			
No	7 (47)	9 (47)			
Brain metastasis present			0.613		
Yes	1 (7)	3 (16)			
No	14 (93)	16 (84)			
Location metastases at diagnosis					
Bone	2 (13)	9 (47)			
Lung	9 (60)	16 (84)			
Lymph node	12 (80)	12 (63)			
GI	2 (13)	2 (11)			
Adrenal gland	0 (0)	2 (11)			
Liver	2 (13)	4 (21)			
Cutaneous Subcutaneous	7 (47)	4 (21)			
Spleen	1 (7) 1 (7)	4 (21) 1 (5)			
WHO ECOG			0.471		
0	7 (47)	8 (42)	17 =		
1	7 (47)	11 (58)			
2	1 (7)	0 (0)			
Cycles immunotherapy, median (range)	19 (6-18)	4 (1-9)	<0.001		
Best Overall Response			<0.001		
PD		11 (57.9)			
SD		8 (42.1)			
PR	4 (26.7)				
CR	11 (73.3)				
Progressive disease			<0.001		
Yes	4 (27)	19 (100)			
No	11 (73)	0 (0)			

Differences in pathway activity between primary tumor samples and matching metastasis

To determine the PAS, all samples were analyzed using the OncoSIGNal test, measuring the functional activity of the TGF-\u03b3, Hh, MAPK, AR, NOTCH, PI3K, JAK/ STAT1-2, and NFxB pathways. PAS were significantly higher in the metastatic tumor samples (n=31) for TGF- β (p=0.010) and Hh (p<0.010) compared to the primary tumor samples. Looking at the responders and non-responders in a subgroups analysis, this PAS increase was only statistically significant for non-responders, for both TGF-B (p=0.044) and Hh (p=0.003). For MAPK (p<0.01), JAK/STAT1-2 (p<0.01), and NFκB (p=0.03) the mean PAS was significantly lower in the metastases compared to the primary tumor samples. This decrease was predominantly seen in non-responders in the JAK/STAT1-2 (p=0.01) and NF κ B (p=0.023) pathway. In the MAPK pathway, the decrease in PAS was observed in both the responders (p=0.024) and non-responders (p=0.002) (figure 1).

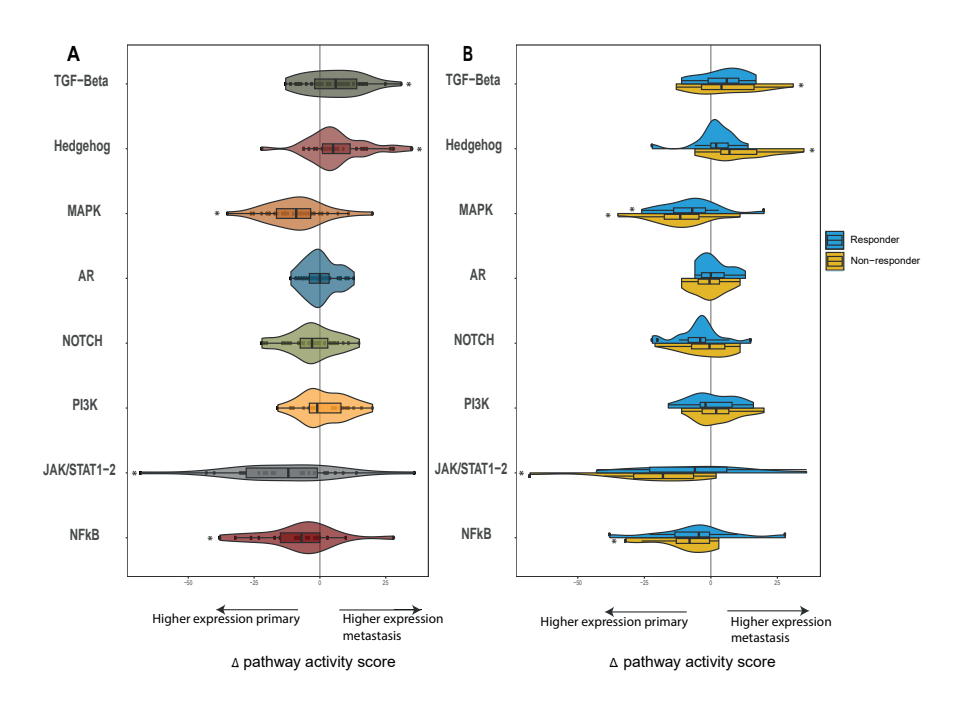


Figure 1: The mean change in pathway activity score (PAS) is reflected for the selected pathways (TGF-Beta, Hedgehog, MAPK, AR, NOTCH, PI3K, JAK/STAT1-2 and NFkB). The change in pathway score is shown as the delta of the pathway scores, calculated by subtracting the PAS of the primary tumor from that of the matching metastatic tumor sample. A The delta pathway activity score for the entire patient cohort and B for responders (blue) and non-responders (yellow).

Predictive value of pathway activity scores on treatment response

To investigate the predictive value of the TGF- β pathway, the mean PAS for both responders and non-responders to ICI was determined (**table 3 and supplementary figures S1 and S2**). Pathway scores from the primary tumor samples were comparable among responders and non-responders for all pathways. No association between PAS and survival in the primary tumor samples was found. For the metastatic tumor samples, the mean TGF- β PAS was also comparable between responders and non-responders (53.9 vs 56.8, p=0.265). Univariate cox-regression analysis showed no significant association between TGF- β PAS and PFS (HR 1.047, 95%CI, 0.995-1.101, p=0.078) (**supplementary figure S3**). No association with OS was detected.

The mean Hh score was significantly higher for non-responders compared to responders (41.6 vs 35.7, p=0.038) (**table 3 and supplementary figures S1 and S2**). High Hh PAS was associated with resistance to ICI in the metastatic tumor samples (OR 0.904 95% CI 0.817-1.00, p=0.049) in the univariate analysis. This association was confirmed by multivariate analysis, where Hh came out as the sole (negative) predictor associated with response (OR 0.884, 95% CI 0.789-0.990, p=0.033). In the metastatic samples a higher Hh PAS was associated with shorter PFS (HR 1.077, 95%CI 1.016-1.141, p=0.012) in the multivariate analysis. OS was comparable for Hh and all other PAS.

Table 3: Mean PAS for responders and non-responders to immune checkpoint inhibition.

	Primary tumor tissue (n = 31)			Metastatic tumor tissue (n= 34)		
Pathway (mean [range])	Responder (n = 14)	Non-responder (n = 17)	p-value	Responder (n = 15)	Non-responder (n = 19)	p-value
TGF-β	50.86 [36-60]	50.00 [32-63]	0.751	53.87 [42-68]	56.84 [45-77]	0.265
Hh	33.64 [24-49]	32.06 [19-48]	0.569	35.73 [27-45]	41.63 [31-58]	0.038
MAPK	55.71 [25-66]	56.53 [43-73]	0.810	47.47 [35-69]	46.21 [34-59]	0.664
AR	28.43 [20-37]	27.41 [20-35]	0.542	28.47 [21-37]	27.84 [20-39]	0.721
NOTCH	67.50 [52-85]	64.53 [53-74]	0.301	63.27 [50-76]	62.79 [43-84]	0.880
PI3K	37.71 [25-49]	38.59 [30-56]	0.741	39.60 [30-50]	40.26 [31-54]	0.784
JAK/STAT1-2	54.23 [20-77]	56.25 [28-84]	0.784	45.53 [14-80]	41.17 [16-79]	0.562
NFκB	65.92 [35-82]	69.45 [51-80]	0.476	58.15 [35-79]	61.94 [40-79]	0.441

pSMAD2 levels not associated with treatment response

As a second method to investigate the predictive value of the TGF- β pathway, the expression of SMAD2 was evaluated. In an enlarged cohort, largely overlapping with the PAS analysis, sixty-five melanoma samples were immunohistochemically stained using a recombinant monoclonal anti-phospho-SMAD2 antibody. This cohort encompassed 30 primary and 35 metastatic tumor samples, of whom 25 and 32 overlapped with the cohort for the PAS analysis. **Figure 2** shows an example of a positive and a negative pSMAD2 staining and the corresponding Hematoxylin and Eosin (H&E) stain.

Of the primary tumor samples, 16 (53%) tumors showed a positive staining (36% responders vs 69% non-responders (p=0.141)). Of the metastatic tumor samples, 17 (51%) metastases showed a positive staining (47% responders vs 53% non-responders (p=1.00)) (**table 4**). No association between pSMAD2 staining and treatment response in either the primary tumor samples or metastasis was identified. Neither was a significant association between pSMAD2 staining and survival found. Mean TGF- β PAS were comparable for the pSMAD2 positive and negative samples in both the primary tumors (0.221) and metastasis (p=0.261) (**supplementary figure S4**).

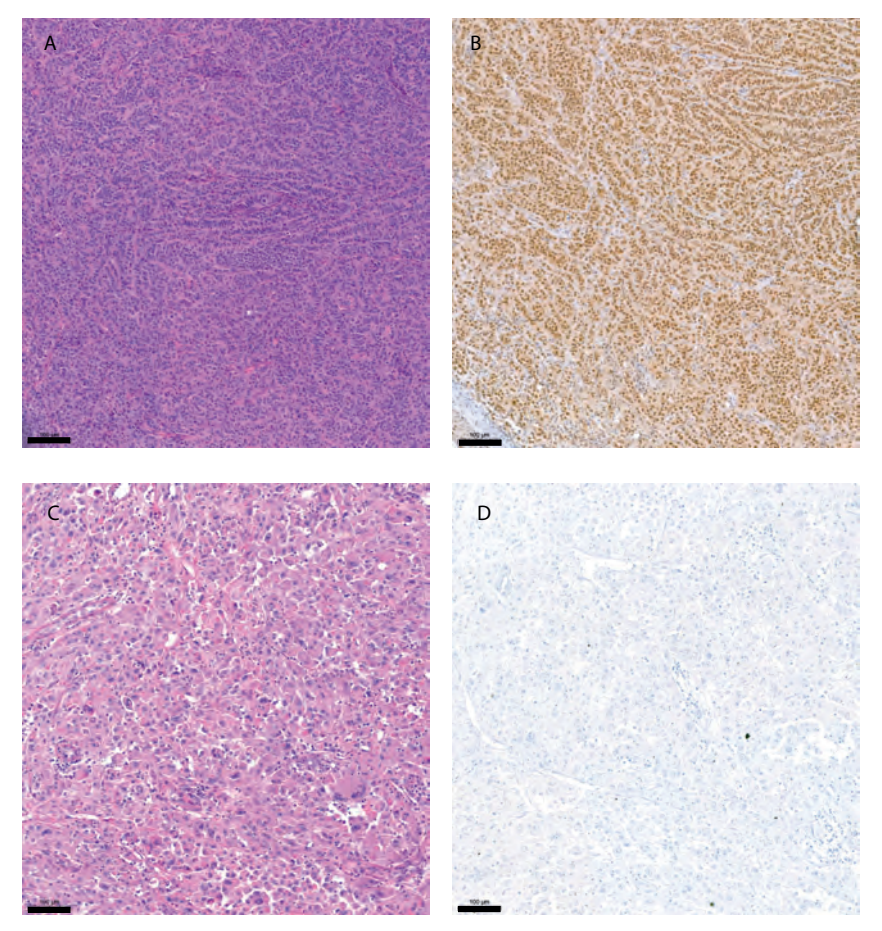


Figure 2: pSMAD2 immunohistochemistry staining. Hematoxylin and Eosin (H&E) stain of a primary melanoma tumor sample (A), and corresponding sample with a positive immunohistochemistry (IHC) staining using a pSMAD2 antibody (B). Figure 2C and 2D showing an H&E stain of a small intestine melanoma metastasis and corresponding negative IHC staining using a pSMAD2 antibody. Yardstick represents 100um.

Table 4: anti-phospho-SMAD2 scores by immunohistochemistry.

	pSMAD2 score		
	Negative	Positive	p-value
Primary tumor samples			0.141
Non-responder	9	5	
Responder	5	11	
Metastatic tumor samples			1.00
Non-responder	9	9	
Responder	9	8	

Discussion

In this study the predictive role of the TGF- β pathway to treatment response with ICI in patients with melanoma was studied. No association between treatment response and TGF-β pathway activity in both primary tumor samples and metastases was found, neither could we identify a clear association with survival. Although significant changes in PAS between primary tumor samples and metastasis were identified in multiple pathways including TGF-B only a consistent association between high Hh pathway scores and resistance to ICI was detected.

Several studies have successfully investigated the value of quantification of PAS using the OncoSIGNal test to predict treatment response and clinical benefit in various cancer types. In salivary duct cancer, the AR pathway predicts clinical benefit, and in patients treated with androgen deprivation therapy the TGF-β and NOTCH pathways could have a prognostic value. (26, 28) In metastatic castration resistant prostate cancer low AR and NOTCH activity and increased Hh pathway activity were associated with resistance to androgen receptor inhibitors. (35). In primary breast cancer, it was reported that immunosuppressive regulatory T-cells were characterized by a high TGF-β and NOTCH PAS. (33) In this study we measured TGF-β pathway activity in patients with melanoma, using the OncoSIGNal pathway analysis. The results were validated using immunohistochemistry for an anti-phospho-SMAD2 antibody, as SMAD2 is a hallmark protein in the TGF-\beta pathway, and elevated SMAD2 levels have been associated with an immune-suppressive microenvironment in melanoma mouse models. (36) No significant association between a positive pSMAD2 IHC staining and elevated TGF-\(\beta \) pathway activity measured by means of mRNA target gene expression was found. In non-small cell lung cancer, SMAD2 was positively associated with PD-L1 expression, suggesting its use as a biomarker for treatment response. (37) Some studies in colorectal cancer and urothelial cell carcinoma suggest a predictive role of the TGF-β pathway for treatment response to ICI. (7, 9) However, the current results in this study do not support the hypothesis that activity of the TGF-\beta pathway is predictive for treatment response to ICI in patients with melanoma.

Several studies are currently investigating the effect of agents blocking TGF-B signaling. This includes agents affecting the TGF-B signaling pathway as monotherapy, or in combination with anti-PD-(L)1 inhibitors. (11, 12, 38-40) Up to now, clinical trials showed only limited effect in treating patients with TGF-β blocking agents and reported substantial toxicity in some cases. (39, 41) Fresolimumab (GC1008), a human IgG4 monoclonal antibody, showed reasonable toxicity, most frequently inducing keratoacanthomas and hyperkeratosis but also squamous cell carcinoma of the skin. However, its effectiveness was limited, with an overall response rate of 3.5% in a study that included mostly patients with advanced melanoma. (42) Bifunctional agents combining TGF- β /PD-L1 inhibition, of which Bintrafusp alfa is the most well-studied, have shown a more favorable toxicity profile, although fatal adverse events such as interstitial lung disease have been reported. (43) The efficacy of Bintrafusp alfa is currently under investigation in several phase I-III trials. (43, 44) Overall, clinical trials blocking TGF- β signaling are in an early stage and require further investigation. In melanoma, studies investigating TGF- β blocking agents are scarce and response rates are low, which is in line with the lack of correlation between response and TGF- β pathway activity in this study.

Disease characteristics, e.g. LDH level and presence of brain metastases, impact the chance of response but are unable to select responders from non-responders. While specific biomarkers such as PD-L1, tumor mutational burden (TMB), and the composition of the TME may to some extent predict response in specific tumor types, this might not be the case in others. Within the tumor, programmed cell death ligand 1 (PD-L1) is the most studied biomarker, based on its mechanism of interaction with PD-1. T-cells can be deactivated when engagement between PD-1 and PD-L1 occurs. Blocking PD-(L)1 can prevent cancer cells from inactivating T-cells. High (TMB) is associated with response and survival to ICI. (45) Samstein et al. found that patients with the 20% highest TMB in various cancer types had a significantly better survival after treatment with ICI. (46) In melanoma specifically, a T-cell infiltrated TME, PD-L1 expression on peripheral T-cells, abundance of specific gut-microbiome genera, and an interferon-gamma signature have been associated with response to ICI. (47-50) However, it has become increasingly clear that these biomarkers do not unequivocally predict response to ICI. (51) For example, the European Medicine Agency (EMA) declined approval of pembrolizumab for TMB-H due to concerns about the large variability in response rates among different tumor types in the KEYNOTE-158 trial. (52) This could also be the case for TGF-β activity, where its use as a predictive biomarker might be of value in urothelial cell carcinoma and colorectal cancer, but not melanoma. Marathesian et al described that enrichment of the fibroblast TGF-β response results in immune evasion by restricting T-cells in the TME, thereby creating non-responding tumors. (9) One could hypothesize that the lack of predictive value of TGF-β in melanoma is related to the composition of the TME, with a relatively lower frequency of cancer-associated-fibroblasts in melanoma compared to colorectal or urothelial cell carcinoma. (53)

We identified Hh PAS as potential predictive biomarker associated with treatment response to ICI in patients with melanoma. An elevated Hh PAS activity correlated

with a shorter PFS and resistance to ICI. Furthermore, in line with previous studies investigating the role of the Hh pathway in metastasis development, we reported a significant increase in Hh PAS between primary tumor samples and metastasis. The Hh pathway is a highly conserved and essential signaling pathway in embryonic development and tissue maintenance. It regulates various processes including cell differentiation, proliferation, and tissue patterning. (54) Hh signaling has also been reported to promote tumor associated macrophage polarization to suppress cytotoxic T-cell recruitment. Furthermore, Hh pathway activation has been described to cause accumulation of regulatory T-cells and increased expression of PD-(L)1. (22, 55) In basal cell carcinoma, genetic alterations resulting in aberrant activation of the Hh PAS are frequently present. Protein patched homolog 1 (PTCH1), a transmembrane receptor protein acting as tumor suppressor, and transmembrane protein smoothened (SMO) are often affected. SMO activation leads to a signaling cascade that involves the transcription of Hh target genes, initializing cell proliferation and leading towards tumor growth. (56) Two Hh inhibitors, Sonidegib and Vismodegib, are approved by the Food and Drug Administration (FDA) and European Medicines Agency (EMA) for treatment in (metastatic) basal cell carcinoma. Both drugs are inhibiting SMO with response rates ranging between 45-60% for locally advanced disease. (57) Due to the absence of Hh pathway associated driver mutations, Hh inhibition has no place in the treatment for melanoma. (58) Unfortunately, Hh inhibition has not been successful in other cancer types besides basal cell carcinoma, possibly due to several factors such as the non-canonical activation of the Sonic hedgehog pathway and gene amplifications. (59, 60) Based on our results linking an elevated Hh pathway activity and resistance to ICI, Hh inhibition might positively impact the TME. Therefore further exploration of the combination therapy with Hh inhibitors and ICI seems opportune.

This study has some limitations. The study was retrospectively designed, and focused exclusively on patients receiving monotherapy ICI. This limits the generalizability of the findings to those treated with dual ICI. While our results provide initial insights into the relationship between TGF-β signaling and ICI resistance in melanoma, and although a clear distinction was defined between responders and non-responders, the relatively small sample size in this exploratory study may limit the detection of significant trends. To provide further confirmation, future studies should be directed at extending this cohort, preferable in a prospective clinical trial.

In conclusion, despite the pathophysiological rationale, TGF-β pathway activation showed no significant relation with treatment response to ICI monotherapy or survival in patients with melanoma. Based on this finding, we expect limited efficacy of agents blocking TGF- β signaling in melanoma. Prospective trials will shine light on the clinical effect of these agents. In contrast, the Hedgehog pathway activity was identified as a possible predictive biomarker associated with both treatment response and survival and warrants further investigation.

Data availability statement

The data that support the findings of this study are available from the corresponding author upon reasonable request.

Conflict of interest

K.F. Bol: consultancy fees (all paid to institute) from MSD and Pierre Fabre.

Yvonne Wesseling: Fulltime employee InnoSIGN Anne van Brussel: Fulltime employee InnoSIGN Diederick Keizer: Fulltime employee InnoSIGN The other authors report no conflict of interest.

Author Contributions

Conceptualization, H.M.W.V., K.F.B., S.G.v.R, methodology, S.G.v.R., H.M.W.V., K.F.B., formal analysis, S.G.v.R., H.M.W.V, K.F.B.; investigation. S.G.v.R., A.L.A., D.V.F.T., C.M.L.H., M.J.B.S, Y.J.W.W., A.C.G.B., D.M.K., H.M.W.V., K.F.B.; resources, S.G.v.R., H.M.W.V., D.V.F.T., K.F.B.; data curation, S.G.v.R., A.L.A., Y.J.W.W., A.C.G.B., D.M.K; writing—original draft preparation, S.G.v.R., H.M.W.V, K.F.B.; writing—review and editing, S.G.v.R., A.L.A., D.V.F.T., C.M.L.H., M.J.B.S, Y.J.W.W., A.C.G.B., D.M.K., H.M.W.V., K.F.B.;; visualization, S.G.v.R. supervision, H.M.W.V. and K.F.B project administration: H.M.W.V. and K.F.B.; funding acquisition, H.M.W.V. and K.F.B.;. All authors have read and agreed to the published version of the manuscript.

References

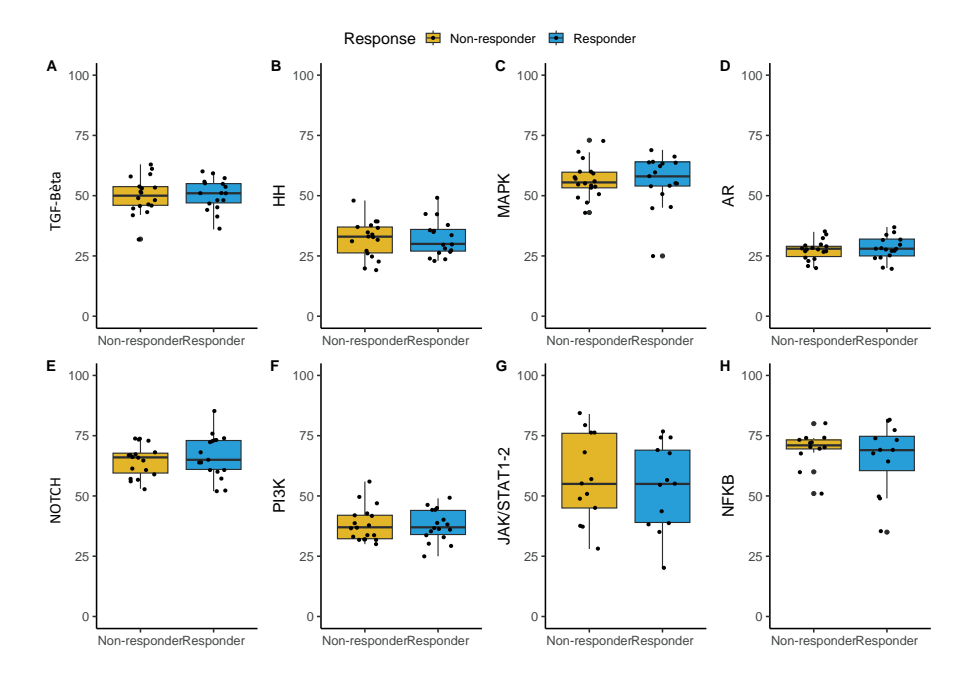
- Sung H, Ferlay J, Siegel RL, Laversanne M, Soerjomataram I, Jemal A, Bray F. Global Cancer Statistics 2020: GLOBOCAN Estimates of Incidence and Mortality Worldwide for 36 Cancers in 185 Countries. CA Cancer J Clin. 2021;71(3):209-49.
- Hodi FS, O'Day SJ, McDermott DF, Weber RW, Sosman JA, Haanen JB, et al. Improved survival with ipilimumab in patients with metastatic melanoma. N Engl J Med. 2010;363(8):711-23.
- 3. Blank CU, Lucas MW, Scolyer RA, van de Wiel BA, Menzies AM, Lopez-Yurda M, et al. Neoadjuvant Nivolumab and Ipilimumab in Resectable Stage III Melanoma. N Engl J Med. 2024.
- 4. Larkin J, Chiarion-Sileni V, Gonzalez R, Grob JJ, Cowey CL, Lao CD, et al. Combined Nivolumab and Ipilimumab or Monotherapy in Untreated Melanoma. N Engl J Med. 2015;373(1):23-34.
- 5. Postow MA, Chesney J, Pavlick AC, Robert C, Grossmann K, McDermott D, et al. Nivolumab and ipilimumab versus ipilimumab in untreated melanoma. N Engl J Med. 2015;372(21):2006-17.
- 6. Wolchok JD, Chiarion-Sileni V, Gonzalez R, Grob JJ, Rutkowski P, Lao CD, et al. Long-Term Outcomes With Nivolumab Plus Ipilimumab or Nivolumab Alone Versus Ipilimumab in Patients With Advanced Melanoma. J Clin Oncol. 2022;40(2):127-37.
- 7. Tauriello DVF, Palomo-Ponce S, Stork D, Berenguer-Llergo A, Badia-Ramentol J, Iglesias M, et al. TGFbeta drives immune evasion in genetically reconstituted colon cancer metastasis. Nature. 2018;554(7693):538-43.
- 8. Loffek S. Transforming of the Tumor Microenvironment: Implications for TGF-beta Inhibition in the Context of Immune-Checkpoint Therapy. J Oncol. 2018;2018:9732939.
- Mariathasan S, Turley SJ, Nickles D, Castiglioni A, Yuen K, Wang Y, et al. TGFbeta attenuates tumour response to PD-L1 blockade by contributing to exclusion of T cells. Nature. 2018;554(7693):544-8.
- Gordian E, Welsh EA, Gimbrone N, Siegel EM, Shibata D, Creelan BC, et al. Transforming growth factor beta-induced epithelial-to-mesenchymal signature predicts metastasis-free survival in nonsmall cell lung cancer. Oncotarget. 2019;10(8):810-24.
- Tauriello DVF, Sancho E, Batlle E. Overcoming TGFbeta-mediated immune evasion in cancer. Nat Rev Cancer. 2022;22(1):25-44.
- 12. Ciardiello D, Elez E, Tabernero J, Seoane J. Clinical development of therapies targeting TGFbeta: current knowledge and future perspectives. Ann Oncol. 2020;31(10):1336-49.
- 13. Massague J. TGFbeta in Cancer. Cell. 2008;134(2):215-30.
- 14. Morikawa M, Koinuma D, Miyazono K, Heldin CH. Genome-wide mechanisms of Smad binding. Oncogene. 2013;32(13):1609-15.
- Miyazawa K, Miyazono K. Regulation of TGF-beta Family Signaling by Inhibitory Smads. Cold Spring Harb Perspect Biol. 2017;9(3).
- Bu MT, Chandrasekhar P, Ding L, Hugo W. The roles of TGF-beta and VEGF pathways in the suppression of antitumor immunity in melanoma and other solid tumors. Pharmacol Ther. 2022;240:108211.
- Lainé A, Labiad O, Hernandez-Vargas H, This S, Sanlaville A, Léon S, et al. Regulatory T cells promote cancer immune-escape through integrin ανβ8-mediated TGF-β activation. Nat Commun. 2021;12(1):6228.
- Li Z, Wang F, Dang J, Cheng F, Zheng F. Bidirectional regulation between tumor cell-intrinsic PD-L1 and TGF-β1 in epithelial-to-mesenchymal transition in melanoma. Transl Cancer Res. 2022;11(10):3698-710.

- Tuncer E, Calcada RR, Zingg D, Varum S, Cheng P, Freiberger SN, et al. SMAD signaling promotes melanoma metastasis independently of phenotype switching. J Clin Invest. 2019;129(7):2702-16.
- 20. Ma D, Qiao L, Guo B. Smad7 suppresses melanoma lung metastasis by impairing Tregs migration to the tumor microenvironment. Am J Transl Res. 2021;13(2):719-31.
- Wang P, Fan J, Chen Z, Meng ZQ, Luo JM, Lin JH, et al. Low-level expression of Smad7 correlates with lymph node metastasis and poor prognosis in patients with pancreatic cancer. Ann Surg Oncol. 2009;16(4):826-35.
- 22. Petty AJ, Li A, Wang X, Dai R, Heyman B, Hsu D, et al. Hedgehog signaling promotes tumor-associated macrophage polarization to suppress intratumoral CD8+ T cell recruitment. J Clin Invest. 2019;129(12):5151-62.
- 23. Grund-Groschke S, Stockmaier G, Aberger F. Hedgehog/GLI signaling in tumor immunity new therapeutic opportunities and clinical implications. Cell Commun Signal. 2019;17(1):172.
- 24. Eisenhauer EA, Therasse P, Bogaerts J, Schwartz LH, Sargent D, Ford R, et al. New response evaluation criteria in solid tumours: revised RECIST guideline (version 1.1). Eur J Cancer. 2009;45(2):228-47.
- 25. Verhaegh W, Van de Stolpe A. Knowledge-based computational models. Oncotarget. 2014;5(14):5196-7.
- 26. Lassche G, Tada Y, van Herpen CML, Jonker MA, Nagao T, Saotome T, et al. Predictive and Prognostic Biomarker Identification in a Large Cohort of Androgen Receptor-Positive Salivary Duct Carcinoma Patients Scheduled for Combined Androgen Blockade. Cancers (Basel). 2021;13(14).
- 27. Sieuwerts AM, Inda MA, Smid M, van Ooijen H, van de Stolpe A, Martens JWM, Verhaegh WFJ. ER and PI3K Pathway Activity in Primary ER Positive Breast Cancer Is Associated with Progression-Free Survival of Metastatic Patients under First-Line Tamoxifen. Cancers (Basel). 2020;12(4).
- 28. van Boxtel W, Verhaegh GW, van Engen-van Grunsven IA, van Strijp D, Kroeze LI, Ligtenberg MJ, et al. Prediction of clinical benefit from androgen deprivation therapy in salivary duct carcinoma patients. Int J Cancer. 2020;146(11):3196-206.
- van de Stolpe A, Verhaegh W, Blay JY, Ma CX, Pauwels P, Pegram M, et al. RNA Based Approaches to Profile Oncogenic Pathways From Low Quantity Samples to Drive Precision Oncology Strategies. Front Genet. 2020;11:598118.
- 30. van Lieshout L, van de Stolpe A, van der Ploeg P, Bowtell D, de Hullu J, Piek J. Signal Transduction Pathway Activity in High-Grade, Serous Ovarian Carcinoma Reveals a More Favorable Prognosis in Tumors with Low PI3K and High NF-kappaB Pathway Activity: A Novel Approach to a Long-Standing Enigma. Cancers (Basel). 2020;12(9).
- 31. van Ooijen H, Hornsveld M, Dam-de Veen C, Velter R, Dou M, Verhaegh W, et al. Assessment of Functional Phosphatidylinositol 3-Kinase Pathway Activity in Cancer Tissue Using Forkhead Box-O Target Gene Expression in a Knowledge-Based Computational Model. Am J Pathol. 2018;188(9):1956-72.
- 32. van Weelden WJ, van der Putten LJM, Inda MA, van Brussel A, Snijders M, Schriever LMM, et al. Oestrogen receptor pathway activity is associated with outcome in endometrial cancer. Br J Cancer. 2020;123(5):785-92.
- Wesseling-Rozendaal Y, van Doorn A, Willard-Gallo K, van de Stolpe A. Characterization of Immunoactive and Immunotolerant CD4+ T Cells in Breast Cancer by Measuring Activity of Signaling Pathways That Determine Immune Cell Function. Cancers (Basel). 2022;14(3).
- 34. Voorneveld PW, Jacobs RJ, De Miranda NF, Morreau H, van Noesel CJ, Offerhaus GJ, et al. Evaluation of the prognostic value of pSMAD immunohistochemistry in colorectal cancer. Eur J Cancer Prev. 2013;22(5):420-4.

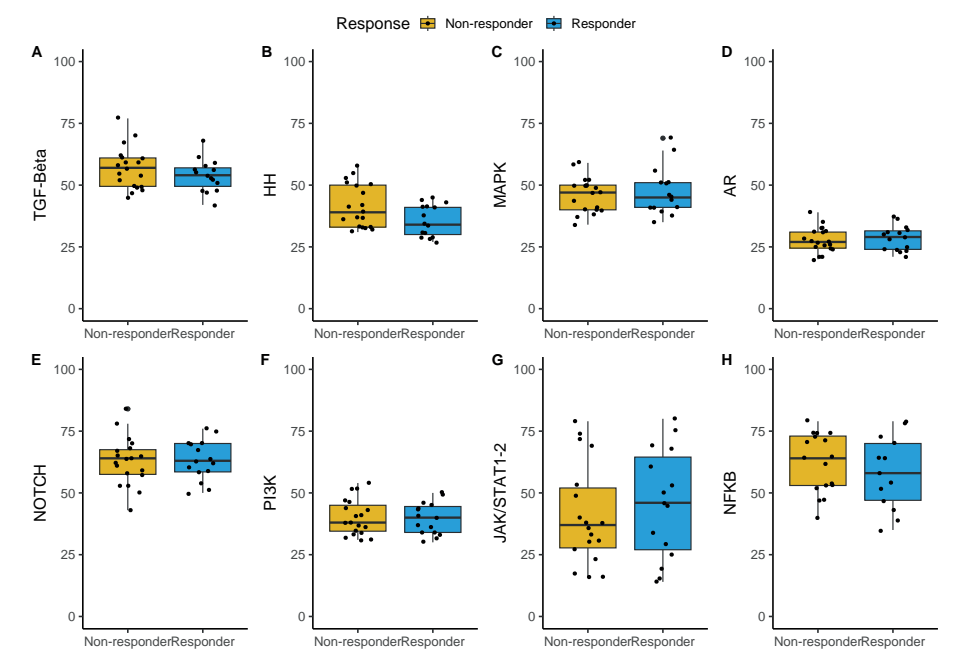
- Menssouri N, Poiraudeau L, Helissey C, Bigot L, Sabio J, Ibrahim T, et al. Genomic profiling of metastatic castration-resistant prostate cancer samples resistant to androgen-receptor pathway inhibitors. Clin Cancer Res. 2023.
- 36. Zhou WJ, Wang HY, Zhang J, Dai HY, Yao ZX, Zheng Z, et al. NEAT1/miR-200b-3p/SMAD2 axis promotes progression of melanoma. Aging (Albany NY). 2020;12(22):22759-75.
- David JM, Dominguez C, McCampbell KK, Gulley JL, Schlom J, Palena C. A novel bifunctional anti-PD-L1/TGF-beta Trap fusion protein (M7824) efficiently reverts mesenchymalization of human lung cancer cells. Oncoimmunology. 2017;6(10):e1349589.
- 38. Paz-Ares L, Kim TM, Vicente D, Felip E, Lee DH, Lee KH, et al. Bintrafusp Alfa, a Bifunctional Fusion Protein Targeting TGF-beta and PD-L1, in Second-Line Treatment of Patients With NSCLC: Results From an Expansion Cohort of a Phase 1 Trial. J Thorac Oncol. 2020;15(7):1210-22.
- 39. Melisi D, Oh DY, Hollebecque A, Calvo E, Varghese A, Borazanci E, et al. Safety and activity of the TGFbeta receptor I kinase inhibitor galunisertib plus the anti-PD-L1 antibody durvalumab in metastatic pancreatic cancer. J Immunother Cancer. 2021;9(3).
- Wheatley-Price P, Chu Q, Bonomi M, Seely J, Gupta A, Goss G, et al. A Phase II Study of PF-03446962 in Patients with Advanced Malignant Pleural Mesothelioma. CCTG Trial IND.207. J Thorac Oncol. 2016;11(11):2018-21.
- Teixeira AF, Ten Dijke P, Zhu HJ. On-Target Anti-TGF-beta Therapies Are Not Succeeding in Clinical Cancer Treatments: What Are Remaining Challenges? Front Cell Dev Biol. 2020;8:605.
- 42. Morris JC, Tan AR, Olencki TE, Shapiro GI, Dezube BJ, Reiss M, et al. Phase I study of GC1008 (fresolimumab): a human anti-transforming growth factor-beta (TGFbeta) monoclonal antibody in patients with advanced malignant melanoma or renal cell carcinoma. PLoS One. 2014;9(3):e90353.
- 43. Yoo C, Oh DY, Choi HJ, Kudo M, Ueno M, Kondo S, et al. Phase I study of bintrafusp alfa, a bifunctional fusion protein targeting TGF-β and PD-L1, in patients with pretreated biliary tract cancer. J Immunother Cancer. 2020;8(1).
- 44. Tan B, Khattak A, Felip E, Kelly K, Rich P, Wang D, et al. Bintrafusp Alfa, a Bifunctional Fusion Protein Targeting TGF-beta and PD-L1, in Patients with Esophageal Adenocarcinoma: Results from a Phase 1 Cohort. Target Oncol. 2021;16(4):435-46.
- 45. Hugo W, Zaretsky JM, Sun L, Song C, Moreno BH, Hu-Lieskovan S, et al. Genomic and Transcriptomic Features of Response to Anti-PD-1 Therapy in Metastatic Melanoma. Cell. 2016;165(1):35-44.
- 46. Samstein RM, Lee CH, Shoushtari AN, Hellmann MD, Shen R, Janjigian YY, et al. Tumor mutational load predicts survival after immunotherapy across multiple cancer types. Nat Genet. 2019;51(2):202-6.
- 47. Grasso CS, Tsoi J, Onyshchenko M, Abril-Rodriguez G, Ross-Macdonald P, Wind-Rotolo M, et al. Conserved Interferon-γ Signaling Drives Clinical Response to Immune Checkpoint Blockade Therapy in Melanoma. Cancer Cell. 2020;38(4):500-15.e3.
- 48. Jacquelot N, Roberti MP, Enot DP, Rusakiewicz S, Ternès N, Jegou S, et al. Predictors of responses to immune checkpoint blockade in advanced melanoma. Nat Commun. 2017;8(1):592.
- Lee KA, Thomas AM, Bolte LA, Björk JR, de Ruijter LK, Armanini F, et al. Cross-cohort gut microbiome associations with immune checkpoint inhibitor response in advanced melanoma. Nat Med. 2022;28(3):535-44.
- 50. Costa Svedman F, Das I, Tuominen R, Darai Ramqvist E, Höiom V, Egyhazi Brage S. Proliferation and Immune Response Gene Signatures Associated with Clinical Outcome to Immunotherapy and Targeted Therapy in Metastatic Cutaneous Malignant Melanoma. Cancers (Basel). 2022;14(15).

- Morrison C, Pabla S, Conroy JM, Nesline MK, Glenn ST, Dressman D, et al. Predicting response to checkpoint inhibitors in melanoma beyond PD-L1 and mutational burden. J Immunother Cancer. 2018;6(1):32.
- 52. Marabelle A, Fakih M, Lopez J, Shah M, Shapira-Frommer R, Nakagawa K, et al. Association of tumour mutational burden with outcomes in patients with advanced solid tumours treated with pembrolizumab: prospective biomarker analysis of the multicohort, open-label, phase 2 KEYNOTE-158 study. Lancet Oncol. 2020;21(10):1353-65.
- 53. Joshi RS, Kanugula SS, Sudhir S, Pereira MP, Jain S, Aghi MK. The Role of Cancer-Associated Fibroblasts in Tumor Progression. Cancers (Basel). 2021;13(6).
- 54. Carballo GB, Honorato JR, de Lopes GPF, Spohr T. A highlight on Sonic hedgehog pathway. Cell Commun Signal. 2018;16(1):11.
- 55. de la Roche M, Ritter AT, Angus KL, Dinsmore C, Earnshaw CH, Reiter JF, Griffiths GM. Hedgehog signaling controls T cell killing at the immunological synapse. Science. 2013;342(6163):1247-50.
- 56. Nguyen NM, Cho J. Hedgehog Pathway Inhibitors as Targeted Cancer Therapy and Strategies to Overcome Drug Resistance. Int J Mol Sci. 2022;23(3).
- 57. Migden MR, Guminski A, Gutzmer R, Dirix L, Lewis KD, Combemale P, et al. Treatment with two different doses of sonidegib in patients with locally advanced or metastatic basal cell carcinoma (BOLT): a multicentre, randomised, double-blind phase 2 trial. Lancet Oncol. 2015;16(6):716-28.
- 58. Grund-Gröschke S, Ortner D, Szenes-Nagy AB, Zaborsky N, Weiss R, Neureiter D, et al. Epidermal activation of Hedgehog signaling establishes an immunosuppressive microenvironment in basal cell carcinoma by modulating skin immunity. Mol Oncol. 2020;14(9):1930-46.
- Giroux-Leprieur E, Costantini A, Ding VW, He B. Hedgehog Signaling in Lung Cancer: From Oncogenesis to Cancer Treatment Resistance. Int J Mol Sci. 2018;19(9).
- 60. Giammona A, Crivaro E, Stecca B. Emerging Roles of Hedgehog Signaling in Cancer Immunity. Int J Mol Sci. 2023;24(2).

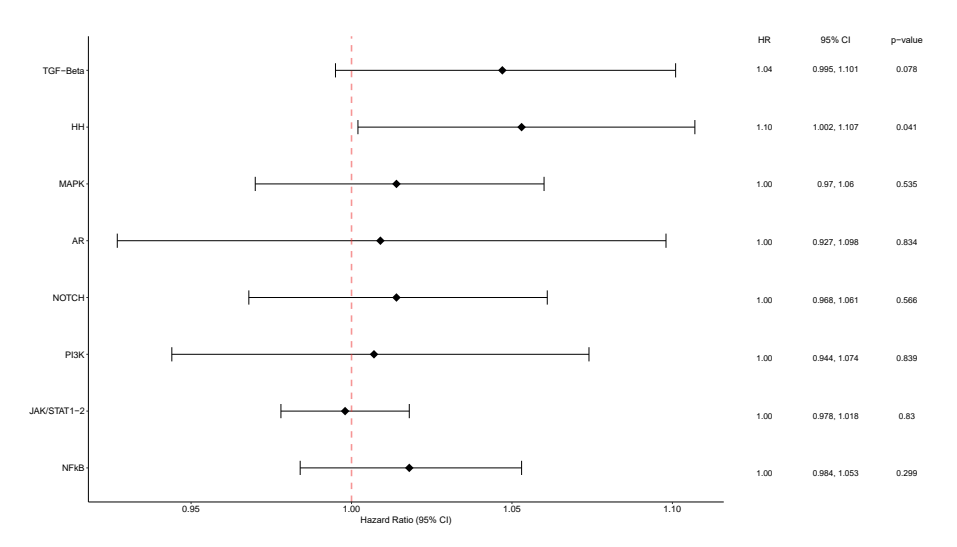
5



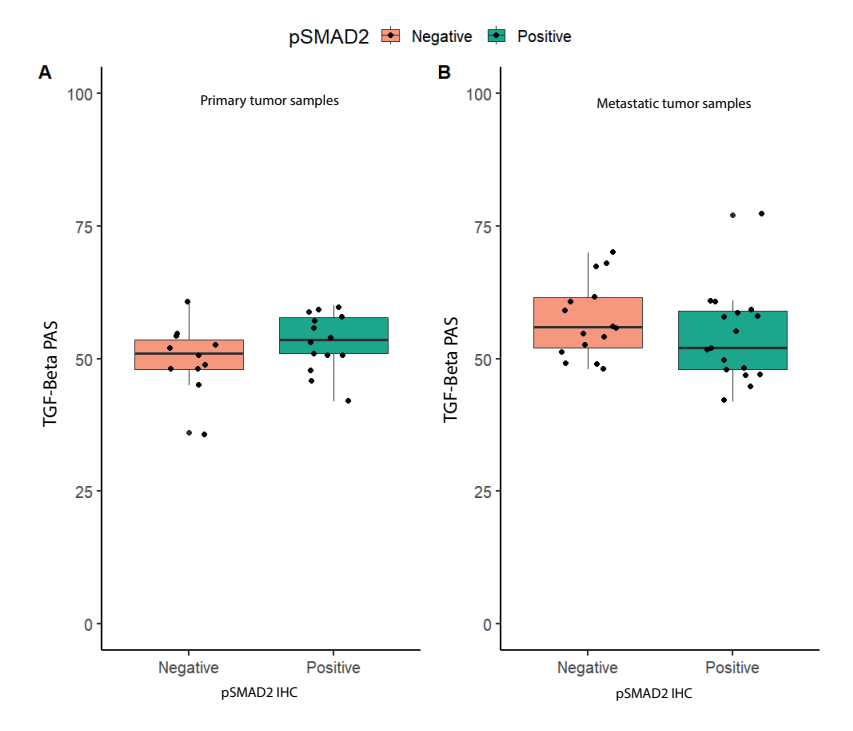
Supplementary Figure S1: Individual Signal Transduction Pathway scores in primary tumor samples. Boxplots reflecting the individual pathway activity scores in primary tumor samples for TGF- β , Hh, MAPK, AR, NOTCH, PI3K, JAK/STAT1-2, and NFkB pathways. Abbreviations: Transforming growth factor bèta (TGF- β), Hedgehog (Hh), Mitogen-Activated Protein Kinase (MAPK), Androgen Receptor (AR), Phosphoinositide 3-Kinase (PI3K), Janus Kinase/signal transducer and activator of transcription (JAK-STAT1/2) and Nuclear Factor kappa B (NFkB).



Supplementary Figure S2: Individual Signal Transduction Pathway scores in metastatic tumor samples. Boxplots reflecting the individual pathway activity scores in metastatic tumor samples for TGF- β, Hh, MAPK, AR, NOTCH, PI3K, JAK/STAT1-2, and NFkB pathways. Abbreviations: Transforming growth factor bèta (TGF-β), Hedgehog (Hh), Mitogen-Activated Protein Kinase (MAPK), Androgen Receptor (AR), Phosphoinositide 3-Kinase (PI3K), Janus Kinase/signal transducer and activator of transcription (JAK-STAT1/2) and Nuclear Factor kappa B (NFκB).



Supplementary figure S3: Univariate cox regression analysis on progression free survival in metastatic tumor samples. Forrest plot reflecting the univariate cox regression analysis on progression free survival (PFS) for individual pathway activity scores in metastatic tumor samples (TGF- β, Hh, MAPK, AR, NOTCH, PI3K, JAK/STAT1-2, and NFkB pathways). Abbreviations: Transforming growth factor bèta (TGF-B), Hedgehog (Hh), Mitogen-Activated Protein Kinase (MAPK), Androgen Receptor (AR), Phosphoinositide 3-Kinase (PI3K), Janus Kinase/signal transducer and activator of transcription (JAK-STAT1/2) and Nuclear Factor kappa B (NFxB).



Supplementary figure S4: Correlation TGF-Beta PAS and pSMAD2 staining. Anti-phospho-SMAD2 scores by immunohistochemistry (IHC) were matched with the corresponding TGF-Beta pathway activity scores for the primary tumor samples (A) and metastatic tumor samples (B).





Chapter 6

The prognostic relevance of MRI characteristics in myxofibrosarcoma patients treated with neoadjuvant radiotherapy

Stefan G. van Ravensteijn*, Maikel J.L. Nederkoorn*, Tom C.P. Wal, Yvonne M.H. Versleijen-Jonkers, Pètra M. Braam, Uta E. Flucke, Johannes J. Bonenkamp, Bart H.W. Schreuder, Carla M.L. van Herpen, Johannes H.W. de Wilt, Ingrid M.E. Desar** and Jacky W.J. de Rooy**

^{*} These authors contributed equally to this work

^{**} These authors contributed equally to this work

Abstract

To improve local control, neoadjuvant radiotherapy (nRT) followed by surgery is standard of care in myxofibrosarcoma (MFS) because of their infiltrative growth pattern. Nevertheless, local recurrence rates are high. Data on prognostic factors for poor clinical outcomes are lacking. This retrospective study therefore investigates the prognostic relevance of Magnetic Resonance Imaging (MRI) characteristics before and after nRT in 40 MFS patients, and their association with Disease-Free Survival (DFS) and Overall Survival (OS). A vascular pedicle, defined as extra-tumoral vessels at the tumor periphery, was observed in 12 patients (30.0%) pre-nRT and remained present post-nRT in all cases. Patients with a vascular pedicle had worse DFS (HR 5.85; 95% CI 1.56-21.90; p=0.009) and OS (HR 9.58; 95% CI 1.91-48.00; p=0.006). An infiltrative growth pattern, referred to as a tail sign, was observed in 22 patients (55.0%) pre-nRT and in 19 patients (47.5%) post-nRT, and was post-nRT associated with worse DFS (HR 6.99; 95% CI 1.39-35.35; p=0.019). The percentage of tumor necrosis estimated by MRI was increased post-nRT, but was not associated with survival outcomes. The presence of a tail sign or vascular pedicle on MRI could support the identification of patients at risk for poor clinical outcomes after nRT.

Introduction

Myxofibrosarcoma (MFS) is a histological subtype of Soft Tissue Sarcoma (STS), histologically characterized by pleomorphism, myxoid stroma and curvilinear vasculature. (1) This malignant lesion of mesenchymal origin represents approximately 5% of all sarcoma entities, with an age-standardized incidence rate of 0.19 per 100,000 persons-year in Europe. (2) MFS most commonly presents in the extremities or trunk of patients in the sixth to eight decades of life, with a particular predilection for the lower limbs. (1, 3) The mainstay of treatment for localized primary disease involves surgical resection, commonly applied in conjunction with neoadjuvant radiotherapy (nRT) to optimize local control. MFS is described as a locally aggressive tumor with a distinctive infiltrative pattern of growth, resulting in particularly high rates of local recurrence (LR), ranging from 20-60%. (3-12) Distant metastasis will eventually develop in 20-40% of patients, despite adequate treatment of the primary tumor. (3-12) Several prognostic factors for LR and overall survival (OS) have been described in MFS, including tumor size, and patient age and sex. (3-6, 8, 11, 13) A recently published large series from the Netherlands comprising 908 MFS patients reported a median OS of 155 months, which was significantly lower in patients who experienced LR (64.0 months) or metastatic disease (34.3 months). (3) A comprehensive understanding of prognostic factors for patients at risk for poor clinical outcomes despite adequate initial treatment might support the optimization of primary treatment and follow up schedules.

Recently, neoadjuvant radiotherapy has been replacing adjuvant radiotherapy as the preferred treatment modality, as it enables more accurate definition of the treatment field and therefore limits damage to adjacent structures. (14, 15) The role of nRT has been investigated in different histological subtypes of STS, but not in MFS, where tumor-positive surgical margins and high tumor necrosis have been identified as predictors for worse clinical outcome. (16-21) A high percentage of tumor necrosis, histologically assessed, after nRT is the most commonly used surrogate marker for treatment response, however this has not been validated in STS and small studies present conflicting data. (18-20, 22)

Magnetic Resonance Imaging (MRI) is standard of care in MFS diagnosis and restaging after nRT. Specific MRI features at diagnosis, in particular the presence of longitudinal spreading, also referred to as a tail sign, has been recognized as an MRI predictor prognostic for LR and worse OS. (5, 6, 23, 24) The value of post-nRT MRI characteristics as prognostic factors for disease recurrence or OS remains ambiguous and should be explored in further detail. Being able to identify high-risk patients in

an early stage might support the development of intensified primary treatment and follow up strategies for these patients. We therefore aim to evaluate the prognostic relevance of MRI characteristics in MFS patients who received nRT.

Methods

Study objectives

The primary objective of this retrospective study was to evaluate the prognostic relevance of pre- and post-nRT MRI characteristics in MFS patients. The secondary objective of this study was to identify factors prognostic for DFS and OS. In addition, the effects of the WHO-performance status, surgical margin status, the time interval between nRT and restaging MRI, and the time interval between nRT and surgery on DFS and OS were investigated.

Study population

Data from patients diagnosed with MFS and treated with nRT in a tertiary sarcoma expertise center in the Netherlands between 2014 and 2022 were retrospectively collected. Histological diagnosis of MFS was confirmed by an experienced sarcoma pathologist (U.E.F.). Patients were included in this study if both pre- and post-nRT MRI data were available. This study was conducted according to the principles of the declaration of Helsinki. Written informed consent was provided by all participating subjects (NCT05373810).

Magnetic resonance imaging

Only patients with MRI examinations with the following minimum requirements were included in this study: all MRI studies were performed on a 1.5 Tesla scanner using a protocol including T1-weighted (T1w) and T2-weighted (T2w) sequences with fat saturation, and T1w images with fat saturation after intravenous administration of Gadolinium (Gd). All MRI studies, both pre- and post-nRT, were revised by an experienced musculoskeletal radiologist (J.W.J.d.R.). The musculoskeletal radiologist was blinded to the clinical and histopathological data.

Data on pre- and post-nRT MRI characteristics were systematically collected. Gd-enhancement was evaluated on Tiw sequences with fat saturation using the grading system proposed by Sambri et al. (5, 6) Tiw, T2w and Gd-enhanced studies were used to evaluate the parameters described below, including the presence of peritumoral edema or intratumoral signs of bleeding, vascular pedicle, necrosis percentage, tumor volume and tumor size. Myxoid matrix content was recognized

as the presence of high signal on fluid-sensitive sequences (T2w), slightly less than the signal of water. (5, 6) A vascular pedicle was defined as abnormal tortuous feeding extra-tumoral vessels, whether or not coalescing as a clump, at one site along the lesion periphery. This peri-tumoral neo-angiogenesis can be identified as prominent flow voids (i.e. signal loss). (25, 26) The percentage of tumor necrosis was evaluated using Tiw sequences with fat saturation after Gd contrast enhancement on a semi-quantitively base (<50.0% or ≥50.0%). Tumor size was measured as the largest diameter of the mass in any direction of the imaging plane. Tumor shape was classified as monolobular, lobular or polylobulated. Tumor location was recorded as superficial (above the fascia) or deep (below the fascia). The number of anatomical compartments involved was registered, as was the tumor demarcation (unsharp, moderately sharp, sharp). The presence of an infiltrative growth pattern, referred to as a tail sign, was determined and differentiated from peritumoral edema by its enhancement on post-contrast images. A tail sign was deemed present if the tail was at least ten millimeters (mm) in length and two mm in width. (23, 27)

Clinical and histopathological data

Clinical data were retrieved from a prospective clinical registry database and included patient age and BMI at diagnosis, sex, tumor site, WHO-performance status, date and dose schedule of nRT, timing of MRI studies, the occurrence of LR, time interval between surgery and LR, treatment for LR, the occurrence of metastasis, time interval between surgery and metastasis, treatment for metastasis and date of death or last follow-up. Histopathological data included tumor grading and classification of surgical margins according to the guidelines of the American Joint Committee on Cancer (Ro: tumor-free margin, R1: microscopic positive margin and R2: macroscopic positive margin). (28)

Statistical analysis

Descriptive statistics were used to describe baseline patient characteristics. Mean or median values were described as applicable. Continuous variables were compared through t-test or Mann-Whitney U test. To compare categorical variables, McNemar-(Bowker) tests were used. Values were considered significant with a p-value ≤ 0.05 . Univariate survival analyses were performed according to the Kaplan-Meier method. Multivariable cox-regression was performed using forward wald selection. Variables that revealed a p-value ≤0.10 were included in the multivariable model. Statistical analyses were performed using IBM SPSS statistics 25 (version 3.6.2) and RStudio (version 1.1.463).

Results

The total cohort comprised 40 MFS patients. Patient characteristics are depicted in **Table 1**. The majority of primary MFS tumors were located in the lower extremities (77.5%). Most lesions were located below the fascia (70.0%) and were of high histologic grade (92.5%). The most frequently applied nRT dose was 50 Gray (Gy) in 25 fractions (25 × 2 Gy) (87.5%). Four patients (10.0%) received 45 Gy in 15 fractions (15 × 3 Gy) and one patient (2.5%) received 25 Gy in 5 fractions (5 × 5 Gy) based on the physicians' choice. All patients with MFS involving the extremities who received nRT underwent limb-sparing resection. The median time intervals between nRT and restaging MRI or surgery were 32 (range 12-61) days and 51 (range 26-117) days, respectively. Negative surgical margins (R0), were reported in 90.0% of cases. Microscopic-positive surgical margins (R1) were described in 5.0% of patients and 5.0% of cases had macroscopic-positive surgical margins (R2).

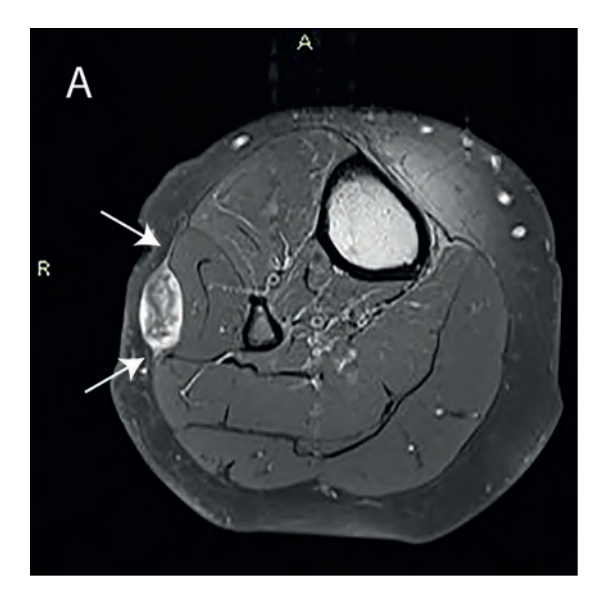
Neoadjuvant radiotherapy induced changes on MRI characteristics

Pre-nRT MRI studies were predominantly performed at the primary referral center and therefore there was a large variance in MRI devices and pulse sequences. An overview of the observed pre- and post-nRT MRI characteristics is provided in **Table 2**. The median tumor diameter (81 mm pre-nRT versus (vs) 92 mm post-nRT, p=0.002) and median tumor volume (224 cm³ pre-nRT vs 298 cm³ post-nRT, p=0.008) were significantly increased post-nRT. The amount of patients with a tumor necrosis percentage \geq 50.0% significantly increased post-nRT (10.0% pre-nRT vs 45.0% post-nRT, p=0.046). Three patients showed no signs of tumor necrosis post-nRT. Furthermore, there was a significant increase in the number of cases that showed tumor bleeding (47.5% pre-nRT vs 67.5% post-nRT, p=0.021). Peritumoral edema was present in 97.5% of cases pre-nRT and in 100.0% of cases post-nRT (p=1.000).

Table 1: Baseline patient and MRI characteristics. All MRI characteristics reflected in this table were described based on pre-nRT imaging.

Number of patients = 40	
Gender n (%)	
Male	23 (57.5)
Female	17 (42.5)
Median BMI at diagnosis (range)	25.2 (19.8-45.3)
Median age in years at diagnosis (range)	67 (48-86)
Primary tumor site n (%)	
Upper leg	24 (60.0)
Lower leg	7 (17.5)
Lower arm	2 (5.0)
Shoulder	2 (5.0)
Knee	2 (5.0)
Upper arm	1 (2.5)
Abdominal wall	1 (2.5)
Thoracic wall	1 (2.5)
WHO-performance status (%)	
0	24 (60.0)
1	16 (40.0)
Radiotherapy dosing schedule (Gy) n (%)	
50 Gy in 25 fractions	35 (87.5)
45 Gy in 15 fractions	4 (10.0)
25 Gy in 5 fractions	1 (2.5)
Surgical margin	
Ro	36 (90.0)
R1	2 (5.0)
R2	2 (5.0)
Tumor grading n (%)	
High grade	37 (92.5)
Low grade	2 (5.0)
Unknown	1 (2.5)
Tumor depth on MRI, n (%)	
Deep	28 (70.0)
Superficial	12 (30.0)
Myxoid type based on MRI, n (%)	
Grade 0	5 (12.5)
Grade 1	9 (22.5)
Grade 2	21 (52.5)
Grade 3	5 (12.5)
Gadolinium-enhancement on MRI, n (%)	
Grade 0	6 (15.0)
Grade 1	8 (20.0)
Grade 2	11 (27.5)
Grade 3	15 (37.5)

A vascular pedicle, defined as abnormal tortuous feeding extra-tumoral vessels, whether or not coalescing as a clump, at one site along the lesion periphery (**Figure 1**), was observed in 12 patients pre-nRT (30.0%) and remained present post-nRT in all cases. No new cases with a vascular pedicle were identified on post-nRT MRI. When a vascular pedicle was present, 1 out of 12 patients had tumor positive surgical margins, categorized as R1 or R2. In the absence of a vascular pedicle, 3 out of 28 patients had tumor-positive surgical margins (p=0.824). An infiltrative pattern with extensions of \geq 10 mm in length and \geq 2 mm in width (**Figure 1**), also referred to as a tail sign, was present in 22 cases pre-nRT (55.0%) and in 19 cases (47.5%) post-nRT (p=0.453). All lesions with a tail sign observed post-nRT were already observed pre-nRT. No new cases with a tail sign-containing lesion were identified post-nRT. Furthermore, no significant changes were observed in tail sign length (p=0.134) or tail sign width (p=0.201) post-nRT. In the presence of a tail sign post-nRT, 4 out of 19 patients had tumor-surgical margins. In its absence, 0 out of 21 patients had tumor positive surgical margins (p=0.027).



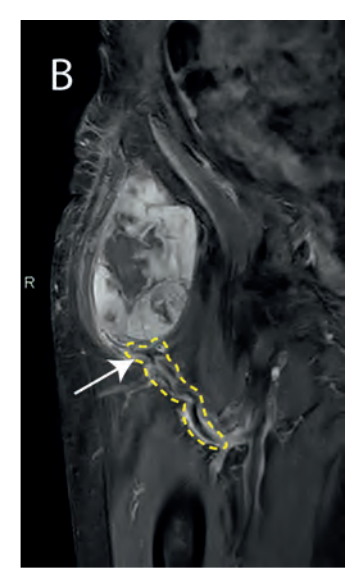


Figure 1: (**A**) Axial contrast enhanced T1-weighted image with fat saturation of a right lower leg with a superficial myxofibrosarcoma. Arrows are indicating the tail sign. (**B**) Coronal contrast-enhanced T1 weighted image of a right upper leg with a deep myxofibrosarcoma. The area outlined in yellow highlights the pathologic tumor-feeding vasculature and the arrow indicates the vascular pedicle.

 Table 2: Pre-and post-neoadjuvant radiotherapy MRI characteristics.

MRI Characteristic	Pre-radiotherapy MRI	Post-radiotherapy MRI	<i>p</i> -value
Median tumor diameter in mm (range)	81 (16-231)	92 (0-273)	0.002
Median tumor volume in cm³ (range)	224 (2.6 – 3114.3)	298 (1.2 – 4440.8)	0.008
Tail sign present n (%)	22 (55.0)	19 (47.5)	0.453
Median tail sign length in mm (range)	30 (10-60)	27(12-91)	0.134
Median tail sign width in mm (range)	5 (2-11)	6 (2-21)	0.201
Vascular pedicle present n (%)			1.000
Yes	12 (30.0)	12 (30.0)	
No	28 (70.0)	28 (70.0)	
Necrosis % n (%)			0.046
<50.0%	34 (85.0)	21 (52.5)	
>50.0%	4 (10.0)	18 (45.0)	
Unassessable	2 (5.0)	1 (2.5)	
T1 00			
Edema n (%)			1.000
Present	39 (97.5)	40 (100.0)	
Not present	1 (2.5)	0 (0.0)	
Tumor demarcation n (%)			0.317
Unsharp	5 (12.5)	3 (7.5)	
Moderately sharp	6 (15.0)	7 (17.5)	
Sharp	29 (72.5)	29 (72.5)	
Unassessable		1 (2.5)	
Neurovascular relation n (%)			0.135
No relation	32 (80.0)	36 (90.0)	0.155
Close relation	6 (15.0)	3 (7.5)	
Encasement	2 (5.0)	1(2.5)	
	2 (3.0)	1 (2.3)	
Number of compartments n (%)			1.000
1	30 (75.0)	29 (72.5)	
2/3	10 (25.0)	11 (27.5)	
Tumor bleeding n (%)			0.021
Present	19 (47.5)	27 (67.5)	
Not present	21 (52.5)	13 (32.5)	
Tumor shape n (%)			0.607
Homogenous	2 (5.0)	3 (7.5)	/
Lobular	5 (12.5)	5 (12.5)	
Polylobular	32 (80.0)	30 (75.0)	
Multi-locular	1 (2.5)	1 (2.5)	
Unassessable	· (~·J)	1(2.5)	
CHASSESSADIC		1 (4.3)	

Prognostic relevance of post-nRT MRI characteristics

The median follow up after surgery was 44 (range 2-103) months. Throughout the follow up period, LR occurred in four patients (10.0%) and nine patients (22.5%) developed distant metastases. Nine patients (22.5%) deceased of whom seven passed of disease-related causes. **Figure 2** depicts the Kaplan-Meier estimates for DFS and OS for the entire patient cohort over time. Median DFS and OS were not reached during the follow up period.

An exploratory multivariable cox regression analysis was performed using forward Wald selection on the MRI characteristics depicted in **Table 2**, with the inclusion of WHO-performance status, surgical margin, tumor depth, myxoid type on MRI and Gd-enhancement. The presence of a vascular pedicle (Hazard ratio (HR) 5.85; 95% Confidence interval (CI) 1.56-21.90; p=0.009) and a tail sign (HR 6.99; 95% CI 1.39-35.35; p=0.019) post-nRT were associated with worse DFS. The presence of a vascular pedicle post-nRT was the sole factor associated with worse OS (HR 9.58; 95% CI 1.91-48.00; p=0.006). **Figure 3** depicts the Kaplan-Meier estimates for DFS and OS in relation to the presence of a vascular pedicle or tail sign post-nRT. None of the other remaining patient- or MRI- characteristics post-nRT demonstrated a significant association with DFS or OS.

Discussion

In this large retrospective MFS series investigating the prognostic relevance of MRI characteristics in patients who received nRT, the presence of a vascular pedicle or tail sign on post-nRT MRI was prognostic for worse survival outcomes. The presence of a vascular pedicle on post-nRT MRI was prognostic for both worse DFS and OS, whereas the post-nRT presence of a tail sign-containing lesion was exclusively prognostic for worse DFS. These MRI characteristics could serve as prognostic biomarkers to support the non-invasive identification of patients at risk for worse clinical outcomes in an early stage.

We identified a vascular pedicle in 30.0% of cases post-nRT, of whom 41.7% eventually developed LR (n=1, 8.3%) or distant metastasis (n=4, 33.3%). In the absence of a vascular pedicle, only 25.0% of cases developed LR (n=2, 7.1%), distant metastasis (n=4, 14.3%) or both (n=1, 3.6%). We found no relationship between the presence of a vascular pedicle and surgical margin status. Furthermore, we observed no changes in the presence of a vascular pedicle between pre- and post-nRT MRI. This suggests that the presence of a vascular pedicle on pre-nRT MRI has similar prognostic value

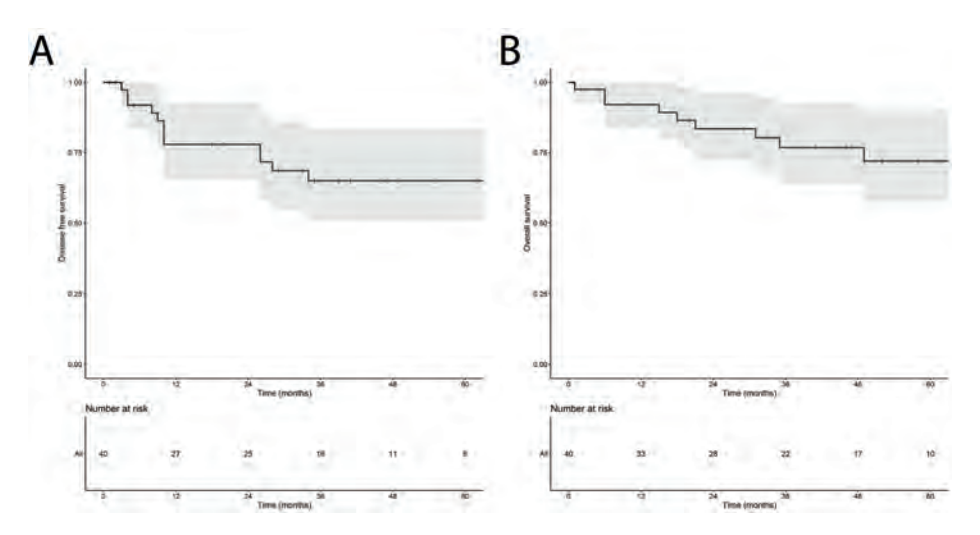


Figure 2: Kaplan-Meier estimate reflecting the disease-free survival (A) and overall survival (B) of the cohort of 40 myxofibrosarcoma patients, including the 95% confidence interval.

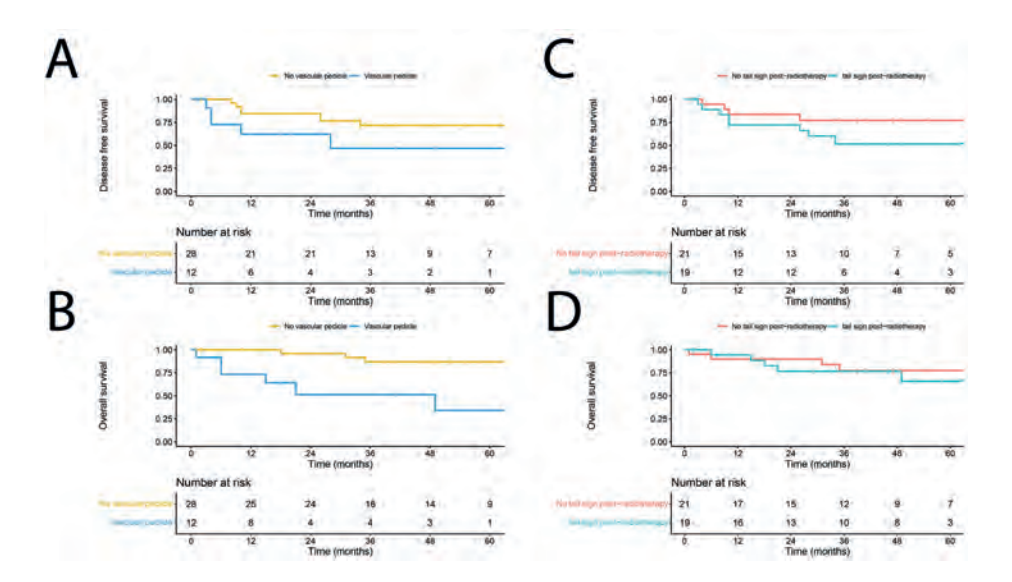


Figure 3: Kaplan-Meier estimate reflecting the disease-free survival (DFS) (A) and overall survival (OS) (B) of myxofibrosarcoma in the presence or absence of a vascular pedicle on MRI, and DFS (C) and OS (**D**) of patients in the presence or absence of a tail sign on post-neoadjuvant radiotherapy MRI.

to its presence on post-nRT MRI. While the presence of a vascular pedicle has been reported in different histological subtypes of STS, this feature has not yet been described in MFS. Ledoux et al. identified abnormal peritumor vascularization in 17% of STS patients using MRI in a cohort of 157 STS cases, including 24 MFS patients. The authors found that peritumoral flow-voids might be associated with higher risk of metastatic relapse and poorer OS. They hypothesize that abnormal vascularization might favor the occurrence of hematogenous metastasis through formation of endovascular thrombi of tumor cells. (26, 29) In the current study we report that patients with a vascular pedicle, either defined as a real clump of peri-tumoral vessels or as abnormal feeding peri-tumoral vascularization, are at increased risk of developing recurrent disease after nRT. Since most patients with disease recurrence had metastatic disease, we suggest that the vascular pedicle could be involved in the hematogenic spread of cancer cells. Future studies with the use of Dynamic Contrast Enhanced (DCE)-MRI may quantify tumor related perfusion and further characterize peritumoral microstructures. Further research is needed to investigate the optimal surgical strategy regarding a vascular pedicle. One might hypothesize that, when a surgeon is informed about the presence of a vascular pedicle, this should be resected also to further prevent hematogenic spread of cancer cells. The same holds for considerations regarding adjuvant systemic therapy.

The presence of a tail sign on MRI is the most recognized feature prognostic for worse DFS in MFS. In this study, we report the presence of a tail sign in 55.0% of cases pre-nRT and in 47.5% of cases post-nRT. This finding is in line with previous studies describing the presence of tail-like lesions in MFS. Lefkowitz et al. reported the presence of a tail sign in 64.0-77.0% of cases on MRI in a cohort of 44 MFS patients, which was associated with worse DFS but not OS. We found a relationship between the presence of a tail sign and tumor-positive surgical margins. This finding could be consistent with the worse DFS observed in the presence of a tail sign. The presence of a tail sign has also been reported as an independent adverse prognostic factor for local control and metastasis-free survival after surgery in a cohort of 89 STS. (30) The histological effect of nRT on tail-like lesions was investigated in a cohort of 18 STS cases, comprising 8 MFS patients and 10 cases of undifferentiated pleomorphic sarcoma. Viable tumor cells remained present after treatment with nRT in 8/18 cases, of whom three patients developed locally recurrent disease. (31) We found no significant changes after nRT in presence, length or width of the tail sign. The complete disappearance or shrinkage of tail-like lesions after neoadjuvant treatment has been reported in 33.3% of cases in a cohort of 36 STS patients, including 13 MFS cases, but did not impact the oncological outcomes. (32)

Tumor necrosis after nRT is the most studied prognostic factor in sarcoma. We found no correlation between the tumor necrosis percentage estimated by MRI and survival outcomes. Quantification of the tumor necrosis percentage by means of MRI is challenging due to tissue heterogeneity, inter-observer variability and a wide variety of pulse sequences. Diffusion Weighted Imaging (DWI)-MRI is not yet implemented in standard care while it has the best capacity to quantify tumor necrosis. In case of histopathological assessment, the estimation of the tumor necrosis percentage is subject to selection of microscopic fields and sampling heterogeneity. Furthermore, within the European Organisation for Research and Treatment of Cancer (EORTC) scoring system for necrosis, cutoff percentages have been arbitrarily chosen. (33) Not surprisingly, data on the tumor necrosis percentage in STS in relation to clinical outcomes are contradictory. (18, 20) The data obtained in this study support the conclusion that, in contrast to bone sarcomas, tumor necrosis has no clear prognostic value in MFS. (19, 34)

The current integration of nRT into the standard of care of MFS is hindered by the increased incidence of wound healing complications compared to adjuvant radiotherapy. Because of the lack of literature on the nRT-to-surgery-time interval and its prognostic value in STS, we explored the influence of the time interval between the end of nRT and surgery on DFS and OS in MFS, and could not identify a clear cutoff. Currently, the EORTC recommends that imaging should not be performed earlier than 4 weeks after nRT. (35) Collier et al. reported in a large retrospective database study investigating the nRT-surgery interval in STS, that a delay in surgery up to 120 days after nRT was not associated with worse survival. (36) An interval of six weeks between the end of nRT and surgery was associated with fewer wound complications in another study. (37) The time interval between the end of nRT and surgery in STS warrants further investigation to minimize wound complications after nRT without affecting survival outcomes.

The next step after our retrospective study, should be to perform a prospective trial using multiparametric MRI in a cohort of MFS patients to assess tumor cellularity and vascularization after nRT. Multiparametric MRI should be performed at multiple time points between end of nRT and planned surgery using the recommendations of the EORTC Soft Tissue and Bone Sarcoma Imaging Group. (35, 38, 39) In the past, several adjuvant chemotherapy trials in different histological subtypes of STS failed in improving the survival of heterogeneous cohorts of STS patients. This has been attributed to the lack of selection of real high-risk patients with chemotherapysensitive STS histiotypes. (40) The use of MRI characteristics as prognostic

biomarkers to select high-risk patients and to individualize further follow-up or treatment should be investigated in further detail.

Conclusions

The presence of a tail sign after nRT is prognostic for worse DFS and the presence of a vascular pedicle is prognostic for both worse DFS and OS, both pre- and post-nRT. These MRI characteristics could serve as biomarkers to support the identification of MFS patients at risk for dismal clinical outcomes in an early stage

References

- Vanni S, De Vita A, Gurrieri L, Fausti V, Miserocchi G, Spadazzi C, et al. Myxofibrosarcoma 1 landscape: diagnostic pitfalls, clinical management and future perspectives. Ther Adv Med Oncol. 2022;14:17588359221093973.
- Amadeo B, Penel N, Coindre J-M, Ray-Coquard I, Ligier K, Delafosse P, et al. Incidence and time trends of sarcoma (2000-2013): results from the French network of cancer registries (FRANCIM). BMC Cancer. 2020;20(1):190.
- van der Horst CAJ, Bongers SLM, Versleijen-Jonkers YMH, Ho VKY, Braam PM, Flucke UE, et 3. al. Overall Survival of Patients with Myxofibrosarcomas: An Epidemiological Study. Cancers (Basel). 2022;14(5).
- Look Hong NJ, Hornicek FJ, Raskin KA, Yoon SS, Szymonifka J, Yeap B, et al. Prognostic factors and outcomes of patients with myxofibrosarcoma. Ann Surg Oncol. 2013;20(1):80-6.
- Spinnato P, Clinca R, Vara G, Cesari M, Ponti F, Facchini G, et al. MRI Features as Prognostic 5. Factors in Myxofibrosarcoma: Proposal of MRI Grading System. Acad Radiol. 2021;28(11):1524-9.
- Sambri A, Spinnato P, Bazzocchi A, Tuzzato GM, Donati D, Bianchi G. Does pre-operative MRI predict the risk of local recurrence in primary myxofibrosarcoma of the extremities? Asia Pac J Clin Oncol. 2019;15(5):e181-e6.
- Odei B, Rwigema JC, Eilber FR, Eilber FC, Selch M, Singh A, et al. Predictors of Local Recurrence in Patients With Myxofibrosarcoma. Am J Clin Oncol. 2018;41(9):827-31.
- Mühlhofer HML, Lenze U, Gersing A, Lallinger V, Burgkart R, Obermeier A, et al. Prognostic Factors and Outcomes for Patients With Myxofibrosarcoma: A 13-Year Retrospective Evaluation. Anticancer Res. 2019;39(6):2985-92.
- Sanfilippo R, Miceli R, Grosso F, Fiore M, Puma E, Pennacchioli E, et al. Myxofibrosarcoma: Prognostic Factors and Survival in a Series of Patients Treated at a Single Institution. Annals of Surgical Oncology. 2011;18(3):720-5.
- Stojadinovic A, Leung DHY, Hoos A, Jaques DP, Lewis JJ, Brennan MF. Analysis of the Prognostic Significance of Microscopic Margins in 2,084 Localized Primary Adult Soft Tissue Sarcomas. Annals of Surgery. 2002;235(3):424-34.
- Huang H-Y, Lal P, Qin J, Brennan MF, Antonescu CR. Low-grade myxofibrosarcoma: a clinicopathologic analysis of 49 cases treated at a single institution with simultaneous assessment of the efficacy of 3-tier and 4-tier grading systems. Human Pathology. 2004;35(5):612-21.
- Teurneau H, Engellau J, Ghanei I, Vult von Steyern F, Styring E. High Recurrence Rate of Myxofibrosarcoma: The Effect of Radiotherapy Is Not Clear. Sarcoma. 2019;2019:8517371.
- Sambri A, Bianchi G, Righi A, Ferrari C, Donati D. Surgical margins do not affect prognosis in high grade myxofibrosarcoma. European Journal of Surgical Oncology (EJSO). 2016;42(7):1042-8.
- Müller DA, Beltrami G, Scoccianti G, Frenos F, Capanna R. Combining limb-sparing surgery with radiation therapy in high-grade soft tissue sarcoma of extremities - Is it effective? European Journal of Surgical Oncology (EJSO). 2016;42(7):1057-63.
- 15. Callaghan CM, Hasibuzzaman MM, Rodman SN, Goetz JE, Mapuskar KA, Petronek MS, et al. Neoadjuvant Radiotherapy-Related Wound Morbidity in Soft Tissue Sarcoma: Perspectives for Radioprotective Agents. Cancers (Basel). 2020;12(8).
- 16. Gingrich AA, Bateni SB, Monjazeb AM, Darrow MA, Thorpe SW, Kirane AR, et al. Neoadjuvant Radiotherapy is Associated with Ro Resection and Improved Survival for Patients with Extremity Soft Tissue Sarcoma Undergoing Surgery: A National Cancer Database Analysis. Ann Surg Oncol. 2017;24(11):3252-63.

- 17. Gannon NP, King DM, Ethun CG, Charlson J, Tran TB, Poultsides G, et al. The role of radiation therapy and margin width in localized soft-tissue sarcoma: Analysis from the US Sarcoma Collaborative. J Surg Oncol. 2019;120(3):325-31.
- Gannon NP, Stemm MH, King DM, Bedi M. Pathologic necrosis following neoadjuvant radiotherapy or chemoradiotherapy is prognostic of poor survival in soft tissue sarcoma. Journal of Cancer Research and Clinical Oncology. 2019;145(5):1321-30.
- 19. Lozano-Calderón SA, Albergo JI, Groot OQ, Merchan NA, El Abiad JM, Salinas V, et al. Complete tumor necrosis after neoadjuvant chemotherapy defines good responders in patients with Ewing sarcoma. Cancer. 2023;129(1):60-70.
- Salah S, Lewin J, Amir E, Abdul Razak A. Tumor necrosis and clinical outcomes following neoadjuvant therapy in soft tissue sarcoma: A systematic review and meta-analysis. Cancer Treatment Reviews. 2018;69:1-10.
- 21. Bonvalot S, Wunder J, Gronchi A, Broto JM, Turcotte R, Rastrelli M, et al. Complete pathological response to neoadjuvant treatment is associated with better survival outcomes in patients with soft tissue sarcoma: Results of a retrospective multicenter study. Eur J Surg Oncol. 2021;47(8):2166-72.
- Reijers SJM, Gennaro N, Bruining A, van Boven H, Snaebjornsson P, Bekers EM, et al. Correlation of radiological and histopathological response after neoadjuvant radiotherapy in soft tissue sarcoma. Acta Oncologica. 2023:1-8.
- 23. Yoo HJ, Hong SH, Kang Y, Choi J-Y, Moon KC, Kim H-S, et al. MR imaging of myxofibrosarcoma and undifferentiated sarcoma with emphasis on tail sign; diagnostic and prognostic value. European Radiology. 2014;24(8):1749-57.
- 24. Kikuta K, Kubota D, Yoshida A, Morioka H, Toyama Y, Chuuman H, Kawai A. An analysis of factors related to the tail-like pattern of myxofibrosarcoma seen on MRI. Skeletal Radiol. 2015;44(1):55-62.
- Swami VG, Demicco EG, Naraghi A, White LM. Soft tissue solitary fibrous tumors of the musculoskeletal system: spectrum of MRI appearances and characteristic imaging features. Skeletal Radiol. 2022;51(4):807-17.
- Ledoux P, Kind M, Le Loarer F, Stoeckle E, Italiano A, Tirode F, et al. Abnormal vascularization of soft-tissue sarcomas on conventional MRI: Diagnostic and prognostic values. European Journal of Radiology. 2019;117:112-9.
- 27. Lefkowitz RA, Landa J, Hwang S, Zabor EC, Moskowitz CS, Agaram NP, Panicek DM. Myxofibrosarcoma: prevalence and diagnostic value of the "tail sign" on magnetic resonance imaging. Skeletal Radiol. 2013;42(6):809-18.
- 28. Amin MB, Greene FL, Edge SB, Compton CC, Gershenwald JE, Brookland RK, et al. The Eighth Edition AJCC Cancer Staging Manual: Continuing to build a bridge from a population-based to a more "personalized" approach to cancer staging. CA Cancer J Clin. 2017;67(2):93-9.
- 29. Setsu N, Yoshida A, Takahashi F, Chuman H, Kushima R. Histological analysis suggests an invasion-independent metastatic mechanism in alveolar soft part sarcoma. Hum Pathol. 2014;45(1):137-42.
- 30. Iwata S, Yonemoto T, Araki A, Ikebe D, Kamoda H, Hagiwara Y, Ishii T. Impact of infiltrative growth on the outcome of patients with undifferentiated pleomorphic sarcoma and myxofibrosarcoma. J Surg Oncol. 2014;110(6):707-11.
- 31. Imanishi J, Slavin J, Pianta M, Jackett L, Ngan SY, Tanaka T, et al. Tail of Superficial Myxofibrosarcoma and Undifferentiated Pleomorphic Sarcoma After Preoperative Radiotherapy. Anticancer Res. 2016;36(5):2339-44.
- 32. Aiba H, Ikuta K, Asanuma K, Kawanami K, Tsukushi S, Matsumine A, et al. Effect of Neoadjuvant Therapies on Soft Tissue Sarcomas with Tail-like Lesions: A Multicenter Retrospective Study. Cancers (Basel). 2021;13(15).

- 33. Wardelmann E, Haas RL, Bovée JVMG, Terrier P, Lazar A, Messiou C, et al. Evaluation of response after neoadjuvant treatment in soft tissue sarcomas; the European Organization for Research and Treatment of Cancer-Soft Tissue and Bone Sarcoma Group (EORTC-STBSG) recommendations for pathological examination and reporting. European Journal of Cancer. 2016;53:84-95.
- 34. Tsuda Y, Tsoi K, Parry MC, Stevenson JD, Fujiwara T, Sumathi V, Jeys LM. Impact of chemotherapyinduced necrosis on event-free and overall survival after preoperative MAP chemotherapy in patients with primary high-grade localized osteosarcoma. Bone Joint J. 2020;102-b(6):795-803.
- 35. Messiou C, Bonvalot S, Gronchi A, Vanel D, Meyer M, Robinson P, et al. Evaluation of response after pre-operative radiotherapy in soft tissue sarcomas; the European Organisation for Research and Treatment of Cancer-Soft Tissue and Bone Sarcoma Group (EORTC-STBSG) and Imaging Group recommendations for radiological examination and reporting with an emphasis on magnetic resonance imaging. Eur J Cancer. 2016;56:37-44.
- 36. Collier CD. Kim C-Y. Liu RW. Getty PI. The Interval Between Preoperative Radiation and Surgery Is Not Associated with Overall Survival for Soft-tissue Sarcomas: An Analysis of the National Cancer Database. Clinical Orthopaedics and Related Research®. 2021;479(3):506-17.
- 37. Collier CD, Su CA, Reich MS, Tu L-A, Getty PJ. Six-Week Interval Between Preoperative Radiation and Surgery Is Associated With Fewer Major Wound Complications in Soft Tissue Sarcoma. American Journal of Clinical Oncology. 2020;43(7):491-5.
- 38. Soldatos T, Ahlawat S, Montgomery E, Chalian M, Jacobs MA, Fayad LM. Multiparametric Assessment of Treatment Response in High-Grade Soft-Tissue Sarcomas with Anatomic and Functional MR Imaging Sequences. Radiology. 2016;278(3):831-40.
- 39. Winfield JM, Miah AB, Strauss D, Thway K, Collins DJ, deSouza NM, et al. Utility of Multi-Parametric Quantitative Magnetic Resonance Imaging for Characterization and Radiotherapy Response Assessment in Soft-Tissue Sarcomas and Correlation With Histopathology. Front Oncol. 2019;9:280.
- 40. Woll PJ, Reichardt P, Le Cesne A, Bonvalot S, Azzarelli A, Hoekstra HJ, et al. Adjuvant chemotherapy with doxorubicin, ifosfamide, and lenograstim for resected soft-tissue sarcoma (EORTC 62931): a multicentre randomised controlled trial. Lancet Oncol. 2012;13(10):1045-54.





Chapter 7

Summary, discussion, and future perspectives

As described in the general introduction, while many tumor types have seen advances in treatment development resulting in improved survival rates, this is not the case for angiosarcomas (AS), where poor survival rates remain unchanged over the past decade. There is a clear unmet need for new systemic treatment options in this rare cancer.

Immune checkpoint inhibition (ICI) has revolutionized the treatment in solid tumors, but this progress has not extended to sarcomas in general, nor to AS in particular. Even within AS, subgroups can be identified with distinct characteristics. These subgroup specific tumor characteristics could provide valuable information for designing personalized treatment strategies, including possible susceptibility to ICI.

Here, we will discuss the heterogeneity of AS and the possible role of ICI in AS treatment.

Meanwhile we will describe how our results contribute to the current understanding of treatment strategies in AS and outline future perspectives. Selecting the right patient for the right treatment will provide access to ICI for patients likely to respond, improving their overall survival and quality of life. Furthermore, it will save non-responding patients from ineffective treatments and unnecessary toxicity, but also protect society from the coexisting financial toxicity. To better select future patients, we have investigated promising prognostic biomarkers. To identify patients likely to respond to ICI, we will also discuss potential predictive biomarkers for treatment response.

Defining AS subgroups based on immunological and genomic profiles

Traditionally, literature distinguishes AS subgroups based on their anatomical site, with different classifications used in various studies. (1, 2) These classifications are determined by location of the primary tumor, not on immunological and/or genomic profiles. Based on the data described in this thesis, I propose making a clear and universal distinction between AS subgroups, into primary (pAS) and secondary AS (sAS) based on etiology. Making a distinction based on etiology could assist in the development of tailored treatment strategies for AS subgroups, and in particular in identifying patients susceptible to ICI based treatment.

Immunological profiles of pAS and sAS

In chapter 2 of this thesis, we investigated the largest group of AS currently described in literature, including 257 unique AS patients. We reported that there is a large heterogeneity between AS subgroups, showing distinct differences in the immunological and genomic profiles between pAS and sAS. One of the main findings was a significantly higher T-cell density in sAS compared to pAS. A high T-cell density was in particular found in UV-AS, and Stewart Treves AS and to a lesser extent in radiotherapy associated AS (RT-AS). A T-cell rich tumor microenvironment (TME), especially by means of CD8⁺ T-cells, has been reported as a favorable prognostic factor with regard to survival outcomes in other high grade sarcomas. (3) In the CEMangio clinical trial (chapter 4) we also showed that T-cell infiltration is a predictive biomarker as there was a significantly higher CD3+, CD4+, and CD8+ T-cell density in sAS responders to ICI. (4) However, in our study the patient who exhibited a complete response had a relatively low T-cell density, showing the limited sensitivity of the biomarker, possibly due to tumor heterogeneity. Therefore, T-cell density alone from a single tumor biopsy is unlikely to reliably predict response to ICI. Tertiary lymphoid structures (TLS) are aggregates of CD4+ and CD8+ T-cells, dendritic cells, and B-cell follicles that develop in non-lymphoid tissue like tumors, and showed significant associations with response and survival to ICI in multiple tumor types including STS as shown in the PEMBROSARC study. (5) Future research could investigate the role of TLS in AS. Combining T-cell density with the presence of TLS and other biomarkers, such as TMB and PD-L1, could be a next step, as it is increasingly clear that one sole factor like CD8+ T-cell density cannot unequivocally predict treatment response.

Spatial heterogeneity within the TME by lymphocytes, both between tissue sites and within tissue samples can be substantial. (6) Consequently, a single biopsy may not accurately reflect the overall immune landscape of the tumor, potentially leading to an over- or underestimation of the prediction of response to ICI. In the future, this limitation could possibly be overcome by visualizing the entire tumor distribution of T-cells by means of for example CD8+ targeted positron emission tomography (PET) imaging. (7) The use of anti-CD8 radiolabeled minibodies such as 89Zr-Df-IAB22M2C has been reported as safe, and can potentially become a non-invasive biomarker in predicting early response to ICI as shown in phase I-II studies. (7, 8)

Genomic profiles of pAS and sAS

To study heterogeneity between AS subgroups, we conducted next generation sequencing (NGS) as described in chapter 2 and chapter 4. We identified (likely) pathogenic mutations in the vast majority of pAS and sAS tumors, many of which that could serve as druggable targets, and reported distinct differences in the genomic profiles between pAS and sAS. With limited treatment options existing for AS, we propose early stage implementation of NGS in all advanced AS to identify these druggable targets.

One of our main findings was a significantly higher number of DNA damage response (DDR) mutations in sAS compared to pAS. Tumors with DDR mutations also showed a higher T-cell density compared to tumors without DDR mutations. DDR mutations inhibit DNA repair, and thereby increase tumor mutational burden (TMB), upregulate programmed death ligand-1 (PD-L1) expression and cause reshaping of the immune environment. (9, 10) DDR pathway mutated tumors tend to have more neoantigens that can be recognized by the immune system, which can be beneficial to ICI effectiveness. In contrast to our hypothesis, in the CEMangio clinical trial, we did not find a significant association between DDR pathway mutation presence and response to ICI. This might be the result of the small number of patients included in this study. Several clinical trials in other tumor types are currently investigating combination therapies using DDR pathway inhibitors with ICIs to increase response to ICI. For example, in refractory gastric cancer patients, combination therapy with the ATR inhibitor ceralasertib and the PD-1 inhibitor durvalumab showed promising results including durable responses. (11) Furthermore, in metastatic triple negative breast cancer, the PARPi niraparib combined with the PD-1 inhibitor Pembrolizumab showed a tolerable safety profile and promising antitumor activity. (12) As our understanding of the efficacy and safety of combined DDR inhibition and ICI treatment improves, and given the considerable number of DDR mutations in sAS, designing a clinical trial that investigates the combination treatment of ICI and DDR inhibitors in sAS should be considered.

MYC amplification is traditionally used to differentiate between AS subgroups, and has also been proposed as a prognostic biomarker. (13) In **chapter 2** and **chapter 3**, we confirmed that, while the majority of RT-AS and Stewart Treves AS showed MYC amplifications, it was also detected in pAS such as non-UV primary skin AS, primary breast AS, and soft tissue AS. Therefore, relying solely on MYC to distinguish pAS from sAS seems an unreliable method. While MYC might serve as both a predictive biomarker for ICI response, and as a prognostic biomarker, we could not confirm this hypothesis in our retrospective and prospective studies. MYC proteins are associated with tumorigenesis and therapeutic resistance through gene amplification, translocation, and mRNA upregulation. They are known to remodulate the TME, leading to ICI treatment resistance. Interestingly, patients with AS displaying MYC protein overexpression had significantly shorter OS than those without. However, this finding should be interpreted with caution since established prognostic

indicators such as size, age, stage at diagnosis, or differences in treatment could act as confounding factors. Furthermore, in chapter 3 we showed that correlation between MYC amplification and MYC protein expression is poor, suggesting that other mechanisms are at play leading towards MYC protein overexpression. (14, 15) While MYC amplification status does not seem like a viable prognostic or predictive biomarker, MYC inhibitors are currently investigated in several phase I-II clinical trials. The selective MYC inhibitor OMO-103 showed an acceptable safety profile in a phase I/II clinical trial for solid cancers. (16) The high prevalence of MYC in both pAS and sAS may become relevant if these MYC targeted therapies evolve.

The findings in this thesis highlight the heterogeneity within AS, showing clear differences between pAS and sAS based on immunological and genomic profiles. Incorporating AS heterogeneity into future clinical studies is of vital importance to improve treatment-related outcomes. Improved patient selection will result in increased chances of treatment response, subsequently protecting non-responding patients from futile treatments and unnecessary toxicity.

Clinical application of immune checkpoint inhibition in AS

The results from chapters 2 and 3, showing a highly T-cell infiltrated TME and frequent DDR gene mutations, especially in sAS, have led to the design of a prospective clinical trial investigating monotherapy ICI in sAS. In the CEMangio trial, described in **chapter 4**, we demonstrated the modest effectivity of the PD-1 inhibitor cemiplimab in the treatment of locally advanced and metastatic sAS. We report a best overall response rate (BORR) of 27.8%, a median progression free survival (PFS) of 3.7 months, and a median overall survival (OS) of 13.1 months. The time to response was 2.6 months and duration of response 6.9 months. Two patients (11%) experience an ongoing complete response. Only one other prospective clinical trial investigating ICI in AS has been published so far. Wagner et al. treated 16 AS patients with a combination of the PD-1 inhibitor nivolumab and ipilimumab, a checkpoint inhibitor of Cytotoxic T-Lymphocyte-Associated Antigen 4 (CTLA-4), and reported an overall response rate of 25%. The majority of responders (75%) were patients with AS of the scalp and face, which is considered to be the effect of UV exposure, as proposed in this thesis these patients would be classified as sAS. (17) Furthermore, two retrospective cohort studies have been published, reporting similar response rates ranging from 20-25% in cohorts treating a combined cohort of pAS and sAS with ICI-based regimens. (18, 19) These findings collectively suggest a comparable efficacy across different studies and treatment protocols, highlighting the potential of ICI as a viable therapeutic option for AS. The results from the CEMangio study showed comparable response rates with the trial that prospectively investigated dual ICI blockade in AS. Although patient numbers in both studies are low, this could still be a relevant finding, given the increased chance of toxicity in dual ICI. Grade 3-4 treatment related adverse events are reported in 10–17% of patients with various solid tumors treated with monotherapy anti-PD-1 agents and in up to 55% of the patients treated with combined anti-PD1 and anti-CTLA-4 agents. (20, 21)

In the Netherlands the PASKWILL criteria are used to systematically evaluate new oncologic agents, to determine their possible place in daily clinical practice. (22) The CEMangio trial by a small margin failed to meet the PASKWILL criteria for nonrandomized studies, where a duration of response of 8 months is required in case of a response rate of 30-40%. We have, however, prospectively shown that, in a tumor type presumed non-responsive to ICI, a subset of patients clearly benefits from ICI treatment. In alignment with the ESMO Rare Cancer Agenda 2030, we recognize that in rare cancers like AS, a higher degree of uncertainty needs to be tolerated, not only in selecting methodologies for new clinical trials, but also in making new drugs available for daily clinical practice. We confirmed that UV-AS, particularly those patients with a high TMB (TMB-H; ≥10 mutations per megabase (mut/Mb)) benefited from ICI treatment. With a response rate of 66% in UV-AS (n=3, 100% TMB-H), our data align with response rates reported across studies in patients with other solid TMB-H tumors ranging from 50-70%. The Federal Drug Administration (FDA) has approved pembrolizumab for unresectable or metastatic TMB-H solid tumors. The European Medicine Agency (EMA) on the other hand declined approval for TMB-H due to concerns about the large variability in response rates among different tumor types in the KEYNOTE-158 trial. (23) We propose that UV-AS, especially with TMB-H, represent a specific subgroup for whom ICI should be considered as standard of care treatment. (17, 24) In the CEMangio trial, none of the three Stewart-Treves AS responded to treatment. The low CD4+ and CD8+ T-cell density and low TMB in all three patients could be a possible explanation for their lack of response. Interestingly, in contrast to our results, clinical benefit has been described previously in a limited number of Stewart-Treves AS treated with an ICI-based regimen.(19) Our findings suggest that the possible sensitivity to ICI in Stewart-Treves AS reported earlier, may not be as definitive. It is important to note that both studies included only a small number of Stewart-Treves AS cases, which may limit the generalizability of these findings. A next step could be expansion towards a multinational clinical trial, treating a larger group of sAS patients with monotherapy ICI, to further investigate possible predictive biomarkers for ICI response in sAS patients. Given the rarity of AS, conducting this clinical trial under the banner of the European Organisation for Research and Treatment of Cancer (EORTC) and/or in collaboration with EURACAN would be of great value. EURACAN, is a European collaboration network connecting healthcare providers and patient representatives. For rare cancers in particular, multinational collaboration is essential to ensure sufficient patient enrollment in order to produce generalizable results.

Future research on ICI in STS should not be limited to the locally advanced or metastatic setting alone. With high recurrence rates of up to 50% after primary surgical treatment, future research should also focus on ICI in the neoadjuvant setting. (25) Recently published studies provided solid evidence on the additional value of ICI in the neoadjuvant treatment of melanoma and colorectal cancer. (26-28) These studies demonstrated that administering ICI before surgery can lead to significant improvements in patient outcomes, including higher recurrence-free survival rates. These findings underscore the importance of investigating ICI in the neoadjuvant context for STS, where similar strategies could potentially reduce recurrence rates and improve long-term outcomes.

Predictive and prognostic biomarkers and their clinical implications

Not only in AS, but in almost all tumor types, we are unable to identify which patients will experience a durable response to treatment, and therefore all eligible patients are treated, even though the majority will not experience a durable response. Patient selection is essential to avoid unnecessary treatment and subsequent risk of toxicity for non-responders to ICI. Despite this need, and extensive research, an unambiguous predictive biomarker to identify patients that will respond to ICI remains absent. Therefore in this thesis we aimed to identify possible predictive biomarkers for ICI response in sAS. In the CEMangio clinical trial (chapter 4) we showed that, although not unambiguously, a high TMB and T-cell density were associated with response to ICI. Furthermore we looked into other promising biomarkers associated with response to ICI or survival, such as circulating tumor DNA (ctDNA) and the gut microbiome. Recent insights indicate that the gut microbiome may also play a role in determining the effectiveness of ICI treatment. Our analysis revealed a significantly higher relative abundance of Colidextribacter in responders to ICI, which aligns with previous reports. (29) Presence of Ruminococcus gnavus and Pseudoflavonifractor was significantly associated with non-response to ICI, in concordance with earlier studies. (30) While initial reports pointed to the significant influence of specific genera such as Akkermansia on ICI response, subsequent research suggests that this relationship is far more complex. (30, 31) Although certain genera might indicate a likelihood of ICI response in particular cohorts, the variation of microbiomes, populations and tumor characteristics poses challenges to the reproducibility and general applicability of these findings. Several studies have demonstrated that fecal microbiota transplantations (FMT) can positively influence ICI response, indicating that the gut microbiome may function not only as a predictive biomarker, but also a potential therapeutic target. (32)

Circulating tumor DNA (ctDNA) is not only increasingly recognized as a prognostic biomarker, it also shows great promise as an early, non-invasive, predictor of response to ICI treatment in several tumor types including STS. (33-36) We reported the presence of a common mutation or amplification that can be used for ctDNA analysis in the majority of sAS. We showed a decline in ctDNA, as early as three weeks after ICI treatment initiation, preceding radiological response. We also demonstrated a clear increase of ctDNA in cases with evolving radiological disease progression. Real time monitoring by means of ctDNA could enable clinicians so assess effectiveness of ICI sooner than radiological imaging, that often is conducted after 12 weeks of treatment, allowing for timely adjustment of the treatment plan, and avoiding unnecessary toxicity and costs. This highlights the potential of ctDNA as a valuable tool in optimizing patient management. A considerable number of clinical trials is currently evaluating the clinical use of ctDNA in ICI treated patients.

TGF-β is a potential predictive biomarker for ICI response based on its interaction with the TME as suggested in other tumor types. (37, 38) In **chapter 5**, we investigated the predictive role of the TGF-β pathway to ICI treatment response in patients with melanoma. In contrast to our hypothesis, no association between treatment response and TGF-β pathway activity in both primary tumor samples and metastases was found. Neither could we identify a clear association with survival. The results were validated using immunohistochemistry for an anti-phospho-SMAD2 antibody, as SMAD2 is a hallmark protein in the TGF-β pathway. (39) Our data is in line with disappointing clinical trial outcomes with TGF-b blocking agents in solid tumors. This includes compounds influencing the TGF-b signaling pathway as monotherapy, or in combination with ICI. (40-46) The use of bifunctional agents, combining TGF-b/PD-L1 inhibition, of which Bintrafusp alfa is the most well-studied, are currently under investigation in phase I-III trials. (47, 48) Overall, clinical trials blocking the TGF-b pathway are in an early stage and require further investigation.

Although not part of our research question, we identified Hedgehog (Hh) pathway activity as potential predictive biomarker associated with ICI treatment response in patients with melanoma. An elevated Hh pathway activity score correlated with a shorter PFS and resistance to ICI. The Hh pathway is known to regulate cell differentiation, proliferation, and tissue patterning. (49) Additionally, Hh pathway activation has been reported to lead to an accumulation of regulatory T-cells and upregulation of PD-(L)1 expression. (50, 51) Unfortunately, Hh inhibition has not

been successful in other cancer types besides basal cell carcinoma, possibly due to several factors such as the non-canonical activation of the Hh pathway and gene amplifications. (52, 53) Given our findings that associate elevated Hh pathway activity with resistance to ICI, inhibiting the Hh pathway could positively impact the TME and thereby increase susceptibility to ICI. Thus, further investigation into the combination therapy with Hh inhibitors and ICI is warranted in melanoma.

Overall, in this thesis we have examined various predictive biomarkers, and found associations between response to ICI and T-cell density, TMB-H, the gut microbiome and ctDNA levels in AS. However, none of these biomarkers can predict response to ICI with 100% accuracy. It seems increasingly likely that future approaches will need to focus on a combination of biomarkers in blood, tumor tissue and stool samples to reach an acceptable accuracy. As a first step, Chang et al showed that a score called LORIS (logistic regression-based immunotherapy-response score) outperformed known predictive single markers such as PD-L1 and TMB. LORIS makes use of six features, including TMB and neutrophil-to-lymphocyte ratio, to predict treatment response. (54) Furthermore, by using artificial intelligence on large collected clinical trial datasets integrating additional biomarkers such as T-cell density, gutmicrobiome data, combined with histology and radiology results, might result in a predictive tool for improved patient selection as a next step for future ICI patient selection. These predictive tools could be optimized for individual tumor types.

Prognostic biomarkers can also play a key role in the development of personalized treatment strategies. Being able to identify high-risk patients in an early stage, especially in a curative setting, might support the development of intensified primary treatment and follow-up strategies for these patients. This is in particular relevant for patients diagnosed with Myxofibrosarcoma (MFS), a subgroup of STS with a high disease recurrence risk in 20-40% of patients, due to an infiltrative growth pattern. (55-62) Magnetic Resonance Imaging (MRI) is already in use for response evaluation after neoadjuvant radiotherapy (nRT) in MFS. While the presence of a vascular pedicle has been reported in different histological subtypes of STS, this feature had not yet been described in MFS. (63, 64) In chapter 6, we described the presence of a vascular pedicle or tail sign on post-nRT MRI as a prognostic biomarker for worse survival outcomes. We found a relationship between the presence of a tail sign and tumor-positive surgical margins. This finding could be consistent with the worse DFS observed in the presence of a tail sign. As most patients with disease recurrence had metastatic disease, we suggest that the vascular pedicle could be involved in the hematogenic spread of cancer cells. The use of MRI characteristics as prognostic biomarkers to select high-risk patients to individualize further follow-up and treatment schedules should be investigated in further detail. Studies could focus on the value of MRI characteristics in selecting the right patients for (neo)adjuvant chemotherapy. In the past, several adjuvant chemotherapy trials in different histological subtypes of STS failed to improve the survival of heterogeneous cohorts of STS patients. This has been attributed to the lack of selection of real highrisk patients with chemotherapy-sensitive STS histiotypes. (65) The importance of adherence to the recommendations of the EORTC Soft Tissue and Bone Sarcoma Imaging Group to ensure adequate multiparametric MRIs protocols and reliable radiological judgements should be stressed out. (66, 67)

Conclusion

In this thesis we demonstrated the significant immunological and genomic heterogeneity between pAS and sAS, which has clear implications for patient tailored treatment strategies. Our findings support the universal distinction between AS subgroups based on etiology rather than anatomical location. We have prospectively shown that a subset of sAS patients, previously thought unlikely to benefit from ICI, can obtain durable responses to ICI treatment. In the current era of ICI and targeted therapies, identifying patients who are likely to respond to treatment is crucial to avoid subjecting non-responding patients to ineffective treatments and experiencing unnecessary toxicity. We have identified several predictive biomarkers associated with treatment response to ICI in AS, including T-cell density, TMB-H, the gut microbiome, and ctDNA levels. These findings allow for further exploration of these biomarkers in future clinical trials.

Finally, based on the results of this thesis, we propose specific treatment strategies for future clinical trials, emphasizing the role of ICI in both advanced and (neo) adjuvant settings for sAS. Additionally, we recommend studies using combination therapies incorporating DDRi and ICI to enhance therapeutic efficacy. Our findings represent a significant step forward in the development of personalized, biomarker-driven treatment approaches, with the potential to improve patient outcomes and reshape therapeutic strategies for patients with rare sarcoma.

References

- Painter CA, Jain E, Tomson BN, Dunphy M, Stoddard RE, Thomas BS, et al. The Angiosarcoma 1 Project: enabling genomic and clinical discoveries in a rare cancer through patient-partnered research. Nat Med. 2020:26(2):181-7.
- Espejo-Freire AP, Elliott A, Rosenberg A, Costa PA, Barreto-Coelho P, Jonczak E, et al. Genomic Landscape of Angiosarcoma: A Targeted and Immunotherapy Biomarker Analysis. Cancers (Basel). 2021;13(19).
- Boxberg M, Steiger K, Lenze U, Rechl H, von Eisenhart-Rothe R, Wortler K, et al. PD-L1 and PD-1 3. and characterization of tumor-infiltrating lymphocytes in high grade sarcomas of soft tissue prognostic implications and rationale for immunotherapy. Oncoimmunology. 2018;7(3):e1389366.
- D'Angelo SP, Richards AL, Conley AP, Woo HJ, Dickson MA, Gounder M, et al. Pilot study of bempegaldesleukin in combination with nivolumab in patients with metastatic sarcoma. Nat Commun. 2022;13(1):3477.
- Italiano A, Bessede A, Pulido M, Bompas E, Piperno-Neumann S, Chevreau C, et al. Pembrolizumab in soft-tissue sarcomas with tertiary lymphoid structures: a phase 2 PEMBROSARC trial cohort. Nat Med. 2022;28(6):1199-206.
- van Wilpe S, Gorris MAJ, van der Woude LL, Sultan S, Koornstra RHT, van der Heijden AG, et al. Spatial and Temporal Heterogeneity of Tumor-Infiltrating Lymphocytes in Advanced Urothelial Cancer. Front Immunol. 2021:12:802877.
- Farwell MD, Gamache RF, Babazada H, Hellmann MD, Harding JJ, Korn R, et al. CD8-Targeted PET Imaging of Tumor-Infiltrating T Cells in Patients with Cancer: A Phase I First-in-Humans Study of (89)Zr-Df-IAB22M2C, a Radiolabeled Anti-CD8 Minibody. J Nucl Med. 2022;63(5):720-6.
- Pandit-Taskar N, Postow MA, Hellmann MD, Harding JJ, Barker CA, O'Donoghue JA, et al. Firstin-Humans Imaging with (89)Zr-Df-IAB22M2C Anti-CD8 Minibody in Patients with Solid Malignancies: Preliminary Pharmacokinetics, Biodistribution, and Lesion Targeting. J Nucl Med. 2020;61(4):512-9.
- Brown JS, Sundar R, Lopez J. Combining DNA damaging therapeutics with immunotherapy: more haste, less speed. Br J Cancer. 2018;118(3):312-24.
- Sun W, Zhang Q, Wang R, Li Y, Sun Y, Yang L. Targeting DNA Damage Repair for Immune Checkpoint Inhibition: Mechanisms and Potential Clinical Applications. Front Oncol. 2021;11:648687.
- Kwon M, Kim G, Kim R, Kim KT, Kim ST, Smith S, et al. Phase II study of ceralasertib (AZD6738) in combination with durvalumab in patients with advanced gastric cancer. J Immunother Cancer. 2022;10(7).
- 12. Vinayak S, Tolaney SM, Schwartzberg L, Mita M, McCann G, Tan AR, et al. Open-label Clinical Trial of Niraparib Combined With Pembrolizumab for Treatment of Advanced or Metastatic Triple-Negative Breast Cancer. JAMA Oncol. 2019;5(8):1132-40.
- 13. Wang J, Zhang R, Lin Z, Zhang S, Chen Y, Tang J, et al. CDK7 inhibitor THZ1 enhances antiPD-1 therapy efficacy via the p38alpha/MYC/PD-L1 signaling in non-small cell lung cancer. J Hematol Oncol. 2020;13(1):99.
- 14. Gurel B, Iwata T, Koh CM, Jenkins RB, Lan F, Van Dang C, et al. Nuclear MYC protein overexpression is an early alteration in human prostate carcinogenesis. Mod Pathol. 2008;21(9):1156-67.
- Morrison C, Radmacher M, Mohammed N, Suster D, Auer H, Jones S, et al. MYC amplification and polysomy 8 in chondrosarcoma: array comparative genomic hybridization, fluorescent in situ hybridization, and association with outcome. J Clin Oncol. 2005;23(36):9369-76.

- Garralda E, Beaulieu ME, Moreno V, Casacuberta-Serra S, Martínez-Martín S, Foradada L, et al. MYC targeting by OMO-103 in solid tumors: a phase 1 trial. Nat Med. 2024;30(3):762-71.
- Wagner MJ, Othus M, Patel SP, Ryan C, Sangal A, Powers B, et al. Multicenter phase II trial (SWOG S1609, cohort 51) of ipilimumab and nivolumab in metastatic or unresectable angiosarcoma: a substudy of dual anti-CTLA-4 and anti-PD-1 blockade in rare tumors (DART). J Immunother Cancer. 2021;9(8).
- Ravi V, Subramaniam A, Zheng J, Amini B, Trinh VA, Joseph J, et al. Clinical activity of checkpoint inhibitors in angiosarcoma: A retrospective cohort study. Cancer. 2022;128(18):3383-91.
- 19. Rosenbaum E, Antonescu CR, Smith S, Bradic M, Kashani D, Richards AL, et al. Clinical, genomic, and transcriptomic correlates of response to immune checkpoint blockade-based therapy in a cohort of patients with angiosarcoma treated at a single center. J Immunother Cancer. 2022;10(4).
- Larkin J, Chiarion-Sileni V, Gonzalez R, Grob JJ, Cowey CL, Lao CD, et al. Combined Nivolumab and Ipilimumab or Monotherapy in Untreated Melanoma. N Engl J Med. 2015;373(1):23-34.
- 21. Postow MA, Chesney J, Pavlick AC, Robert C, Grossmann K, McDermott D, et al. Nivolumab and ipilimumab versus ipilimumab in untreated melanoma. N Engl J Med. 2015;372(21):2006-17.
- 22. NVMO. PASKWILL Criteria https://www.nvmo.org/over-de-adviezen/2021 [
- 23. Marabelle A, Fakih M, Lopez J, Shah M, Shapira-Frommer R, Nakagawa K, et al. Association of tumour mutational burden with outcomes in patients with advanced solid tumours treated with pembrolizumab: prospective biomarker analysis of the multicohort, open-label, phase 2 KEYNOTE-158 study. Lancet Oncol. 2020;21(10):1353-65.
- 24. Florou V, Rosenberg AE, Wieder E, Komanduri KV, Kolonias D, Uduman M, et al. Angiosarcoma patients treated with immune checkpoint inhibitors: a case series of seven patients from a single institution. J Immunother Cancer. 2019;7(1):213.
- 25. Fury MG, Antonescu CR, Van Zee KJ, Brennan MF, Maki RG. A 14-year retrospective review of angiosarcoma: clinical characteristics, prognostic factors, and treatment outcomes with surgery and chemotherapy. Cancer J. 2005;11(3):241-7.
- 26. Blank CU, Lucas MW, Scolyer RA, van de Wiel BA, Menzies AM, Lopez-Yurda M, et al. Neoadjuvant Nivolumab and Ipilimumab in Resectable Stage III Melanoma. N Engl J Med. 2024.
- 27. Patel SP, Othus M, Chen Y, Wright GP, Jr., Yost KJ, Hyngstrom JR, et al. Neoadjuvant-Adjuvant or Adjuvant-Only Pembrolizumab in Advanced Melanoma. N Engl J Med. 2023;388(9):813-23.
- 28. Chalabi M, Fanchi LF, Dijkstra KK, Van den Berg JG, Aalbers AG, Sikorska K, et al. Neoadjuvant immunotherapy leads to pathological responses in MMR-proficient and MMR-deficient early-stage colon cancers. Nat Med. 2020;26(4):566-76.
- Newsome RC, Gharaibeh RZ, Pierce CM, da Silva WV, Paul S, Hogue SR, et al. Interaction of bacterial genera associated with therapeutic response to immune checkpoint PD-1 blockade in a United States cohort. Genome Med. 2022;14(1):35.
- 30. Lee KA, Thomas AM, Bolte LA, Björk JR, de Ruijter LK, Armanini F, et al. Cross-cohort gut microbiome associations with immune checkpoint inhibitor response in advanced melanoma. Nat Med. 2022;28(3):535-44.
- 31. Routy B, Le Chatelier E, Derosa L, Duong CPM, Alou MT, Daillere R, et al. Gut microbiome influences efficacy of PD-1-based immunotherapy against epithelial tumors. Science. 2018;359(6371):91-7.
- 32. Routy B, Lenehan JG, Miller WH, Jr., Jamal R, Messaoudene M, Daisley BA, et al. Fecal microbiota transplantation plus anti-PD-1 immunotherapy in advanced melanoma: a phase I trial. Nat Med. 2023;29(8):2121-32.

- Tolmeijer SH, van Wilpe S, Geerlings MJ, von Rhein D, Smilde TJ, Kloots ISH, et al. Early Ontreatment Circulating Tumor DNA Measurements and Response to Immune Checkpoint Inhibitors in Advanced Urothelial Cancer. Eur Urol Oncol. 2024;7(2):282-91.
- 34. Raja R, Kuziora M, Brohawn PZ, Higgs BW, Gupta A, Dennis PA, Ranade K. Early Reduction in ctDNA Predicts Survival in Patients with Lung and Bladder Cancer Treated with Durvalumab. Clin Cancer Res. 2018;24(24):6212-22.
- 35. Bratman SV, Yang SYC, Iafolla MAJ, Liu Z, Hansen AR, Bedard PL, et al. Personalized circulating tumor DNA analysis as a predictive biomarker in solid tumor patients treated with pembrolizumab. Nature Cancer. 2020;1(9):873-81.
- 36. Bui NQ, Nemat-Gorgani N, Subramanian A, Torres IA, Lohman M, Sears TJ, et al. Monitoring Sarcoma Response to Immune Checkpoint Inhibition and Local Cryotherapy with Circulating Tumor DNA Analysis. Clin Cancer Res. 2023;29(14):2612-20.
- 37. Tauriello DVF, Palomo-Ponce S, Stork D, Berenguer-Llergo A, Badia-Ramentol J, Iglesias M, et al. TGFbeta drives immune evasion in genetically reconstituted colon cancer metastasis. Nature. 2018;554(7693):538-43.
- 38. Mariathasan S, Turley SJ, Nickles D, Castiglioni A, Yuen K, Wang Y, et al. TGFbeta attenuates tumour response to PD-L1 blockade by contributing to exclusion of T cells. Nature. 2018;554(7693):544-8.
- Zhou WJ, Wang HY, Zhang J, Dai HY, Yao ZX, Zheng Z, et al. NEAT1/miR-200b-3p/SMAD2 axis promotes progression of melanoma. Aging (Albany NY). 2020;12(22):22759-75.
- 40. Paz-Ares L, Kim TM, Vicente D, Felip E, Lee DH, Lee KH, et al. Bintrafusp Alfa, a Bifunctional Fusion Protein Targeting TGF-beta and PD-L1, in Second-Line Treatment of Patients With NSCLC: Results From an Expansion Cohort of a Phase 1 Trial. J Thorac Oncol. 2020;15(7):1210-22.
- 41. Melisi D, Oh DY, Hollebecque A, Calvo E, Varghese A, Borazanci E, et al. Safety and activity of the TGFbeta receptor I kinase inhibitor galunisertib plus the anti-PD-L1 antibody durvalumab in metastatic pancreatic cancer. J Immunother Cancer. 2021;9(3).
- 42. Wheatley-Price P, Chu Q, Bonomi M, Seely J, Gupta A, Goss G, et al. A Phase II Study of PF-03446962 in Patients with Advanced Malignant Pleural Mesothelioma. CCTG Trial IND.207. J Thorac Oncol. 2016;11(11):2018-21.
- 43. Ciardiello D, Elez E, Tabernero J, Seoane J. Clinical development of therapies targeting TGFbeta: current knowledge and future perspectives. Ann Oncol. 2020;31(10):1336-49.
- 44. Tauriello DVF, Sancho E, Batlle E. Overcoming TGFbeta-mediated immune evasion in cancer. Nat Rev Cancer. 2022;22(1):25-44.
- Teixeira AF, Ten Dijke P, Zhu HJ. On-Target Anti-TGF-beta Therapies Are Not Succeeding in Clinical Cancer Treatments: What Are Remaining Challenges? Front Cell Dev Biol. 2020;8:605.
- 46. Morris JC, Tan AR, Olencki TE, Shapiro GI, Dezube BJ, Reiss M, et al. Phase I study of GC1008 (fresolimumab): a human anti-transforming growth factor-beta (TGFbeta) monoclonal antibody in patients with advanced malignant melanoma or renal cell carcinoma. PLoS One. 2014;9(3):e90353.
- 47. Tan B, Khattak A, Felip E, Kelly K, Rich P, Wang D, et al. Bintrafusp Alfa, a Bifunctional Fusion Protein Targeting TGF-beta and PD-L1, in Patients with Esophageal Adenocarcinoma: Results from a Phase 1 Cohort. Target Oncol. 2021;16(4):435-46.
- 48. Yoo C, Oh DY, Choi HJ, Kudo M, Ueno M, Kondo S, et al. Phase I study of bintrafusp alfa, a bifunctional fusion protein targeting TGF-beta and PD-L1, in patients with pretreated biliary tract cancer. J Immunother Cancer. 2020;8(1).
- 49. Carballo GB, Honorato JR, de Lopes GPF, Spohr T. A highlight on Sonic hedgehog pathway. Cell Commun Signal. 2018;16(1):11.

- 50. Petty AJ, Li A, Wang X, Dai R, Heyman B, Hsu D, et al. Hedgehog signaling promotes tumor-associated macrophage polarization to suppress intratumoral CD8+ T cell recruitment. J Clin Invest. 2019;129(12):5151-62.
- 51. de la Roche M, Ritter AT, Angus KL, Dinsmore C, Earnshaw CH, Reiter JF, Griffiths GM. Hedgehog signaling controls T cell killing at the immunological synapse. Science. 2013;342(6163):1247-50.
- 52. Giroux-Leprieur E, Costantini A, Ding VW, He B. Hedgehog Signaling in Lung Cancer: From Oncogenesis to Cancer Treatment Resistance. Int J Mol Sci. 2018;19(9).
- 53. Giammona A, Crivaro E, Stecca B. Emerging Roles of Hedgehog Signaling in Cancer Immunity. Int J Mol Sci. 2023;24(2).
- 54. Chang TG, Cao Y, Sfreddo HJ, Dhruba SR, Lee SH, Valero C, et al. LORIS robustly predicts patient outcomes with immune checkpoint blockade therapy using common clinical, pathologic and genomic features. Nat Cancer. 2024.
- 55. Look Hong NJ, Hornicek FJ, Raskin KA, Yoon SS, Szymonifka J, Yeap B, et al. Prognostic factors and outcomes of patients with myxofibrosarcoma. Ann Surg Oncol. 2013;20(1):80-6.
- 56. Spinnato P, Clinca R, Vara G, Cesari M, Ponti F, Facchini G, et al. MRI Features as Prognostic Factors in Myxofibrosarcoma: Proposal of MRI Grading System. Acad Radiol. 2021;28(11):1524-9.
- 57. Sambri A, Spinnato P, Bazzocchi A, Tuzzato GM, Donati D, Bianchi G. Does pre-operative MRI predict the risk of local recurrence in primary myxofibrosarcoma of the extremities? Asia Pac J Clin Oncol. 2019;15(5):e181-e6.
- 58. Odei B, Rwigema JC, Eilber FR, Eilber FC, Selch M, Singh A, et al. Predictors of Local Recurrence in Patients With Myxofibrosarcoma. Am J Clin Oncol. 2018;41(9):827-31.
- van der Horst CAJ, Bongers SLM, Versleijen-Jonkers YMH, Ho VKY, Braam PM, Flucke UE, et al. Overall Survival of Patients with Myxofibrosarcomas: An Epidemiological Study. Cancers (Basel). 2022;14(5).
- 60. Mühlhofer HML, Lenze U, Gersing A, Lallinger V, Burgkart R, Obermeier A, et al. Prognostic Factors and Outcomes for Patients With Myxofibrosarcoma: A 13-Year Retrospective Evaluation. Anticancer Res. 2019;39(6):2985-92.
- 61. Sanfilippo R, Miceli R, Grosso F, Fiore M, Puma E, Pennacchioli E, et al. Myxofibrosarcoma: Prognostic Factors and Survival in a Series of Patients Treated at a Single Institution. Annals of Surgical Oncology. 2011;18(3):720-5.
- 62. Teurneau H, Engellau J, Ghanei I, Vult von Steyern F, Styring E. High Recurrence Rate of Myxofibrosarcoma: The Effect of Radiotherapy Is Not Clear. Sarcoma. 2019;2019:8517371.
- 63. Ledoux P, Kind M, Le Loarer F, Stoeckle E, Italiano A, Tirode F, et al. Abnormal vascularization of soft-tissue sarcomas on conventional MRI: Diagnostic and prognostic values. European Journal of Radiology. 2019;117:112-9.
- 64. Setsu N, Yoshida A, Takahashi F, Chuman H, Kushima R. Histological analysis suggests an invasion-independent metastatic mechanism in alveolar soft part sarcoma. Hum Pathol. 2014;45(1):137-42.
- 65. Woll PJ, Reichardt P, Le Cesne A, Bonvalot S, Azzarelli A, Hoekstra HJ, et al. Adjuvant chemotherapy with doxorubicin, ifosfamide, and lenograstim for resected soft-tissue sarcoma (EORTC 62931): a multicentre randomised controlled trial. Lancet Oncol. 2012;13(10):1045-54.
- 66. Tsuda Y, Tsoi K, Parry MC, Stevenson JD, Fujiwara T, Sumathi V, Jeys LM. Impact of chemotherapy-induced necrosis on event-free and overall survival after preoperative MAP chemotherapy in patients with primary high-grade localized osteosarcoma. Bone Joint J. 2020;102-b(6):795-803.
- 67. Soldatos T, Ahlawat S, Montgomery E, Chalian M, Jacobs MA, Fayad LM. Multiparametric Assessment of Treatment Response in High-Grade Soft-Tissue Sarcomas with Anatomic and Functional MR Imaging Sequences. Radiology. 2016;278(3):831-40.





Epilogue

The safety risk of information overload and bureaucracy in oncology clinical trial conduct

Stefan G. van Ravensteijn, Mirte Meijerink, Renée Nijenhuis-van Schayk, Ingrid M.E. Desar, Kalijn F. Bol, Carla M.L. van Herpen, Henk M.W. Verheul

Abstract

Performance of clinical trials has led to major therapeutic developments and substantial improvements in the field of medical oncology. To ensure patient's safety, regulatory aspects for proper clinical trial conduct has been increased over the past two decades, but seems to cause information overload and ineffective bureaucracy, possibly even impacting patient safety. To put this in perspective, after the implementation of Directive 2001/20/EC in the European Union, a 90 percent increase in trial launching time, a 25 percent decrease in patient participation and a 98 percent rise in administrative trial costs were reported. The time to initiate a clinical trial has increased from a few months to several years in the past three decades. Moreover, there is a serious risk that information overload with relatively unimportant data endangers the decision-making processes and distracts from essential patient safety information. It is now a critical moment in time to improve efficient clinical trial conduct for our future patients diagnosed with cancer. We are convinced that a reduction of the administrative regulations, information overload, and simplification of the procedures for trial conductance may improve patient safety. In this Current Perspective we give insight in the current regulatory aspects of clinical research, evaluate the practical consequences of these regulations, and propose specific improvements for optimal clinical trial conduct.

Introduction

In the past decades, there have been major diagnostic and therapeutic developments in the field of medical oncology that have led to a better prognosis for many subgroups of patients with cancer. [1] These advancements have been made possible by proper performance of clinical trials. Until 2007 the number of patients participating in cancer-related research increased steadily, but this augmentation of inclusion of patients has come to a halt. [2] In recent years, we have witnessed a dramatic surge in the information load to which both patients and research teams are exposed without clear evidence to what extent this bureaucracy contributes to (patient) safety. [3-8] There is a serious risk that information overload with relatively unimportant data endanger the decision-making processes and distract from essential patient safety information. [5] Information overload has a negative effect on productivity and working environment happiness in all parts of society. [9] For example emergency physicians reported stress, tension, and impaired decision making due to overwhelming amounts of information, while alert fatigue has been described to negatively influence clinical decision making in regular patient care. [10, 11] In the study of Singh et al. 87% of the primary care physicians reported excessive amounts of alerts, and 30% missed test results that led to care delays. [12] It is undisputed that guidelines and regulations are essential to safeguard the process of clinical trials. However, the administrative burden and information load has increased to such extend that it may endanger progress of research and the potential benefit for patients. To put this in perspective, after the implementation of Directive 2001/20/ EC in the European Union (EU), a 90 percent increase in trial launching time, a 25 percent decrease in patient participation and a 98 percent rise in administrative trial costs were reported. [2, 3, 13] Between the 1990s and 2017, trial participating costs per patient increased from 3000-5000 USD to 88.000-156.000 USD. [3, 6, 14]

In this Current Perspectives we give insight in the current regulatory aspects of clinical research and propose specific improvements for optimal clinical trial conduct. First, we discuss the historical context of the regulations. Next, we evaluate the practical consequences and impact of these regulations in recent years. Finally, we propose and describe several initiatives designed to limit the information overload and bureaucratic burden for proper and safe clinical trial conduct and the relief they may offer in the near future. Consequently, we envision that more patients will be able to participate in clinical trials and effective treatment strategies will be approved in standard care faster.

History

In the 20th century, after the second World War, as a response to the horrific experiments conducted by Nazi-Germany rules and guidelines were created to streamline clinical research and protect safety of participating patients. This process started with the Nuremberg code in 1947, followed by the acceptance of the Declaration of Helsinki in 1964. [15]

The international quality standard Good Clinical practice (GCP) was implemented in 1996. GCP guidelines are implemented by the Food and Drug Administration (FDA) in the United States and by means of Directive 2001/20/EC in the EU. [13, 16] Under this directive, almost all studies are subject to the new legislation and have to adhere to its regulatory requirements. Strict rules were implemented with regards to amendments, reporting, monitoring, and registration of adverse events. [2, 3, 6, 14, 17]

In 2014 Clinical Trials Regulation No. 536/2014 was endorsed in the EU but due to several delays it was only implemented as of January 31st, 2022. The goal of this regulation is to stimulate clinical research and harmonize regulations within the EU while retaining the highest standards of safety and standardized timelines. [2, 18]

Practical consequences and impact of intensified regulations and increasing information load and possible solutions

Do these regulations contribute to patient safety? Evidence is lacking while the downside of growing bureaucracy and information overload may even have a negative impact on patient safety.

A defensive interpretation of GCP has become imbedded in the daily practice of clinical research. [19] For example, GCP states that "an investigator must have the right qualifications, and should maintain a list of appropriately qualified persons". This results in extensive documentation with resumes, training logs, and delegation logs for each individual study. The excessive amount of documentation to which researchers are exposed may lead to a false sense of security when investigators are overwhelmed instead of being trained for a trial. We propose standardized internal training procedures and documentation that can provide evidence of qualification for standard operating procedures (SOPs). [19] Another option could be standardization of all the different documentation formats. This could further be supported by the

removal of the requirement for "wet ink" signatures. Miller et al. demonstrated that the use of digital signatures could lead to 19% savings in labor compared to wet ink signatures and 85% of the participants preferred it. No statistical difference was reported in error rates, and time to complete documents was significantly shorter. [20] If standardized formats and digital signatures were to be implemented, this could lead to a great relief in administration burden.

A new industry in the form of Contract Research Organizations (CROs) has been developed to support the pharmaceutical companies and the clinical investigators in the labyrinth of regulations, but are often contributing to the information overload. [17] This labyrinth of regulations was made visual by Dilts and his colleagues, describing 239 working steps, 52 major decision points, 20 processing loops and 11 stopping points required to activate a clinical study. [4] The number of steps and the time it takes have only grown in recent years. [21, 22] As a result, time to initiate a clinical trial has increased from a few months to more than a year the past three decades. [3, 4]

Over time, adverse event (AE) monitoring and the number of queries have increased significantly. The communication presented to research teams has become progressively labor intensive. Part of the requested information is irrelevant for proper conduct of a trial, for example AEs that are disease-related rather than treatment-related. [23] E-mails frequently report (Serious) Adverse Events ((S)AEs) or Suspected Unexpected Severe Adverse Reactions (SUSARs) that are neither serious nor unexpected. Jarow et al. showed that of all safety reports presented to the FDA, only 14% were informative. [24] Another contributing factor is the enormous number of queries sent to a research team. Due to this overwhelming amount of information, chances of overlooking a real SAE increases. Information overload in the form of overabundance of clinically irrelevant information, poor data display and excessive alerting in electronic health records has been associated with higher error rates and increased physician cognitive load. [25] Clinical Trials Regulation No 536/2014 describes that safety reporting between investigator and sponsor are dictated by the clinical trial protocol. It offers an opportunity for drafting protocols to prevent excessive reporting, which can be done for example by more cyclic safety reviews in which AEs are clustered and by only reporting actionable and treatment-related AEs. Streamlining AE reporting by itself, as also stated by the American Society of Clinical Oncology (ASCO), will improve patient safety and at the same time reduce the information overload. [23]

Between 1979 and 2002 treatment-related deaths in clinical trials have decreased from 0.8% to 0.5%.[11] In perspective, the fatal AE incidence rate for standard of

care bevacizumab is 2.9%. [26] Meanwhile, regulatory delays in development of effective therapies potentially result in tens to hundreds of thousands of life-years lost in patients, unable to timely participate in a clinical trial. [6, 7] In our view the information overload by itself has become a (safety) risk in clinical trial conduct.

Future perspectives

Participation in a clinical trial must be as safe as possible. This safety can be approved by strict regulations for proper trial conduct. However, one should also realize that bureaucracy and information overload itself might be a risk factor for patient safety. Without disputing the relevance of each regulation independently, implementation of a large number of guidelines and regulations over a relatively short period of time will most probably increase the administrative workload, slowdown clinical research programs and increase costs, requiring specific vigilance for the future of investigator initiated trials. Although it is challenging to evaluate the effect of individual regulations, it is of great importance that impact assessments are conducted.

We are convinced that a reduction of the administrative regulations, information overload, and simplification of the procedures for trial conductance may improve patient safety. A view which is supported by surveys by the European Society for Medical Oncology (ESMO). [21] By reducing the amount of information presented, the risk of missing vital data reduces. [10, 12, 23, 25] More sites will be able to participate in a clinical trial and sites will be able to conduct more clinical trials, enhancing development of new treatment and thereby positively impacting future patients.

It is important to mention that several new initiatives to simplify trial conduct have already been proposed, such as the implementation of digital signatures, in order to limit bureaucracy. [20, 27] Decreasing administrative burden could also be achieved when standardized formats are implemented and accepted by the different pharmaceutical companies, hospitals, and regulatory authorities, a vision that is also reflected in the ASCO strategy to improve clinical research and cancer care. [28] Regarding the communication with pharmaceutical companies about possible new clinical trials, stimulating the use of master confidential disclosure agreements (CDAs), valid for all proposed new clinical trials, could eliminate the burden of individual CDAs for each new study. If we limit the number of queries, take a critical look at which SUSARs, SAEs, and AEs need to be reported, eliminate reporting of AEs related to disease progression and clustering AEs in cyclic reports, this could be a major step in the right direction. [23] Finally we envision the creation of one universal investigator

platform, used by all the pharmaceutical companies, for entering all required data for an individual clinical trial potentially decreasing the bureaucratic burden dramatically.

Several organizations such as the ASCO and ESMO have taken up the call from many clinicians in the field to rationalize the bureaucracy and limit the amount of information presented. [21, 28] The ASCO's Research Task Force identified five goals in order to create a more accessible and efficient clinical research system, while protecting patient safety: Goal 1: Ensure That Clinical Research Is Accessible, Affordable, and Equitable, Goal 2: Design More Pragmatic and Efficient Clinical Trials, Goal 3: Minimize Administrative and Regulatory Burdens on Research Sites, Goal 4: Recruit, Retain, and Support a Well-Trained Clinical Research Workforce and Goal 5: Promote Appropriate Oversight and Review of Clinical Trial Conduct and Results. [28] If medical oncologists and patient advocates join forces with CROs, pharmaceutical companies, and regulatory authorities, we are convinced that clinical trials will become more attractive for patients, researchers, and organizations. It will stimulate investigator-initiated trials, limit the administrative burden in trials driven by pharmaceutical companies, and improve patient safety at the same time.

With major efforts put in clinical trials, we aim to prolong median progression-free survival or disease free survival with several months while years are lost in this bureaucratic, inefficient, and expensive system without proven benefit on patient safety. It is now a critical moment in time to improve efficient clinical trial conduct for our future patients diagnosed with cancer. Reduction of unnecessary bureaucracy and proper evaluation of implementation of new administrative regulations will allow for more efficiently organized clinical trial conduct, improving the outcome of our future patients faster.

References

- Arnold, M., et al., Progress in cancer survival, mortality, and incidence in seven high-income countries 1995-2014 (ICBP SURVMARK-2): a population-based study. Lancet Oncol, 2019. 20(11): p. 1493-1505.
- Tenti, E., et al., Main changes in European Clinical Trials Regulation (No 536/2014). Contemp Clin Trials Commun, 2018. 11: p. 99-101.
- Steensma, D.P. and H.M. Kantarjian, Impact of cancer research bureaucracy on innovation, costs, and patient care. J Clin Oncol, 2014. 32(5): p. 376-8.
- Dilts, D.M., et al., Steps and time to process clinical trials at the Cancer Therapy Evaluation Program. J Clin Oncol, 2009. 27(11): p. 1761-6.
- 5. Roetzel, P.G., Information overload in the information age: a review of the literature from business administration, business psychology, and related disciplines with a bibliometric approach and framework development. Business Research, 2019. 12(2): p. 479-522.
- Stewart, D.J., S.N. Whitney, and R. Kurzrock, Equipoise lost: ethics, costs, and the regulation of cancer clinical research. J Clin Oncol, 2010. 28(17): p. 2925-35.
- 7. Penninckx, B., et al., A systemic review of toxic death in clinical oncology trials: an Achilles' heel in safety reporting revisited. Br J Cancer, 2012. 107(1): p. 1-6.
- Klerings, I., A.S. Weinhandl, and K.J. Thaler, Information overload in healthcare: too much of a good thing? Z Evid Fortbild Qual Gesundhwes, 2015. 109(4-5): p. 285-90.
- 9. Dean, D. and C. Webb, Recovering from information overload. 2011.
- Sbaffi, L., et al., Information Overload in Emergency Medicine Physicians: A Multisite Case Study Exploring the Causes, Impact, and Solutions in Four North England National Health Service Trusts. J Med Internet Res, 2020. 22(7): p. e19126.
- 11. Ancker, J.S., et al., Effects of workload, work complexity, and repeated alerts on alert fatigue in a clinical decision support system. BMC Med Inform Decis Mak, 2017. 17(1): p. 36.
- 12. Singh, H., et al., Information overload and missed test results in electronic health record-based settings. JAMA Intern Med, 2013. 173(8): p. 702-4.
- 13. Directive 2001/20/EC of the European Parliament and of the Council of 4 April 2001 on the approximation of the laws, regulations and administrative provisions of the member states relating to the implementation of good clinical practice in the conduct of clinical trials on medicinal products for human use. Med Etika Bioet, 2002. 9(1-2): p. 12-9.
- Pascarella, G., et al., Costs of clinical trials with anticancer biological agents in an Oncologic Italian Cancer Center using the activity-based costing methodology. PLoS One, 2019. 14(1): p. e0210330.
- 15. Declaration of Helsinki. New England Journal of Medicine, 1964. 271(9): p. 473-&.
- 16. Welzing, L., et al., Consequences of Directive 2001/20/EC for investigator-initiated trials in the paediatric population--a field report. Eur J Pediatr, 2007. **166**(11): p. 1169-76.
- 17. Gobbini, E., et al., Effect of Contract Research Organization Bureaucracy in Clinical Trial Management: A Model From Lung Cancer. Clin Lung Cancer, 2018. 19(2): p. 191-198.
- Regulation (EU) No 536/2014 of the European Parliament and of the Council of 16 April 2014 on clinical trials in medicinal products for human use and repealing Directive 2001/20/EC. 2014: Off. J. 2014; L 158: pp. 1022.
- den Heijer, J.M., et al., Good Clinical Trials by removing defensive interpretation of Good Clinical Practice guidelines. Br J Clin Pharmacol, 2021. 87(12): p. 4552-4559.
- 20. Miller, T.M., et al., 21 Code of Federal Regulations Part 11-Compliant Digital Signature Solution for Cancer Clinical Trials: A Single-Institution Feasibility Study. JCO Clin Cancer Inform, 2020. 4: p. 854-864.

- 22. Lacombe, D., et al., Clinical research in Europe: Who do we do all that for? Journal of Cancer Policy, 2020. 23.
- 23. Levit, L.A., et al., Streamlining Adverse Events Reporting in Oncology: An American Society of Clinical Oncology Research Statement. J Clin Oncol, 2018. 36(6): p. 617-623.
- 24. Jarow, J.P., et al., The Majority of Expedited Investigational New Drug Safety Reports Are Uninformative. Clin Cancer Res, 2016. **22**(9): p. 2111-3.
- 25. Nijor, S., et al., Patient Safety Issues From Information Overload in Electronic Medical Records. Journal of Patient Safety, 9900: p. 10.1097/PTS.000000000000002.
- 26. Ranpura, V., S. Hapani, and S. Wu, Treatment-related mortality with bevacizumab in cancer patients: a meta-analysis. JAMA, 2011. 305(5): p. 487-94.
- 27. Bleiberg, H., et al., A need to simplify informed consent documents in cancer clinical trials. A position paper of the ARCAD Group. Ann Oncol, 2017. 28(5): p. 922-930.
- Pennell, N.A., et al., American Society of Clinical Oncology Road to Recovery Report: Learning From the COVID-19 Experience to Improve Clinical Research and Cancer Care. J Clin Oncol, 2021. 39(2): p. 155-169.

Nederlandse samenvatting

Immuun checkpointremmers (ICR) blokkeren specifieke signalen die immuuncellen beperken in hun activiteit tegen kankercellen. Door deze blokkade kunnen immuuncellen de kankercellen beter herkennen en vernietigen. ICR hebben de behandelmogelijkheden voor veel verschillende vormen van kanker drastisch veranderd. Ondanks indrukwekkende resultaten waarbij een klein deel van de patiënten langdurig baat heeft van behandeling met ICR, profiteert een aanzienlijk deel van de patiënten helaas niet. Voor de behandeling van sarcomen zijn ICR niet geregistreerd. Sarcomen zijn echter een heterogene tumorsoort, met meer dan 100 verschillende subtypen. Sommige subtypen, zoals angiosarcomen, zouden baat kunnen hebben van behandeling met ICR. Het identificeren van specifieke subgroepen, die mogelijk gevoelig zijn voor ICR, kan de overleving van deze patiënten aanzienlijk verbeteren. Het is van groot belang om patiënten te selecteren die baat hebben bij de behandeling, en om patiënten die niet zullen reageren te behoeden voor ineffectieve behandelingen en onnodige bijwerkingen.

In dit proefschrift onderzochten we de verschillen tussen angiosarcoom subgroepen en beschrijven we specifieke subgroepen die gevoelig zouden kunnen zijn voor ICR. Verder bestudeerden we veelbelovende biomarkers om patiënten te identificeren die mogelijk gunstig reageren op behandeling. Tevens onderzochten we prognostische biomarkers, die van belang kunnen zijn bij het aanpassen van behandelingen of follow-up controles bij patiënten met een hoog of laag risico op terugkeer van de ziekte.

Het immunologische en genomische landschap van angiosarcomen

Angiosarcomen zijn zeldzame en agressieve wekedelen sarcomen. Angiosarcomen kunnen worden onverdeeld in twee verschillende groepen. Primaire angiosarcomen ontstaan op verschillende anatomische locaties in het lichaam, met onbekende etiologie. Secundaire angiosarcomen ontstaan door externe DNA-schade, zoals ultravioletstraling, radiotherapie of chronisch lymfoedeem (Stewart-Treves angiosarcomen). De behandelmogelijkheden voor angiosarcomen zijn zeer beperkt, en indien een operatie niet mogelijk is of wanneer er sprake is van uitgezaaide ziekte bestaat de behandeling voornamelijk uit chemotherapie. De overleving van angiosarcoom patiënten is de afgelopen tien jaar niet verbeterd, en is gemiddeld slechts 5 tot 10 maanden vanaf het moment van diagnose van lokaal vergevorderde of uitgezaaide ziekte. In tegenstelling tot veel andere tumoren zijn ICR niet geregistreerd voor de behandeling van angiosarcomen. Sarcomen worden over het algemeen beschouwd als "koude tumoren" met weinig immuuncellen in de tumor,

waardoor de kans op een gunstig effect op ICR klein wordt geacht. Sarcomen zijn echter een heterogene ziekte met meer dan 100 subtypen, waarbij sommige subtypen mogelijk baat kunnen hebben bij behandeling met ICR.

In **hoofdstuk 2** van dit proefschrift beschrijven we het immunologische en genomische landschap van 257 angiosarcomen. We toonden aan dat er een grote heterogeniteit is tussen primaire en secundaire angiosarcomen, op basis van de immunologische en genomische profielen. Bij secundaire angiosarcomen werd een significant hogere dichtheid van immuuncellen waargenomen. In 84% van de geteste tumoren werd een pathogene mutatie gevonden, en in veel gevallen werd een mutatie of amplificatie gevonden die een aangrijpingspunt zou kunnen zijn voor een behandeling.

Het MYC-gen speelt een rol bij groei en deling van cellen. In het geval van een fout in dit gen, bijvoorbeeld een MYC-amplificatie, kan dit gen overactief worden. Er kan dan ongecontroleerde celgroei plaatsvinden. De aanwezigheid van een MYC-amplificatie wordt in de literatuur beschreven bij een meerderheid van de angiosarcomen die ontstaan na een eerdere behandeling met bestraling, zoals bijvoorbeeld bij een behandeling voor borstkanker. In **hoofdstuk 3** toonden we aan dat MYC-amplificaties inderdaad aanwezig zijn bij de meerderheid van de angiosarcomen die ontstaan door een eerdere bestraling, maar ook voorkomen bij andere angiosarcoom subgroepen. Op basis van deze data lijkt het gebruik van enkel MYC om angiosarcoom subgroepen van elkaar te onderscheiden geen goed diagnosticum. MYC wordt daarnaast in verband gebracht met een kleinere kans op een gunstig effect van behandeling met ICR. In onze studie was een MYC-amplificatie niet geassocieerd met overleving. Het bepalen van de MYC-amplificatiestatus op basis van een techniek genaamd fluorescentie in situ hybridisatie is duurder en tijdrovender dan het gebruik van immuunhistochemie om MYC-eiwitexpressie te bepalen, daarom onderzochten we de concordantie tussen beide technieken. De overeenstemming tussen beide technieken bleek slecht, en wij concludeerden op basis van onze resultaten dat het gebruik van immuunhistochemie niet als vervangende marker kan worden gebruikt om de MYC-amplificatiestatus te bepalen.

In hoofdstukken 2 en 3 lieten wij zien dat er sterke aanwezigheid was van immuuncellen bij secundaire angiosarcomen. Tevens toonden wij aan dat er sprake was van frequente mutaties in het DNA-schade herstel, hetgeen is geassocieerd met een mogelijk gunstig effect op behandeling met ICR. Op basis van deze data hebben wij een prospectieve klinische studie opgezet waarin wij de effecten van ICR onderzochten bij secundaire angiosarcomen. In de CEMangio studie, beschreven in hoofdstuk 4, demonstreerden we de effectiviteit van het middel cemiplimab bij de behandeling van lokaal vergevorderde en uitgezaaide secundaire angiosarcomen. In totaal reageerde 27,8% van de patiënten op de behandeling, met een mediane progressievrije overleving van 3,7 maanden en een mediane overleving van 13,1 maanden. De mediane tijd tot respons was 2,1 maanden en de duur van de respons tot ziekteprogressie was 6,9 maanden. De bijwerkingen van de behandeling waren acceptabel. Om toekomstige patiënten beter te selecteren voor ICR, voerden we genomische en immunologische analyses uit. Bij de meerderheid van de patiënten werd een DNA-mutatie of amplificatie geïdentificeerd. Twee van de drie patiënten met een tumor met relatief veel mutaties (een hoge tumor-mutational burden) reageerden goed op de behandeling. In tegenstelling tot onze hypothese vonden we geen associatie tussen de aanwezigheid van mutaties in het DNA-schadeherstel en de effectiviteit van ICR. Echter zou de grote aanwezigheid van deze mutaties een nieuw aangrijpingspunt kunnen vormen voor een combinatiebehandeling met ICR en specifieke remmers van het DNA-schadeherstel.

Tevens toonden we in de CEMangio studie aan dat patiënten die reageerden op behandeling met ICR een significant hogere dichtheid hadden van specifieke immuuncellen, namelijk T-helper cellen en cytotoxische T-cellen. Daarnaast onderzochten wij de waarde van het darm-microbioom, waarbij aanwezigheid van de bacterie Colidextribacter significant was geassocieerd met een goede respons op ICR. Met de opkomst van poeptransplantaties en probiotica als aanvullende behandeloptie kan het microbioom mogelijk niet alleen fungeren als een voorspeller op de kans om op ICR te reageren, maar ook als een therapeutisch aangrijpingspunt. Daarnaast onderzochten wij in hoofdstuk 4 de waarde van circulerend tumor DNA (ctDNA). In onze studie was een daling in ctDNA al na 3 weken aantoonbaar, en dit liep vooruit op een gunstige afname van de tumoromvang die later werd gemeten met een CTscan. Een toename in ctDNA liep vooruit op een toename van de tumoromvang. Het gebruik van ctDNA kan artsen in staat stellen de effectiviteit van ICR eerder te beoordelen dan met conventionele beeldvormende onderzoeken, die vaak pas na 12 weken plaatsvinden. Hierdoor kan een tijdige aanpassing van het behandelplan plaatsvinden voor de patiënt. Deze bevinding benadrukt het potentieel van ctDNA als waardevol toekomstig hulpmiddel voor het optimaliseren van de patiëntenzorg.

Predictieve en prognostische biomarkers en klinische toepasbaarheid

Tot heden zijn wij niet goed in staat om accuraat te voorspellen welke patiënten wel, en welke patiënten niet zullen reageren op een behandeling. Om deze reden worden grote groepen patiënten behandeld, ook al zal een meerderheid van deze

patiënten niet langdurig reageren op de behandeling. Patiënten selectie is essentieel om onnodige behandelingen, en het daaruit voortvloeiend risico op bijwerkingen bij niet reagerende patiënten, en dientengevolge hoge kosten voor de maatschappij te beperken.

In hoofdstuk 5 hebben wij onderzoek verricht naar predictieve biomarkers bij de behandeling met ICR. Een predictieve biomarker is een biologische eigenschap die kan voorspellen hoe een patiënt zal reageren op een specifieke behandeling. Tot heden ontbreekt een eenduidige accurate predictieve biomarker voor ICR. Wij onderzochten de voorspellende waarde van TGF-ß bij de behandeling met ICR van melanoom patiënten. TGF-ß is een potentiële predictieve biomarker vanwege de interactie met de tumormicro-omgeving. In onze retrospectieve cohortanalyse van 40 melanoom patiënten, allemaal behandeld ICR, vonden we echter geen verband tussen de behandelrespons en TGF-β activiteit. Ook vonden wij geen verband tussen TGF-\beta activiteit en overleving. Door te kijken naar SMAD2, een kenmerkend eiwit betrokken bij de TGF-ß signaleringsroute, werden de resultaten van het onderzoek gevalideerd. Onderzoek naar middelen die TGF-ß activiteit blokkeren tonen tot heden teleurstellende resultaten, hetgeen in overeenstemming is met het gebrek aan correlatie tussen respons en TGF-β activiteit in onze studie.

In **hoofdstuk 5** onderzochten we ook andere biomarkers die mogelijk betrokken zijn bij respons op ICR, waaronder hedgehog activiteit. De hedgehog signaleringsroute reguleert verschillende processen, waaronder celgroei. We toonden aan dat een verhoogde hedgehog activiteit correleerde met een kortere progressievrije overleving en resistentie tegen ICR. Hedgehog-remming kan mogelijk een positieve invloed hebben op de tumormicro-omgeving, en daarom zouden toekomstige studies zich kunnen richten op een combinatie behandeling met ICR en hedgehog remming.

Prognostische biomarkers kunnen ook een belangrijke rol spelen bij het ontwikkelen van een geïndividualiseerd behandelplan. Het identificeren van patiënten met een hoog risico op een recidief door middel van een prognostische biomarker zou kunnen helpen bij de ontwikkeling van geïntensiveerde behandelingsschema's voor deze patiënten. In hoofdstuk 6 beschrijven wij de prognostische waarde van Magnetic Resonance Imaging (MRI), in een onderzoek met 40 patiënten die zijn gediagnostiseerd met een myxofibrosarcoom. Myxofibrosarcoom is een type wekedelen sarcoom met een hoge kans op een (lokale) terugkeer van ziekte na behandeling. Patiënten gediagnosticeerd met een lokaal myxofibrosarcoom worden in opzet genezend behandeld met radiotherapie gevolgd door een operatie. Wij toonden aan dat specifieke patiëntkenmerken zoals de aanwezigheid van een vaatkluwen op MRI-beelden een slechtere (ziektevrije) overleving hadden. Een infiltratief groeipatroon was tevens geassocieerd met een slechtere ziektevrije overleving. De aanwezigheid van een infiltratief groeipatroon of vaatkluwen op MRI zouden kunnen helpen bij het identificeren van patiënten met een hoog risico op slechte klinische uitkomsten, en ondersteuning kunnen bieden bij het individualiseren van follow-up en behandeling.

Tot slot bespreken we in **hoofdstuk 7** de belangrijkste bevindingen van dit proefschrift en geven we onze visie op de ontwikkeling van op ICR gebaseerde behandelstrategieën bij angiosarcomen.

Epiloog: Het verrichten van klinische wetenschappelijke studies

In hoofdstuk 8 geven we inzicht in de huidige regelgeving in het kader van het verrichten van klinisch wetenschappelijk onderzoek. We evalueren de praktische gevolgen van deze regelgeving en doen voorstellen voor specifieke verbeteringen om de regeldruk te verminderen. Het uitvoeren van wetenschappelijk onderzoek heeft geleid tot belangrijke ontwikkelingen in de behandeling van kankerpatiënten. Om de veiligheid van patiënten te waarborgen, is de regelgeving omtrent het verrichten van klinisch onderzoek de afgelopen twee decennia sterk toegenomen. Als gevolg van deze regeldruk is er een ineffectieve bureaucratie ontstaan, die mogelijk zelfs de veiligheid van patiënten beïnvloedt. We hebben een dramatische toename gezien in de tijd en kosten die gepaard gaan met het opstarten van nieuwe studies, en mede daardoor een afname in deelnamemogelijkheden voor patiënten. Het beperken van deze bureaucratie door middel van het gebruik van digitale handtekeningen en het beperken van onnodige correspondentie, zou een belangrijke stap in de goede richting kunnen zijn. Wij zijn groot voorstander van het oprichten van één universeel platform voor onderzoekers, dat door alle farmaceutische bedrijven wordt gebruikt, voor het invoeren van alle vereiste gegevens voor een klinische studie. Dit uniforme platform zou de bureaucratie aanzienlijk kunnen verminderen. Als oncologen en patiëntvertegenwoordigers de krachten bundelen met farmaceutische bedrijven en regelgevende instanties, zijn wij ervan overtuigd dat klinische studies aantrekkelijker worden voor patiënten, onderzoekers en organisaties. Dit zal het opzetten en verrichten van klinische studies stimuleren, de administratieve last verminderen en tegelijkertijd de veiligheid van patiënten verbeteren.

In dit proefschrift hebben wij aangetoond dat er aanzienlijke immunologische en genomische verschillen bestaan tussen primaire en secundaire angiosarcomen, wat duidelijke implicaties heeft voor toekomstige behandelstrategieën. We hebben laten zien dat een subgroep van angiosarcoom patiënten een duurzame respons kan

bereiken door behandeling met ICR. Tevens hebben wij verschillende biomarkers geïdentificeerd, die geassocieerd zijn met een gunstig effect op ICR bij angiosarcomen, waaronder de dichtheid van immuuncellen in de tumormicro-omgeving, ctDNA, tumor-mutational burden en het darm-microbioom. Tot slot stellen wij op basis van de bevindingen in de proefschrift specifieke behandelstrategieën voor toekomstig onderzoek met ICR voor in de (neo)adjuvante setting. Aanvullend hierop komen wij met voorstellen voor toekomstige studies waarbij ICR wordt gecombineerd met andere middelen, zoals een combinatiebehandeling met ICR en specifieke remmers van het DNA-schadeherstel, om de effectiviteit van de behandeling te verbeteren. Onze bevindingen zijn een belangrijke stap vooruit in de ontwikkeling van gepersonaliseerde, biomarker gedreven behandelingen voor patiënten met zeldzame sarcomen.

List of abbreviations

AE	Adverse Event	ECRO	ESMO Clinical Research Observatory
APC	Adenomatous Polyposis Coli	EGFR	Epidermal Growth Factor Receptor
AR	Androgen Receptor	EHR	Electronic Health Records
AS	Angiosarcoma	ECOG	Eastern Cooperative Oncology Group
ASCO	American Society of	ESCA	European Society for Clinical Analysis
	Clinical Oncology	ESMO	European Society for
ATR	Ataxia Telangiectasia		Medical Oncology
	and Rad3-Related	FDA	Food and Drug Administration
BRAF	B-Raf Proto-Oncogene	FISH	Fluorescence in situ Hybridization
BORR	Best Overall Response Rate	FFPE	Formalin-Fixed Paraffin-Embedded
CD	Cluster of Differentiation	FoxP3+	Forkhead Box P3 Positive
CDKN2A	Cyclin-Dependent Kinase		(T-regulatory cells)
	Inhibitor 2A	GCP	Good Clinical Practice
CHEK2	Checkpoint Kinase 2	Gd	Gadolinium
CNA	Copy Number Alterations	H&E	Hematoxylin and Eosin
CNV	Copy Number Variation	Hh	Hedgehog
COSMIC	Catalogue of Somatic Mutations	ICI	Immune Checkpoint Inhibition
	in Cancer	IHC	Immunohistochemistry
CR	Complete Response	IQR	Interquartile Range
CRKL	C-RELA Kinase-Like Gene	IFN-γ	Interferon Gamma
ctDNA	Circulating Tumor DNA	ICR	Immune Checkpoint Receptor
CRO	Contract Research Organization	LR	Local Recurrence
CTCAE	Common Terminology Criteria for	MAPK	Mitogen-Activated Protein Kinase
	Adverse Events	MFS	Myxofibrosarcoma
CTLA-4	Cytotoxic T-Lymphocyte-Associated	MSI	Microsatellite Instability
	Antigen 4	MYC	Proto-oncogene MYC
CDA	Confidential Disclosure Agreement	NGS	Next-Generation Sequencing
DDR	DNA Damage Response	NLR	Neutrophil-to-Lymphocyte Ratio
DDRi	DNA Damage Response Inhibitor	NK cells	Natural Killer cells
DCE-MRI	Dynamic Contrast-Enhanced	NRAS	Neuroblastoma RAS Viral
	Magnetic Resonance Imaging		Oncogene Homolog
DFS	Disease-Free Survival	OS	Overall Survival
DNA	Deoxyribonucleic Acid	OSI	Oncological Soft Imaging
DWI	Diffusion Weighted Imaging	PARP	Poly(ADP-Ribose) Polymerase
EORTC	European Organisation for Research	PARPi	Poly-ADP Ribose
	and Treatment of Cancer		Polymerase Inhibitors
EMA	European Medicine Agency	PD	Progressive Disease
LIMA	European Medicine Agency	צט	rrogressive Disease

PD-1 Programmed Cell Death-1
PD-L1 Programmed Death-Ligand 1
PFS Progression-Free Survival
PI3K Phosphoinositide 3-Kinase
PLR Platelet-to-Lymphocyte Ratio

PR Partial Response

RAD54L RAD54-Like DNA Repair Protein
RECIST Response Evaluation Criteria in

Solid Tumors

RT Radiotherapy RT-AS Radiotherapy-

associated Angiosarcoma

SNPs Single Nucleotide Polymorphisms
SOP Standard Operating Procedure

STS Soft Tissue Sarcomas

T1w T1-weighted (MRI sequence)
T2w T2-weighted (MRI sequence)
TGF-β Transforming Growth Factor-Beta
TILs Tumor-Infiltrating Lymphocytes
TMB Tumor Mutational Burden

TMA Tissue Microarray

TME Tumor Microenvironment
TSO500 Tumor Sequencing Panel 500

UV Ultraviolet

ТМВ-Н

UV-AS Ultraviolet-associated Angiosarcoma

High Tumor Mutational Burden

VAF Variant Allele Frequency
WHO World Health Organization

Data management

Ethics and privacy

This thesis is based on the results of research involving human participants, which were conducted in accordance with relevant national and international legislation and regulations, guidelines, codes of conduct and Radboudumc policy. The recognized Medical Ethics Review Committee 'METC Oost-Nederland' has given approval to conduct these studies (chapter 4) (file number: NL74804.091.21). The institutional ethical review committee CMO Radboudumc, Nijmegen, the Netherlands has given approval to conduct these studies (CMO Radboudumc dossier number: 2017-3164 (chapter 2,3, chapter 6), 2021-12959 (chapter 4), 2016-2686, (chapter 5)).

According to Dutch legalization, data collection from electronic patient files was performed by personnel with a treatment relationship with the patient and the researcher(s) upon consent by the study participant. The privacy of the participants in these studies was warranted by the use of pseudonymization. The pseudonymization key was stored on a secured network drive that was only accessible to members of the project who needed access to it because of their role within the project. The pseudonymization key was stored separately from the research data.

For chapters 2, 3, 4, 5 and 6, either informed consent was obtained from participants to collect and process their data, or data was used that was previously collected in the context of healthcare. Consent for reuse of the data was not obtained. To ensure responsible reuse of healthcare data, specific informed consent procedures were followed that are aligned with applicable laws, regulations, and the national Code of Conduct for Health Research

Data collection and storage

Data for chapters 2, 3, 4 and 6 was collected through electronic Case Report Forms (eCRF) in Castor EDC. Data were converged from Castor EDC to SPSS (SPSS Inc., Chicago, Illinois, USA) and R statistics for data interpretation. Pseudonymized data were stored and analyzed on the department server and in Castor EDC and are only accessible by project members working at the Radboudumc. Additionally, part of the data for chapter 2, 3, 4 and 5 were obtained through laboratory experiments. Data from chapters 2, 3, 4, 5 and 6 were analyzed and stored on the department server.

Availability of data

All studies are published open access, or will be submitted for open access publication. The data will be archived for a minimum of 15 years after termination of the study. The metadata for chapters 2, 3, 4, 5, and 6 are published in Data Sharing Collections (DSC's) in the Radboud Data Repository. The datasets underlying these chapters are not published in the DSC's as data from patients treated in other hospitals were involved or patients did not give permission to reuse nor share their data. The datasets are thus only available for reuse for future research after a renewed permission by the participants.

Chapter	DAC	RDC	DSC	DSC License
2	-	-	DOI: https://doi.org/10.34973/r8wq-fe88	CC-BY-NC-ND 4.0
3	-	-	DOI: https://doi.org/10.34973/j5dg-mr17	CC-BY-NC-ND 4.0
4	-	-	DOI: https://doi.org/10.34973/da1h-ya12	CC-BY-NC-ND 4.0
5	-	-	DOI: https://doi.org/10.34973/fk96-hx66	CC-BY-NC-ND 4.0
6	-	-	DOI: https://doi.org/10.34973/r8wq-fe88	CC-BY-NC-ND 4.0

DAC = Data Acquisition Collection, RDC = Research Documentation Collection, DSC = Data Sharing Collection

List of publications

Part of this thesis

van Ravensteijn, S.G., Versleijen-Jonkers, Y.M.H., Hillebrandt-Roeffen, M.H.S., Weidema, M.E., Nederkoorn, M.J.L., Bol, KF., Gorris, M.A.J., Verrijp, K., Kroeze, L.I., de Bitter, T.J.J., de Voer, R.M., Flucke, U.E., & Desar, I.M.E. (2022). Immunological and Genomic Analysis Reveals Clinically Relevant Distinctions between Angiosarcoma Subgroups. Cancers, 14(23), 5938. https://doi.org/10.3390/cancers14235938

van Ravensteijn, S.G., Hogeboom-Gimeno, A.G., Desar, I.M.E., Hillebrandt-Roeffen, M.H.S., van Cleef, P.H.J., Bonenkamp, J.J., Flucke, U.E., & Versleijen-Jonkers, Y.M.H. (2023). MYC amplification in angiosarcoma depends on etiological/clinical subgroups – Diagnostic and prognostic value. *Annals of Diagnostic Pathology*, 63, 152096, https://doi.org/10.1016/j.anndiagpath.2022.152096.

van Ravensteijn, S.G., Amir, A.L., Tauriello, D.V.F., van Herpen, C.M.L., Boers-Sonderen, M.J., Wesseling, Y.J.W., van Brussel, A.C.G., Keizer, D.M., Verheul, H.M.W., & Bol, K.F. (2024). Exploring the relation between TGF-β pathway activity and response to checkpoint inhibition in patients with metastatic melanoma, Clinical and Experimental Immunology, Uxae108, https://doi.org/10.1093/cei/uxae108

van Ravensteijn, S.G., de Haan, J.J., Gelderblom, H., Nederkoorn, M.J.L., Hillebrandt-Roeffen, M.H.S., Gorris, M.A.J., de Bitter, T.J.J., Boleij, A., Gusinac, A., Ederveen, T.H.A., Flucke, U.E., Bonenkamp, J.J., Speetjens, F.M., Kaal, S.E.J., Smits, M., Bol, K.F., van Herpen, C.M.L., Versleijen-Jonkers, Y.M.H., Desar, I.M.E.. Cemiplimab in locally advanced or metastatic secondary angiosarcomas (CEMangio): A phase II clinical trial and biomarker analyses. Clinical Cancer Research, 2025 Jul 9. doi: 10.1158/1078-0432.CCR-25-0311

van Ravensteijn, S.G., Nederkoorn, M.J.L., Wal, T.C.P., Versleijen-Jonkers, Y.M.H., Braam, P.M., Flucke, U.E., Bonenkamp, J.J., Schreuder, B.H.W., van Herpen, C.M.L., de Wilt, J.H.W., Desar, I.M.E., & de Rooy, J.W.J. (2023). The Prognostic Relevance of MRI Characteristics in Myxofibrosarcoma Patients Treated with Neoadjuvant Radiotherapy. Cancers, 15(10), 2843. https://doi.org/10.3390/cancers15102843

van Ravensteijn, S.G., Meijerink, M., Nijenhuis-van Schayk, R., Desar, I.M.E., Bol, K.F., van Herpen, C.M.L., & Verheul, H.M.W. (2023). The safety risk of information overload and bureaucracy in oncology clinical trial conduct. *European Journal of Cancer*, 183, 90-94. https://doi.org/10.1016/j.ejca.2023.01.018

Scientific publications outside of this thesis

van Ravensteijn S.G., van Merrienboer B., van Asten S., Pruijt J., Hilbink, M., & Tol, J. (2021). Oxaliplatin infusion-related venous pain: prevention by simultaneous intravenous fluids. *BMJ Supportive & Palliative Care*. 11(2), 226-229. https://doi.org/10.1136/bmjspcare-2019-002177.

Uijen, M.J., Weijers, J.A., Lassche, G., van Ravensteijn, S.G., van Rijk, M.C., Lubeek, S.F., van Engen-van Grunsven, A.C., Amir, A.L., Driessen, C.M., & van Herpen, C.M.L., (2023). Cutaneous lymphangitis carcinomatosa in salivary duct carcinoma. Journal of Clinical Pathology, 76(3), 211-213. https://doi.org/10.1136/jcp-2022-208564.

PhD portfolio of Stefanus Gerardus van Ravensteijn

Department: Medical Oncology

PhD period: 01-09-2020 - 1-1-2023 and 01-06-2024 - 06-01-2025

PhD Supervisor(s): Prof. Dr. C.M.L. (Carla) van Herpen, Prof. Dr. H.M.W. (Henk) Verheul,

PhD Co-supervisor(s): Dr. I.M.E. (Ingrid) Desar, Dr. K.F. (Kalijn) Bol

Training activities	Hours
Courses	
EBROK (2020)	34.00
RIHS - Introduction course for PhD candidates (2020)	15.00
Radboudumc - Scientific integrity (2021)	20.00
Vitaal bedreigde patiënt (2022)	16.00
Radboudumc - Re-registration BROK (2023)	5.00
Seminars	
JNVMO Oncology Lectures (2021)	12.00
JNVMO oncology lectures (2021)	4.00
Brabants Mamma symposium (2023)	4.00
JNVMO oncology lectures (2023)	8.00
JNVMO oncology lectures (2023)	8.00
JNVMO oncology lectures (2024)	8.00
ESMO preceptorship metastatic bladder and kidney cancer (2024)	17.00
Weekly meeting PhD/laboratory (2025)	100.00
Conferences	
Bridging Radiotherapy & Immunotherapy (2021)	10.00
AACR annual meeting + poster presentation (2022)	48.00
Dutch Sarcoma Group Symposium + oral presentation (2022)	16.00
ASCO annual meeting poster presentation (2022)	16.00
Nederlandse internistendagen + oral presentation (2022)	16.00
AACR annual meeting attendance + poster presentation (2023)	48.00
ASCO annual meeting poster presentation (2023)	16.00
NVMO post-ASCO (2023)	8.00
Post-ASCO meeting Onco-Oost (2023)	4.00
Post-ESMO Onco-Oost (2023)	4.00
NVMO oncologiedagen (2023)	16.00
ESMO Sarcoma and Rare Cancers poster presentation (2024)	8.00
Nijmegen Prostate Cancer Prospects (2024)	16.00
ASCO annual meeting + oral presentation (2024)	48.00
Post-ASCO meeting + oral presentation (2024)	16.00
Post-ESMO NVMO (2024)	6.00
Other	
Peer review (2020)	8.00
IMPROVER project (2021)	42.00
Phase I study physician meetings (2022)	50.00
Journal club (2020-2025)	20.00
Supervision of internships / other	
Supervision student (2022)	40.00
Total	707.00

Curriculum Vitae

Stefanus Gerardus van Ravensteijn werd op 16 juni 1991 geboren te Oss. Na het afronden van het Gymnasium aan het Titus Brandsma Lyceum in Oss, startte hij in 2009 met de studie geneeskunde aan de Radboud Universiteit in Nijmegen. Zijn coschappen sloot hij af met een keuzecoschap op de afdeling interne geneeskunde en een onderzoeksstage bij de afdeling hematologie, waarna hij in 2016 zijn artsendiploma behaalde.



Na het afronden van de studie geneeskunde startte hij direct met de opleiding tot internist in het Jeroen Bosch Ziekenhuis te 's-Hertogenbosch (opleider Dr. W. Smit), waarna hij deze na 3 jaar in 2019 verder vervolgde in het Radboudumc te Nijmegen (opleider Dr. G.M.M. Vervoort).

In 2018 maakte hij voor het eerst kennis met het verrichten van wetenschappelijk onderzoek, waarbij hij keek naar de toegevoegde waarde van gelijktijdige vochttoediening tijdens de behandeling met Oxaliplatin, ter preventie van pijnklachten tijdens infusie met dit chemotherapeuticum. Dit resulteerde in zijn eerste posterpresentatie op een internationaal congres en een wetenschappelijke publicatie.

In september 2020 heeft Stefan zijn opleiding onderbroken voor promotieonderzoek onder begeleiding van Prof. Dr. C.M.L. van Herpen, Prof. Dr. H.M.W. Verheul, Prof. dr. I.M.E. Desar en Dr. K.F. Bol. Het onderzoek richtte zich onder meer op het identificeren van patiënten die een kans hebben op een gunstig effect van behandeling met immunotherapie. Tijdens zijn promotieonderzoek zette hij onder meer een klinische studie op waarbij patiënten met een inoperabel secundair angiosarcoom werden behandeld met immunotherapie. Tevens verrichte hij poliklinische zorg voor patiënten die werden behandeld in verschillende Fase I studies.

De resultaten van zijn onderzoeken presenteerde hij op verschillende nationale en internationale congressen. In 2024 presenteerde hij de resultaten van de klinische studie tijdens een mondelinge presentatie op het Amerikaanse oncologiecongres (ASCO).

77

Naast zijn promotieonderzoek, heeft Stefan in januari 2023 zijn opleiding tot internist hervat, met als differentiatie medische oncologie, welke in maart 2025 werd afgerond. Vanaf april 2025 is Stefan werkzaam als internist-oncoloog in het Catharina Ziekenhuis te Eindhoven. Stefan woont samen met Carlyn en hun dochter Livia in Berghem.

Dankwoord

Dit proefschrift was niet tot stand gekomen zonder de samenwerking, hulp en inzet van vele anderen. Ik wil daarvoor iedereen heel hartelijk bedanken.

Allereerst wil ik alle patiënten en hun families bedanken die deel hebben genomen aan de studies en/of op een andere wijze hebben bijgedragen aan de totstandkoming van dit proefschrift. Zonder jullie deelname hadden wij niet de kennis kunnen verkrijgen die is beschreven in dit proefschrift. Dit onderzoek is door hen, en voor hen gedaan.

Prof. dr. van Herpen, beste Carla, als AIOS kwam ik met je praten over een mogelijk promotietraject. Vanaf het allereerste begin heb jij mij de ruimte gegeven om mijn eigen weg te vinden binnen het promotietraject. Dankzij jouw inzet voor de Fase I-poli kreeg ik de mogelijkheid om onderzoek te combineren met de directe patiëntenzorg. Je hebt mij gesteund in het maken van mijn eigen keuzes, waarbij je tegelijkertijd waakte over de grote lijnen en de structuur van het promotietraject. Die combinatie van begeleiding en vertrouwen heeft mij gestimuleerd om met enthousiasme en toewijding aan mijn onderzoek te werken. Dank je wel voor je betrokkenheid en ruimte die je me hebt gegeven om te groeien als onderzoeker én als persoon.

Prof. dr. Verheul, beste Henk, met een kopje koffie begon mijn promotietraject, een moment dat het startsein bleek voor een bijzonder leerzame en waardevolle periode. In eerste instantie richtte mijn onderzoek zich met name op Fase I-studies, maar al snel verschoof de focus naar zowel klinisch als preklinisch onderzoek bij sarcomen. Vanaf het begin straalde jij vertrouwen uit. Je daagde me uit om niet alleen de klinische kant van het onderzoek te verkennen, maar juist ook preklinisch onderzoek te verrichten. Daardoor kreeg ik de kans om te werken aan diverse studies en om congressen te bezoeken zoals de AACR in New Orleans en Orlando, wat waardevolle ervaringen zijn geweest. Ik wil je ontzettend bedanken voor de mooie, inspirerende en leerzame tijd als jouw promovendus.

Prof. dr. Desar, beste Ingrid, gedurende mijn promotieonderzoek was je niet alleen mijn copromotor, maar ook opleider. Toen mijn promotieonderzoek een andere richting insloeg, bood jij mij direct de ruimte en mogelijkheid om binnen het sarcomenonderzoek te werken aan prachtige klinische en preklinische studies. Die kans heeft mijn promotietraject enorm verrijkt. Ik waardeer het enorm dat jouw deur altijd openstond voor advies, of het nu ging om grote beslissingen of om kleine, praktische vragen. Je zorgde voor structuur wanneer dat nodig was, maar gaf mij

tegelijkertijd alle ruimte om eigen keuzes te maken en mijn eigen pad te volgen. Die ruimte gaf je niet alleen binnen het onderzoek, maar ook als opleider. Dank voor jouw vertrouwen, begeleiding en steun gedurende dit traject.

Dr. Bol, beste Kalijn, jouw scherpzinnigheid, behulpzaamheid en laagdrempelige houding maakten het ontzettend prettig om met je samen te werken. Je bent enorm gedreven en je passie voor preklinisch onderzoek werkt aanstekelijk. Hier heb ik ontzettend veel van geleerd. Mede dankzij jou heb ik me verder kunnen verdiepen in immunologisch onderzoek, en verliep de samenwerking met het Tumor Immunologie Laboratorium heel goed. Heel veel dank voor je betrokkenheid en waardevolle begeleiding.

De leden van de manuscriptcommissie, Prof. dr. I.C.M van der Geest, Prof. dr. J.A. Schalken en Dr. W.J. van Houdt, wil ik hartelijk danken voor het lezen en beoordelen van dit proefschrift.

Dr. Versleijen-Jonkers, beste Yvonne, heel veel dank voor je hulp en begeleiding bij het sarcomenonderzoek. De samenwerking met jou heb ik als bijzonder prettig ervaren. Het contact was altijd laagdrempelig en er was altijd ruimte om te sparren, vragen te stellen of ideeën uit te wisselen. Jouw betrokkenheid en inhoudelijke bijdrage hebben een belangrijke rol gespeeld in dit traject.

Beste Melissa, heel veel dank voor je hulp bij de vele studies die in dit proefschrift zijn beschreven. Jouw ondersteuning heeft een grote bijdrage geleverd aan het tot stand komen van dit proefschrift. Bedankt voor de fijne samenwerking.

Bij de CEMangio-studie kijk ik terug op een hele fijne samenwerking met de deelnemende centra, veel dank dat dit zo voorspoedig is verlopen!

Prof. dr. K.C.P. Vissers, beste Kris, hartelijk dank voor je begeleiding als mentor tijdens mijn promotieonderzoek. Onze gesprekken waren voor mij van grote waarde.

Ik wil natuurlijk alle coauteurs die hebben meegewerkt aan (een deel van) dit proefschrift bedanken, maar ik zou graag een aantal personen nog expliciet willen noemen.

In het bijzonder wil ik alle (oud-) collega-onderzoekers van de medische oncologie bedanken voor de fijne sfeer, hulp en alle gezelligheid. Bedankt Jetty, Iris, Ilse, Eline, Niels, Peter, Kim, Sophie, Lotte, Dide, Sarah, Gerben, Maike, Sandra, Merle, Sofie en Maikel. Koffie drinken, sparren over welke kant je op moet met je discussie, ondersteuning bij een R-script dat nog wat verbetering kon gebruiken, of gezellig samen naar een congres gaan, zijn onmisbaar tijdens een promotietraject. Jetty, Jorien en Dennis, bedankt voor de hele leuke tijd en vele potjes Ligretto tijdens de AACR in Orlando, en natuurlijk het uitstapje naar Disney. Ilse, Eline en Niels, samen met jullie kijk ik terug op een fantastische ASCO en een mooie tijd in Chicago, waar ik alles heb geleerd over deepdish pizza! Go Cubs!

Alle collega (oud) fellows van de medische oncologie, wat een fijne groep om je opleiding mee te mogen doorlopen. Heel veel dank voor de mooie samenwerking en ik kijk uit naar de volgende etentjes!

Dank tevens aan de collega's van het researchteam van de medische oncologie. Een speciaal woord van dank voor het Fase 1 researchteam! Bedankt voor de mooie samenwerking afgelopen jaren. Francine, bedankt voor je hulp bij de Fase 1 studies en de CEMangio, maar ook voor de koffie en gezellige gesprekken!

Daarnaast wil ik graag alle medewerkers van de afdeling en polikliniek medische oncologie bedanken voor de hulp bij alle onderzoeken, het geven van de behandelingen en het bieden van een luisterend oor aan de patiënten.

Mark Gorris en Kiek Verrijp, veel dank voor de fijne samenwerking vanuit het Tumor Immunologie Lab bij de verschillende studies beschreven in dit proefschrift.

Veel dank aan alle collega's van de Vakgroep Interne Geneeskunde van het Catharina Ziekenhuis. Sinds april 2025 ben ik gestart als oncoloog in het Catharina Ziekenhuis, en ik voel me helemaal opgenomen als onderdeel van de vakgroep.

Een goede werk-privébalans is essentieel voor het goed functioneren op de werkvloer tijdens een promotietraject. Graag wil ik alle vrienden en vriendinnen bedanken voor de mooie en leuke dingen die we de afgelopen jaren samen hebben mogen doen.

Beste Hechte Helden, Anne en Marel, Gerardo, Jaap en Naomi, Janneke en Remo, Karlijn en Ole, Luuk en Javi, Merijn en Eveline, Niels en Aria, Sifra, Teun en Simone en Ward. Al sinds de middelbare school zijn we vrienden. Ik ben enorm dankbaar voor onze mooie vriendschap, de fantastische vakanties die we hebben gehad met elkaar, en de mooie herinneringen die we hebben gemaakt. Van Chili tot Salt Lake, en van Enkhuizen tot Berghem, de afstand is groter geworden dan vroeger op het TBL,

maar als we elkaar weer zien is alles zoals vanouds. Bedankt voor alle interesse en mooie momenten!

Beste leden van het 23° bestuur van het SOOS! Beste Ayla, Eline, Joey, Joyce, Niels, Tess en Sjef. Sinds het SOOS bestuur kennen we elkaar, inmiddels zijn we 15 jaar verder, en nog steeds vrienden. Mede dankzij jullie steun is dit proefschrift tot stand gekomen.

Beste Laura en Sietse, bedankt voor de gezellige CPK avonden! Ik kijk al uit naar de volgende editie.

Beste Annemarije, al sinds onze coschappen zijn we vrienden, dank voor je steun, luisterend oor en de gezellige spelletjesavonden.

Beste Maren en Leon, bedankt voor jullie steun en afleiding. Oorspronkelijk vrienden van Carlyn, maar inmiddels zijn jullie ook mijn vrienden geworden. Bedankt voor de gezellige avondjes, het dromen over, en plannen van mooie verre reizen en de heerlijke etentjes buiten de deur!

Beste Thijs, al sinds onze jeugd zijn we vrienden. Vele jaren gingen we samen met de families op vakantie naar Frankrijk, Italië en op de camping in Nederland. De vakanties hebben plaatsgemaakt voor game- en borrel avonden. Inmiddels ben je zelfs overbuurman geworden! Ik ben enorm dankbaar voor onze mooie vriendschap door alle jaren heen. Ik wil je bedanken voor al je steun, luisterende oor en de mooie dingen die we samen hebben gedeeld. Ik prijs me enorm gelukkig met jou als paranimf aan mijn zijde vandaag! Beste Minette, bedankt voor je vriendschap, de spelletjesavonden en alle gezellige momenten!

Lieve Ria, wat was opgroeien met jou in de buurt fijn! Bedankt voor alle mooie momenten die we hebben gehad samen! Jou zorgzaamheid, aandacht en betrokkenheid hebben mij mede gevormd tot de persoon die ik nu ben. Peter, veel dank voor je interesse in het onderzoek.

Beste familie van Lith en van Ravensteijn. Bedankt voor jullie interesse en betrokkenheid tijdens mijn promotieonderzoek. Ik geniet enorm van alle gezellige familiemomenten, en natuurlijk de spelletjes met Pasen en Kerst!

Lieve familie Kouwenberg, lieve Peter en Gerry, ik wil jullie bedanken dat jullie mij hebben opgenomen in jullie familie. Ik voel me bij jullie thuis, en jullie zijn me dierbaar. Bedankt voor jullie oprechte betrokkenheid en interesse in mijn onderzoek. Ik vind het erg mooi dat ik dit moment met jullie mag delen.

Lieve Myrlon en Rens, met zijn drieën opgroeien, daar zit geen saai moment bij. Waar we vroeger nog weleens botsten achter in de auto naar Frankrijk, is onze band nu ijzersterk. De vele gezellige avonden en mooie momenten koester ik enorm. Lieve Pauline, wat een gezellige en fijne aanvulling ben jij voor onze familie. Bedankt voor al je interesse! Ik kijk er enorm naar uit om ons aankomende nichtje te ontmoeten!

Lieve papa en mama, bedankt voor jullie onvoorwaardelijke steun en liefde. Jullie rotsvaste vertrouwen en het feit dat jullie er altijd voor me zijn betekent enorm veel. Mede dankzij jullie is dit proefschrift zo geworden. Ik realiseer me hoeveel geluk ik heb met jullie als mijn ouders, en van alle ondersteuning die jullie bieden, ik hou van jullie.

Lieve Livia, jij bent het allermooiste wat mij ooit is overkomen. Ik ben enorm trots en dankbaar dat ik jou papa mag zijn. Elke dag met jou is een cadeau! Ik kijk ernaar uit om je te zien opgroeien, en om je de wereld te laten zien!

Allerliefste Carlyn, jij bent de liefde van mijn leven, mijn beste vriendin. Bij jou voel ik me thuis, waar ter wereld we dan ook zijn. Bedankt voor al je onvoorwaardelijke steun en liefde. Ik kijk uit naar alle mooie avonturen die we samen gaan beleven, de landen die we gaan ontdekken, maar vooral naar de tijd die we samen met elkaar en Livia doorbrengen. Ik hou van jou!



